2022

Mechanisms and Treatment of Pain-Depressed Behavior in Male and Female Mice

Clare M. Diester
Virginia Commonwealth University

Mechanisms and Treatment of Pain-Depressed Behavior in Male and Female Mice

A dissertation submitted in partial fulfillment of the requirements for the degree of Doctor of Philosophy at Virginia Commonwealth University

by

Clare M. Diester
Master of Science in Forensic Science, Virginia Commonwealth University, 2017
Bachelor of Science, University of Missouri, 2015

Advisor: S. Stevens Negus, Ph.D.
Professor of Pharmacology and Toxicology
Virginia Commonwealth University

Virginia Commonwealth University
Richmond, Virginia
December 2021

Acknowledgements

Try as I might, there are simply no words to properly express my deep gratitude to everyone who has supported me these past four years. I could never have accomplished the work described in this dissertation while going through a knee surgery and a global pandemic (!) without the most incredible mentors, colleagues, friends, and family.

To my mentor Dr. Steve Negus: being your mentee will likely be one of the best decisions I will make during my scientific career. It has been an honor to learn from such a remarkable scientist and genuinely wonderful person. I will carry your lessons with me for the rest of my life and owe so much of who I have become to your patient guidance. To Dr. Matt Banks: thank you for your inspirational conversations and humoring my sporadic "Hey, Matt?" questions throughout the day. I have been incredibly fortunate to share an office space with you and Steve that has been filled with so much laughter and pure scientific curiosity. To my committee members: Dr. John Bigbee, you are such a joy to learn from, and I am so grateful for the constant support you have provided me. Dr. Aron Lichtman, thank you for all the guidance you have given me throughout my doctoral training. Your energy is absolutely inspirational, and I have had so much fun being an "honorary" member of your laboratory. Dr. Gretchen Neigh, you have taught me so much about leading by example. Thank you for allowing me to use the instrumentation in your laboratory and providing invaluable insight for the design and interpretation of my doctoral research. Dr. Sim-Selley, thank you for providing a wonderful education experience in Principles, for allowing me to create my own little bench space in your lab, and for your support during my doctoral research. To Dr. Bill Dewey, Dr. Krista Scoggins, Dr. Jill Bettinger, and Dr. Keith Shelton, thank you for your academic support. To Dr. Michael Grotewiel, you have been incredibly impactful on my doctoral training, and I am lucky to have such a wonderfully empathetic individual to oversee my graduate education. Thank you to the members of the Banks and Negus laboratory (especially our amazing lab technician Sam), and to all of my wonderful friends that have supported me along my graduate journey, especially Jacy, Erica, Lesley, Jimmy, Jordan, Ashley, Cody, Tyson, and Victoria. Your encouragement means the world to me and has helped provide the foundation that allows me to take risks and grow. Thank you to my family, especially my father for the unconditional support and company during late night experiments, and my astonishingly wonderful twin sister. I will forever feel like I have found a cheat code in life by having you as my twin. To my dear Vassilis, thank you for your unwavering support, and for your invaluable help with the neurochemical portion of this dissertation. Your curiosity is positively infections, and you have changed how I view the world around me.

To quote my dad, "Starting something is easy. The hardest thing to do is finish something well." This process has not been easy, but all of these individuals have made this the most fun job I have ever had, and I will always cherish the memories from my PhD.

Table of Contents

List of Abbreviations

2-AG = 2-arachidonyl glycerol

AEA = anandamide

ANOVA = Analysis of variance

$CB_{1/2}R$ = cannabinoid 1 & 2 receptors

$COX = cyclooxygenase_{1/2}$

DA = dopamine

DH = dorsal horn

DRG = dorsal root ganglia

eCB = endodannabinoid

FAAH = fatty acid amide hydrolase

fMRI = functional magnetic resonance imaging

GABA = gamma-aminobutyric acid

GAD = glutamate decarboxylase

IASP = International Association for the Study of Pain

IP acid = intraperitoneal lactic acid

LHb = lateral habenula

MAGL = monoacylglycerol lipase

MOR = mu-opioid receptor

NAc = nucleus accumbens

NIH = National Institutes of Health

NMDA = N-methyl-D-aspartate

NSAID = non-steroidal anti-inflammatory drug

PAG = periaqueductal gray

PB = parabrachial nucleus

PBS = phosphate-buffered saline

RMC = red nucleus

RMTg = rostromedial tegmental nucleus

SABV = Sex as a Biological Variable

SC = subcutaneous

SEM = standard error of the mean

SI = primary somatosensory cortex

SN = substantia nigra

TH = tyrosine hydroxylase

THC = Δ9-tetrahydrocannibinol

VSCC = voltage-sensitive calcium channel

VTA = ventral tegmental area

List of Compounds

Chapter II:

Ketoprofen

Chapter III:

Ketoprofen

Oxycodone

Amphetamine

Diazepam

Chapter IV:

Δ9-tetrahydrocannibinol

MJN110

JZL184

JZL195

SA57

URB597

PF3845

Rimonabant

SR141716A

Chapter V:

MJN110

Structure of Compounds

Chapter II:

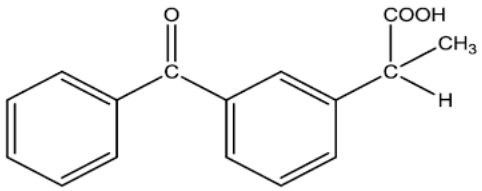

Ketoprofen

Chapter III:

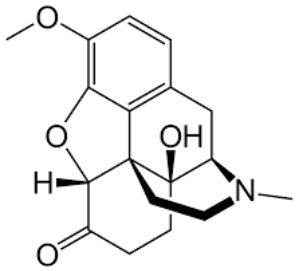

Oxycodone

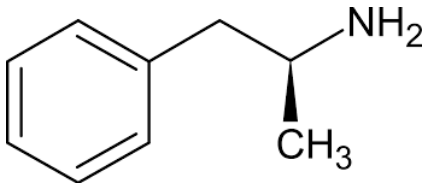

Amphetamine

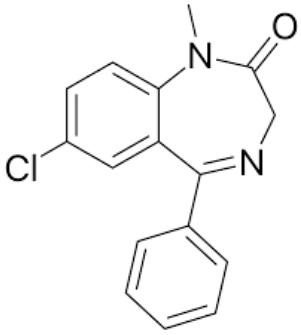

Diazepam

Chapter IV:

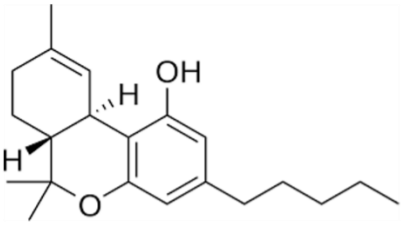

THC

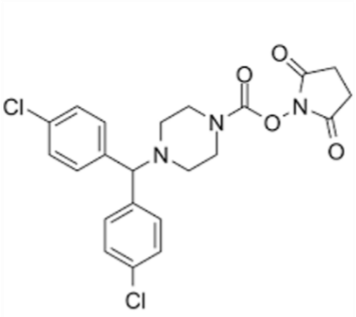

MJN110

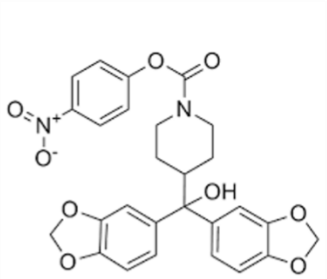

JZL184

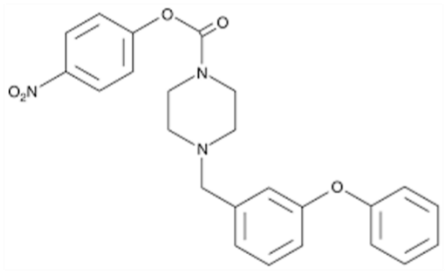

JZL195

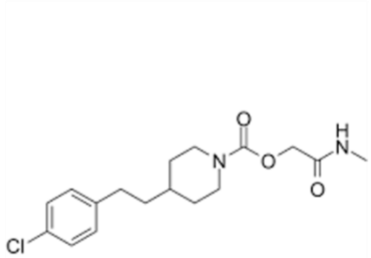

SA57

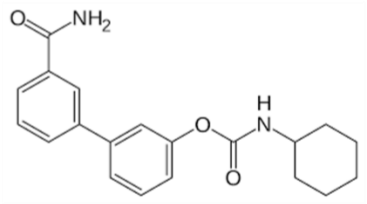

URB597

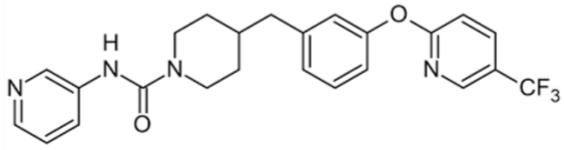

PF3845

Chapter V:

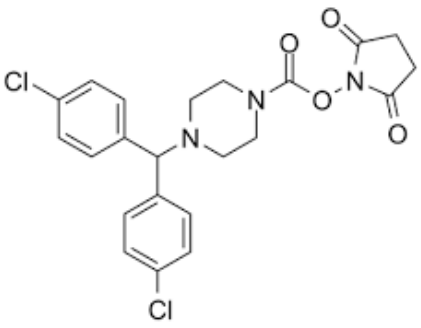

MJN110

Abstract

MECHANISMS AND TREATMENT OF PAIN-DEPRESSED BEHAVIORS IN MALE AND FEMALE MICE

A dissertation submitted in partial fulfillment of the requirements for the degree of Doctor of Philosophy at Virginia Commonwealth University, 2021

Advisor: S. Stevens Negus, PhD

One of the largest discrepancies between preclinical and clinical assessment of pain and analgesia is the type of behavioral endpoint used. Although most preclinical research has historically focused on drug effectiveness to block reflexive withdrawal behaviors stimulated by a noxious stimulus, increasing evidence shows that drug-induced restoration of pain-depressed behaviors provides increased clinical translation with decreased susceptibility to false-positives. Accordingly, the first portion of this dissertation designed a behavioral battery that featured pain-depressed behaviors as well as more conventional pain-stimulated behaviors for testing candidate analgesics in male and female mice. The main findings are as follows. (1) Intraperitoneal injection of dilute lactic acid (IP acid) served as an effective visceral chemical noxious stimulus to produce concentration-dependent stimulation of two behaviors (stretching and facial grimace; pain-stimulated behaviors) and depression of two behaviors (rearing and nesting; pain-depressed behaviors). (2) Pharmacological characterization with two positive control analgesics (ketoprofen, oxycodone) and two active negative controls (diazepam, amphetamine) validated a strategy for distinguishing analgesics from nonanalgesics by profiling drug effects in this battery of complementary pain-stimulated and pain-depressed behaviors along with two additional pain-independent behaviors (nesting and locomotor activity in the absence of the IP acid noxious stimulus). (3) A National Institutes of Health mandate for consideration of Sex as a Biological

Variable (SABV) was published at the start of this dissertation research. Accordingly, we developed an experimental design for considering SABV when sex differences are not the principle independent variable, with emphases on exploratory power analyses (effect size, power, predicted N) and segregation of data by sex to allow transparent analysis of SABV and help guide future study designs.

The second portion of this dissertation applied this behavioral battery and SABV data-analysis strategy to evaluate a spectrum of endocannabinoid (eCB) catabolic enzyme inhibitors ranging in selectivity for the eCB catabolic enzymes monoacylglycerol lipase (MAGL) and fatty acid amide hydrolase (FAAH), which have received increasing interest for development of candidate analgesics. The main findings are as follows: (1) antinociceptive effectiveness decreased as MAGL-selectivity decreased, with the most MAGL-selective inhibitor MJN110 producing the most effective antinociceptive profile, (2) time course and antagonism studies for MJN110 showed a long duration of antinociceptive action (40min – 6hrs), mediation by CB_1R but not CB_2R, a tendency for greater effects in females, and (3) repeated administration of MJN110 produced partial but sustained attenuation of IP acid-induced depression of nesting, with segregation of data by sex demonstrating sustained but weak antinociception in males and variable effects following repeated dosing in females.

Overall, these data provide a framework for predicting the analgesic potential of test drugs in preclinical pain models in male and female mice, and suggest that MJN110 may have only partial effectiveness as a candidate analgesic for treatment of visceral episodic pain.

Chapter I: Introduction

I. Core Pain-Related Measures in Preclinical and Clinical Research: Discrepancies Highlight Roadmap for Improved Preclinical Assessments

Pain is a leading global health problem (Goldberg, 2011) and major reason for healthcare utilization in the United States (St. Sauver et al., 2013). Almost 40 million people undergo surgery that often produces acute pain, and more than 100 million Americans suffer from chronic pain each year, costing the United States over $600 billion annually (Institute of Medicine, 2011; Chapman and Vierck, 2017; Pogatzki-Zahn, 2021). For the first time since 1979, the International Association for the Study of Pain (IASP) updated their definition of pain, describing it as, "an unpleasant sensory and emotional experience associated with, or resembling that associated with, actual or potential tissue damage." Despite decades of research, the most commonly used analgesics continue to be non-steroidal anti-inflammatory drugs (NSAIDs) and μ-opioid receptor (MOR) agonists that were introduced over a century ago (Kissin, 2010; Obeng et al., 2021). Use of these compounds is constrained by limited clinical efficacy for some pain indications (Finnerup et al., 2015) and by side effects that include gastric ulceration for NSAIDs and abuse liability and potentially lethal respiratory depression for MOR agonists that have contributed in part to the current public health crisis. The opioid crisis in particular has invigorated efforts to discover new, effective, and safe medications for pain treatment (Skolnick and Volkow, 2016; Volkow and Collins, 2017).

Preclinical testing in laboratory animals will likely play an important role in this drug-discovery effort, but preclinical-to-clinical translation has been poor in analgesic drug development, with numerous candidate analgesic compounds (e.g. NK-1 antagonists) appearing highly effective preclinically and failing in clinical trials (Mogil, 2009; Yezierski and Hansson,

2018; Negus, 2019; Tappe-Theodor et al., 2019; Gonzalez-Cano et al., 2020; Kandasamy and Morgan, 2020). Experimental evaluation of pain inherently involves delivery of a noxious stimulus with the intent of producing a pain state (primary independent variable) followed by measurement of different behaviors interpreted as evidence of that pain state (dependent variable). In preclinical research, noxious stimuli are often classified as either acute, inflammatory ± evocation with an acute stimulus, neuropathic ± evocation with an acute stimulus, or a disease state (e.g. bone cancer) ± evocation with an acute stimulus (Negus, 2019). While large strides have been made in preclinical development of noxious stimuli to model clinically-relevant pain indications (Le Bars et al., 2001; Mogil, 2009; Deuis et al., 2017; Munro et al., 2017), less progress has been made regarding pain-related behaviors, with one of the largest discrepancies between preclinical and clinical pain assessment being the type of behavioral endpoint used to indicate the presence of a pain state and impact of a drug treatment.

Clinical pain in human medicine is primarily measured via verbal reporting, whereas preclinical pain research has focused almost exclusively on reflexive withdrawal behaviors stimulated by noxious stimuli. This creates a major discrepancy for translational research because verbal behavior cannot be measured in animals, and suppression of nocifensive withdrawal reflexes is not a priority for analgesic administration in humans. For example, 2016 CDC guidelines recommend the primary goal in clinical pain treatment to be decreasing pain-related functional impairments rather than solely decreasing pain intensity (Ballantyne and Sullivan, 2015; Dowell et al., 2016; Negus, 2019; Tappe-Theodor et al., 2019; Kandasamy and Morgan, 2020). Moreover, pain is a multi-faceted experience comprised of sensory and affective dimensions that manifests as a constellation of unconditioned and learned behaviors in both humans and animals, with adequate assessment likely requiring evaluation of multiple behaviors

relative to different pain indications that are mediated by different neural circuits (Garcia-Larrea and Peyron, 2013; Negus, 2019).

Pain-related behaviors can be classified into the two following categories: (1) pain-stimulated behaviors, which increase in rate, frequency, duration, or intensity following delivery of a noxious stimulus, and (2) pain-depressed behaviors, which decrease in rate, frequency, duration, or intensity following delivery of a noxious stimulus. While pain-stimulated behaviors possess clinical face validity for reflexive pain-related behaviors (e.g., removing your hand from a hot surface), they are highly susceptible to false positives such as general motor sedatives and do not model the primary clinical goal for functional restoration of behavior. Accordingly, our lab and others have argued for the inclusion of pain-depressed behaviors, which are not susceptible to false positives from general motor sedatives, are one of the main endpoints used in veterinary medicine for diagnosis and treatment of pain, and possess increased clinical translation by modeling the primary treatment goal for restoring pain-related functional impairment (e.g. pain decreasing ability to sleep, move, work, eat) (Stevenson et al., 2009; de la Puente et al., 2017; Negus, 2019; Tappe-Theodor et al., 2019; Kandasamy and Morgan, 2020). Figure I.I illustrates the key differences in drug effects on pain-stimulated vs pain-depressed behaviors, with particular emphasis placed on susceptibility to false positives.

II. Design and Pharmacological Characterization of a Behavioral Battery for Testing Candidate Analgesics in Male and Female Mice

The goal of Chapter III was to validate a battery of pain-stimulated and pain-depressed behaviors for use in mice to test candidate analgesics, as complementary assessment of both pain-stimulated and pain-depressed behaviors not only broadens the scope and translational

relevance of preclinical behavioral testing, but also protects against false-positive effects from drugs that produce sedation or motor impairment (Figure I.I) (Negus, 2019). Intraperitoneal injection of dilute lactic acid (IP acid) served as an acute visceral noxious stimulus that models inflammation-associated tissue acidosis as one contributor to inflammatory pain from various pain indications, including post-surgical inflammation (Koster et al., 1959; Holzer, 2009; Stevenson et al., 2009; Cobos et al., 2012; McMahon et al., 2013; de la Puente et al., 2017; Spahn et al., 2017). IP acid has the experimental advantage of providing fine-tuned control of noxious stimulus intensity and the transient nature allows replicable effects with repeated administration in within-subject experimental designs (Le Bars et al., 2001; Stevenson et al., 2009; Negus, 2018).

Additionally, care was taken to include behavioral endpoints reflecting sensory and affective dimensions of pain that are likely mediated by different neural circuits (Garcia-Larrea and Peyron, 2013). One feature of behaviors interpreted as evidence of the "sensory" dimension of pain is their focus on the body part affected by the putative noxious stimulus. For example, delivery of a noxious thermal stimulus to a rodent's hind paw may elicit both a reflexive paw-withdrawal response and more complicated paw-licking/grooming responses. In contrast, behaviors interpreted as evidence of the "affective" dimensions of pain involve more general changes in behavior not specifically directed to the site of noxious stimulus delivery. For example, noxious stimuli can elicit common facial grimacing behaviors and signs of general behavioral depression regardless of the site where the noxious stimulus is delivered. These different sensory and affective pain behaviors appear to involve overlapping but dissociable CNS pathways. Additionally, local spinal cord circuits have been shown to be sufficient to mediate simple reflexive pain behaviors in spinalized subjects, whereas higher order somatotopically

organized pathways (e.g., spinothalamocortical pathway) appear to be involved in coordinating more complex behaviors such as licking/grooming of a pain state (Grossman et al., 1982; Le Bars et al., 2001). Conversely, affective behaviors are thought to involve spinal-bulbar-limbic circuits that have a lower level of somatotopic organization (Price, 2003; Almeida et al., 2004).

Drug effects in this dissertation were examined on four different IP acid-induced pain-related behaviors: (1) stimulation of a stretching (or writhing) response as a conventional pain-stimulated behavior somatotopically directed to the site of noxious stimulus delivery and potentially relying on spinal circuits (Collier et al., 1968; Clement et al., 2000; Le Bars et al., 2001), (2) stimulation of facial grimace as a pain-stimulated behavior directed to a remote site away from the noxious stimulus and hence requiring supraspinal circuits and potentially reflecting affective pain behaviors (Langford et al., 2010; Matsumiya et al., 2012), (3) depression of rearing as an unconditioned and high-frequency vertical locomotor behavior (Cho et al., 2013; Cobos and Portillo-Salido, 2013), and (4) depression of nesting as a robust and adaptive ethological behavior (Jirkof, 2014; Negus et al., 2015). Drug effects were also evaluated on two additional pain-independent behaviors in the absence of the IP acid noxious stimulus: (1) nesting to assess drug-induced disruption of an adaptive ethological behavior and (2) horizontal locomotor activity that could be either increased or decreased by test drugs.

To validate this behavioral battery for both clinically effective and ineffective drugs as recommended for translational research (Ferreira et al., 2019), effects were compared for two mechanistically distinct but clinically effective positive-control analgesics (ketoprofen and oxycodone) and two negative-control drugs that are not clinically indicated for use as analgesics but do produce robust behavioral effects in mice (diazepam and amphetamine). Ketoprofen is a cyclooxygenase$_{1/2}$ (COX) inhibitor representative of NSAID analgesics, whereas oxycodone is

an MOR agonist representative of opioid analgesics (Kantor, 1986; Kalso, 2005; McMahon et al., 2013; Brunton et al., 2018). Diazepam is a GABA type A ($GABA_A$)-receptor positive allosteric modulator that produces general motor suppression, and amphetamine is a substrate at dopamine and norepinephrine transporters that produces dopamine and norepinephrine release and subsequent psychomotor-stimulant behavioral effects (Calcaterra and Barrow, 2014; Hutson et al., 2014; Brunton et al., 2018). We hypothesized that ketoprofen and morphine would alleviate both IP acid–stimulated and IP acid–depressed behaviors at doses that did not alter pain-independent behaviors, whereas diazepam and amphetamine would not. Results of this work were then used in Chapter IV as an empirical framework to interpret effects produced by a series of candidate analgesic targeting the endocannabinoid system.

III. Responding to the NIH Mandate for Consideration of Sex as a Biological Variable in Preclinical Research

At the time this dissertation research began, the National Institutes of Health (NIH) issued a policy promoting the inclusion of male and female subjects in preclinical biomedical research (Miller et al., 2017). This policy acknowledged that sex differences are not the primary variable of interest in much preclinical research, but that absent an explicit scientific rationale to exclude either males or females, both sexes should be included and the data-analysis plan should address the role of sex as a biological variable (SABV). As further guidance for addressing this new mandate, the policy articulated "The Four C's of Studying Sex to Strengthen Science" (https://orwh.od.nih.gov/sex-gender/nih- policy-sex-biological-variable)(NIH, 2015): (1) Consider (design studies that take sex into account, or explain why it is not incorporated), (2) Collect (tabulate sex-based data), (3) Characterize (analyze sex-based data), and (4)

Communicate (report and publish sex-based data). As sex differences were not the primary aim for the present studies and sample sizes required to detect sex differences were unknown, we designed an experimental framework in Chapter II to address "The Four C's of Studying Sex to Strengthen Science" when sex is not the primary variable of interest. In this framework, the "Consider" mandate for experimental design that takes sex into account is addressed through inclusion of both males and females, the "Collect" mandate for tabulating sex-based data is addressed through segregation of data by sex following analysis of primary variable(s) in data pooled across sex, the "Characterize" mandate is addressed by using ANOVAs to analyze sex-based differences with existing sample sizes and power analyses to guide both interpretation of the ANOVA results and design of any future studies that might focus on sex differences, and the "Communicate" mandate for reporting and publishing sex-based data is addressed through reporting results of ANOVAs (F statistics) and power analyses (effect size, power, predicted Ns) as a useful array of statistical outcome measures.

Ultimately, three categories of sex differences have been described: Type 1 ("sexual dimorphism"; qualitatively different phenotypes between sexes), Type 2 ("sex differences"; quantitatively different phenotypes), and Type 3 ("sex convergence and divergence"; similar phenotypes with different biological mechanisms) (McCarthy et al., 2012). The analysis proposed in Chapter II will be more sensitive to Type 1 than Type 2 differences, but in either case, it can provide preliminary information on the existence of phenotypic sex differences. In contrast, this approach will not detect Type 3 differences. As a result, even if adequately powered statistical analysis indicates that a phenotypic sex difference is absent, it remains possible that the convergent phenotypes could have sexually divergent underlying mechanisms. It is also important to note that all experiments contain multiple secondary variables, many of

which have been shown to significantly impact experimental outcomes and clinical translation (e.g. importance for utility of outbred strains compared to inbred rodent strains (Tuttle et al., 2018b)). The experimental design and analysis framework described in Chapter II can be applied for analysis of a variety of secondary variables (not just sex), with inclusion of these additional secondary analyses dependent upon the research group and experimental question.

With these caveats in mind, we utilized the strategy detailed in Chapter II for preliminary analysis of sex effects in studies that include both sexes but do not aim to focus on sex as a primary variable of interest. In those instances, we suggest that priority of analyses should follow standard statistical assessment with priority placed on adequately powered primary variables based on initial study design, followed by segregation of data by sex when underpowered for direct sex comparisons to avoid potential masking of effects (Miller et al., 2017; Tannenbaum et al., 2019; Galea et al., 2020) and inclusion of power analyses (effect size, power, predicted N) to help guide both interpretation of current results and design of any future studies targeting possible sex differences.

IV. Targeting the Endocannabinoid System Main Degradative Enzymes for Assessment of Candidate Analgesics

Neurons communicate nociceptive information from the periphery to the CNS through excitatory transmission, with clinical pain states often involving hyperactivity of these pathways (Basbaum et al., 2009; Dostrovsky and Craig, 2013; Heinricher and Fields, 2013). Current clinically used analgesics have receptor targets throughout these neural pathways that mediate the sensory and affective dimensions of pain. For example, the spinal cord, spinal-thalamic-cortical and spinal-bulbar-limbic circuits are rich in MORs (Mansour et al., 1987; Mansour et al.,

1995; Stein, 2016), which are the primary target for opioid analgesics like oxycodone. These main pain-processing pathways are also rich in cannabinoid 1 and 2 receptors ($CB_{1/2}$Rs) that mediate a form of feedback inhibition (Herkenham et al., 1991; Tsou et al., 1998; Reggio, 2010; Blankman and Cravatt, 2013; Ohno-Shosaku and Kano, 2014). More specifically, $CB_{1/2}$Rs are $G_{i/o}$ G-protein coupled receptors (GPCRs) that can be activated by exogenous orthosteric agonists (e.g. Δ9-tetrahydrocannabinol (THC)) or by endogenous lipids, with the two main endocannabinoid (eCB) lipids being 2-arachidonyl glycerol (2-AG) and anandamide (AEA) (Devane et al., 1992; Mechoulam et al., 1995). CB_1Rs are widely expressed throughout the central and peripheral nervous system, and CB_2Rs are predominately expressed on peripheral immune cells.

Unlike neurotransmitters that are released from presynaptic vesicles to produce effects on postsynaptic terminals, excitatory anterograde transmission within pain-processing pathways will elicit post-synaptic synthesis of 2-AG and AEA. As illustrated in Figure I.II, these highly lipophilic molecules activate presynaptic CB_1Rs through retrograde signaling, leading to inhibition of adenylyl cyclase, enhancement of inwardly rectifying potassium channels, and inhibition of calcium channels, effectively dampening further anterograde neurotransmitter release (Reggio, 2010; Lu and Mackie, 2016). 2-AG and AEA signaling is terminated primarily via the enzymes monoacylglycerol lipase (MAGL), which hydrolyzes 2-AG into arachidonic acid (AA) and glycerol in the presynaptic nerve terminal, and fatty-acid amide hydrolase (FAAH), which hydrolyzes AEA into AA and ethanolamine in the postsynaptic terminal. Both pharmacological inhibition and genetic knock-out of these enzymes produce dramatic increases in their respective eCB brain lipid levels, indicating these enzymes as key regulators for 2-AG

and AEA signaling *in vivo* (Cravatt et al., 2001; Long et al., 2009a; Chanda et al., 2010; Niphakis et al., 2013).

Previous studies have shown that the eCB system acts as an on-demand feedback-inhibition mechanism to dampen the hyperactive excitatory signaling seen in both acute and chronic pain states (Meng, 1998; Guindon and Hohmann, 2009; Reggio, 2010; Woodhams et al., 2017). More specifically, delivery of a noxious stimulus recruits the eCB system in the periphery (Hohmann, 2002; Guindon and Beaulieu, 2009; Kaczocha et al., 2018), dorsal horn of the spinal cord (Richardson et al., 1998; Nyilas et al., 2009; Woodhams et al., 2017), and neural circuits associated with both acute and chronic pain states (Sagar et al., 2009; Woodhams et al., 2017). Accordingly, great interest has been placed on targeting the eCB system for development of candidate analgesics. Multiple studies have shown poor clinical efficacy alongside unwanted psychomimetic and motor-impairing effects with $CB_{1/2}R$ agonists as analgesics (Raft et al., 1977; Greenwald and Stitzer, 2000; Wallace et al., 2007; Kraft et al., 2008; Babalonis et al., 2019; Mun et al., 2020). This year, the IASP released a statement that they "…do not endorse the general use of cannabinoids to treat pain" due to a lack of evidence following a systematic review of current clinical evidence for cannabinoids as analgesics by the Presidential Task Force on Cannabis and Cannabinoid Analgesia (Rice et al., 2021).

Instead of globally activating all $CB_{1/2}Rs$ throughout the CNS and periphery via exogenous agonists, increasing evidence suggests analgesic potential for enhanced signaling of the eCB system through inhibition of the main degradative catabolic enzymes MAGL and FAAH (Schlosburg et al., 2009; Fowler, 2012; Donvito et al., 2018). Compared to exogenous agonists, development of MAGL- and FAAH-selective inhibitors allows researchers increased temporal and spatial selectivity as enhanced inhibitory signaling of $CB_{1/2}Rs$ will only be produced where

2-AG and/or AEA is being synthesized. Additionally, MAGL and FAAH inhibitors possess dual inhibitory capacity for neuronal signaling and proinflammatory mediators through decreased production of AA, suggesting potential antinociceptive effectiveness in pain states involving inflammatory mechanisms, especially for MAGL-selective inhibitors as 2-AG has been shown as a major source of AA in the brain (Ahn et al., 2009; Long et al., 2009a; Nomura et al., 2011; Kinsey et al., 2013; Ignatowska-Jankowska et al., 2015a; Thompson et al., 2020).

Pharmacological inhibition of MAGL and FAAH elicits antinociceptive effects in neuropathic, inflammatory, and thermal preclinical pain models (Long et al., 2009a; Schlosburg et al., 2009; Nomura et al., 2011; Booker et al., 2012; Fowler, 2012; Kwilasz et al., 2014; Dalmann et al., 2015; Burston et al., 2016; Wilkerson et al., 2018; Habib et al., 2019; Thompson et al., 2020). Moreover, inhibitors selective for MAGL and FAAH did not produce classic cannabimimetic effects in mice, suggesting an increased safety profile compared to orthosteric $CB_{1/2}R$ agonists (Ignatowska-Jankowska et al., 2015a). Despite these promising preclinical reports, failure of a FAAH inhibitor in a clinical trial for pain due to osteoarthritis of the knee, and neurological effects by the FAAH inhibitor BIA 10-2474 case doubts on the clinical utility of FAAH inhibitors as candidate analgesics (Huggins et al., 2012; von Schaper, 2016; Weber et al., 2020). However, the discovery a microdeletion in a *FAAH* pseudogene in a patient with pain insensitivity and elevated AEA levels has reinvigorated these efforts (Habib et al., 2019). Clinical results have not yet been published with MAGL-selective or dual MAGL/FAAH inhibitors for pain indications; however, the MAGL-selective inhibitor Lu AG06466 (formerly ABX-1431) successfully completed a phase 1b study in Tourette Syndome with no serious adverse effects and is currently in clinical trials for multiple diseases, including fibromyalgia (Abide Therapeutics, 2017; Cisar et al., 2018; Muller-Vahl et al., 2021).

eCB catabolic enzyme inhibitors have been evaluated in a limited range of preclinical pain assays predominantly focused on sensory pain-stimulated behaviors and have not been extensively evaluated in preclinical studies that include assays of pain-depressed behaviors. The existing data for pain-depressed behaviors suggest that MAGL inhibitors may be more effective than FAAH inhibitors (Kwilasz et al., 2014; Wilkerson et al., 2018). Accordingly, Chapter IV utilized the battery of pain-stimulated, pain-depressed, and pain-independent mouse behaviors validated and pharmacologically characterized in Chapter III to compare the direct $CB_{1/2}R$ agonist THC to the following spectrum of eCB catabolic enzyme inhibitors: the MAGL-selective inhibitors MJN110 and JZL184, the dual MAGL/FAAH inhibitors JZL195 and SA57, and the FAAH-selective inhibitors URB597 and PF3845 (see Figure IV.I). We predicted a more favorable profile of antinociceptive effects without motor impairment for MAGL-selective inhibitors than for dual or FAAH-selective inhibitors or THC. Additionally, previous work has shown the antinociceptive effects of MAGL and FAAH to be $CB_{1/2}R$-mediated in neuropathic and inflammatory pain models, with some inconsistencies for the involvement of CB_2R in MAGL effects (Kinsey et al., 2009; Naidu et al., 2010; Booker et al., 2012; Ignatowska-Jankowska et al., 2015b; Burston et al., 2016; Thompson et al., 2020). Accordingly, the time course and $CB_{1/2}R$ antagonism were assessed for the most effective eCB catabolic enzyme inhibitor.

Additionally, there is increasing evidence for sex differences in cannabinoid antinociception (Cooper and Craft, 2018; Blanton et al., 2021), along with evidence for sex differences in pain processing (Greenspan et al., 2007; Sorge et al., 2011; Fullerton et al., 2018). As this study was designed for primary analysis of eCB candidate analgesic effects and not for detection of sex differences, we included equal numbers of male and female mice and analyzed

results for sex differences using the stepwise strategy developed in Chapter II and utilized in Chapter III.

The data in Chapter IV demonstrate that MJN110, the most MAGL-selective inhibitor, produced the most effective antinociceptive profile among the eCB catabolic enzyme inhibitors, with significant antinociception without motor disruption on three of the four IP acid-induced behaviors at a dose of 1.0 mg/kg (Figure IV.VII). While the interaction between sex and treatment was not significant, a main effect of sex in IP acid-depressed nesting suggests an increased effect in females compared to males, especially at 1.0 mg/kg (Supp. Figure IV.I D). While these acute antinociceptive effects support further consideration of MAGL-inhibitors (especially MJN110) as candidate analgesics, other groups evaluating the effects of repeated administration of MAGL inhibitors suggest tolerance may develop to these acute antinociceptive effects. Previous studies evaluating repeated administration of MJN110 in chronic models of cancer-induced bone pain (CIBP) and osteoarthritic pain report sustained antinociceptive effects following repeated MJN110 administration (Burston et al., 2016; Thompson et al., 2020), with Burston *et al.* showing development of antinociceptive tolerance to be dose-dependent, with higher doses (5 mg/kg) producing tolerance to antinociceptive effects on monosodium iodoacetate-stimulated behaviors.

Studies investigating the MAGL inhibitor JZL184 also demonstrate antinociceptive tolerance following persistent pharmacological inhibition or genetic disruption of MAGL to be dose-dependent. More specifically, repeated administration of 4 mg/kg JZL184 did not produce tolerance in a variety of behavioral and neurochemical measures, while 40 mg/kg JZL184 produced functional tolerance of antinociceptive effects on pain-stimulated behaviors in inflammatory and neuropathic pain models (Schlosburg et al., 2010; Ghosh et al., 2013; Kinsey

et al., 2013). Mechanisms underlying this development of tolerance were shown to be mediated through CB_1Rs as repeated dosing of 40 mg/kg JZL184 produced cross-tolerance to CB_1R agonists, reduced CB_1R function (assessed via agonist-stimulated [^{35}S]GTPγS binding), reduced CB_1R density (assessed via saturation binding with the CB_1R-selective antagonist [^{3}H]SR141716A) in mouse brain, and increased expression of off-target eCB lipids, such as AEA, palmitoylethanolamine, and *N*-oleoylethanolamine (Schlosburg et al., 2010; Ghosh et al., 2013; Kinsey et al., 2013).

Accordingly, Chapter V of this dissertation focused on evaluating the antinociceptive effectiveness of repeated administration of MJN110 on pain-depressed behavior. For this study, a pain-depressed behavior must be selected that allows the following: (1) stable and reproducible effects in the absence of the noxious stimulus across 7-days, and (2) consistent noxious stimulus-induced depression of the behavior across 7-days. The primary dependent variable in Chapter V for evaluation of noxious stimulus and drug treatment effects was nestlet consolidation, as previous work from our laboratory has demonstrated stable and high rates of nesting across multiple days (Negus et al., 2015). Additionally, IP acid was used as the repeated noxious stimulus as our lab has previously shown that daily administration of IP acid produces reliable depression of operant responding in rats that can be reversed by repeated treatment with clinically-effective analgesics (Altarifi et al., 2015; Lazenka et al., 2018; Legakis et al., 2020). Studies in Chapter V aim to extend the utility of daily administration of IP acid to mice as a model of repeated episodic visceral pain suitable for evaluating effects of repeated test-drug administration. As the temporal pattern of the underlying pain state is often presumed to be relatively constant for periods of weeks to months in most chronic pain research, this repeated

daily IP acid model provides an important tool for repeatable expression of a transient pain state for episodic chronic pain.

V. Nociceptive Circuitry and its Modulation of the Mesolimbic System

As described in Chapter I.II, pain is a multi-faceted experience with both sensory and affective dimensions likely mediated by different neuronal circuits (Garcia-Larrea and Peyron, 2013). The spinothalamocortical tract has been shown as a crucial pathway for mediation of sensory-related neuronal signaling. Following delivery of a noxious chemical, thermal, or mechanical stimulus to the periphery, primary Aδ and C fibers (nociceptors) with cell bodies in the DRG are activated, as illustrated in Figure I.III. These synapse to secondary neurons in the dorsal horn of the spinal cord that decussate and ascend via the spinothalamic tract to synapse in the thalamus. Tertiary thalamic neurons then project to cortical regions, including the somatosensory and motor cortexes, that inform behavioral responses localized to the site of the noxious stimulus. Sensory pain-related behaviors can also be mediated via reflex arcs within the spinal cord, where secondary neurons in the dorsal horn project to cell bodies in the ventral horn of the spinal cord to elicit nocifensive withdrawal responses (see Fig. I.III). In this dissertation, IP acid-induced stimulation of stretching is interpreted as evidence of the "sensory" dimension of pain that may be mediated through signaling in the spinothalamocortical pathway.

The neuronal circuits involved in affective behaviors are less understood. Preclinical pain research utilizes the term "affective" to capture emotional aspects of pain; however, as emotions in preclinical models are inferred from behavioral interpretation of animal subjects, this classification may be more similar to "non-sensory" components of pain-related behaviors that involve more general changes not specifically directed to the site of noxious stimulus delivery.

For example, Chapters III-V have demonstrated IP acid-induced depression of nesting and stimulation of facial grimace, two behaviors shown to be produced regardless of site of noxious stimulus delivery and attenuated by clinically-effective analgesics (Langford et al., 2010; Negus et al., 2015; Oliver et al., 2018; Alexander et al., 2019; Siemian et al., 2021).

Preclinical and clinical evidence across a variety of acute and chronic noxious stimuli suggest that spinal-bulbar-limbic circuits, particularly mesolimbic dopamine (DA) signaling from the ventral tegmental area (VTA) to the nucleus accumbens (NAc), play an important role in "affective" pain-related behaviors (Price, 2003; Almeida et al., 2004; Leitl et al., 2014; Benarroch, 2016; Martikainen et al., 2018; Markovic et al., 2021). Our lab has previously shown that IP acid produces depression of both intracranial self-stimulation (ICSS) and NAc DA levels, with ketoprofen and morphine alleviating both IP acid-induced depression of both behavior and mesolimbic DA (Leitl et al., 2014). This suggests that pain-depressed behaviors are mediated in part by depression of DA signaling in the mesolimbic system. Increasing evidence has shown the rostromedial tegmental nucleus (RMTg), previously called the tail of the VTA, as a critical regulator of the mesolimbic DA system (Taylor et al., 2019; Jhou, 2021). This cluster of GABAergic cells located caudal to the posterior end of the VTA are suggested to act as a "brake" on dopaminergic signaling (Barrot et al., 2012; Jhou, 2021), and has been shown to play an important role in coding of aversive stimuli, pain, and antinociception (Barrot et al., 2012; Taylor et al., 2019; Markovic et al., 2021).

Multiple brain regions shown to be involved in pain-processing have excitatory afferents synapsing in the RMTg (see Figure I.III), including regions associated with ascending pain pathways (e.g. parabrachial nucleus), descending pain pathways (e.g. periaqueductal gray), and the "affective" dimension of pain (e.g. lateral habenula) (Barrot et al., 2012; Dostrovsky and

Craig, 2013; Heinricher and Fields, 2013; Zhang et al., 2020). Additionally, both opioids and cannabinoids have been shown to produce disinhibition of DA neurons in the VTA through inhibition of RMTg GABAergic neurons (Barrot et al., 2012; Jhou, 2021). An interesting point should be made regarding opioid receptor activation on the cell bodies vs. terminals of RMTg GABAergic neurons. Opioids administered in the VTA (more anterior) can bind MORs on RMTg GABAergic synaptic terminals to produce local disinhibition of DA signaling. However, small doses of opioids targeted to the RMTg produce widespread disinhibition of DA neurons in the VTA, effectively amplifying disinhibitory effects of smaller opioid doses (Kaufling et al., 2009; Jalabert et al., 2011; Matsui and Williams, 2011; Barrot et al., 2012). As pointed out in Barrot *et al*, care should be taken when evaluating opioid or cannabinoid effects in the VTA, as the posterior VTA overlap with the RMTg may produce different neuronal and behavioral effects.

Based on this evidence, we hypothesize that IP acid-depressed behaviors are mediated in part by depression of DA signaling in the mesolimbic system. More specifically, we propose that NAc DA signaling is depressed by IP acid in part via pain-related activation of RMTg GABAergic neurons and subsequent inhibition of VTA DA neurons. Moreover, we hypothesize that antinociceptive effects of MAGL inhibitors like MJN110 may be mediated in part by inhibition of these pain-activated RMTg GABAergic neurons. To evaluate this hypothesis, the neuroanatomical signaling of the IP acid noxious stimulus must first be characterized. Accordingly, this dissertation includes an appendix aimed to develop an immunohistochemical method for assessment of IP acid-induced neuronal activation in mouse spinal cord, NAc, VTA, and RMTg.

Expression of the immediate early gene transcription factor cFos was used as a correlate of neuronal activation. Under basal conditions cFos is expressed at relatively low levels in neurons and glial cells. cFos expression is rapidly induced in neurons activated by a variety of stimuli, with neuronal activity increasing synaptic intracellular Ca^{2+} levels through N-methyl-D-aspartate (NMDA) and voltage-sensitive calcium channels (VSCCs), which then activates the ERK/MAPK pathway that phosphorylates transcription factors Elk-1/SRF and CREB on the *cfos* promoter, leading to transcription and translation of the cFos protein. Finally, cFos forms a heterodimer with c-Jun to form the AP-1 early response transcription factor (Cruz et al., 2013; Chung, 2015; McReynolds et al., 2018). Time course for cFos production has been well characterized, with *cfos* mRNA peaking around 30 minutes and cFos protein peaking between 1-3 hrs after stimulus delivery (McReynolds et al., 2018). Accordingly, studies in the appendix collected tissue 60-70 minutes after stimulus administration for cFos detection, which agrees with previous work evaluating visceral noxious stimulus-induced cFos expression in rodent brain (Sinniger et al., 2004; Jurik et al., 2015).

Similar to how functional magnetic resonance imaging (fMRI) methods draw activity-based conclusions from indirect changes in blood oxygenation, cFos is not a direct measure of neuronal activation but rather a measure of calcium-mediated signaling pathways. Electrophysiological methods would be necessary to directly measure neuronal activation; however, characterization of neuronal activity across large tissue areas is not easily amenable to electrophysiological recordings. cFos mRNA and/or protein expression offers a relatively simple method for evaluating large sections of tissue following a wide variety of stimuli, with activity profiles helping guide more specific manipulations intended to evaluate the degree to which activation of a given neural circuit is necessary and/or sufficient for a given behavioral response.

While cFos immunohistochemistry allows identification of the location of activated neurons, additional labeling with other markers is required for chemical phenotyping of activated neurons. Chemical phenotyping of RMTg GABAergic neurons in this dissertation work was attempted by targeting the enzyme glutamate decarboxylase (GAD), which functions to convert glutamate into GABA (Molinoff, 2011). GAD has two main isoforms: GAD65, which is predominantly expressed in synaptic terminals, and GAD67, which is expressed more diffusely throughout the axon and cell body (Esclapez et al., 1994; Ge et al., 2019). Identification of DA neurons in the VTA was also performed in this dissertation by targeting tyrosine hydroxylase (TH), the rate-limiting enzyme for catecholamine biosynthesis that converts tyrosine to DOPA, which is then converted to DA by dopamine-β-hydroxylase (Sanders-Bush and Hazelwood, 2011). While TH is not selective for DA neurons as norepinephrine (NE) is synthesized from dopamine, noradrenergic neurons are not located in the VTA or RMTg, allowing anatomical specificity for TH to accurately identify DA neurons in the VTA (Molinoff, 2011).

Figure I.I

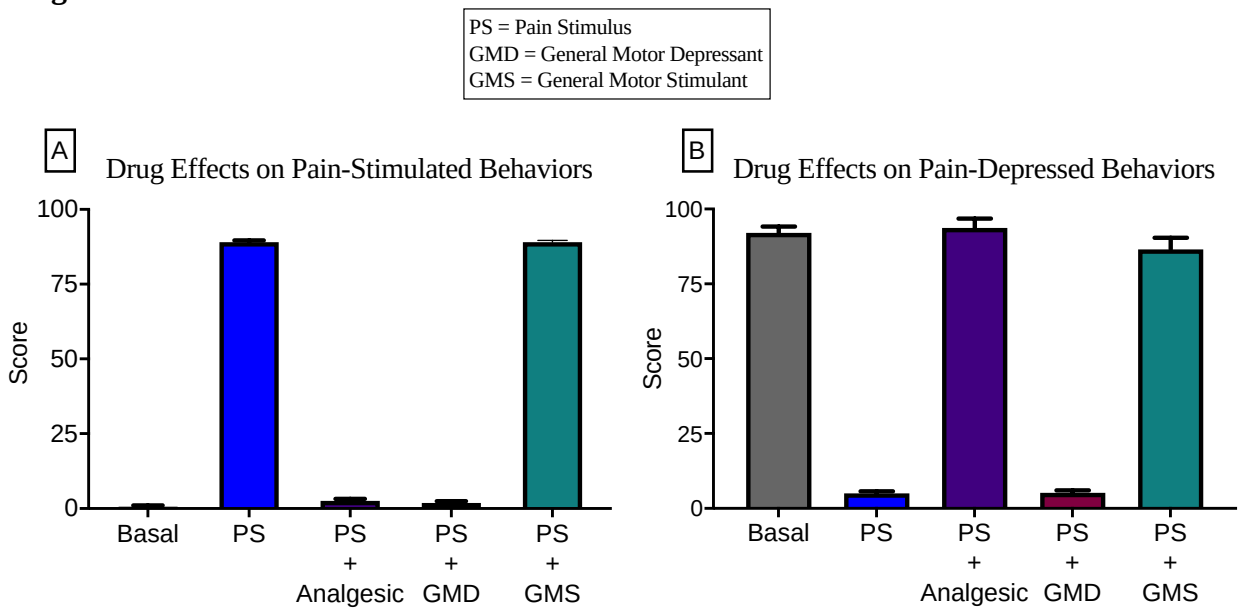

<u>Figure I.I:</u> Example data demonstrating fundamental differences in susceptibility of pain-stimulated and pain-depressed behaviors for false-positives. (A) Baseline rates of pain-stimulated behaviors are very low and increase following delivery of a noxious stimulus. Delivery of an effective analgesic decreases the behavior; however, these decreases are indistinguishable from depression from drugs that produce general behavioral suppression. (B) Baseline rates of pain-depressed behaviors are high and decrease following delivery of a noxious stimulus. Delivery of an effective analgesic produces functional restoration of the pain-depressed behavior. Importantly, drugs that decrease general behavior will produce either no change or exacerbation of the pain-related behavioral depression. Drugs that produce general motor stimulation may produce false-positive effects on pain-depressed endpoints. While general motor depressants can simultaneously depress all behavior, general motor stimulants increase a subset of behaviors as animals can only express a limited number of behaviors at one time. This suggests a higher likelihood for false positives from general motor depressants on pain-stimulated behaviors.

Figure I.II

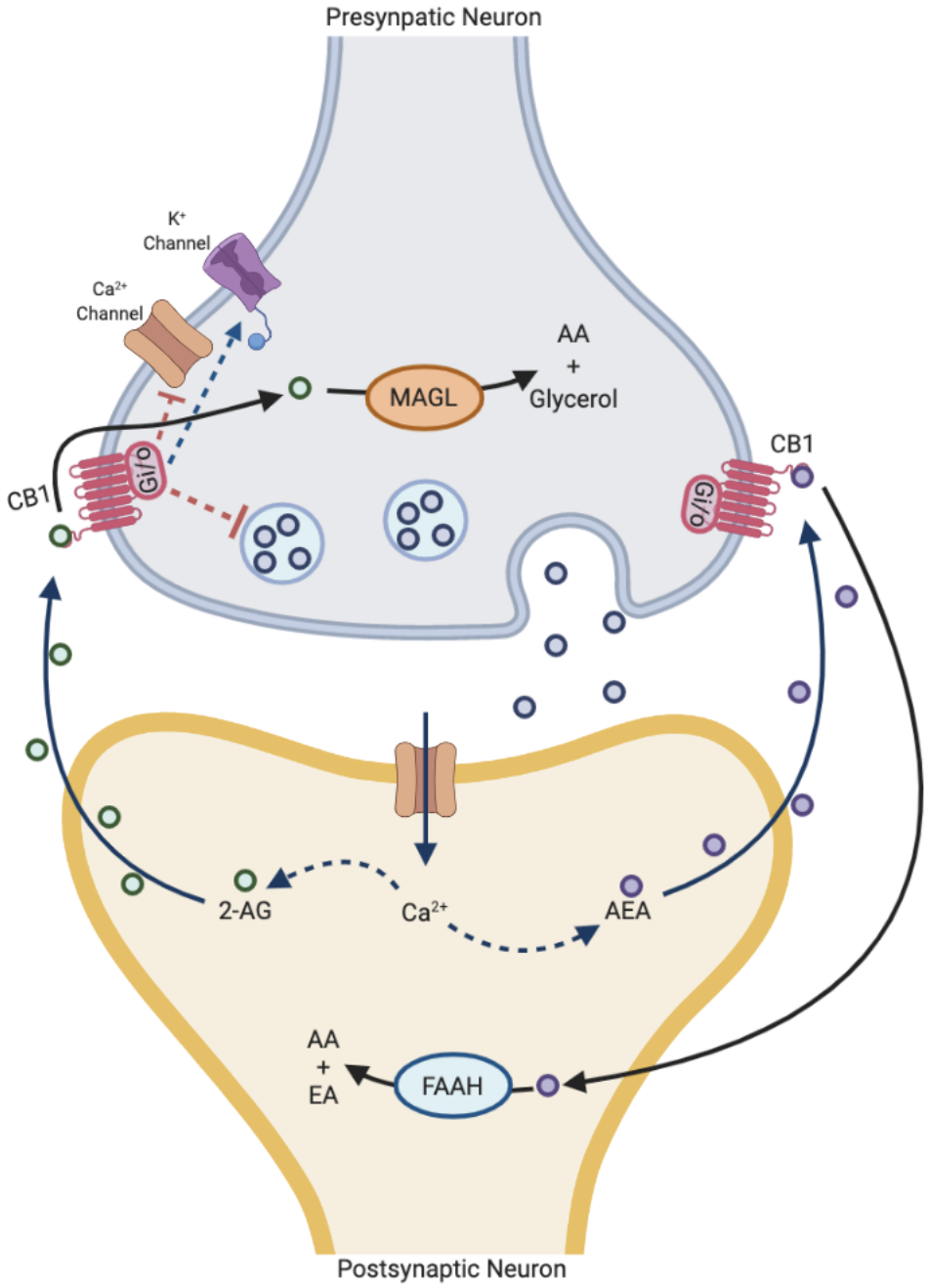

<u>Figure I.II</u>: Simplified overview of endocannabinoid system components at the neuronal synapse. Vesicular release of excitatory or inhibitory neurotransmitters from the presynaptic nerve terminal (blue) produces postsynaptic activity (yellow), leading to increased intracellular levels of Ca^{2+} and synthesis of 2-AG and AEA. These highly lipophilic molecules travel across

the synapse to bind and produce retrograde signaling on the presynaptic nerve terminal via CB_1Rs. Activation of these $G_{i/o}$-coupled GPCRs inhibits adenylyl cyclase, enhances inwardly rectifying potassium channels, and inhibits calcium channels, effectively dampening further anterograde neurotransmitter release (Reggio, 2010; Lu and Mackie, 2016). 2-AG signaling is terminated through degradation by MAGL into AA and glycerol in the presynaptic nerve terminal, and AEA signaling is terminated through degradation by FAAH into AA and EA in the postsynaptic nerve terminal. 2-AG: 2-arachidonyl glycerol; AEA: anandamide; CB_1Rs: cannabinoid 1 receptors; GPCRs: G-protein coupled receptors; MAGL: monoacylglycerol lipase; AA: arachidonic acid; FAAH: fatty acid amide hydrolase; EA: ethanolamine.

Figure I.III

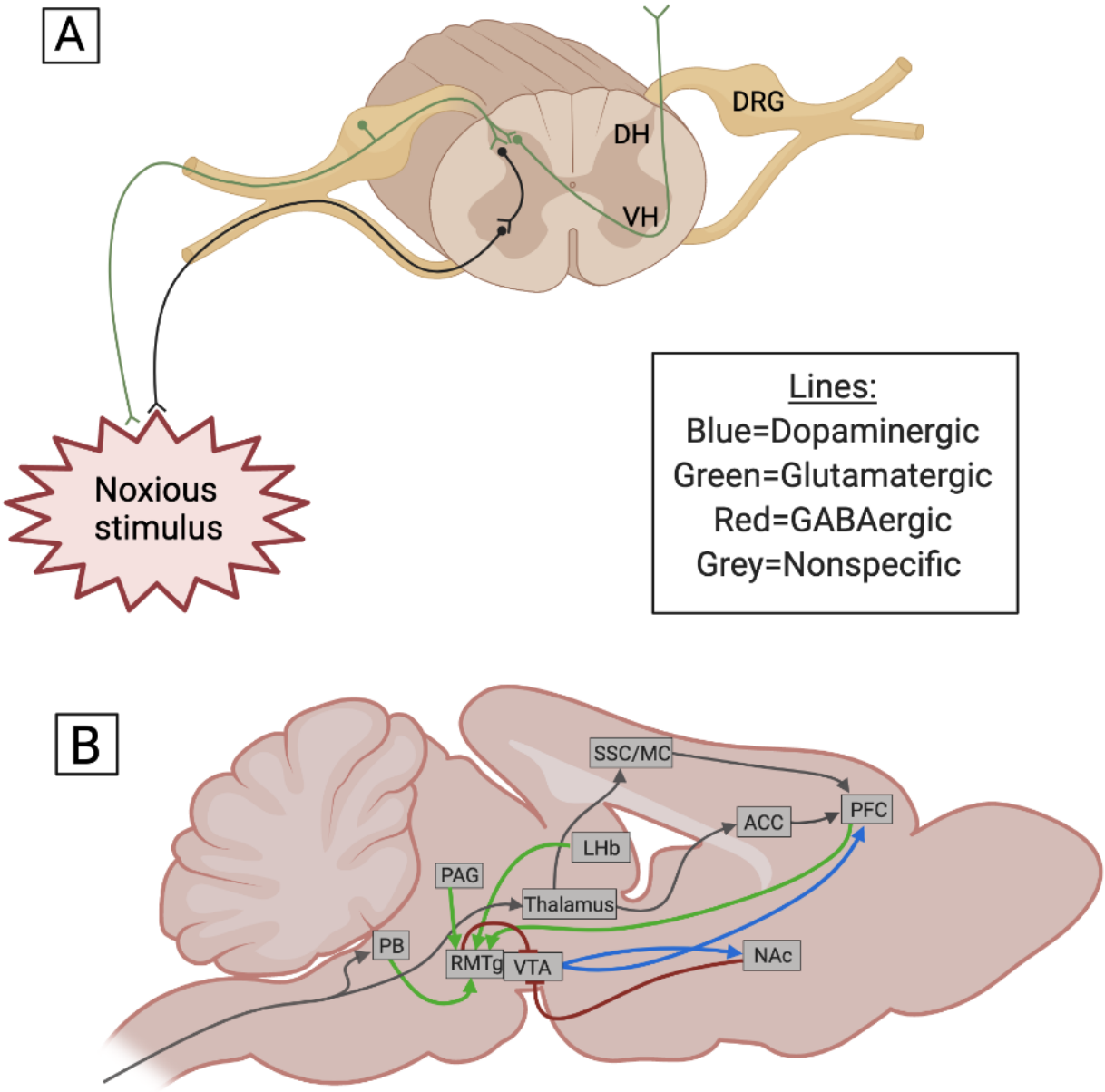

Figure I.III: Illustration of spinal and supra-spinal nociceptive pathways that can modify mesolimbic dopamine signaling via the RMTg. (A) A peripheral noxious stimulus will activate primary nociceptive neurons with cell bodies in the DRG that synapse onto secondary neurons in the dorsal horn of the spinal cord. These can either synapse onto tertiary cells in the ventral horn as part of a reflexive arc to elicit nocifensive responses, or decussate and ascend via the

spinothalamic tract to synapse on tertiary neurons in the thalamus (B). These tertiary thalamic neurons then project to the somatosensory and motor cortexes, completing the three-neuron spinothalamocortical ascending pain pathway. Quaternary afferents can then project to other regions, such as the PFC, which can modulate dopaminergic activity in the VTA through excitatory projections to the RMTg. The spinal-bulbar-limbic pathway can also modulate mesolimbic signaling, with ascending spinal afferents synapsing in the PB, which stimulates the RMTg that then inhibits VTA signaling. The PAG, which mediates descending pain pathway signaling, also has afferent projections to the RMTg. Additionally, the LHb provides a large number of excitatory inputs to the RMTg. Abbreviations: DH = dorsal horn; VH = ventral horn; DRG = dorsal root ganglia; PB = parabrachial nucleus; PAG = periaqueductal gray; RMTg = rostromedial tegmental nucleus; VTA = ventral tegmental nucleus; LHb = lateral habenula; NAc = nucleus accumbens; SSC = somatosensory cortex; MC = motor cortex; ACC = anterior cingulate cortex; PFC = prefrontal cortex.

Chapter II: Experimental Design and Analysis for Consideration of Sex as a Biological Variable

(This chapter is an adapted form of the Diester *et al.* 2019 article published in Neuropsychopharmacology, PMCID: PMC6897955)

Introduction

The National Institutes of Health (NIH) issued a policy in 2015 to promote inclusion of both male and female subjects in preclinical biomedical research (Miller et al., 2017). As guidance to address this policy, NIH has articulated "The Four Cs of Studying Sex to Strengthen Science" (https://orwh.od.nih.gov/sex-gender/nih- policy-sex-biological-variable): (1) Consider (design studies that take sex into account, or explain why it is not incorporated), (2) Collect (tabulate sex-based data), (3) Characterize (analyze sex-based data), and (4) Communicate (report and publish sex-based data). This article describes a general, multi-step approach to address The Four Cs when investigation of sex differences is not the primary aim, and sample sizes required to detect sex differences are not known.

We acknowledge that there are many instances where sex may be a top priority; however, as written, the NIH policy and associated "Four C's" guidance recognize that this is not invariably the case. The factors that may contribute to an individual researcher's prioritization of sex differences among all possible independent variables are beyond the scope of this chapter. In those instances where sex is not the primary variable of interest, we suggest that priority of analyses should be assigned to those primary variables that have been adequately powered based on initial study design with additional analyses of secondary variables such as sex addressed through appropriately designed follow-up studies.

The expression and treatment of pain constitute one domain in which sex differences are apparent in both humans and laboratory animals (Greenspan et al., 2007), and preclinical research is playing a major role in analgesic drug development in response to the NIH "Helping to End Addiction Long-term" (HEAL) initiative. Accordingly, this is one area where preclinical research is active, the new NIH policy is pertinent, and inclusion of both males and females is warranted.

Materials and Methods

Subjects

Adult male and female ICR mice (Envigo, Frederick, MD) were 6-8 weeks old upon arrival and housed in an AAALAC approved facility. All subjects were littermates group-housed 3/cage, with a cardboard tube added to the cage environment for additional enrichment to decrease fighting. Throughout the study, mice had ad libitum access to food (Teklad LM-485 Mouse/Rat Diet, Harlan Laboratories) and water, and were maintained on a 12-hour light/dark cycle (lights on from 6:00AM to 6:00PM) in a temperature-controlled room, with testing occurring during the light phase. All subjects were acclimated to the vivarium for at least one week before beginning studies and acclimated to the experimental room for at least 1 day before the first test day and at least 1 hour before testing.

Stretching Assay

For this illustrative study, which used methods similar to those previously described (Bagdas et al., 2016), adult male and female mice received an intraperitoneal injection of dilute lactic acid (IP acid) as an acute visceral pain stimulus immediately before being placed into 4-inch diameter

plexiglass cylinders for 20-min periods of videotaped observation. Two observers blinded to experimental treatment scored each video by counting the number of pain-related stretches (defined as contraction of the abdomen followed by extension of the hind limbs). Observer scores for each session were averaged for subsequent analysis. The cyclooxygenase inhibitor ketoprofen was also evaluated for its effectiveness to block IP acid effects in a separate group (Bagdas et al., 2016). The following steps in experimental design and analysis were incorporated to address The Four Cs.

Data Analysis

Experimental design to address The Four Cs

The following steps in experimental design and analysis were incorporated to address The Four Cs:

(1) IP acid alone was tested in one group of 12 mice, ketoprofen + IP acid was tested in a separate group of 12 mice, and each group contained equal numbers of male and female mice (N = 6/sex). The total group size, which was modestly larger than the N = 6-10 mice used in our previous study with only males (Bagdas et al., 2016), was selected based on the observation that confidence-interval widths for any normally distributed population decline with increasing sample size and approach an asymptote at approximately N = 12 (van Belle, 2008). We further chose to constitute this N = 12 group size with equal numbers of N = 6 mice per sex in part to comply with published guidance by the *British Journal of Pharmacology* for use of equal sample sizes of $N \geq 5$ across groups (Curtis et al., 2015). However, it is important to note that NIH guidance does not specify minimum group sizes or allocations by sex, and our approach could be used regardless of the numbers of males and females included in a study.

(2) Sex was not the primary independent variable of interest in this study, so the primary analysis pooled data from both sexes and used repeated-measures one-way ANOVA (Prism 8.0, Graph-Pad, La Jolla, CA) to evaluate effects of IP acid or ketoprofen dose. A significant ANOVA was followed by Dunnett's post hoc test to compare acid or ketoprofen effects to vehicle effects. The criterion for significance for this and all other statistical tests was $p < 0.05$.

(3) Secondary analyses to address sex as a biological variable proceeded in two steps. First, data in each panel of Fig. 1 were segregated by sex and analyzed by repeated-measures one-way ANOVA. Second, data from males and females in each panel were also analyzed by two-way ANOVA with sex as a between-subjects factor and IP acid or ketoprofen dose as a within-subjects factor. A significant interaction was followed by a Holm-Sidak post hoc test.

(4) Lastly, all one-way and two-way ANOVA results were submitted to power analyses to calculate three variables (a) Cohen's f effect size, (b) achieved power (1-β), and (c) the total number of animals predicted as necessary to detect a significant effect given the empirically determined effect size and criterion levels of $\alpha = 0.05$ and power (1-β) = 0.8 (G*Power (Faul et al., 2007), free and publicly available: http://www.gpower.hhu.de).

Power analyses

Power analysis complements the ANOVA results in three ways. First, "effect size" provides a basis for comparing the magnitude of sex differences or other effects across studies (Nakagawa

and Cuthill, 2007). In this data set, for example, all of the effect sizes for IP acid alone were greater than the effect sizes for ketoprofen antinociception.

Second, "power" provides a basis for confidence in drawing conclusions based on the ANOVA results. In particular, just as "α" values specify the probability of a Type 1 (false-positive) error, so the "β" values specify the probability of a Type 2 (false-negative) error. Moreover, just as convention accepts $\alpha \leq 0.05$ as an acceptable criterion for Type 1 errors in concluding that an effect is PRESENT, so convention also generally accepts $\beta \leq 0.2$ as an acceptable criterion for Type 2 errors in concluding that an effect is ABSENT (Marino, 2018). Insofar as the term "power" represents 1-β, then this criterion is equivalent to power ≥ 0.8. Given this criterion, it is appropriate to conclude that an effect of sex (or any other variable) is absent only if the experiment is sufficiently powered to reach that conclusion at power ≥ 0.8.

Lastly, the "predicted N" can inform experimental design for future studies that might pursue evaluation of sex differences. Thus, the effect size observed for a treatment in an initial sample of subjects from some population can be used to predict the sample size required to achieve target statistical criteria (e.g., $\alpha \leq 0.05$, $\beta \leq 0.2$) for confidence in reaching positive or negative conclusions regarding that treatment effect in other subjects from that population. Importantly, this prediction is founded on the assumption that the effect size observed in the initial sample size is representative of the whole population, but this of course is an empirical question (see (Marino, 2018) for commentary). In this study for example, power analysis predicts that total sample sizes of 56 (28/ sex) and 16 (8/sex) would be required to adequately characterize the presence or absence of a main effect of sex and a dose × sex interaction, respectively, for two-

way ANOVA of effects produced by IP acid alone. Similarly, samples sizes would need to be increased to 15 (males) or 10 (females) to adequately characterize effects of ketoprofen by one-way ANOVA in males or females alone.

Results

Primary and secondary ANOVA analyses

The data to illustrate this approach are shown in Figure 1 and Table 1. Primary repeated-measures one-way ANOVA of pooled data showed IP acid to produce a dose-dependent stimulation of stretching and ketoprofen to dose-dependently block IP acid effects. Secondary repeated-measures one-way ANOVA analysis of data from each panel segregated by sex showed IP acid stimulating stretching in both sexes; however, ketoprofen failed to significantly decrease IP acid effects in either sex. For secondary two-way ANOVA with sex as a between-subjects factor and IP acid or ketoprofen dose as a within-subjects factor, IP acid alone produced a significant main effect of acid dose but not of sex. The acid dose x sex interaction was significant, but post hoc analysis did not reveal a sex difference at any acid dose. For ketoprofen + IP acid, there was a significant main effect of ketoprofen dose but not of sex, and the ketoprofen dose x sex interaction was also not significant.

Results and implications from power analyses

In this data set, most sex-based analyses failed to reach the criterion for statistical significance, and even with the significant dose × sex interaction for effects of IP acid alone, the post hoc analysis failed to reveal a significant sex difference at any acid dose. However, power analysis indicated that it would be inappropriate to conclude from these ANOVA results that a sex

difference was absent for either IP acid or ketoprofen, because none of the analyses involving sex achieved power ≥ 0.8. The same principle applies to interpretation of ketoprofen effects in males or females alone. Although ketoprofen failed to produce a significant decrease in IP acid-stimulated stretching in either males or females, power was well under 0.8 in both sexes. Consequently, it would be inappropriate to conclude from these ANOVA results that ketoprofen had no effect. Notably, power ≤ 0.8 is not problematic in the event that a significant effect is deemed to be present, because in these cases, the concern is with potential false-positive conclusions (addressed by α) and not with potential false-negative conclusions (addressed by β). For example, the pooled analysis of ketoprofen effects had power < 0.8 (0.752); however, the ketoprofen data met the criterion for a significant effect, so there was no need to address the potential of a false-negative conclusion.

Discussion

In summary, this approach establishes a general, multi-step approach to address The Four Cs articulated by the National Institutes of Health (NIH) when preclinical investigation of sex differences is not the primary aim and sample sizes required to detect sex differences are not known. Inclusion of both males and females is responsive to the "Consider" mandate for the experimental design that takes sex into account. The pooling of data across sex permits focus on the primary variable(s) of interest, while segregation of data by sex addresses the "Collect" mandate for tabulating sex-based data. The secondary analyses address the "Characterize" mandate by using ANOVAs to analyze sex-based differences with existing sample sizes and power analyses to guide both interpretation of the ANOVA results and design of any future studies that might focus on sex differences. Finally, the results of ANOVAs (F statistics) and

power analyses (effect size, power, and predicted Ns) provide a useful array of statistical outcome measures that fulfill the “Communicate” mandate for reporting and publishing sex-based data.

Figures

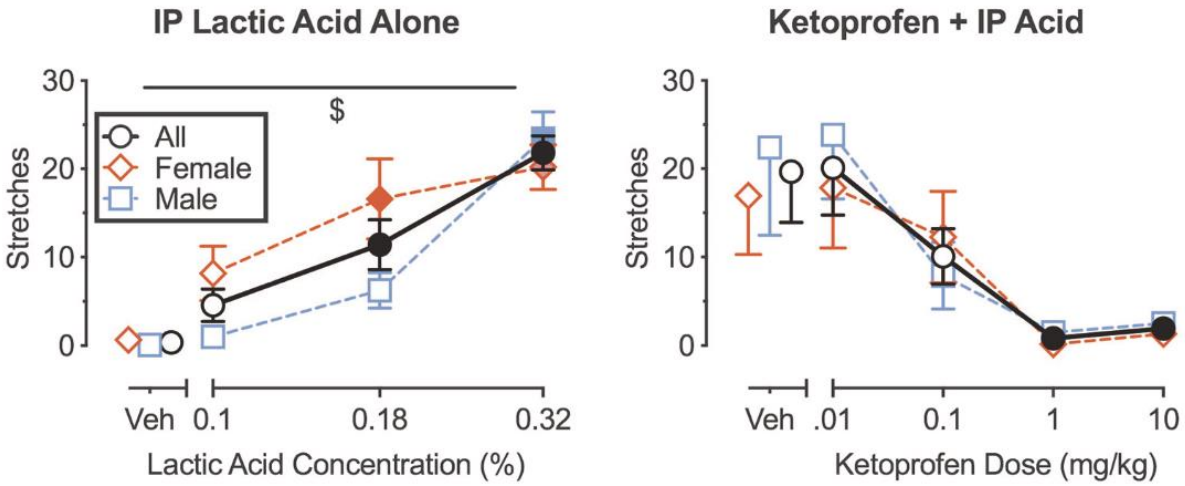

Figure II.I. Effects of IP lactic acid administered alone or after pretreatment with ketoprofen on pain-related stretching behavior in male and female mice. Abscissae: concentration of lactic acid (left panel, diluted in sterile water and administered IP in a volume of 10 ml/kg) or dose of ketoprofen (right panel, administered subcutaneously as a 30-min pretreatment to 0.32% IP acid). Veh = vehicle for IP acid (left panel) or ketoprofen before 0.32% IP acid (right panel). Ordinates: number of stretches observed during a 20-min observation period. Points show mean ± SEM for all mice (black circles, N = 12), just males (blue squares, N = 6), and just females (pink diamonds, N = 6). Filled symbols indicate significantly different from Veh as determined by one-way ANOVA and Dunnett's post hoc test for pooled data, males, or females. $ Indicates a significant sex × dose interaction as determined by two-way ANOVA, but follow-up analysis with the Holm–Sidak post hoc test did not reveal a significant effect of sex at any acid dose. The results of ANOVA and power analysis for data in each panel are shown in Table 1.

Table 1. Summary of power analysis results from one-way and two-way ANOVA of data shown in Fig. 1

Analysis		IP lactic acid alone				Ketoprofen + IP acid			
		F Statistic, *p*-value	Current effect size (Cohen's f)		Current power	Sample size for power ≥ 0.8	F statistic, *p*-value	Current effect size (Cohen's f)	Current power
Sample size for power ≥ 0.8									
From one-way ANOVA	Pooled males + females	F (2.19, 24.07) = 15.29, $p<0.0001$	1.180	0.999	6 (3M, 3F)	F = (1.31, 14.33) = 3.84, $p = 0.0147$	0.79	0.752	14 (7M, 7F)
	Males only	F (1.44, 7.18) = 43.55, $p = 0.0002$	2.951	0.999	4 (All M)	F (1.12, 5.61) = 3.07, $p = 0.1329$	0.785	0.320	15 (All M)
	Females only	F (2.09, 10.43) = 7.84, $p = 0.0079$	1.253	0.879	6 (All F)	F (1.66, 8.29) = 3.84, $p = 0.0714$	0.876	0.494	10 (All F)
From two-way ANOVA	Main effect of dose	F (2.26, 22.64) = 28.10, $p<0.0001$	1.674	1.0	5 (2–3M, 2–3F)	F (1.30, 12.97) = 6.40, $p = 0.0194$	0.80	0.713	14 (7M, 7F)
	Main effect of sex*	F (1.10) = 4.34, $p =$ 0.0639	0.383	0.225	56 (28M, 28F)	F (1,10) = 0.139, p = 0.892	0.079	0.057	>100 (>50M, >50F)
	Dose x sex interact	F (3,30) = 3.06, $p =$ 0.0430	0.553	0.657	16 (8M, 8F)	F = (4, 40) = 0.28, p = 0.8920	0.166	0.104	>100 (>50M, >50F)

For predicted "Sample Size for Power ≥0.8," numbers show the total sample size as well as the allocation to males (M) and females (F) assuming equal representation by both sexes

*To illustrate the approach using Prism 8.0 and G*Power, detailed step-by-step methods are described here for power analysis of the Main Effect of Sex for IP Acid Alone on Stretching

(1) From the two-way ANOVA table in Prism 8.0, calculate partial eta^2 from the sum of squares (SS) values for the main effect of sex (SS_{sex}) and the residual variance unaccounted for by either sex or dose ($SS_{residuals}$) as follows: [10]

$$\text{partial eta}^2 = \frac{SSsex}{SSsex + SSresiduals} = \frac{164.7}{164.7 + 1121} = 0.1281$$

(2) In G × Power select the following:

- Test family: F tests
- Statistical test: ANOVA: fixed effects, special, main effects, and interactions
- Type of power analysis: Post hoc: Compute achieved power – a given α, sample size, and effect size
- Input Parameters: Select "Determine", enter partial eta^2 from step 1 above, and select "Calculate effect size f and transfer to main window"; also enter 0.05 for "α err prob"; 12 for "total sample size"; 1 for "numerator df"; and 2 for "number of groups"
- Output Parameters: Select "Calculate" to calculate output parameters that include "Denominator df "and "Power (1−β err prob)." Select "X–Y plot for range of values" to generate a graph and associated table that relate changes in Power to changes in Total Sample Size and determine from the table the smallest sample size necessary to obtain the desired power. This study selected the sample size necessary to achieve Power≥0.8 (56 total animals)
- Report: "Effect size f" from Input Parameters (Cohen's f), "Power (1−β err prob)" from Output Parameters, and "Total Sample Size" necessary for desired power from Table

(3) To ensure all metrics were entered correctly, check that the degrees of freedom in the "Output parameters" ("Denominator df") of G*Power matches that from the ANOVA table in Prism. If they do not agree, data were not entered correctly

Chapter III: Behavioral Battery for Testing Candidate Analgesics in Mice. I. Validation with Positive and Negative Controls

(Published in Journal of Pharmacology & Experimental Therapeutics: Diester *et al.*, 2021, PMCID: PMC8058504)

Introduction

The goal of this study was to evaluate a battery of pain-stimulated, pain-depressed, and pain-independent behaviors for preclinical pharmacological assessment of candidate analgesics in ICR mice. Intraperitoneal injection of dilute lactic acid (IP acid) served as an acute visceral noxious stimulus to produce the following four pain-related behaviors: 1) stimulation of stretching, 2) stimulation of facial grimace, 3) depression of rearing, and 4) depression of nesting. Additionally, both horizontal locomotor activity and nesting were measured in the absence of the noxious stimulus to assess pain-independent drug effects. As stated in Chapter II, the study design included male and female subjects. These six behaviors were used to compare effects of two mechanistically distinct but clinically effective positive controls (ketoprofen, oxycodone) and two active negative controls that are not clinically approved as analgesics but produce either general motor depression (diazepam) or general motor stimulation (amphetamine).

Materials and Methods

Subjects

Subjects were male and female ICR mice (Harlan Laboratories, Frederick, MD) that were 6-8 weeks old upon arrival to the laboratory. Males weighed 25-45g and females weighed 20-35g throughout the study. In an AAALAC approved facility, mice were housed in cages (31.75cm

long x 23.50 cm wide x 15.25cm deep) with corncob bedding (Harlan Laboratories) and a "nestlet" composed of pressed cotton (Ancare, Bellmore, NY). All mice had ad libitum access to food (Teklad LM-485 Mouse/Rat Diet, Harlan Laboratories) and water, and cages were mounted in a RAIR HD Ventilated Rack (Lab Products, Seaford, DE) in a temperature-controlled room with a 12-hour light/dark cycle (lights on from 6:00 AM to 6:00 PM). Mice used in studies of stretching, grimace, and rearing were littermates group housed 3/cage, and mice used in nesting studies were individually housed. For group-housed mice, a cardboard tube was added to the cage environment to provide enrichment and minimize fighting. All experiments were performed during the light phase of the daily light/dark cycle beginning at least one week after arrival at the laboratory. Additionally, for singly housed mice in nesting studies, experiments were performed in their home cages at least two days after a cage change. Animal-use protocols were approved by the Virginia Commonwealth University Institutional Animal Care and Use Committee and complied with the National Research Council Guide for the Care and Use of Laboratory Animals.

Overview of Experimental Design

The goal of the study was to compare effects of two clinically effective positive-control analgesics (ketoprofen, oxycodone) and two behaviorally active negative controls (diazepam, amphetamine) on a panel of pain-stimulated, pain-depressed, and pain-independent behaviors in mice. Pain-related behaviors were elicited by intraperitoneal (IP) injection of dilute lactic acid as the noxious stimulus, and an initial study determined the potency of IP acid (0-0.32%) to produce these behaviors in two groups of mice. These two groups and all other groups described below consisted of 12 mice (6 males and 6 females) to permit exploratory analysis of sex

differences as described in Chapter II (Diester et al., 2019). One group of mice was used to evaluate IP acid-induced stimulation of abdominal stretching and facial grimace behaviors as well as IP acid-induced depression of rearing. A second group was used to evaluate IP acid-induced depression of nesting behavior. Thus, behavioral assessment focused on two pain-stimulated behaviors (stretching, grimace) and two pain-depressed behaviors (rearing, nesting). In each group, all mice received all IP acid concentrations in a within-subject repeated-measures design. The order of presentation for different acid concentrations was randomized across mice using a Latin-square design, and tests were conducted once per week in each mouse.

On the basis of this initial study, a concentration of 0.32% IP acid was used as the noxious stimulus for all subsequent studies with test drugs. Antinociception dose-effect curves for each test drug were determined in two groups of mice, one to assess drug effects on IP acid-induced changes in stretching, facial grimace, and rearing, and a second to assess drug effects on IP acid-induced depression of nesting. Effects of each test drug on pain-independent behaviors were determined in two additional groups of mice, one to assess drug effects on control nesting in the absence of the IP acid noxious stimulus, and a second to assess drug effects on locomotion in the absence of the noxious stimulus. In each group, all mice received all drug doses, and dose order was randomized across mice using a Latin-square design. Doses for each drug were varied in 0.5 or 1.0 log-unit increments across a ≥10-fold dose range with the intent of progressing from low doses that produced little or no effect to high doses that produced either significant antinociception on one or more endpoints of pain-related behavior or significant changes in nesting or locomotor activity as pain-independent behaviors. Data were analyzed to evaluate the

degree to which each test drug alleviated pain-related behaviors at doses below those that altered pain-independent behaviors.

Test drug doses, pretreatment times, and supporting references were as follows: the cyclooxygenase$_{1/2}$ inhibitor ketoprofen, 0.1-32 mg/kg, 30 min (Negus et al., 2015); the mu-opioid receptor agonist oxycodone, 0.32-10 mg/kg, 30 min (Beardsley et al., 2004); the gamma aminobutyric acid receptor A ($GABA_A$) receptor positive allosteric modulator diazepam, 1-10 mg/kg, 30 min (Rosland et al., 1987; Schwienteck et al., 2017); and the dopamine and norepinephrine transporter substrate amphetamine, 0.32-10 mg/kg, 30 min (Tyler and Tessel, 1979; Nevins et al., 1993).

Behavioral Procedures

***Stretching/Grimace/Rearing Procedure*.** Studies of stretching, grimace, and rearing were conducted in a procedure room separate from the housing room. Mice were acclimated for at least 1 hr to the procedure room at least one day before the first test day, and on all subsequent test days, mice were again acclimated to the procedure room for at least 1 hr before testing. Testing occurred once per week for each subject and was initiated by subcutaneous (SC) administration of the specified test drug dose followed by return of the mouse to its home cage for the pretreatment time specified above. Subsequently, mice received IP acid immediately before being placed into individual plexiglass cylinders (4" diameter) and filmed for 20.5 min without any researchers in the room. Videos were later scored for stretching, facial grimace, and rearing by two trained and blinded observers, and scores across the two observers were averaged. The number of stretches and rears was counted for the first 20-min of the observation period. A

stretch was defined as a horizontal extension of the abdomen followed by extension of at least one hind limb. A rear was defined as vertical extension of the mouse with both front paws off the ground followed by return of at least one front paw to the ground. Importantly, a rear was not counted when a mouse was resting on its hind legs without vertical extension (e.g. during grooming). Facial grimace was scored during the last 0.5 min of the observation period by evaluating ptosis and ear position with criteria similar to those described previously (Langford et al., 2010). Specifically, ptosis was scored on a graded scale with 0 = eyes fully open, 0.5 = eyes half to a quarter closed, and 1 = eyes fully closed. Ear position was also scored on a graded scale by reference to a line drawn following the top of the whisker line along the snout. If the center tip of the mouse's ear was above the line, it was scored as a 0, through the center of the ear was a 0.5, and below was a 1. Scores for ptosis and ear position were assigned based on observer impressions for the entire 0.5 min observation period and summed to yield a total score for each mouse, with a minimum score of 0 and maximum score of 2.

***Nesting Procedure*.** A nesting procedure described previously (Negus et al., 2015) was modified to accommodate testing in the housing room and provide a continuous quantitative dependent variable. Additionally, mice were excluded from nesting studies if they failed to nest during the initial acclimation week in the housing room (3 mice over the course of the study). On test days, which occurred once per week for each subject, mice received a SC injection with the specified test drug before being returned to their home cages on the housing rack. After the specified pre-treatment time, mice were removed from their cage and received either IP acid or vehicle. Old nesting material was removed, two 1-in^2 nestlet squares were placed 11 in apart in the center of the opposing short walls of the cage (see Supp. Figure I), and the mouse was again returned to its

home cage. After a 90-min nesting period with no researcher in the room, the cage top was removed, the position of the nestlets was photographed from above, and the distance between the center of mass for each nestlet was measured to the nearest quarter inch. For the initial study to examine the potency and time course of IP acid effects, nestlet position was also evaluated every 30 min during the 90 min nesting period (Supp. Figure I); however, for all remaining experiments, nestlet position was evaluated only at 90 min to minimize cage disturbances during the experiment. The primary dependent variable was % Maximal Nestlet Consolidation (%MNC), defined as [(11-End)/11] x 100], where 11 and End were the distances in inches between the nestlets at the start and end of the nesting period, respectively.

***Locomotor Procedure*.** Horizontal locomotor activity was assessed during 30-min sessions in 16.8 cm wide x 12.7 cm deep x 12.7 cm high boxes housed in sound-attenuating chambers (Med Associates, St. Albans, VT) and located in a procedure room separate from the housing room. Each box had black plexiglass walls, a clear plexiglass ceiling equipped with a house light, bar floors, and six photobeams arranged at 3 cm intervals across the long wall and 1 cm above the floor. Beam breaks were monitored by a microprocessor operating Med Associates software. The primary dependent variable was the total number of beam breaks, excluding consecutive interruptions of the same beam, during the 30-min session. Test sessions were conducted twice a week with at least 48 hr between sessions. On test days, mice were brought to the procedure room at least 2 hr before session onset. After SC test-drug administration, mice were returned to their home cages for the 30-min pretreatment interval, then placed into the locomotor activity boxes at session onset.

Data Analysis

Stretching, rearing, nesting, and locomotor data were treated as ratio variables and analyzed by parametric statistics, whereas facial grimace was treated as an ordinal variable and analyzed with non-parametric statistics. Data for each treatment on each endpoint were analyzed in four phases as described in Chapter II (Diester et al., 2019). As this study was designed based on power to assess treatment effects for pooled data (N=12), data for males and females were first pooled and evaluated using a repeated-measures one-way ANOVA followed by Dunnett's post hoc test for parametric data or Friedman's test followed by Dunn's post hoc for non-parametric data. Second, data were segregated by sex and evaluated by repeated-measures one-way ANOVA to assess drug effects within each sex, and as with pooled data, a significant ANOVA was followed by Dunnett's post hoc test for parametric data, whereas a significant Friedman's test was followed by Dunn's post hoc for non-parametric data. Third, male and female parametric data for a given endpoint were analyzed by two-way ANOVA to directly compare data from males and females, with sex as a between-subjects factor and IP acid concentration or drug dose as a within-subjects factor. A significant sex x treatment interaction was followed by a Holm-Sidak post hoc test. For non-parametric data, multiple t-tests with correction for multiple comparisons were used. These first three steps of data analysis were performed using GraphPad Prism (LaJolla, CA) with a criterion for significance of $p<0.05$. Lastly, results were submitted to power analyses to calculate the Cohen's f effect size, achieved power (1-β), and the total number of animals predicted as necessary to detect a significant effect given the effect size, $\alpha = 0.05$ and power (1-β) = 0.8 using the free statistical analysis program G*Power (Faul *et al.*, 2007). There is currently no consensus method for power analysis of non-parametric data so grimace data was not submitted for further power analyses in this study (Lehmann, 2006; Motulsky, 2020).

Drugs

Lactic acid (Fisher Scientific, Hampton, NH) was diluted in sterile water and administered IP. Ketoprofen was obtained as a commercially available solution (100 mg/mL; Ford Dodge, IA) and diluted in sterile saline. Oxycodone and amphetamine were provided by the National Institute on Drug Abuse Supply Program (Bethesda, MD), and were prepared in sterile saline. Diazepam was obtained as a commercially available solution (5 mg/ml, Hospira, Lake Forest, IL) and diluted in 1:4:5 ethanol, propylene glycol, and saline. All test drugs were administered SC in volumes of 0.1 to 0.9 ml.

Results

Effects of IP Lactic Acid Alone

Figure III.I shows the effects of IP injection with vehicle or increasing concentrations of lactic acid on stretching, facial grimace, rearing, and nesting behaviors. After IP vehicle, stretching and facial grimace scores were low, whereas rearing and nesting scores were high. IP acid produced concentration-dependent increases in both stretching and grimace, with significant increases for both pain-stimulated behavioral endpoints at 0.18% and 0.32% (see Table III.I for all statistical results with pooled data from both sexes). Conversely, IP acid produced concentration-dependent decreases in rearing and nestlet consolidation, with significant decreases for rears at 0.18% and 0.32% and significant decreases in nesting for all three acid concentrations. The time course of nesting behavior in 30-min intervals after vehicle or acid treatment is shown in Supplemental Figure III.I. Results of statistical analysis to examine sex as a determinant of IP acid effects are shown in Supplemental Table III.I. With these sample sizes, only stretching showed a significant

sex x dose interaction; however, further post hoc analysis showed no difference between males and females for any concentration compared to vehicle (Supp. Fig. III.II). Based on these results, a concentration of 0.32% IP acid was used for all subsequent studies with test drugs.

Overview of Data Presentation

Each test drug was evaluated for its potency and effectiveness to block each of the four IP acid-induced behaviors, and results are shown in Figures III.II-III. Additionally, each test drug was administered alone in the nesting and locomotor procedures to evaluate general behavioral effects in the absence of the IP acid noxious stimulus, and results are shown in Figure III.IV. Figure III.V compares the potencies of each test drug to significantly attenuate IP acid effects and to alter nesting and locomotor behaviors when the test drug was administered alone. An optimal test-drug profile would be significant attenuation of all IP acid-induced behaviors at doses that did not affect nesting or locomotion when the test drug was administered alone. Table I shows the results of ANOVA and power analyses for pooled data across sexes. Supplemental Tables III.I-II show results of ANOVA and power analyses for data segregated by sex. Supplemental Tables III-VII report results of statistical analysis to examine sex as a determinant of effects for each drug on each endpoint, and figures are included for selected effects when there was either a significant main effect of sex or a significant dose x sex interaction.

Effects of Ketoprofen and Oxycodone

Figure II shows the effectiveness of the COX inhibitor ketoprofen and the MOR agonist oxycodone to block IP acid-induced pain-related behaviors. Ketoprofen (0.1-10 mg/kg) significantly blocked IP acid-stimulated stretching and facial grimace, and also blocked IP acid-

induced depression of both rearing and nesting. Ketoprofen alone at doses up to 32 mg/kg had no effect on nesting or locomotion (Figure III.IV). Thus, ketoprofen blocked all IP acid-induced changes in behaviors at doses that had no effect on nesting or locomotion when ketoprofen was administered alone (Figure III.V). Table I summarizes the ANOVA and power analysis results for these pooled data. Results of statistical analysis to examine sex as a determinant of ketoprofen effects are shown in Supplemental Table III.IV. No endpoint showed a significant sex x dose interaction, and only nesting in the presence of IP acid had a significant main effect of sex (greater nesting in females; Supp. Figure III.III).

Oxycodone (0.32-3.2 mg/kg) significantly blocked IP acid-stimulated stretching at all three doses and facial grimace at 1.0 and 3.2 mg/kg. No oxycodone dose tested blocked IP acid-induced depression of rearing, and only 1.0 mg/kg significantly attenuated IP acid-depressed nesting to a mean %MNC of 42.2±10.96. Oxycodone alone significantly decreased nesting at 10 mg/kg, and significantly stimulated locomotion at 3.2 and 10 mg/kg (Figure III.IV). Thus, oxycodone decreased IP acid-stimulation of both stretching and facial grimace and attenuated acid-induced depression of nesting at doses lower than those that produced significant effects on nesting and locomotion when administered alone (Figure III.V). The ANOVA and power analysis results for these pooled data are summarized in Table III.I. Supplemental Table III.V shows the results of the statistical analyses to examine sex as a determinant for oxycodone effects. No endpoint showed a significant main effect of sex for the given sample and effect sizes, and only nesting in the absence of the noxious stimulus produced a significant sex x dose interaction; however, further post hoc analysis did not reveal an individual dose being significantly different between males and females (Supp. Figure III.IV).

Effects of Diazepam and Amphetamine

Figure III.III shows the effects of the $GABA_A$ positive allosteric modulator diazepam and the DAT/NET substrate amphetamine on IP acid-induced pain-related behaviors. The highest dose of diazepam (10 mg/kg) significantly attenuated IP acid-stimulated stretching and grimace, but diazepam did not attenuate IP acid-induced depression of either rearing or nesting; rather, 10 mg/kg diazepam exacerbated IP acid-induced depression of rearing. Diazepam administered alone significantly decreased nesting at 10 mg/kg and significantly decreased locomotion at 3.2 and 10 mg/kg (Figure III.IV). Thus, diazepam reduced IP acid-stimulated stretching and grimace only at a dose that exacerbated IP acid-induced depression of rearing and significantly decreased nesting and locomotion when administered alone (Figure III.V). ANOVA and power analysis data summarizing these results is shown in Table III.I. Results of statistical analysis to examine sex as a determinant of diazepam are shown in Supplemental Table III.VI. No endpoints in the presence of IP acid resulted in a significant sex x dose interaction or main effect of sex for the given sample and effect sizes. Diazepam alone did produce a significant main effect of sex in locomotion, but further post hoc analysis showed no individual dose to be significantly different between males and females (Supplemental Figure III.IV).

Amphetamine (0.32-3.2 mg/kg) significantly reduced IP acid-induced stimulation of both stretching and facial grimace at the highest dose tested. Additionally, 3.2 mg/kg amphetamine attenuated IP acid-induced depression of rearing and nesting. Amphetamine delivered alone (0.32-10 mg/kg) significantly decreased nesting at 10 mg/kg and significantly increased locomotion at both 3.2 and 10 mg/kg (Figure III.IV). Thus, amphetamine blocked all IP acid-induced behaviors, but only at a dose that significantly increased locomotion when administered

in the absence of the noxious stimulus (Figure III.V). Table III.I summarizes the ANOVA and power analysis results for these pooled data. Supplemental Table III.VII shows the results of the statistical analyses to examine sex as a determinant for amphetamine effects. No endpoints showed a significant sex x dose interaction or main effect of sex for the given sample and effect sizes.

Discussion

This study compared the effects of two clinically effective analgesics (ketoprofen and oxycodone) and two active negative controls (diazepam and amphetamine) on a panel of pain-stimulated, pain-depressed, and pain-independent behaviors in male and female mice. There were three main findings. First, IP acid served as an effective chemical noxious stimulus to produce a concentration-dependent stimulation of stretching and facial grimace and depression of rearing and nesting as putative pain-related behaviors. Test drugs could then be evaluated for their profiles of antinociceptive effectiveness to alleviate these IP acid effects. Second, the positive-control analgesics ketoprofen and oxycodone produced antinociception in assays of both pain-stimulated and pain-depressed outcome measures (with ketoprofen being the most effective) at doses below those that altered nesting and/or locomotion in the absence of the IP acid noxious stimulus, whereas the negative controls diazepam and amphetamine did not. These results suggest that analgesic potential of test drugs can be predicted by higher potency to alleviate pain-related stimulation and depression of behavior than to produce pain-independent motor disruption in mice. Lastly, sex differences in drug effects were not a primary focus of the present study, and few sex differences were identified; however, the inclusion of equal numbers of male and female mice permitted exploratory power analysis of sex differences that could guide future

studies designed to focus on sex as a primary variable of interest. Overall, this study outlines an experimental design and framework of results with positive and negative controls that can be used to study and interpret effects of candidate analgesic drugs.

Figures

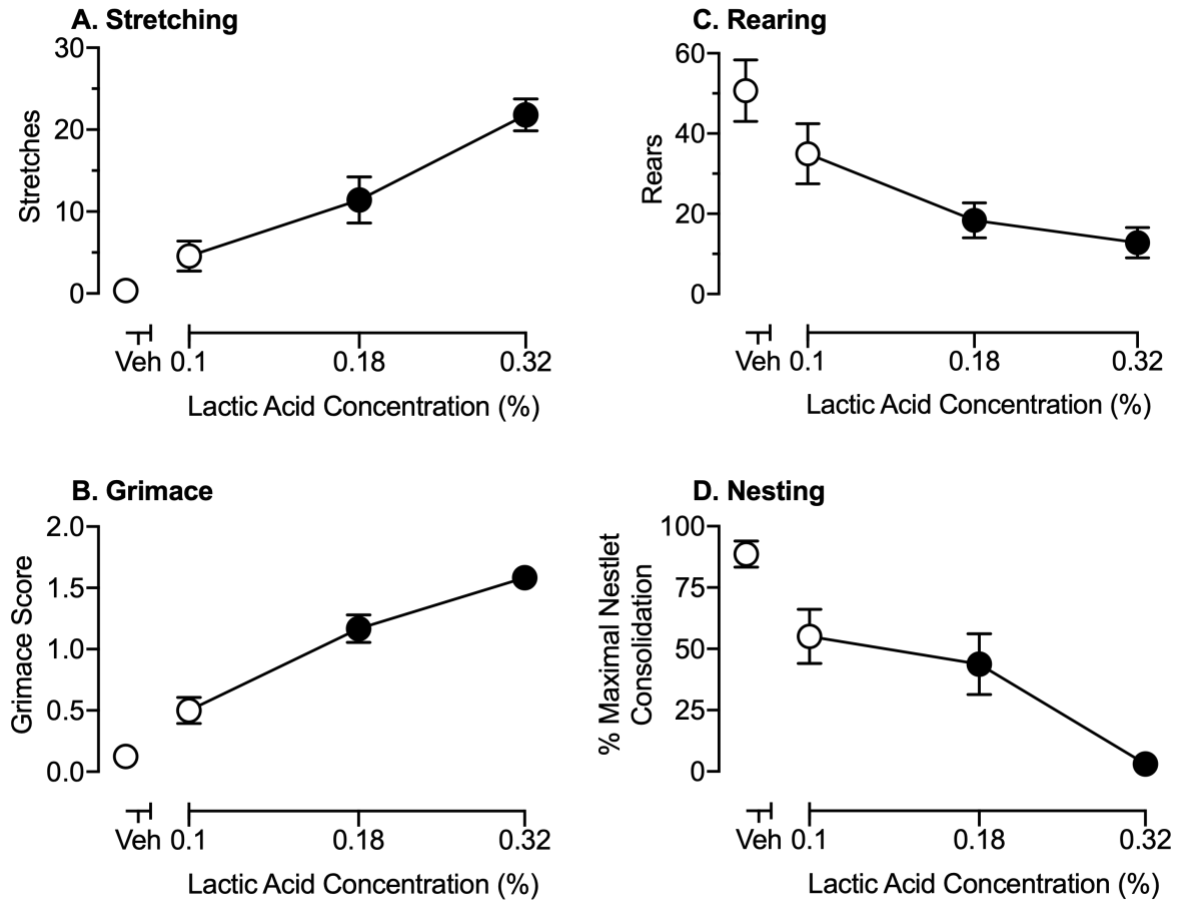

Figure III.I. Effects of intraperitoneal lactic acid (IP Acid) on stretching, facial grimace, rearing, and nesting behaviors in male and female mice. Abscissae: concentration of lactic acid diluted in sterile water and administered intraperitoneally in a volume of 10 ml/kg (log scale). Ordinates: number of stretches (A), grimace score (B), number of rears (C), and nesting expressed as percent maximum nestlet consolidation (D). Each point shows mean ± S.E.M. for 12 mice (6 males, 6 females). Filled symbols indicate a significant difference from vehicle (Veh) as determined by repeated-measures one-way ANOVA and Dunnett's post hoc test for parametric data (A, C, and D) or by Friedman's and Dunn's post hoc test for nonparametric data (B), $P \leq 0.05$. Results of ANOVA and power analysis for each panel are shown in Table III.I.

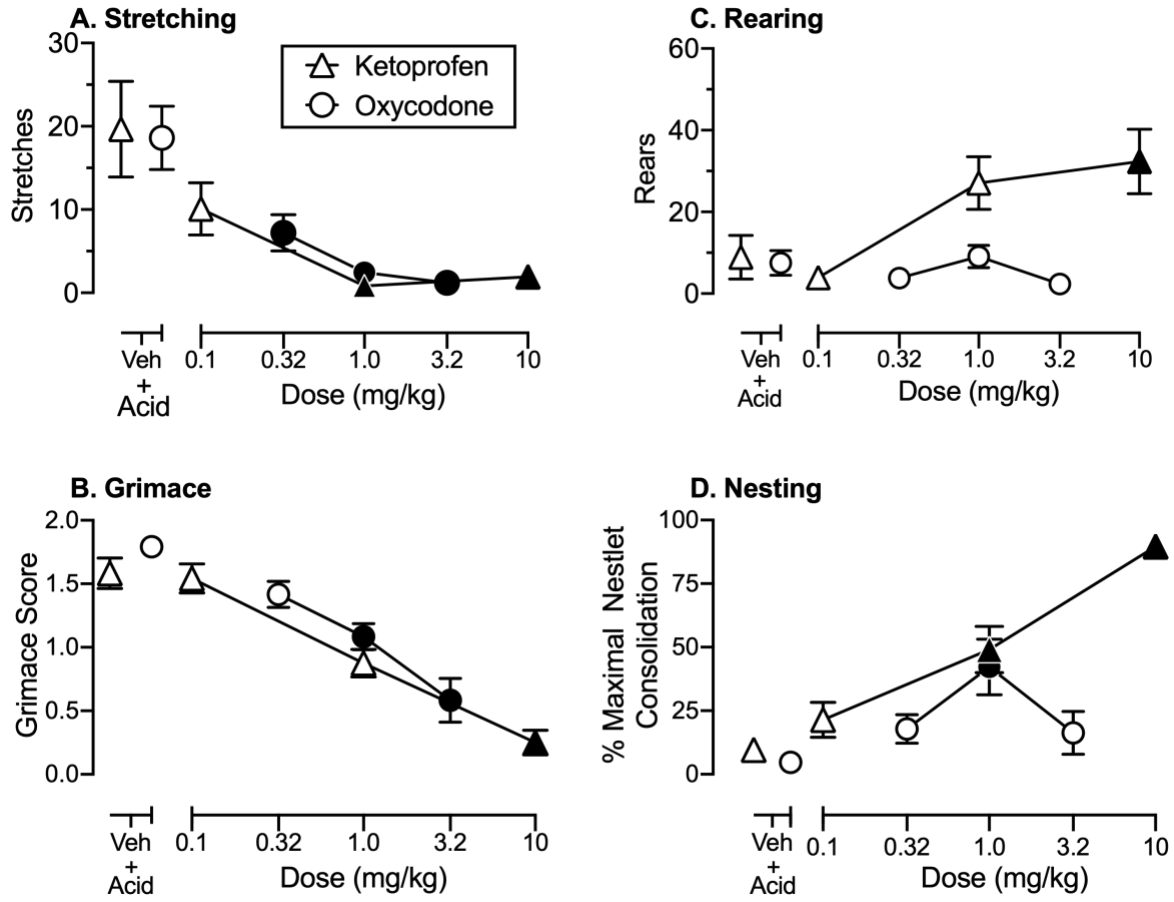

Figure III.II. Effects of the clinically-effective positive controls ketoprofen and oxycodone on IP acid-induced pain behaviors. Abscissae: doses of ketoprofen or oxycodone in mg/kg (log scale). Ordinates: number of stretches (A), grimace score (B), number of rears (C), and nesting expressed as percent maximum nestlet consolidation (D). Each point shows mean ± SEM for 12 mice (6 male, 6 female). Filled symbols indicate a significant difference from vehicle (Veh) as determined by RM one-way ANOVA and Dunnett's post hoc test for parametric data (A, C & D) or by Friedman's and Dunn's post hoc test for nonparametric data (B), $p<0.05$. Results of ANOVA and power analysis data for each panel are shown in Table III.I.

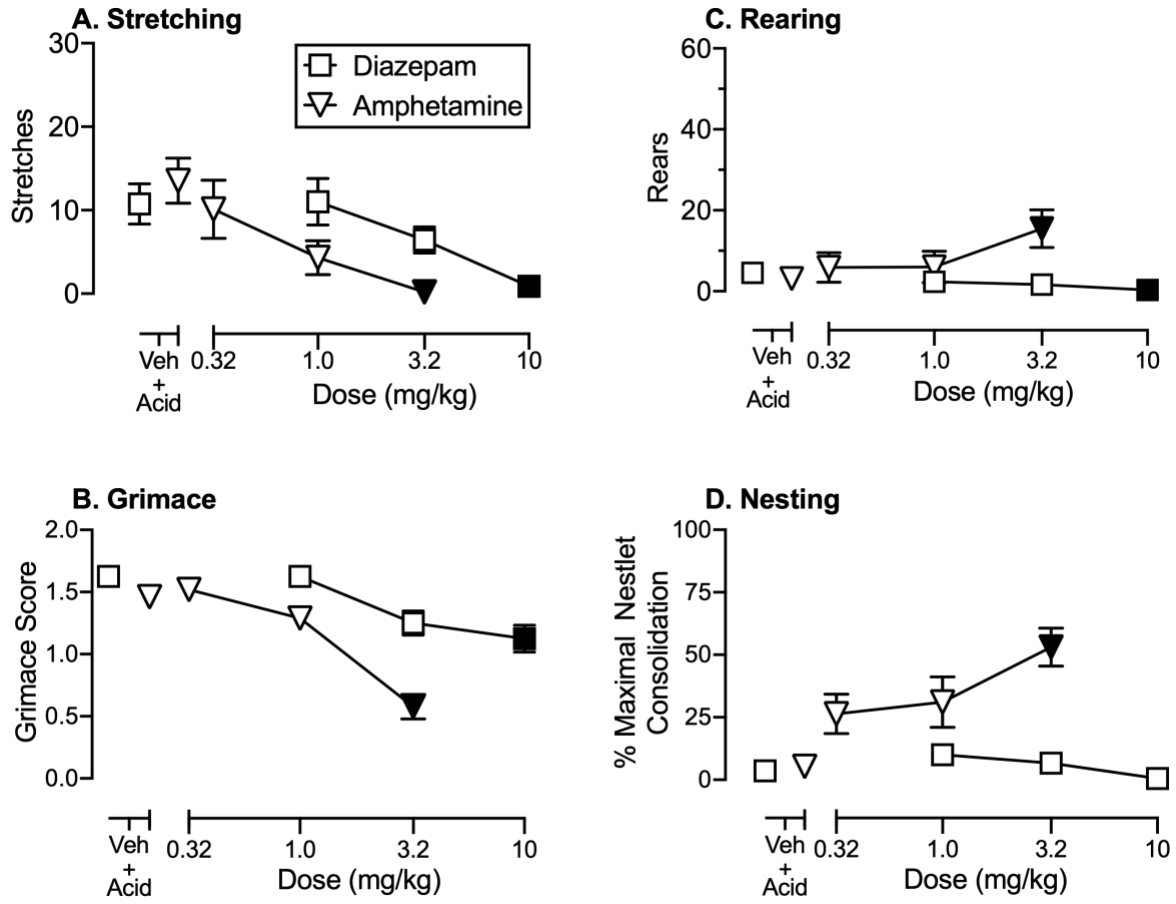

<u>Figure III.III</u>. Effects of the active negative controls diazepam and amphetamine on IP acid-induced pain behaviors. Abscissae: doses of diazepam or amphetamine delivered SC in mg/kg (log scale). Ordinates: number of stretches (A), grimace score (B), number of rears (C), and nesting expressed as percent maximum nestlet consolidation (D). Each point shows mean ± SEM for 12 mice (6 male, 6 female). Filled symbols indicate a significant difference from vehicle (Veh) as determined by RM one-way ANOVA and Dunnett's post hoc test for parametric data (A, C & D) or by Friedman's and Dunn's post hoc test for nonparametric data (B), $p<0.05$. Results of ANOVA and power analysis data for each panel are shown in Table III.I.

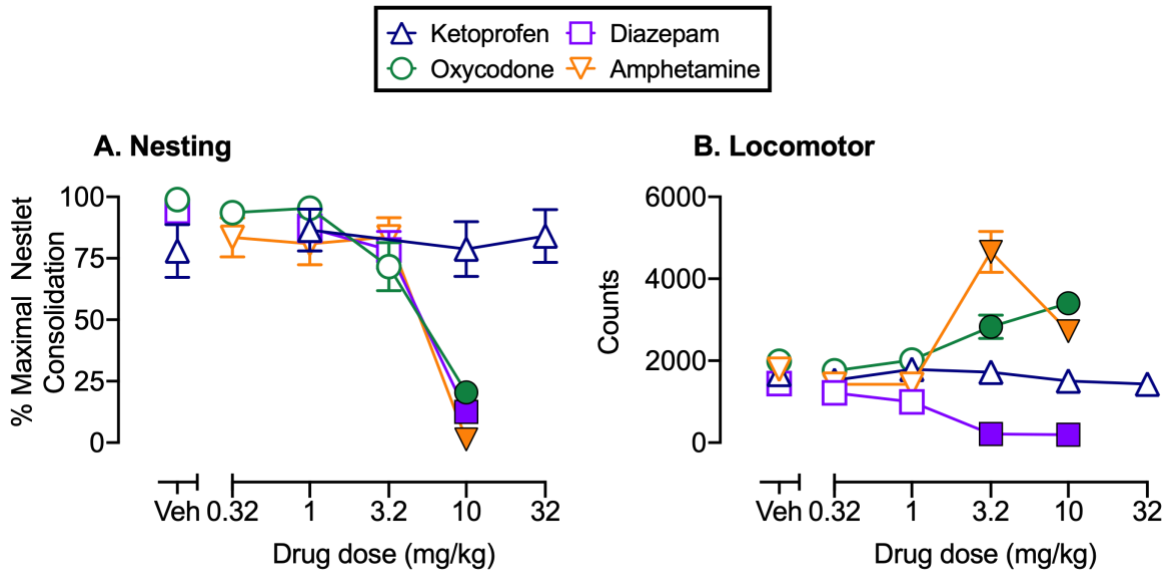

<u>Figure III.IV.</u> Effects of all drugs on nesting and locomotion in the absence of the IP acid noxious stimulus. Abscissae: Doses of ketoprofen, diazepam, oxycodone and amphetamine delivered in mg/kg (log scale). Ordinates: nesting expressed as percent maximum nestlet consolidation (A) and locomotor counts (B). Each point shows mean ± SEM for 12 mice (6 male, 6 female). Filled symbols indicate a significant difference from vehicle (Veh) as determined by RM one-way ANOVA and Dunnett's post hoc test, $p<0.05$. Results of ANOVA and power analysis data for each panel are shown in Table III.I.

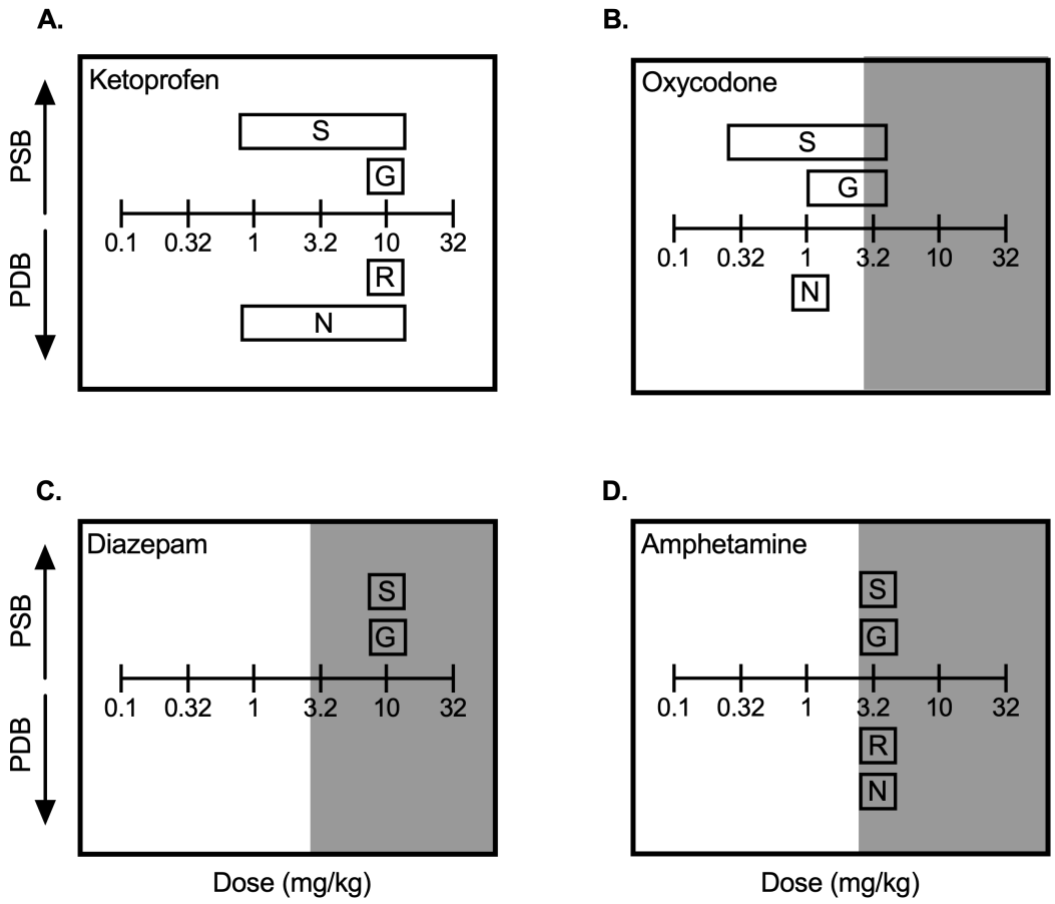

<u>Figure III.V.</u> Drug profiles for comparing potency to produce antinociceptive effects versus general behavioral disruption. Abscissae: Drug dose for either ketoprofen (A), oxycodone (B), diazepam (C) or amphetamine (D). Open bars span the dose range over which each drug significantly attenuated IP acid-induced stimulation of stretching (S) or facial grimace (G) or IP acid-induced depression of rearing (R) or nesting (N). In each panel, bars for pain-stimulated behaviors (PSB) and pain-depressed behaviors (PDB) are shown above and below the dose line, respectively. The gray zone in each panel spans doses over which each drug disrupted nesting and/or locomotion when administered alone in the absence of the IP acid noxious stimulus. Ketoprofen (A) did not alter nesting or locomotion at does up to 32 mg/kg, so no gray zone is indicated.

Table III.I: Summary of power analysis results from pooled one-way ANOVA data from Figures 1-4.

Male and Female	F Statistic, *P* Value	Current Effect Size (Cohen's f)	Current Power	Sample Size: Power ≥ 0.8	Friedman Statistic; *P* Value
IP acid					
Stretch + acid	F (2.188, 24.07) = 15.29; $P < 0.0001$*	1.180	0.999	6	—
Rear + acid	F (1.938, 21.32) = 7.251; $P = 0.0042$*	0.58	0.607	18	—
Grimace	—	—	—	—	F = 31.44; $P < 0.0001$*
Nesting + acid	F (1.888, 20.77) = 16.76; $P < 0.0001$*	1.235	0.998	6	—
Nesting	—	—	—	—	—
Locomotor	—	—	—	—	—
Ketoprofen					
Stretch + acid	F (1.578, 17.36) = 8.075; $P = 0.0052$*	0.856	0.873	11	—
Rear + acid	F (2.403, 26.43) = 6.641; $P = 0.003$*	0.52	0.576	19	—
Grimace	—	—	—	—	F = 26.78; $P < 0.0001$*
Nesting + acid	F (2.188, 24.07) = 29.17; $P < 0.0001$*	1.628	1	4	—
Nesting	F (2.628, 28.94) = 0.158; $P = 0.9037$	0.119	0.074	>100	—
Locomotor	F (2.881, 31.69) = 0.8522; $P = 0.472$	2.531	1	3	—
Oxycodone					
Stretch + acid	F (1.596, 17.55) = 17.10; $P = 0.0002$*	1.18	0.991	7	—
Rear + acid	F (2.066, 22.72) = 3.224; $P = 0.0571$	0.542	0.565	19	—
Grimace	—	—	—	—	F = 25.12; $P < 0.0001$*
Nesting + acid	F (1.634, 17.98) = 4.157; $P = 0.0396$*	0.614	0.603	18	—
Nesting	F (1.806, 19.86) = 43.87; $P < 0.0001$*	2	1	4	—
Locomotor	F (2.755, 30.3) = 15.22; $P < 0.0001$*	1.175	1	5	—
Diazepam					
Stretch + acid	F (2.307, 25.38) = 6.478; $P = 0.0039$*	0.768	0.899	10	—
Rear + acid	F (1.691, 18.6) = 4.033; $P = 0.0409$*	0.605	0.601	18	—
Grimace	—	—	—	—	F = 19.83; $P = 0.0002$*
Nesting + acid	F (2.28, 25.08) = 2.984; $P = 0.0628$	0.52	0.56	19	—
Nesting	F (2.164, 23.8) = 60.51; $P < 0.0001$*	2.343	1	3	—
Locomotor	F (2.54, 27.94) = 10.47; $P = 0.0002$*	0.976	0.992	7	—
Amphetamine					
Stretch + acid	F (2.201, 26.41) = 6.822; $P = 0.0033$*	0.755	0.907	11	—
Rear + acid	F (2.44, 29.28) = 3.131; $P = 0.0496$*	0.511	61	19	—
Grimace	—	—	—	—	F = 25.37; $P < 0.0001$*
Nesting + acid	F (2.041, 22.45) = 5.594; $P = 0.0103$*	0.713	0.81	12	—
Nesting	F (2.641, 29.05) = 36.46; $P < 0.0001$*	1.819	1	4	—
Locomotor	F (1.704, 18.74) = 22.07; $P < 0.0001$*	1.415	1	6	—

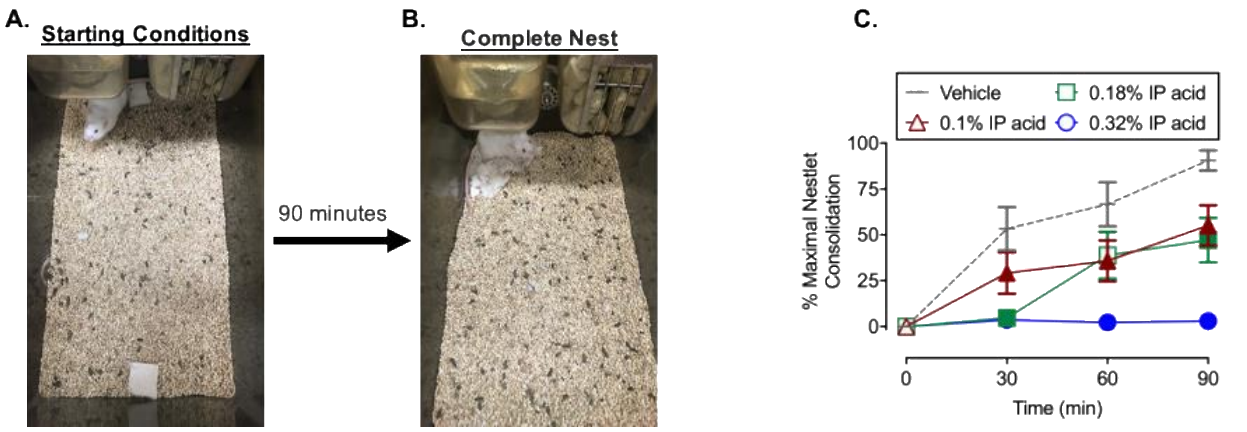

Supplemental Figure III.I. Time course data for nestlet consolidation behavior. Panel A shows a photograph of the starting configuration for each experiment, and panel B shows an example of a complete nest, with a "% Maximal Nestlet Consolidation" (%MNC) of 0% for panel A and 100% for panel B. Panel C shows the time course of nestlet consolidation after vehicle or increasing concentrations of IP lactic acid, with abscissa as time in minutes and the ordinate as %MNC. Each point represents mean ± SEM for 12 mice (6 male, 6 female). Filled symbols indicate a significant difference from vehicle as determined by RM two-way ANOVA and Dunnett's post hoc test, $p<0.05$. For vehicle data, an additional RM one-way ANOVA and Dunnett's post hoc test was performed, with 30 min, 60 min and 90 min being significantly different from 0 min.

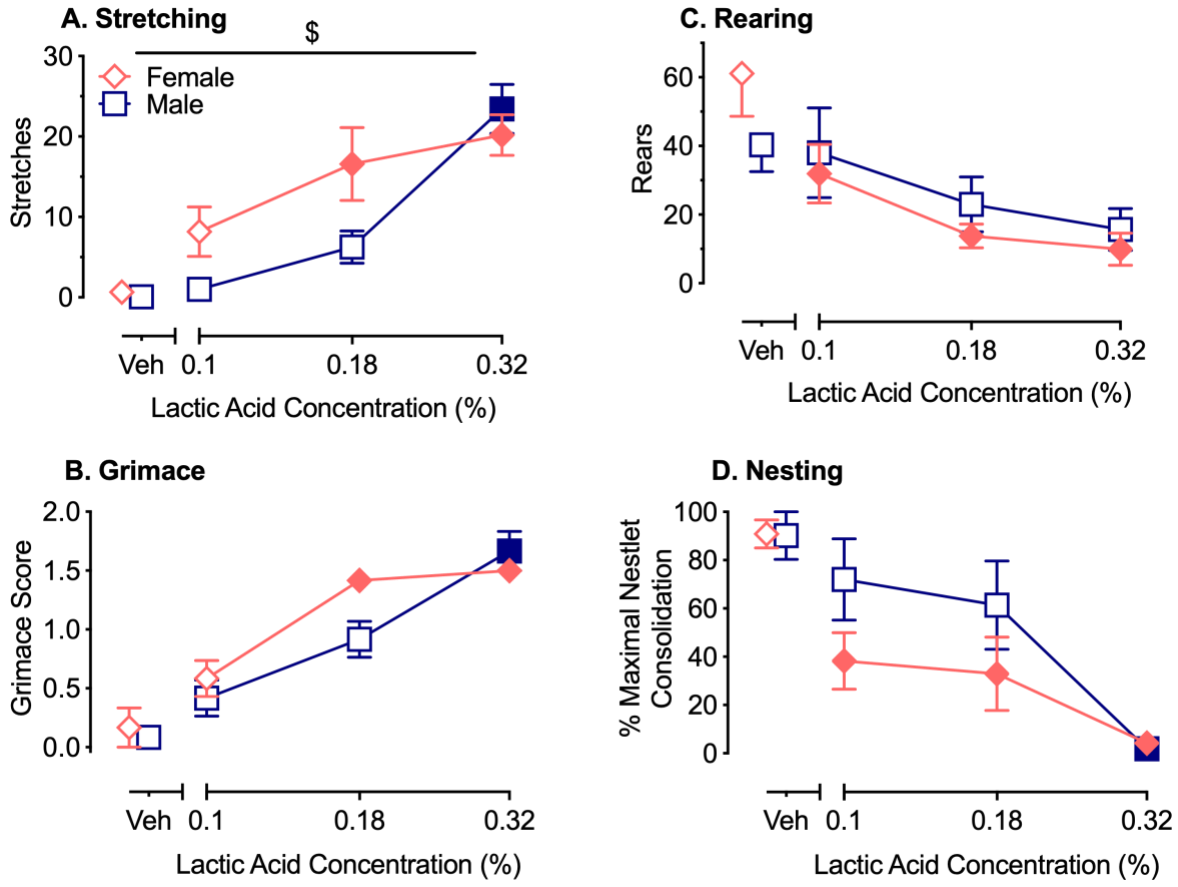

<u>Supplemental Figure III.II.</u> Effects of IP lactic acid on stretching, facial grimace, rearing and nesting behaviors in male and female mice. Abscissae: concentration of lactic acid diluted in sterile water and administered IP in a volume of 10 ml/kg. Ordinates: number of stretches (A), grimace score (B), number of rears (C), and nesting expressed as percent maximum nestlet consolidation (D). All points represent the mean ± SEM for either 6 males (blue) or 6 females (pink). Filled symbols indicate a significant difference from vehicle (Veh) as determined by RM one-way ANOVA and Dunnett's post hoc test for parametric data (A, C & D) or by Friedman's and Dunn's post hoc test for nonparametric data (B), $p<0.05$. $ Indicates a significant sex x dose interaction as determined by 2-way ANOVA and Holm-Sidak post hoc test of data segregated by

sex. Results of ANOVA and power analysis data for each panel are shown in Table III.I. Statistical results for the 2-way ANOVA (parametric) or multiple t-test (non-parametric) data are as follows. (A) Significant main effect of acid dose [$F(2.264, 22.64)=28.10$; $p<0.0001$], but no main effect of sex. Significant sex x dose interaction [$F(3,30)=3.059$; $p=0.043$], but post hoc analysis did not reveal a significant effect of sex at any dose. (B) Significant main effect of dose [$F(2.361, 23.61)=14.28$; $p=<0.0001$], but no significant main effect of sex or sex x dose interaction. (C) No significant difference for any lactic acid concentration between males and females. (D) Significant main effect of dose [$F(1.655, 16.55)=16.90$; $p=0.0002$], but no main effect of sex or sex x dose interaction. Results of ANOVA and power analyses are shown in Supp. Tables III.I-III.

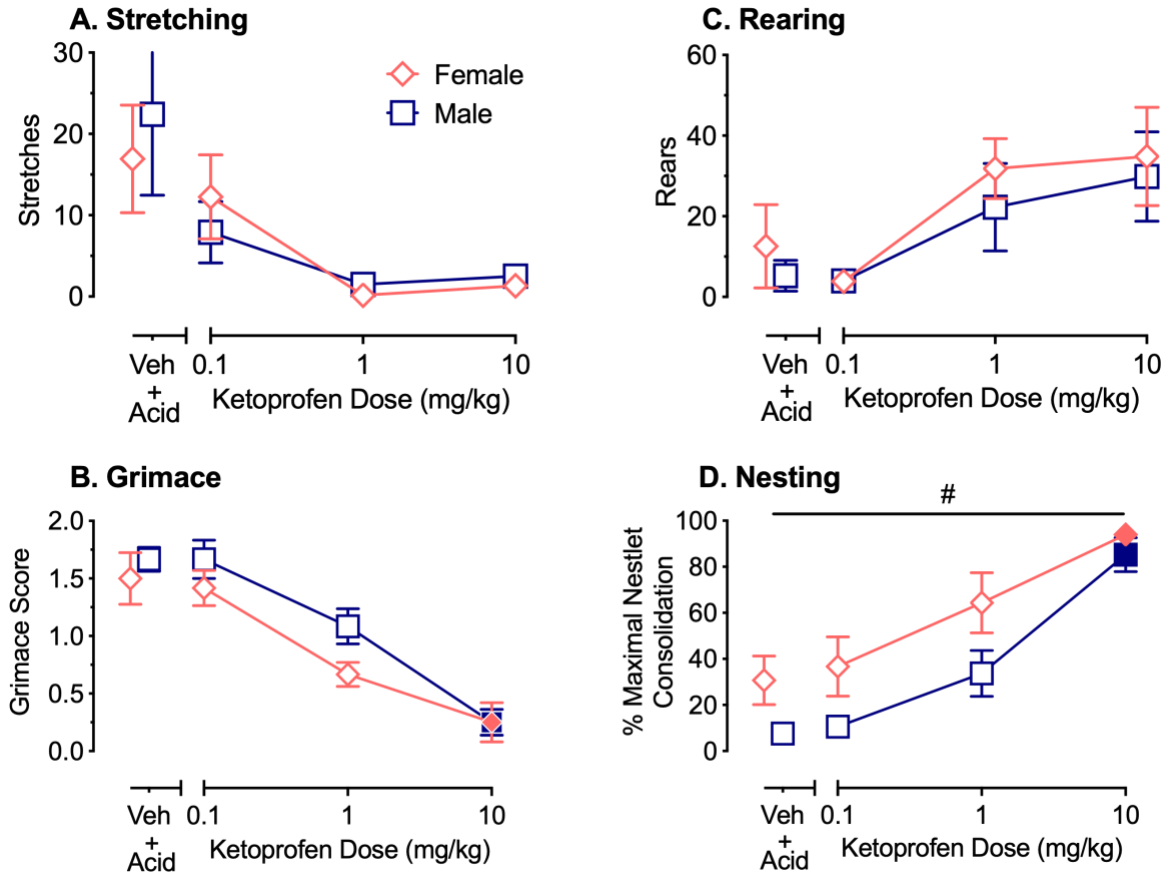

<u>Supplemental Figure III.III.</u> Effects of the clinically-effective positive control ketoprofen on IP acid-induced pain behaviors. Abscissae: doses of ketoprofen delivered SC in a volume of 10 ml/kg. Ordinates: number of stretches (A), grimace score (B), number of rears (C), and nesting expressed as percent maximum nestlet consolidation (D). All points represent the mean ± SEM for either 6 males (blue) or 6 females (pink). Filled symbols indicate a significant difference from vehicle (Veh) as determined by RM one-way ANOVA and Dunnett's post hoc test for parametric data (A, C & D) or by Friedman's and Dunn's post hoc test for nonparametric data (B), $p<0.05$. # Indicates a significant main effect of sex as determined by 2-way ANOVA and Holm-Sidak post hoc test for parametric data segregated by sex. Nonparametric data (B) were assessed for sex differences by multiple t tests using the Holm-Sidak method to correction for

multiple comparisons. Statistical results for the 2-way ANOVA (parametric) or multiple t-test (non-parametric) data are as follows. (A) Significant main effect of dose [$F(1.555, 15.55)=7.64$; $p=0.0075$], but no significant main effect of sex or sex x dose interaction. (B) Significant main effect of dose [$F(2.344, 23.44)=6.151$; $p=0.0052$], but no significant main effect of sex or sex x dose interaction. (C) No significant differences between males and females for any ketoprofen dose. (D) Significant main effect of dose [$F(2.089, 20.89)=28.13$; $p<0.0001$] and significant main effect of sex [$F(1, 10)=9.565$; $p=0.0114$] with data collapsed across dose showing F>M effect [Welch's two-tailed t-test, $p=0.0140$], but no significant sex x dose interaction. Results of ANOVA and power analysis data for each panel are shown in Supp. Tables III.I, II, & IV.

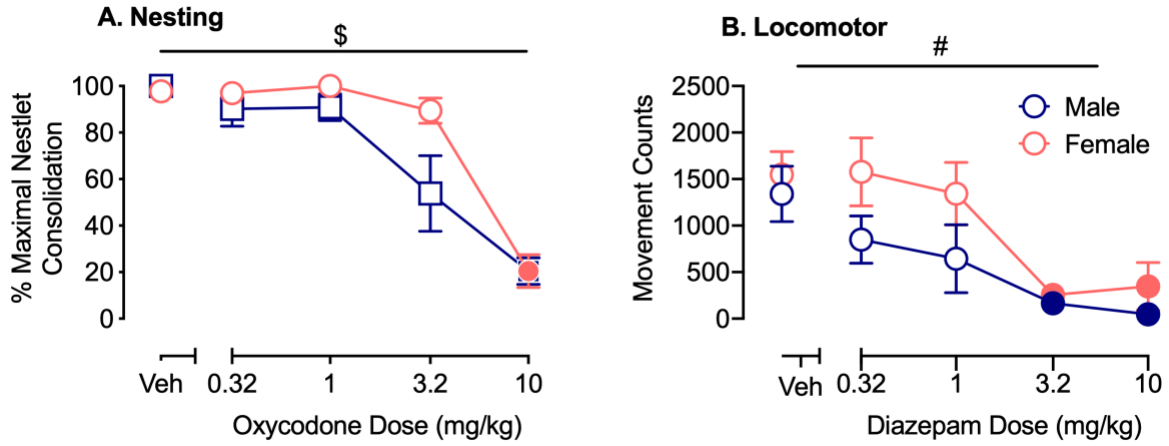

<u>Supplemental Figure III.IV.</u> Effects of oxycodone and diazepam on nesting and locomotion in the absence of the noxious stimulus. Abscissae: doses of oxycodone (A) or diazepam (B) delivered SC in a volume of 10 ml/kg. Ordinates: nesting expressed as percent maximum nestlet consolidation (A) and locomotor counts (B). All points represent the mean ± SEM for either 6 male (blue) or 6 female (pink). Filled symbols indicate a significant difference from vehicle (Veh) as determined by RM one-way ANOVA and Dunnett's post hoc test, $p<0.05$. # Indicates a significant main effect of sex and $ indicates a significant sex x dose interaction as determined by 2-way ANOVA and Holm-Sidak post hoc test for parametric data segregated by sex. Statistical results for the 2-way ANOVA data are as follows. (A) Significant main effect of dose [$F(2.009, 20.09)=50.61$; $p<0.0001$] and sex x dose interaction [$F(4,40)=2.690$; $p=0.0447$] with further post hoc analysis showing no individual dose as significantly different between males and females, and no significant main effect of sex. (B) Significant main effect of dose [$F(2.532, 25.32)=10.13$; $p=0.0003$] and main effect of sex [$F(1, 10)=5.608$; $p=0.0394$] with data collapsed across sex showing a significant F>M effect [Welch's two-tailed t-test, $p=0.0395$], but no significant sex x dose interaction. Results of 1-way ANOVA and power analyses can be found in

Supp. Tables III.I & II, and results of 2-way ANOVA and power analyses can be found in Supp. Table III.V (oxycodone) and Supp. Table III.VI (diazepam).

Supplemental Tables

Supplemental Tables show one-way ANOVA results and power analyses for each drug in males (Table III.I) and females (Table III.II) and two-way ANOVA results and power analyses for each drug with sex included as a variable (Tables III.III-VII). Note that grimace was scored as a nonparametric variable, and as a result, grimace data were not submitted to ANOVA or power analyses. rather, grimace data were evaluated by multiple t-tests with corrections for multiple comparisons using the Friedman statistic.

Supplemental Table III.I

Supplemental Table 1. Summary of power analysis results from male one-way ANOVA data from Figures 1-4

Male	F Statistic, p value	Current Effect Size (Cohen's f)	Current Power	Sample Size: Power≥ 0.8	Friedman statistic; p value
			IP Acid		
Stretch + Acid	F(1.435, 7.175)=43.55; p=0.0002*	2.951	0.99	4	-
Rear + Acid	F(1.746, 8.732)=3.935; p=0.0644	0.449	0.167	29	-
Grimace	-	-	-	-	F=16.25; p<0.0001*
Nesting + Acid	F(1.498, 7.491)=7.253; p=0.022*	1.205	0.735	7	-
Nesting	-	-	-	-	-
Locomotor	-	-	-	-	-
			Ketoprofen		
Stretch + Acid	F(1.244, 6.22)=3.31; p=0.114	0.813	0.363	13	-
Rear + Acid	F(2.131, 10.66_=2.614; p=0.1171	0.509	0.227	21	-
Grimace	-	-	-	-	F=14.37; p=0.0002*
Nesting + Acid	F(1.385, 6.924)=30.18; p=0.0006*	2.458	0.999	4	-
Nesting	F(1.861, 9.303)=0.7242; p=0.5006	0.381	0.136	38	-
Locomotor	F(3.309, 16.55)=0.9731; p=0.4358	0.441	0.226	20	-
			Oxycodone		
Stretch + Acid	F(1.143, 5.714)=8.013; p=0.0295*	1.267	0.675	8	-
Rear + Acid	F(1.825, 9.125)=1.905; p=0.2041	0.617	0.288	16	-
Grimace	-	-	-	-	F=10.86; p=0.0052*
Nesting + Acid	F(1.487, 7.434)=1.977; p=0.2048	0.628	0.263	18	-
Nesting	F(1.695, 8.475)=17.2; p=0.0013*	1.856	0.989	4	-
Locomotor	F(1.759, 8.796)=14.23; p=0.0021*	1.687	0.976	5	-
			Diazepam		
Stretch + Acid	F(2.148, 10.74)=2.668; p=0.1122	0.731	0.43	11	-
Rear + Acid	F(1.868, 9.340)=1.68; p=0.2377	0.579	0.262	18	-
Grimace	-	-	-	-	F=12.00; p=0.0035*
Nesting + Acid	F(1.746, 8.728)=2.229; p=0.1674	0.667	0.321	15	-
Nesting	F(1.303, 6.515)=36.03; p=0.0005*	2.683	1	4	-
Locomotor	F(2.012, 10.06)=4.959; p=0.0316*	0.996	0.676	8	-
			Amphetamine		
Stretch + Acid	F(2.057, 12.34)=6.621; p=0.0107*	1.05	0.833	7	-
Rear + Acid	F(1.754, 10.52)=0.5711; p=0.5599	0.308	0.118	59	-
Grimace	-	-	-	-	F=14.26; p=0.0026*
Nesting + Acid	F(1.416, 7.079)=3.96; p=0.0787	0.89	0.458	11	-
Nesting	F(1.58, 7.9)=31.93; p=0.0002*	2.53	1	4	-
Locomotor	F(1.304, 6.518)=8.839; p=0.0188*	1.33	0.766	7	-

Supplemental Table III.II

Supplemental Table 2. Summary of power analysis results from female one-way ANOVA data from Figures 1-4

Female	F Statistic, p value	Current Effect Size (Cohen's f)	Current Power	Sample Size: Power≥ 0.8	Friedman statistic; p value
	IP Acid				
Stretch + Acid	F(2.086, 10.43)=7.84; p=0.0079*	1.253	0.879	6	-
Rear + Acid	F(1.602, 8.01)=11.71; p=0.0054*	0.745	0.368	13	-
Grimace	-	-	-	-	F=15.79; p<0.0001*
Nesting + Acid	F(1.94, 9.7)=12.36; p=0.0022*	1.57	0.969	5	-
Nesting	-	-	-	-	-
Locomotor	-	-	-	-	-
	Ketoprofen				
Stretch + Acid	F(1.227, 6.134)=5.717; p=0.049*	1.07	0.558	9	-
Rear + Acid	F(2.234, 11.17)=3.673; p=0.0558	0.548	0.265	18	-
Grimace	-	-	-	-	F=12.68; p=0.0012*
Nesting + Acid	F(2.252, 11.26)=7.963; p=0.0060*	1.26	0.903	5	-
Nesting	F(1.885, 9.427)=0.6267; p=0.5463	0.353	0.124	43	-
Locomotor	F(2.131, 10.65)=0.3154; p=0.749	0.25	0.089	76	-
	Oxycodone				
Stretch + Acid	F(1.515, 7.574)=7.773; p=0.0183*	0.245	0.767	7	-
Rear + Acid	F(1.93, 9.649)=1.849; p=0.2093	0.608	0.291	16	-
Grimace	-	-	-	-	F=14.88; p<0.0001*
Nesting + Acid	F(1.525, 7.625)=2.187; p=0.18	0.661	0.29	16	-
Nesting	F(1.745, 8.723)=56.58; p<0.0001*	3.369	1	3	-
Locomotor	F(2.512, 12.56)=4.063; p=0.0366*	0.901	0.665	8	-
	Diazepam				
Stretch + Acid	F(2.188, 10.94)=3.728; p=0.0553	0.863	0.575	9	-
Rear + Acid	F(1.375, 6.873)=2.654; p=0.1458	0.731	0.323	15	-
Grimace	-	-	-	-	F=11.00; p=0.0026*
Nesting + Acid	F(1.448, 7.239)=1.048; p=0.3722	0.157	0.157	31	-
Nesting	F(2.343, 11.72)=24.26; p<0.0001	2.202	1	3	-
Locomotor	F(2.368, 11.84)=5.701; p=0.0154*	1.068	0.798	7	-
	Amphetamine				
Stretch + Acid	F(1.366, 6.83)=11.05; p=0.0101*	1.488	0.867	6	-
Rear + Acid	F(1.113, 5.564)=7.624; p=0.0338*	0.124	0.643	8	-
Grimace	-	-	-	-	F=11.40; p=0.0036*
Nesting + Acid	F(2.069, 10.35)=1.972; p=0.1876	0.327	0.327	15	-
Nesting	F(1.58, 7.9)=31.93; p=0.0002*	2.53	1	4	-
Locomotor	F(1.774, 8.87)=12.36; p=0.0032*	1.572	0.957	5	-

Supplemental Table III.III

Supplemental Table 3. Summary of power analysis results from two-way ANOVA data from Figures 1-4				
	IP Acid			
Main Effect of Dose	F Statistic, p value	Current Effect Size (Cohen's f)	Current Power	Sample Size: Power≥ 0.8
Stretch + Acid	F(2.264, 22.64)=28.10; p<0.0001*	1.674	1	5
Rear + Acid	F(2.361, 23.61)=14.28; p=<0.0001*	1.195	0.999	7
Grimace	-	-	-	-
Nesting + Acid	F(1.655, 16.55)=16.90; p=0.0002*	1.299	1	4
Nesting	-	-	-	-
Locomotor	-	-	-	-
Main Effect of Sex	F Statistic, p value	Current Effect Size (Cohen's f)	Current Power	Sample Size: Power≥ 0.8
Stretch + Acid	F(1,10)=4.337; p=0.0639	0.383	0.225	56
Rear + Acid	F(1,10)=7.98^-5; p=0.993	0.0033	0.05	>100
Grimace	-	-	-	-
Nesting + Acid	F(1, 10)=2.764; p=0.4942	0.297	0.154	92
Nesting	-	-	-	-
Locomotor	-	-	-	-
Dose x Sex Interaction	F Statistic, p value	Current Effect Size (Cohen's f)	Current Power	Sample Size: Power≥ 0.8
Stretch + Acid	F(3,30)=3.059; p=0.043*	0.553	0.657	16
Rear + Acid	F(3,30)=2.4; p=0.0901	0.487	0.538	19
Grimace	-	-	-	-
Nesting + Acid	F(3, 30)=1.086; p=0.37	0.33	0.719	14
Nesting	-	-	-	-
Locomotor	-	-	-	-

Supplemental Table III.IV

Supplemental Table 4. Summary of power analysis results from two-way ANOVA data from Figures 1-4				
	Ketoprofen			
Main Effect of Dose	F Statistic, p value	Current Effect Size (Cohen's f)	Current Power	Sample Size: Power≥ 0.8
Stretch + Acid	F(1.555, 15.55)=7.64; p=0.0075*	0.874	0.844	12
Rear + Acid	F(2.344, 23.44)=6.151; p=0.0052*	0.785	0.881	11
Nesting + Acid	F(2.089, 20.89)=28.13; p<0.0001*	1.677	1	4
Nesting	F(2.518, 25.18)=0.3046; p=0.7877	0.551	0.986	7
Locomotor	F(2.972, 29.72)=0.8099; p=0.4975	0.285	0.527	21
Main Effect of Sex	F Statistic, p value	Current Effect Size (Cohen's f)	Current Power	Sample Size: Power≥ 0.8
Stretch + Acid	F(1,10)=0.051; p=0.8266	0.053	0.053	>100
Rear + Acid	F(1,10)=0.5569; p=0.4727	0.184	0.089	>100
Nesting + Acid	F(1, 10)=9.565; p=0.0114*	0.664	0.547	20
Nesting	F(1, 10)=0.7676; p=0.4015	0.138	0.072	>100
Locomotor	F(1, 10)=0.1317; p=0.7242	0.097	0.061	>100
Dose x Sex Interaction	F Statistic, p value	Current Effect Size (Cohen's f)	Current Power	Sample Size: Power≥ 0.8
Stretch + Acid	F(3,30)=0.4075; p=0.749	0.202	0.121	94
Rear + Acid	F(3,30)=0.1885; p=0.9034	0.139	0.082	>100
Nesting + Acid	F(3, 30)=0.6074; p=0.6154	0.247	0.451	24
Nesting	F(3, 30)=0.8008; p=0.5032	0.283	0.572	19
Locomotor	F(5, 50)=0.4545; p=0.808	0.212	0.42	25

Supplemental Table III.V

Supplemental Table 5. Summary of power analysis results from two-way ANOVA data from Figures 1-4				
	Oxycodone			
Main Effect of Dose	F Statistic, p value	Current Effect Size (Cohen's f)	Current Power	Sample Size: Power≥ 0.8
Stretch + Acid	F(1.703, 17.03)=11.10; p=0.0012*	1.053	1	5
Rear + Acid	F(2.215, 22.15)=2.194; p=0.1310	0.469	0.909	10
Nesting + Acid	F(1.556, 15.56)=3.909; p=0.0509	0.6252	0.97	8
Nesting	F(2.009, 20.09)=50.61; p<0.0001*	2.25	1	<3
Locomotor	F(2.623, 26.23)=15.03; p<0.0001*	1.226	1	4
Main Effect of Sex	F Statistic, p value	Current Effect Size (Cohen's f)	Current Power	Sample Size: Power≥ 0.8
Stretch + Acid	F(1,10)=0.4191; p=0.5320	0.132	0.07	>100
Rear + Acid	F(1,10)=2.704; p=0.1311	0.3168	0.169	81
Nesting + Acid	F(1, 10)=4.764; p=0.0541	0.295	0.153	93
Nesting	F(1, 10)=3.525; p=0.0899	0.377	0.22	58
Locomotor	F(1, 10)=2.829; p=0.1235	0.395	0.236	53
Dose x Sex Interaction	F Statistic, p value	Current Effect Size (Cohen's f)	Current Power	Sample Size: Power≥ 0.8
Stretch + Acid	F(3,30)=0.1605; p=0.9220	0.127	0.142	87
Rear + Acid	F(3,30)=0.4788; p=0.6994	0.219	0.362	30
Nesting + Acid	F(3, 30)=0.3449; p=0.7931	0.186	0.267	41
Nesting	F(4, 40)=2.69; p=0.0447*	0.519	0.996	6
Locomotor	F(4, 40)=0.8627; p=0.4946	0.293	0.672	16

Supplemental Table III.VI

Supplemental Table 6. Summary of power analysis results from two-way ANOVA data from Figures 1-4				
	Diazepam			
Main Effect of Dose	F Statistic, p value	Current Effect Size (Cohen's f)	Current Power	Sample Size: Power≥ 0.8
Stretch + Acid	F(2.305,23.05)=5.979; p=0.0062*	0.773	1	5
Rear + Acid	F(1.726,17.26)=3.896; p=0.0454*	0.624	0.979	8
Nesting + Acid	F(2.284, 22.84)=2.859; p=0.0719	0.534	0.97	8
Nesting	F(2.025, 20.25)=58.87; p<0.0001*	2.43	1	<3
Locomotor	F(2.532, 25.32)=10.13; p=0.0003*	1.226	1	4
Main Effect of Sex	F Statistic, p value	Current Effect Size (Cohen's f)	Current Power	Sample Size: Power≥ 0.8
Stretch + Acid	F(1,10)=0.0307; p=0.8645	0.041	0.052	>100
Rear + Acid	F(1,10)=0.3356; p=0.5752	0.134	0.07	>100
Nesting + Acid	F(1,10)=0.2021; p=0.6626	0.074	0.056	>100
Nesting	F(1, 10)=2.945e-015; p>0.9999	Cannot compute	Cannot compute	Cannot compute
Locomotor	F(1, 10)=5.608; p=0.0394	0.393	0.235	53
Dose x Sex Interaction	F Statistic, p value	Current Effect Size (Cohen's f)	Current Power	Sample Size: Power≥ 0.8
Stretch + Acid	F(3,30)=0.1533; p=0.9268	0.123	0.137	91
Rear + Acid	F(3,30)=0.6254; p0.6042	0.25	0.143	24
Nesting + Acid	F(3, 30)=0.5411; p=0.6579	0.233	0.405	27
Nesting	F(3, 30)=0.7015; p=0.5586	0.265	0.512	21
Locomotor	F(4, 40)=0.6448; p=0.6338	0.078	0.085	>100

Supplemental Table III.VII

Supplemental Table 7. Summary of power analysis results from two-way ANOVA data from Figures 1-4				
	Amphetamine			
Main Effect of Dose	F Statistic, p value	Current Effect Size (Cohen's f)	Current Power	Sample Size: Power≥ 0.8
Stretch + Acid	F(2.041, 22.45)=8.319; p=0.0019*	0.870	1	5
Rear + Acid	F(2.396, 26.36)=3.646; p=0.0331*	0.576	0.994	7
Nesting + Acid	F(2.046, 20.46)=5.158; p=0.0149*	0.682	0.997	6
Nesting	F(2.698, 28.98)=37.33; p<0.0001*	1.932	1	<3
Locomotor	F(1.659, 16.59)=20.42; p<0.0001*	1.428	1	4
Main Effect of Sex	F Statistic, p value	Current Effect Size (Cohen's f)	Current Power	Sample Size: Power≥ 0.8
Stretch + Acid	F(1,11)=4.626; p=0.0546	0.422	0.285	46
Rear + Acid	F(1,11)=0.0625; p=0.8072	0.048	0.053	>100
Nesting + Acid	F(1, 10)=0.8445; p=0.3797	0.0904	0.059	>100
Nesting	F(1, 10)=0.1146; p=0.742	0.062	0.054	>100
Locomotor	F(1, 10)=4.242; p=0.0664	0.303	0.458	88
Dose x Sex Interaction	F Statistic, p value	Current Effect Size (Cohen's f)	Current Power	Sample Size: Power≥ 0.8
Stretch + Acid	F(3, 33)=2.120; p=0.1164	0.439	0.957	9
Rear + Acid	F(3, 33)=1.846; p=0.1580	0.41	0.726	10
Nesting + Acid	F(3, 30)=0.1433; p=0.9332	0.119	0.13	98
Nesting	F(4, 40)=1.262; p=0.3010	0.355	0.851	11
Locomotor	F(4, 40)=0.1765; p=0.9492	0.132	0.161	71

Chapter IV: Behavioral Battery for Testing Candidate Analgesics in Mice. II. Effects of Endocannabinoid Catabolic Enzyme Inhibitors and Δ9-Tetrahydrocannabinol

(Published in Journal of Pharmacology & Experimental Therapeutics: Diester *et al.*, 2021, PMCID: PMC8058502)

Introduction

Enhanced signaling of the endocannabinoid (eCB) system through inhibition of the main eCB catabolic enzymes monoacylglycerol lipase (MAGL) and fatty acid amide hydrolase (FAAH) has received increasing interest for development of candidate analgesics. This study compared the effects of monoacylglycerol lipase (MAGL) and fatty acid amide hydrolase (FAAH) inhibitors with effects of the exogenous cannabinoid 1&2 receptor ($CB_{1/2}R$) agonist Δ9-tetrahydrocannabinol (THC) using the behavioral battery validated in Chapter III. The following spectrum of six eCB catabolic enzyme inhibitors were evaluated: the MAGL-selective inhibitors MJN110 and JZL184, the dual MAGL/FAAH inhibitors JZL195 and SA57, and the FAAH-selective inhibitors URB597 and PF3845. The selectivity of these test compounds for inhibition of MAGL and FAAH in mouse brain tissue is illustrated in Figure IV.I.

Materials and Methods

Subjects

Subjects were male and female ICR mice (Harlan Laboratories, Frederick, MD) that were 6-8 weeks old upon arrival to the laboratory. Males weighed 25-45g and females weighed 20-35g throughout the study. Other details of housing and husbandry are identical to Chapter III.

Overview of Experimental Design

The goal of this study was to compare effects of the direct cannabinoid receptor agonist Δ9-tetrahydrocannabinol (THC) and a series of endocannabinoid (eCB) catabolic enzyme inhibitors

covering a broad spectrum of selectivity for MAGL vs FAAH on a battery of pain-stimulated, pain-depressed, and pain-independent behaviors in mice as described in Chapter III (Diester et al., 2021a). Pain-related behaviors were elicited by intraperitoneal (IP) injection of dilute lactic acid, and antinociception dose-effect curves for each test drug were determined in two groups of mice: (a) one to assess drug effects on IP acid-induced changes in stretching, facial grimace, and rearing, and (b) a second to assess drug effects on IP acid-induced depression of nesting. Two additional groups were used to test effects of each test drug on two pain-independent behaviors: (a) one group to assess control nesting in the absence of the IP acid noxious stimulus, and (b) a second group to assess locomotion in the absence of the noxious stimulus. To further probe the effects observed with the MAGL-selective inhibitor MJN110, two additional nesting groups were used to assess time course and sensitivity to cannabinoid receptor antagonists. Each group consisted of 12 mice (6 males, 6 females) to provide adequate power for detection of drug effects and permit exploratory analysis of sex differences as described in Chapters II and III (Diester et al., 2019). In general, all mice in a given group received all doses of single drug, dose order was randomized across mice using a Latin-square design, and tests were conducted once per week in each mouse. Doses for each drug were varied in 0.5 or 1.0 log-unit increments across a ≥10-fold dose range with the intent of progressing from low doses that produced little or no effect to high doses that produced either significant antinociception on one or more endpoints of pain-related behavior or significant changes in nesting or locomotor activity as pain-independent behaviors. The only exception was for eCB catabolic enzyme inhibitors tested in locomotor studies, in which each group of mice was used to test vehicle and two eCB catabolic enzyme inhibitors at the highest dose tested in antinociception studies. Data were analyzed to evaluate the degree to which each test drug alleviated pain-related behaviors at doses below those that altered pain-independent behaviors.

Test drug doses, pretreatment times, and supporting references were as follows: the cannabinoid receptor$_{1/2}$ direct agonist Δ9-tetrahydrocannibinol, 1.0-30 mg/kg, 30 min (Grim et al., 2017); the selective MAGL>>FAAH inhibitors (Figure IV.I) MJN110, 0.1-10 mg/kg, 2 hours (Niphakis et al., 2013; Ignatowska-Jankowska et al., 2015a) and JZL184, 3.2-32 mg/kg, 2 hours (Long et al., 2009a; Ignatowska-Jankowska et al., 2015a; Wiebelhaus et al., 2015); the dual MAGL=FAAH inhibitor (Figure IV.I) JZL195, 3.2-32 mg/kg, 2 hours (Long et al., 2009c; Anderson et al., 2014; Hruba et al., 2015); the dual MAGL<FAAH inhibitor (Figure I) SA57, 1.0-10 mg/kg, 2 hours (Niphakis et al., 2012; Owens et al., 2016), and the selective MAGL<<FAAH inhibitors (Figure IV.I) URB597, 1.0-10 mg/kg, 60 min (Kinsey et al., 2009; Naidu et al., 2009; Naidu et al., 2010) and PF3845, 1.0-32 mg/kg, 2 hours (Booker et al., 2012; Wiebelhaus et al., 2015).

Behavioral Procedures

Stretching/Grimace/Rearing Procedure. Studies of stretching, grimace, and rearing were conducted using methods identical to those described in Chapter III. A different group of mice was used to test each drug.

Nesting Procedure. Dose-effect studies to evaluate effects of each drug on nesting in the presence or absence of the IP acid noxious stimulus were conducted using methods identical to those described in Chapter III. Two different groups of mice were used to test each drug, one group for dose-effect studies with IP acid, and a second group to test each drug without IP acid. Additionally, time course and antagonism studies were conducted in two additional groups of mice. For time course studies, 1.0 mg/kg MJN110 was administered at different pretreatment times ranging from 10 min to 24 hr, and the sequence of pretreatment times was presented in a Latin-square order across mice. For antagonism studies, mice received a SC pretreatment of vehicle, the CB_1R antagonist rimonabant (3 mg/kg) or the CB_2R antagonist SR144528 (3 mg/kg)

10 minutes before 1.0 mg/kg MJN110 or vehicle, and the nesting session commenced 2hr later. Again, these treatments were administered in a Latin-square design. Antagonist doses and pretreatment times were based on previous studies (Booker et al., 2012; Ignatowska-Jankowska et al., 2015a).

Locomotor Procedure. Locomotor activity studies were conducted using general procedures identical to those described in Chapter III. One group of mice was used to test a range of THC doses. Three additional groups were used to test the eCB enzyme inhibitors, with vehicle and a single high dose of each of two eCB enzyme inhibitors tested in each group.

Data Analysis

Data analysis was identical to that described in Chapter III.

Drugs

Lactic acid (Fisher Scientific, Hampton, NH) was diluted in sterile water and administered IP. Δ9-tetrahydrocannibinol (THC, 20 mg/m in ethanol), JZL184, URB597, and PF3845 were provided by the National Institute on Drug Abuse Supply Program (Bethesda, MD). MJN110 and SA57 were kindly provided by Dr. Michah Niphakis, currently at Lundbeck La Jolla Research Center. JZL195 was purchased from Tocris/Bio-Techne (Minneapolis, MN). The CB_1R antagonist rimonabant (SR141716A) (rimonabant) and CB_2R antagonist SR144528, were provided by the National Institute on Drug Abuse Supply Program (Bethesda, MD). All drugs were prepared in a vehicle of 1:1:18 ethanol, emulphor (Alkamuls-620, Sanofi-Aventis, Bridgewater, NJ), and saline. In general, final concentrations were prepared as clear solutions; however, final concentrations of JZL184 (≥ 1.0 mg/ml) and JZL195 (≥ 3.2 mg/ml) were

suspensions thoroughly shaken immediately before preparation of syringes and injection. All test drugs and antagonists were administered SC in volumes of 0.1 to 0.9 ml.

Results

Overview of Data Presentation

Figures IV.II-V show antinociception dose-effect curves for each drug on each endpoint of IP acid-induced behaviors (stimulation of stretching and facial grimace in left panels, depression of rearing and nesting in right panels). Figure IV.VI shows effects of each compound on nesting and locomotion in the absence of the noxious stimulus to determine IP acid-independent effects of each test drug. Figure IV.VII compares the potencies of each drug to produce antinociceptive effects vs. IP acid-independent effects, in which an ideal drug would produce antinociception at doses below those that produce IP acid-independent effects. Figure IV.VIII shows the time course, $CB_{1/2}R$ antagonism, and sex differences for the MAGL-selective inhibitor MJN110. ANOVA results and power analyses for pooled data across sexes are presented in Table IV.I. Supplemental Tables IV.I-II show ANOVA results for data segregated by sex, and Supplemental Tables IV.III-IX show results from 2-way ANOVA examining sex as a determinant of effects for each test drug on each endpoint. For any significant main effects of sex or sex x dose interactions, additional supplemental figures are added and denoted in the results below.

Effects of Δ9-THC

Figure IV.II shows that the direct $CB_{1/2}$ receptor agonist THC significantly decreased IP acid-stimulated stretching (3.2-10 mg/kg) and facial grimace (10 mg/kg), but failed to alter IP acid-induced depression of either rearing or nesting. Figure IV.VI shows that THC significantly decreased both nesting and locomotion in the absence of the noxious stimulus at 30 mg/kg. Thus, THC displayed a 0.5-1.0 log higher potency to produce antinociception compared to general

motor effects in the absence of the noxious stimulus, but only for IP acid-stimulated behaviors, as it had no significant effect for either IP acid-depressed behavior (Figure IV.VII). Additionally, there were no main effects of sex or dose x sex interactions for any endpoint (Supp. Table IV.III).

Effects of MAGL>>FAAH-selective Inhibitors

Figure IV.III shows antinociceptive effects of the MAGL>>FAAH-selective inhibitors MJN110 and JZL184. MJN110 significantly decreased both IP acid stimulated stretching and grimace at 1.0 mg/kg, but only stretching was significantly decreased at 3.2 mg/kg. MJN110 did not alter IP acid-induced depression of rearing, but doses of 0.32-3.2 mg/kg attenuated IP acid-induced depression of nesting. No dose of MJN110 up to 10 mg/kg altered nesting in the absence of the noxious stimulus, and 3.2 mg/kg did not alter locomotion (Figure IV.VI). Thus, MJN110 produced significant antinociception for three of the four IP acid-induced behaviors at doses that did not alter IP acid-independent behaviors (Figure IV.VII). IP acid-depressed nesting was the only endpoint that showed a significant effect of sex as a determinant of MJN110 effects, where 1-way ANOVAs segregated by sex showed a significant effect for females and not males, and 2-way ANOVA showed a main effect of sex (females > males) (Supp. Figure IV.I, Supp. Tables IV.I, II, & IV). Additional evaluation of sex as a determinant of MJN110 effects on IP acid-induced depression of nesting is described below.

JZL184 did not significantly alter IP acid-stimulated stretching at any dose, but 32 mg/kg JZL184 significantly decreased facial grimace. No dose significantly altered IP acid-induced depression of rearing, but 3.2 and 32 mg/kg attenuated depression of nesting. No dose up to 32 mg/kg of JZL184 altered nesting in the absence of IP acid, and 32 mg/kg did not significantly affect locomotion (Figure IV.VI). Thus, JZL184 produced antinociception for one IP acid-

stimulated behavior (facial grimace) and one IP acid-depressed behavior (nesting) at doses that did not significantly alter IP acid-independent behaviors (Figure IV.VII). Two-way ANOVA of sex differences showed main effects of sex for JZL184 effects on IP acid-stimulated stretching, IP acid-induced depression of rearing (data collapsed across dose show males > females), and nesting in the absence of the noxious stimulus, but there were no sex x dose interactions on any endpoint (Supp. Table IV. IV., Supp. Figure IV.I).

Effects of Dual MAGL and FAAH Inhibitors

Figure IV.IV shows antinociceptive effects of the dual MAGL≅FAAH inhibitor JZL195 and the dual MAGL<FAAH inhibitor SA57. JZL195 significantly blocked IP acid-stimulated stretching at 32 mg/kg but did not block acid-stimulated facial grimace. Although IP acid-depressed rearing was not affected, IP acid-depressed nesting was attenuated at 32 mg/kg. No dose of JZL195 up to 32 mg/kg affected nesting in the absence of IP acid, and 32 mg/kg did not alter locomotor behavior (Figure IV.VI). Thus, JZL195 had antinociceptive effectiveness on one IP acid-stimulated behavior (stretching) and one IP acid-depressed behavior (nesting) at doses that did not produce effects on acid-independent behaviors (Figure IV.VII). In analysis of sex as a determinant of JZL195 effects, there was a main effect of sex in locomotion (females > males), but there were no sex x dose interactions on any endpoint (Supp. Table IV.VI, Supp. Figure IV.II).

SA57 also significantly blocked IP acid-stimulated stretching (10 mg/kg) but not facial grimace. SA57 did not alter IP acid-depressed rearing, but it significantly attenuated IP acid-depressed nesting. No dose of SA57 significantly affected nesting or locomotion in the absence of the noxious stimulus (Figure IV.VI). Thus, like JZL195, SA57 blocked IP acid-stimulated stretching and attenuated IP acid-induced depression of nesting at doses that did not significantly alter

nesting or locomotion when administered alone (Figure IV.VII). For SA57, there was a significant main effect of sex for stretching (females < males) and locomotion (females > males), but there were no sex x dose interactions on any endpoint (Supp. Table IV.VII, Supp. Figure IV.II).

Effects of MAGL<<FAAH-selective Inhibitors

Figure IV.V shows the antinociceptive effectiveness of the MAGL<<FAAH-selective inhibitors URB597 and PF3845. URB597 did not significantly block either IP acid-stimulated behavior at any dose tested, and it also did not alter IP acid-induced depression of rearing. It attenuated IP acid-depressed nesting at 10 mg/kg, and no dose of URB597 significantly affected nesting or locomotion when administered in the absence of IP acid (Figure IV.VI). Thus, URB597 showed antinociceptive effectiveness for only one IP acid-depressed behavior (nesting) at a dose that did not alter nesting or locomotion in the absence of the noxious stimulus (Figure IV.VII). Analysis of sex as a determinant of URB597 effects showed no significant effects of sex (Supp. Table IV.VII).

PF3845 did not produce antinociception on any endpoint. The highest dose of 32 mg/kg significantly decreased nesting in the absence of the noxious stimulus and produced a nonsignificant trend toward reduced locomotion (Figure IV.VI). Thus, PF3845 did not produce antinociceptive effects up to doses that decreased behavior in the absence of the noxious stimulus (Figure IV.VII). There were no sex differences for any endpoints (Supp. Table IV.IX).

Time course, $CB_{1/2}R$ Antagonism, and Sex Differences for MJN110 Effects

Follow-up studies in the assay of IP acid-depressed nesting were conducted with 1.0 mg/kg MJN110 because it was the eCB catabolic enzyme inhibitor that produced antinociception on the

greatest number of endpoints. Results are shown in Figure 8, and statistical results are reported in the figure legend. In time-course studies, MJN110 significantly attenuated IP acid-induced depression of nesting with pretreatment times from 40 min to 6 hr. In antagonism studies, MJN110 antinociception was significantly blocked by the CB_1R antagonist but not by the CB_2R antagonist SR144528. The effects of 2 hr pretreatment with vehicle and 1.0 mg/kg MJN110 were determined in a total of 18 male and 18 female mice from the original study (Figure IV.IIID) and from the two follow-up studies (2hr pretreatment for time-course study, vehicle pretreatment for antagonism study). Figure IV.VIIIC compares effects of vehicle and 1.0 mg/kg MJN110 for all these male and female mice. Two-way ANOVA indicated only significant main effects of dose (1.0 mg/kg MJN110>vehicle) and sex (collapsed data across dose show females > males); the dose x sex interaction approached but did not reach the criterion for statistical significance.

Discussion

There were three main findings in this study. First, THC significantly attenuated IP acid-stimulated stretching and facial grimace at doses that did not produce general motor disruption, but THC did not alleviate IP acid-induced depression of either rearing or nesting. Second, for the eCB catabolic enzyme inhibitors, the MAGL-selective inhibitor MJN110 produced antinociception without motor disruption on three of four endpoints, including significant alleviation of IP acid-induced depression of nesting, whereas the FAAH-selective inhibitor PF3845 failed to produce antinociception on any endpoint up to a dose that produced motor disruption. Other eCB catabolic enzyme inhibitors produced effects between these extremes. Lastly, time course and antagonism studies for MJN110 in the assay of IP acid-induced depression of nesting indicated a long duration of antinociceptive action (40 min to 6 hrs) and mediation by CB_1R but not CB_2R. Overall, these results support further consideration of MAGL-selective inhibitors, especially MJN110, as candidate analgesics.

Figures

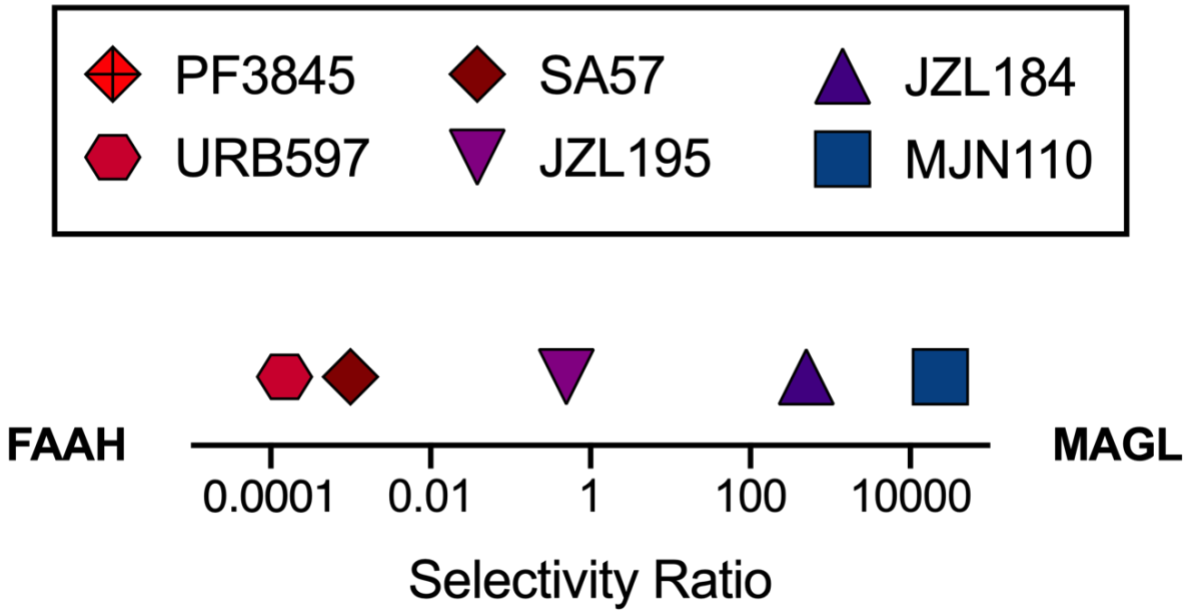

Figure IV.I. Selectivity of test compounds for the main endocannabinoid catabolic enzymes monoacylglycerol lipase (MAGL) and fatty acid amide hydrolase (FAAH) based on competitive substrate binding and activity-based protein profiling (ABPP) assays. Data were obtained from the literature as cited below, with competitive substrate binding used for calculating selectivity if available, and ABPP if no substrate binding data were available. All data are from assays using mouse brain tissue. No data for MAGL binding could be found for either endpoint for PF3845, which is considered to be a highly selective FAAH inhibitor that would fall at the far left of the figure. As a result, no selectivity ratio could be calculated for this inhibitor. PF3845: Ahn et al., 2009 (main paper denoting FAAH selectivity); URB597: Kathuria et al., 2003; SA57: Niphakis et al., 2012; JZL195: Long et al., 2009; JZL184: Long et al., 2009; MJN110: Niphakis et al., 2013.

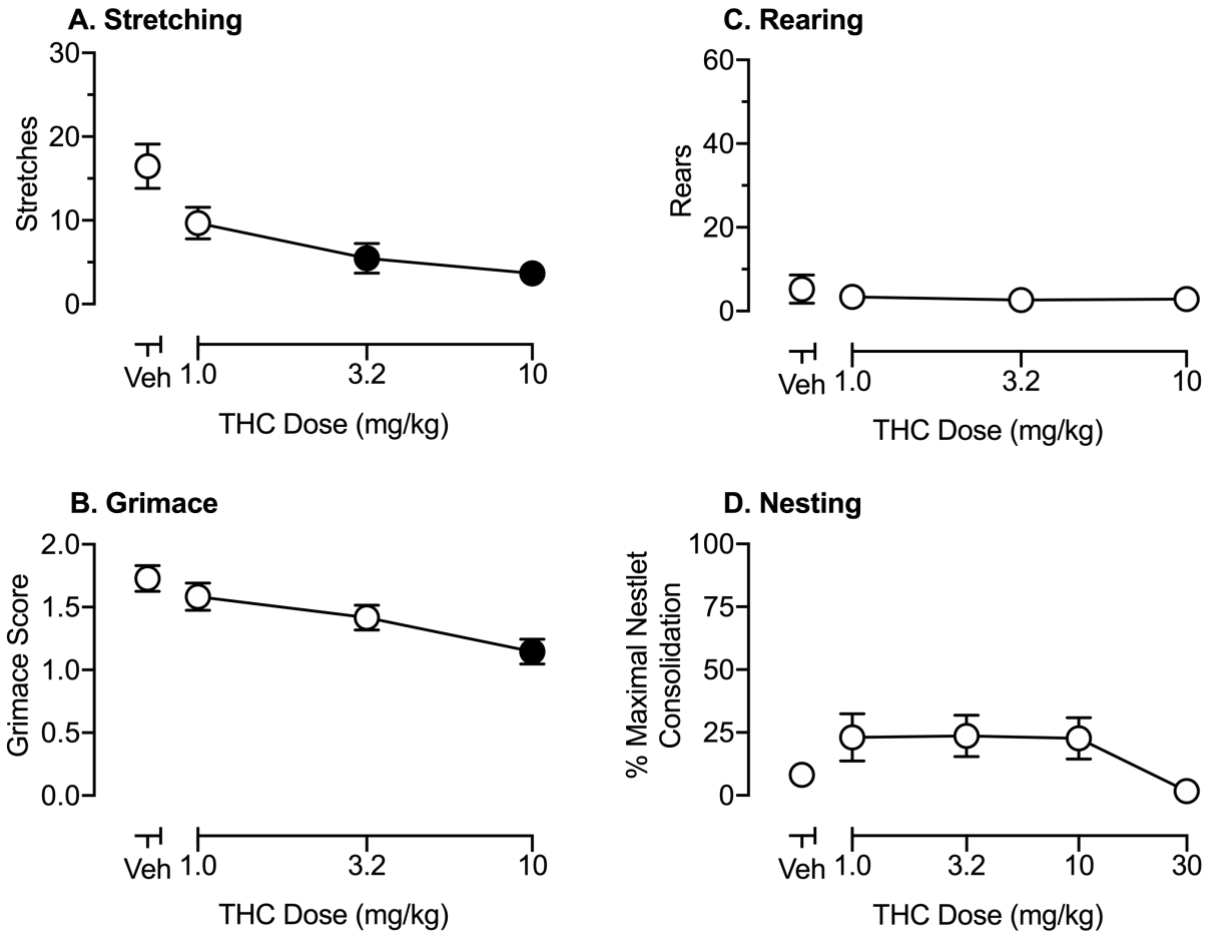

<u>Figure IV.II.</u> Effects of △9-tetrahydrocannabinol (THC) on IP acid-induced stretching, facial grimace, rearing and nesting behaviors in male and female mice. Abscissae: dose of THC delivered SC in mg/kg (log scale). Ordinates: number of stretches (A), grimace score (B), number of rears (C), and nesting expressed as percent maximum nestlet consolidation (D). Each point shows ± SEM for 12 mice (6 male, 6 female). Filled symbols indicate a significant difference from vehicle (Veh) as determined by RM one-way ANOVA and Dunnett's post hoc test for parametric data (A, C & D) or by Friedman's and Dunn's post hoc test for nonparametric data (B), $p<0.05$. Results of ANOVA and power analysis data for each panel are shown in Table IV.1.

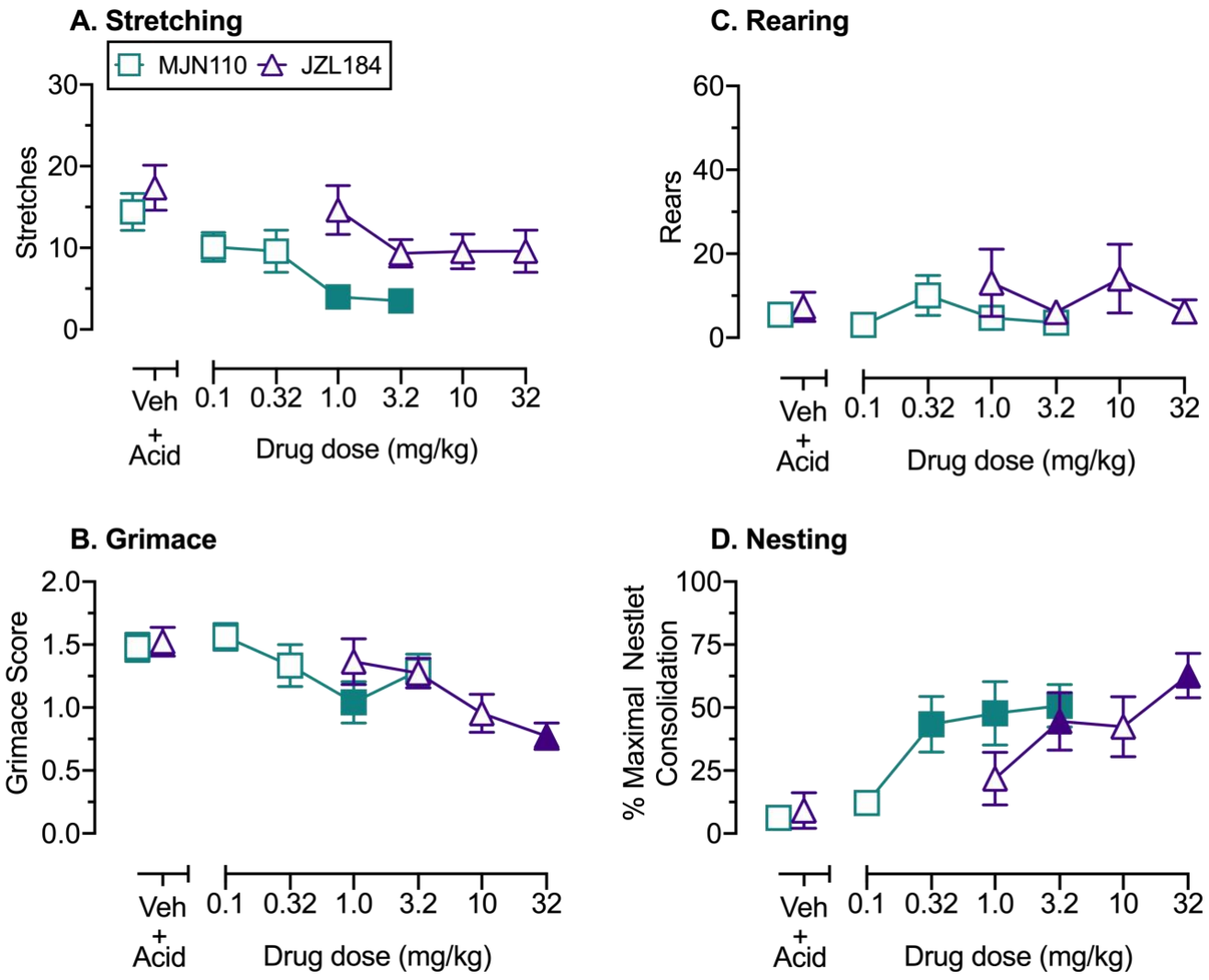

<u>Figure IV.III.</u> Effects of the MAGL-selective inhibitors MJN110 and JZL184 on IP-acid induced stretching, facial grimace, rearing and nesting behaviors in male and female mice. Abscissae: doses of MJN110 or JZL184 in mg/kg (log scale). Ordinates: number of stretches (A), grimace score (B), number of rears (C), and nesting expressed as percent maximum nestlet consolidation (D). Other details as in Figure IV.II.

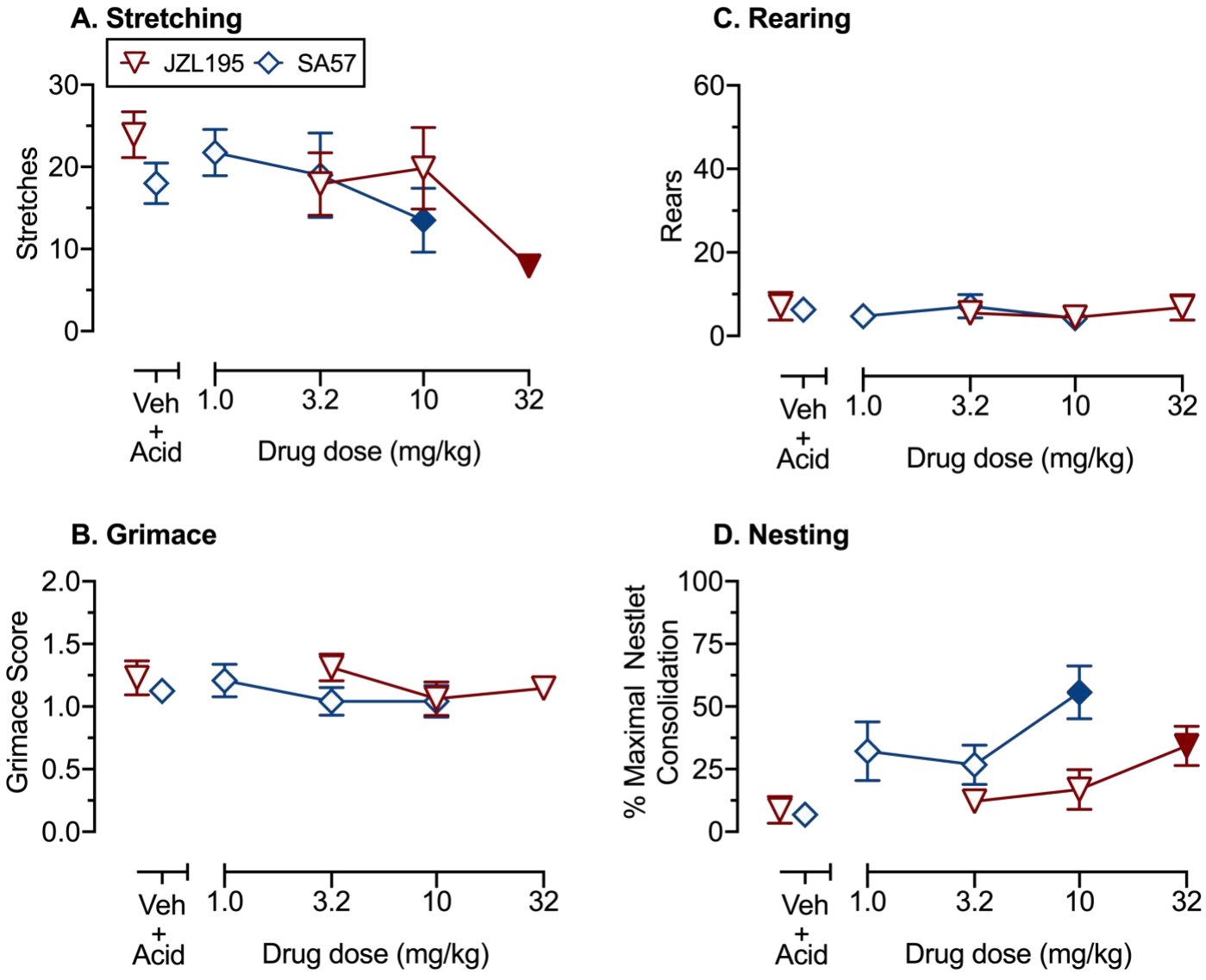

<u>Figure IV.IV.</u> Effects of the dual MAGL and FAAH inhibitors JZL195 and SA57 on IP acid-induced stretching, facial grimace, rearing and nesting behaviors in male and female mice. Abscissae: doses of JZL195 or SA57 in mg/kg (log scale). Ordinates: number of stretches (A), grimace score (B), number of rears (C), and nesting expressed as percent maximum nestlet consolidation (D). Other details as in Figure IV.II.

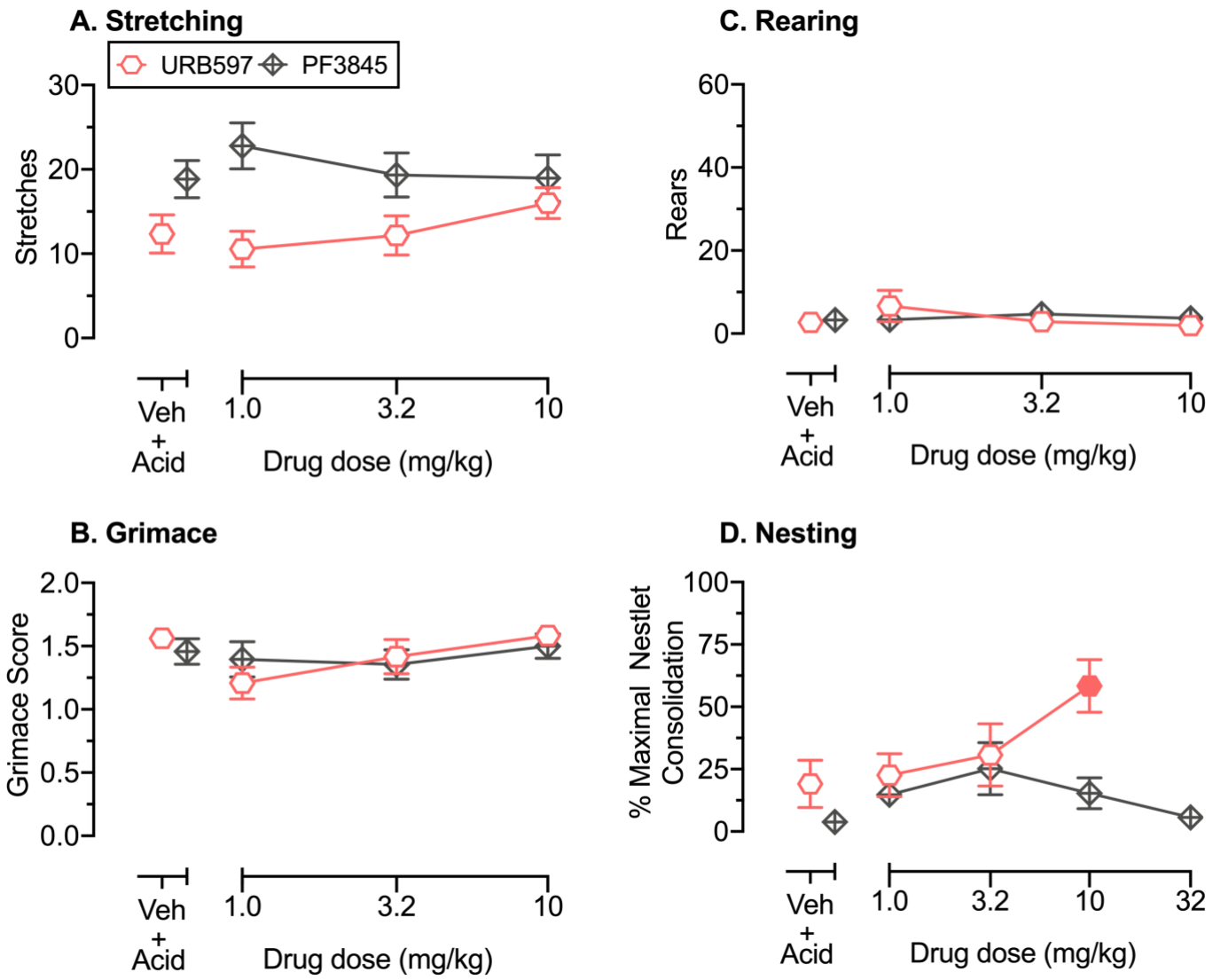

<u>Figure IV.V.</u> Effects of the FAAH-selective inhibitors UR597 and PF3845 on IP acid-induced stretching, facial grimace, rearing and nesting behaviors in male and female mice. Abscissae: doses of UR597 and PF3845 in mg/kg (log scale). Ordinates: number of stretches (A), grimace score (B), number of rears (C), and nesting expressed as percent maximum nestlet consolidation (D). Other details as in Figure IV.II.

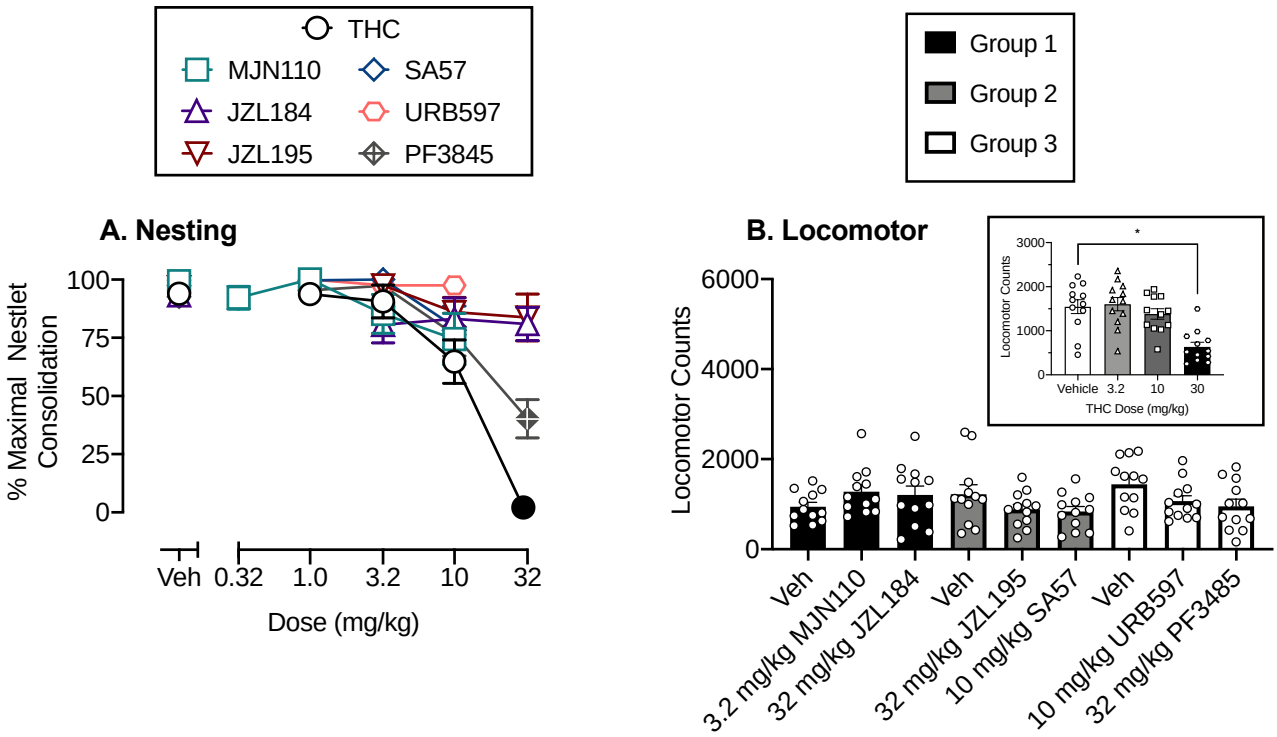

<u>Figure IV.VI.</u> Effects of endocannabinoid catabolic enzyme inhibitors and Δ9-tetrahydrocannabinol (THC) on nesting and locomotor behaviors in male and female mice in the absence of the IP acid noxious stimulus. Abscissae: doses of endocannabinoid catabolic inhibitors or THC in mg/kg. Doses of endocannabinoid catabolic enzyme inhibitors for locomotor studies were the highest tested in antinociception assays, whereas THC (inset in B) was tested across a range of doses. Ordinates: nesting expressed as % maximum nestlet consolidation (A), and locomotor counts (B). Each point shows ± SEM for 12 mice (6 male, 6 female). Filled symbols in Panel A and the asterisk in Panel B inset indicate a significant difference from vehicle (Veh) as determined by RM one-way ANOVA and Dunnett's post hoc test, $p<0.05$. Results of ANOVA and power analysis data for each panel are shown in Table IV.I.

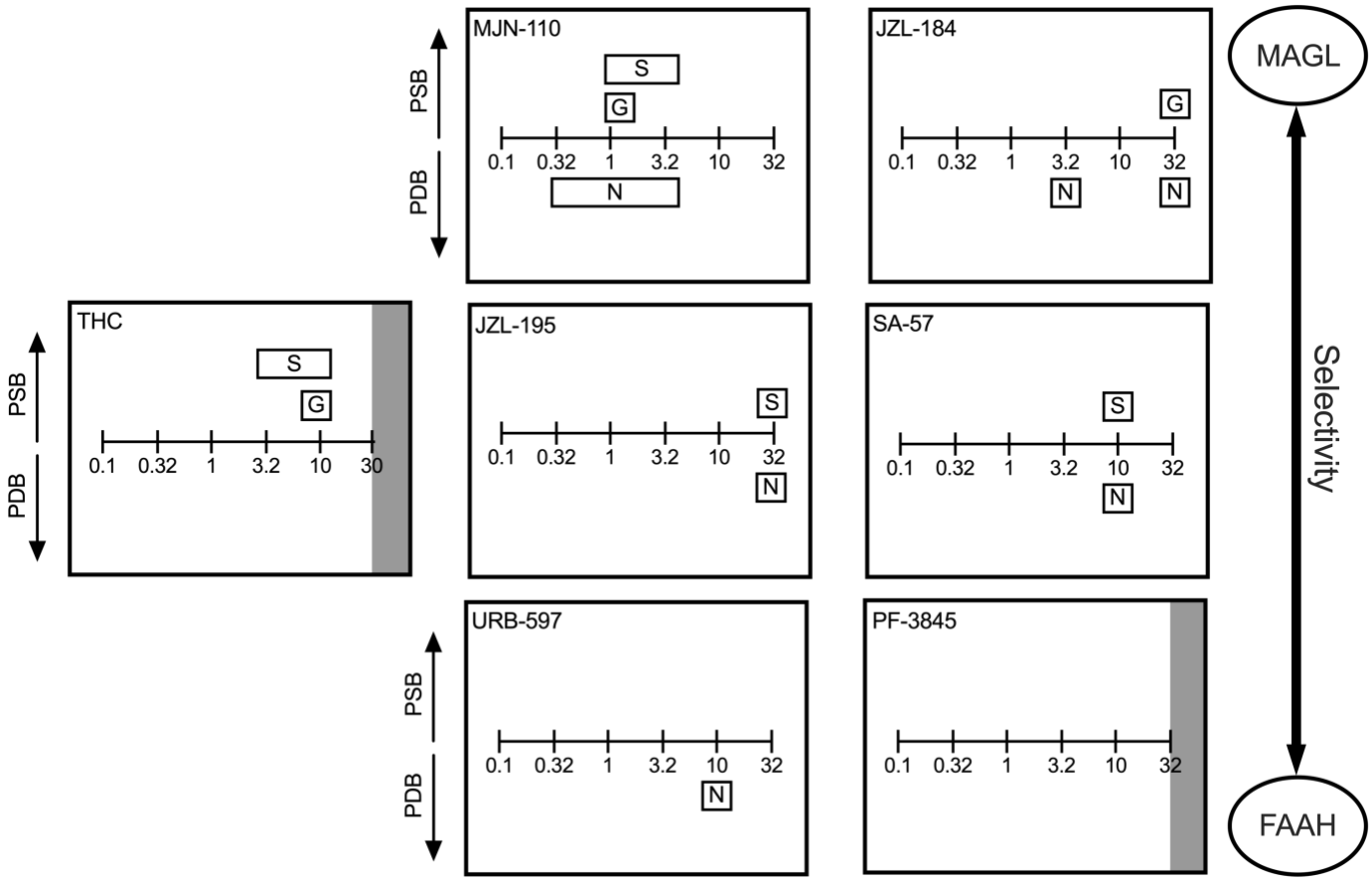

<u>Figure IV.VII.</u> Drug profiles for comparison of potency to produce antinociceptive effects on IP acid-stimulated and IP acid-depressed behaviors versus general behavioral disruption. Abscissae: Drug dose in mg/kg (log scale). Boxed letters (S, G, R, N) denote the dose range over which each drug significantly attenuated IP acid-induced stimulation of stretching (S) or facial grimace (G) or IP acid-induced depression of rearing (R) or nesting (N). In each panel, boxes for pain-stimulated behaviors (PSB) and pain-depressed behaviors (PDB) are shown above and below the dose axis, respectively. The gray zone at the right of edge of panels for THC and PF3845 show doses that produced motor disruption in assays of nesting and/or locomotion in the absence of the IP acid noxious stimulus. For the other drugs, no tested dose altered nesting or locomotion in the absence of the noxious stimulus, and no gray zone is indicated. The test compounds for inhibition of the two main endocannabinoid degradative

enzymes MAGL and FAAH are organized by their selectivity, going from MAGL-selective to FAAH-selective, as indicated by the selectivity arrows on the right.

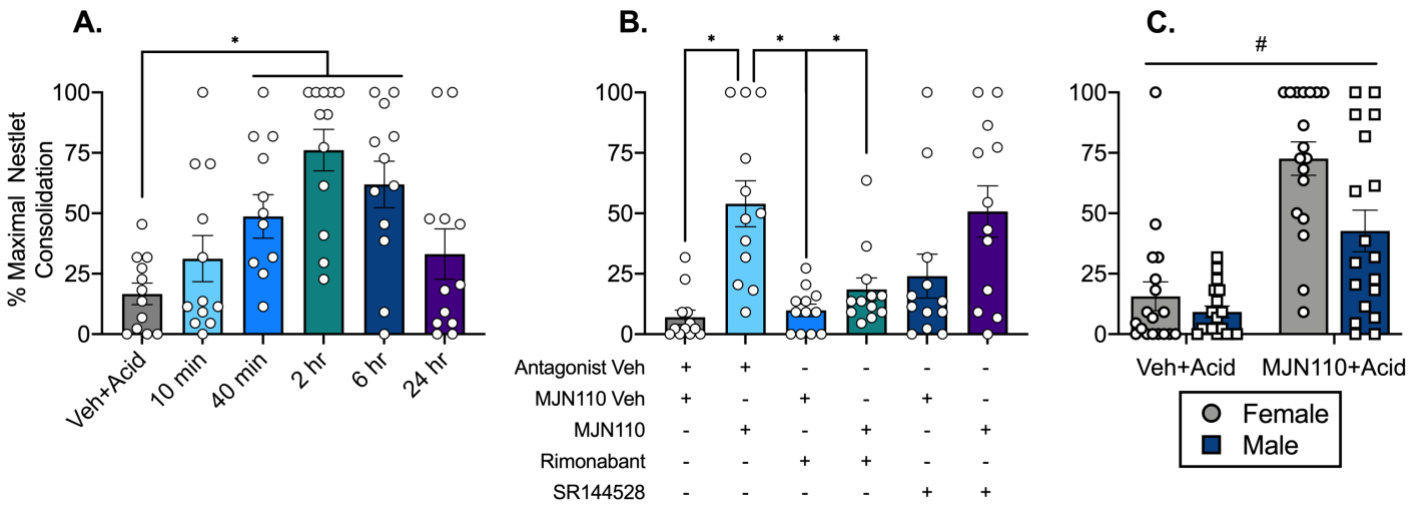

<u>Figure IV.VIII.</u> Effects of time, cannabinoid receptor (CBR) antagonism, and sex on MJN110 attenuation of IP acid-induced depression of nesting in male and female mice. Abscissae: (A) Pre-treatment time of 1.0 mg/kg MJN110 before administration of 0.32% IP acid, (B) treatments for assessment of the CB_1R-selective antagonist rimonabant (3 mg/kg) and the CB_2R-selective antagonist SR144528 (3 mg/kg), and (C) effect of sex on 1.0 mg/kg MJN110 antinociception, all delivered SC in a volume of 10 ml/kg. Ordinates: nestlet consolidation expressed as percent maximal nestlet consolidation. An asterisk (*) indicates a significant difference from or Veh+Acid (A,C) or from Antagonist Veh:MJN110 (B), as determined by RM one-way ANOVA and Dunnett's post hoc test (A,B) or two-way ANOVA and Holm-Šídák post hoc test (C), $p<0.05$. Statistical results are as follows: (A) Significant main effect of time [$F(2.738, 30.12)=7.367$; $p=0.001$]. (B) Significant main effect of treatment [$F(3.931, 43.24)=7.84$; $p<0.0001$]. (C) # Indicates that there were significant main effects of treatment [$F(1, 34)=53.41$; $p<0.0001$], and sex [$F(1, 34)=7.661$; $p=0.0091$] but no treatment x sex interaction [$F(1, 34)=3.605$; $p=0.0661$].

Table IV.I: Summary of power analysis results from pooled one-way ANOVA data from Figures IV.I-IV

Male and Female	F Statistic, *P* Value	Current Effect Size (Cohen's f)	Current Power	Sample Size: Power ≥ 0.8	Friedman Statistic; *P* Value
		△9-Tetrahydrocannabinol			
Stretch + acid	F(2.290, 25.19) = 11.83; *P* = 0.0001*	1.040	0.994	7	—[a]
Rear + acid	F(1.433, 15.77) = 0.362; *P* = 0.6325	0.753	0.94	9	—
Grimace	—	—	—	—	F = 13.09; *P* = 0.0044*
Nesting + acid	F(2.469, 27.16) = 2.083; *P* = 0.1352	0.435	0.431	25	—
Nesting	F(2.351, 25.86) = 45.27; *P* < 0.0001*	0.44	0.427	25	—
Locomotor	F(2.352, 25.87) = 11.64; *P* = 0.0001	1.028	0.994	7	—
		MJN110			
Stretch + acid	F(2.955, 32.51) = 6.231; *P* = 0.0019*	0.753	0.94	9	—
Rear + acid	F(2.045, 22.49) = 0.9844; *P* = 0.3908	0.299	0.201	56	—
Grimace	—	—	—	—	F = 10.65; *P* = 0.0308*
Nesting + acid	F(2.528, 27.80) = 6.5; *P* = 0.0028*	0.768	1	5	—
nesting	F(1.927, 21.19) = 2.789; *P* = 0.0857	0.503	0.407	27	—
Locomotor	F(1.453, 15.98) = 2.166; *P* = 0.1556	0.445	0.33	34	—
		JZL184			
Stretch + acid	F(3.580, 35.80) = 2.726; *P* = 0.0496	0.522	0.662	14	—
Rear + acid	F(1.992, 19.92) = 0.4745; *P* = 0.6283	0.217	0.116	>100	—
Grimace	—	—	—	—	F = 16.66; *P* = 0.0023*
Nesting + acid	F(2.777, 30.55) = 5.316; *P* = 0.0054*	0.695	0.88	11	—
Nesting	F(2.072, 22.79) = 0.6424; *P* = 0.5406	0.241	0.145	84	—
Locomotor	F(1.453, 15.98) = 2.166; *P* = 0.1556	0.445	0.33	34	—
		JZL195			
Stretch + acid	F(2.440, 26.84) = 5.007; *P* = 0.0102*	0.675	0.821	12	—
Rear + acid	F(2.413, 26.55) = 0.2673; *P* = 0.8066	0.157	0.092	>100	—
Grimace	—	—	—	—	F = 1.664; *P* = 0.645
Nesting + acid	F(2.252, 24.78) = 3.782; *P* = 0.0325*	0.587	0.668	16	—
Nesting	F(1.696, 18.65) = 1.157; *P* = 0.3279	0.299	0.184	64	—
Locomotor	F(1.516, 16.68) = 2.768; *P* = 0.1024	0.502	0.416	26	—
		SA57			
Stretch + acid	F(2.256, 24.82) = 4.219; *P* = 0.0228*	0.619	0.718	14	—
Rear + acid	F(2.278, 25.06) = 0.3463; *P* = 0.7377	0.179	0.103	>100	—
Grimace	—	—	—	—	F = 3.058; *P* = 0.3828
Nesting + acid	F(1.972, 21.7) = 4.391; *P* = 0.0255*	0.631	0.691	15	—
Nesting	F(1.109, 12.20) = 5.032; *P* = 0.0413*	0.677	0.565	19	—
Locomotor	F(1.516, 16.68) = 2.768; *P* = 0.1024	0.502	0.416	26	—
		URB597			
Stretch + acid	F(2.643, 29.07) = 1.256; *P* = 0.306	0.337	0.282	38	—
Rear + acid	F(1.346, 14.81) = 1.129; *P* = 0.3258	0.32	0.185	65	—
Grimace	—	—	—	—	F = 6.200; *P* = 0.1023
Nesting + acid	F(2.321, 23.21) = 4.102; *P* = 0.0251*	0.641	0.71	13	—
Nesting	F(1.631, 17.94) = 0.5785; *P* = 0.5373	0.229	0.125	>100	—
Locomotor	F(1.938, 21.31) = 3.418; *P* = 0.0529	0.557	0.57	19	—
		PF3845			
Stretch + acid	F(2.541, 27.95) = 0.5712; *P* = 0.6111	0.227	0.144	82	—
Rear + acid	F(2.051, 22.56) = 0.252; *P* = 0.7847	0.15	0.084	>100	—
Grimace	—	—	—	—	F = 0.0826; *P* = 0.9938
Nesting + acid	F(1.769, 19.46) = 2.045; *P* = 0.160	0.432	0.35	31	—
Nesting	F(2.350, 25.85) = 17.43; *P* < 0.0001*	1.259	0.999	5	—
Locomotor	F(1.938, 21.31) = 3.418; *P* = 0.0529	0.557	0.57	19	—

[a]Dashes indicate statistical analyses that were not conducted in accordance with parametric or nonparametric data.

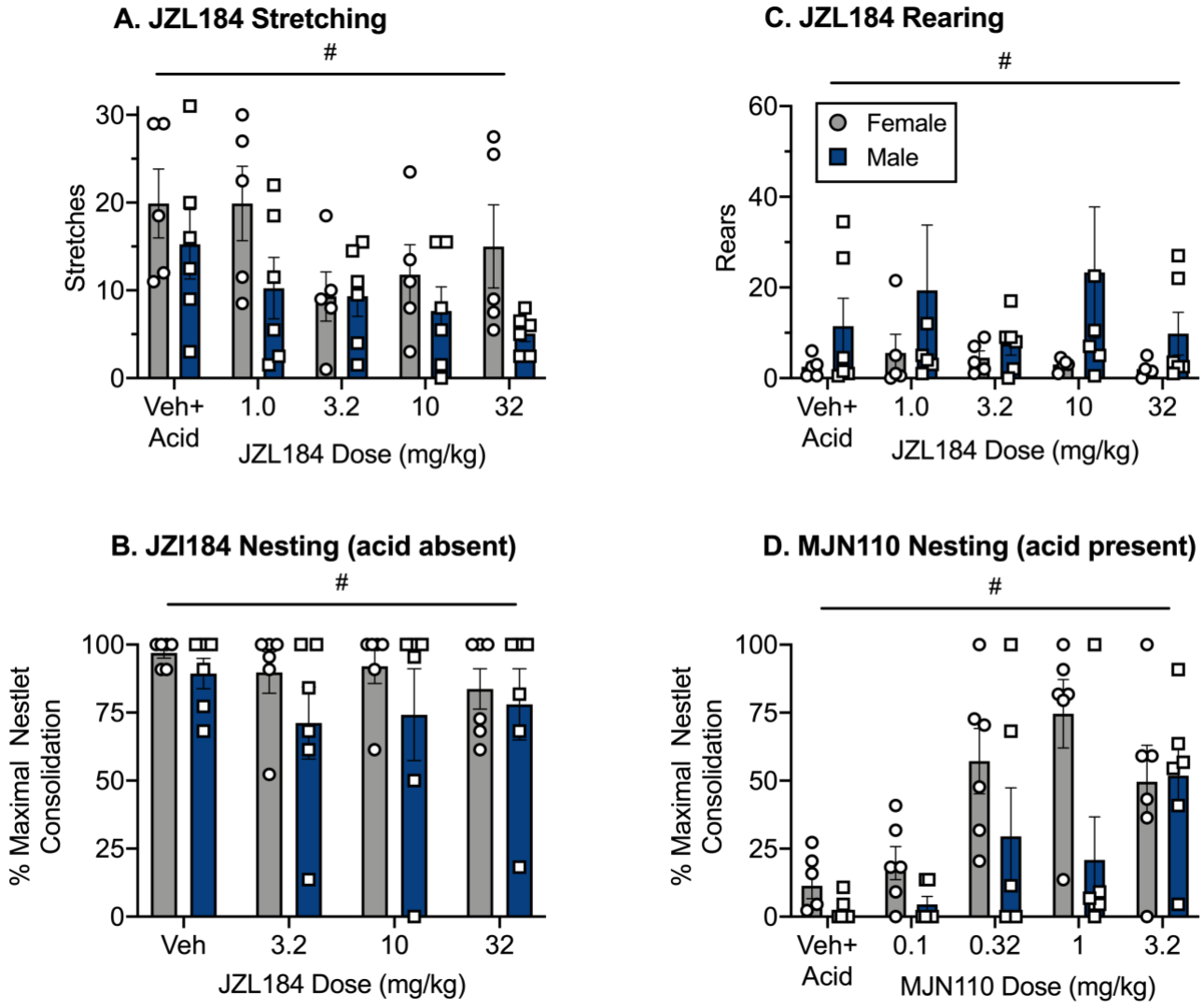

<u>Supplemental Figure IV.I.</u> Endpoints showing a main effect of sex in studies with JZL184 (A,B,C) and MJN110 (D). Abscissae: doses of JZL184 or MJN110 in mg/kg (log scale). Ordinates: number of stretches (A), number of rears (B), and nesting expressed as percent maximum nestlet consolidation (C,D). All points represent the mean ± SEM for either 6 male (blue, squares) or 5-6 female (grey, circles). # Indicates a significant main effect of sex as determined by a 2-way ANOVA and Holm-Sidak post hoc test, with data collapsed across dose showing a significant M>F effect for JZL184 attenuation of IP acid-induced depression of rearing [Welch's two-tailed t-test, p=0.0157] (B) and MJN110 attenuation of IP acid-induced depression of nesting [Welch's two-tailed t-test, p=0.0168] (D). All other statistical results are shown in Supplemental Tables IV.IV and IV.V.

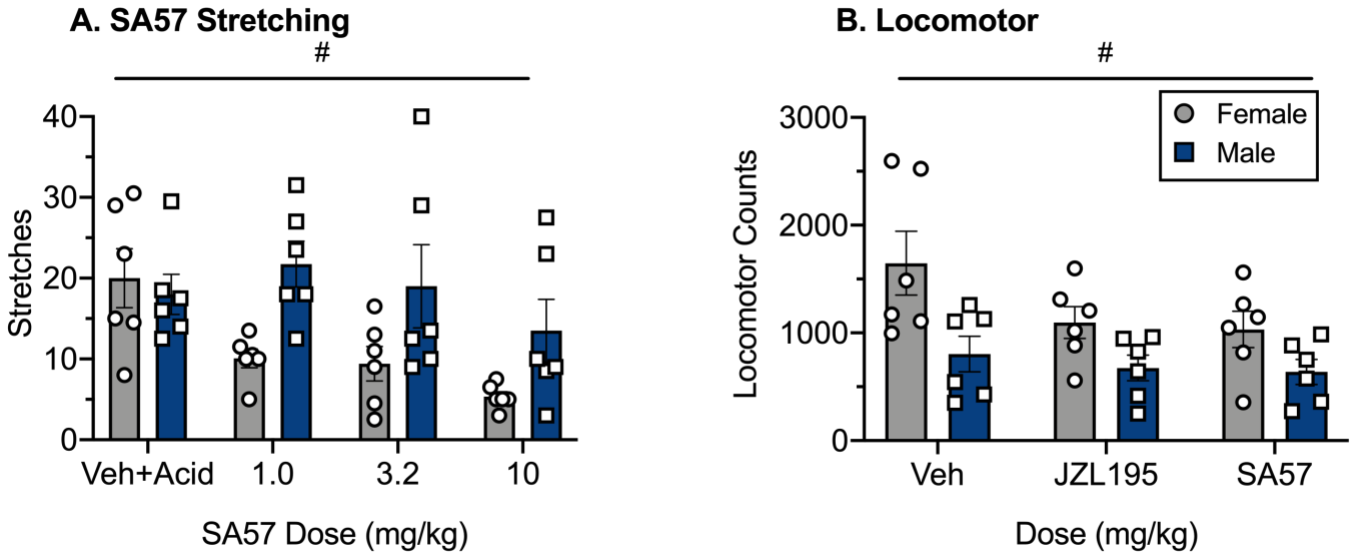

<u>Supplemental Figure IV.II.</u> Sex differences with the dual MAGL and FAAH eCB catabolic enzyme inhibitors JZL195 and SA57 on IP acid-stimulated stretching and locomotion in the absence of IP acid. Abscissae: doses of JZL195 or SA57 in mg/kg (log scale). Ordinates: number of stretches (A) and locomotion in the absence of the noxious stimulus (B). All points represent the mean ± SEM for either 6 male (blue, squares) or 6 female (grey, circles). # Indicates a significant main effect of sex as determined by a 2-way ANOVA and Holm-Sidak post hoc test for parametric data segregated by sex, with statistical results shown in Supplemental Table IV.VI and IV.VII.

Supplemental Tables

Supplemental Tables show one-way ANOVA results and power analyses for each drug in males (Table IV.I) and females (Table IV.II) and two-way ANOVA results and power analyses for each drug with sex included as a variable (Tables IV.III-IX). Note that grimace was scored as a nonparametric variable, and as a result, grimace data were not submitted to ANOVA or power analyses. rather, grimace data were evaluated by multiple t-tests with corrections for multiple comparisons using the Friedman statistic.

Supplemental Table IV.I. Summary of power analysis results from male one-way ANOVA data from Figures IV.II-VI.

Supplemental Table IV.I					
	△9-Tetrahydrocannabinol				
Male & Female	F Statistic, p value	Current Effect Size (Cohen's f)	Current Power	Sample Size: Power≥ 0.8	Friedman statistic; p value
Stretch + Acid	F(1.439, 7.194)=7.872; p=0.0198*	1.260	0.755	7	-
Rear + Acid	F(1.391, 6.957)=0.2079; p=0.7400	0.204	0.07	>100	-
Grimace	-	-	-	-	
Nesting + Acid	F(1.707, 8.536)=0.9699; p=0.4032	0.44	0.16	31	-
Nesting	F(1.614, 8.071)=21.05; p=0.0009*	2.05	0.996	4	-
Locomotor	F(1.772, 8.861)=7.171; p=0.0157*	1.197	0.791	7	-
	MJN-110				
Stretch + Acid	F(2.011, 10.06)=4.235; p=0.0462*	0.921	0.604	9	-
Rear + Acid	F(2.013, 10.07)=0.3134; p=0.7392	0.25	0.087	>100	-
Grimace	-	-	-	-	
Nesting + Acid	F(1.488, 7.442)=2.724; p=0.1355	0.739	0.346	40	-
Nesting	F(1.640, 8.200)=0.6485; p=0.5184	0.36	0.121	46	-
Locomotor	F(1.443, 7.215)=1.244; p=0.3249	0.498	0.178	28	-
	JZL-184				
Stretch + Acid	F(2.766, 13.83)=1.678; p=0.2192	0.579	0.333	14	-

Rear + Acid	F(1.916, 9.578)=0.4136; p=0.6643	0.287	0.098	>100	-
Grimace	-	-	-	-	
Nesting + Acid	F(2.482, 12.41)=4.792; p=0.0235*	0.978	0.737	7	-
Nesting	F(1.865, 9.325)=0.3369; p=0.7081	0.259	0.088	78	-
Locomotor	F(1.443, 7.215)=1.244; p=0.3249	0.498	0.178	28	-
			JZL-195		
Stretch + Acid	F(2.090, 10.45)=5.664; p=0.0207*	1.06	0.75	7	-
Rear + Acid	F(1.365, 6.825)=0.2338; p=0.7162	0.217	0.072	>100	-
Grimace	-	-	-	-	
Nesting + Acid	F(1.526, 7.632)=3.631; p=0.0852	0.853	0.448	11	-
Nesting	F(1.256, 6.281)=0.4887; p=0.5516	0.323	0.095	72	-
Locomotor	F(1.367, 6.833)=0.5788; p=0.5242	0.341	0.106	57	-
			SA-57		
Stretch + Acid	F(1.712, 8.561)=1.295; p=0.3156	0.509	0.201	24	-
Rear + Acid	F(1.301, 6.507)=1.345; p=0.3028	0.519	0.18	27	-
Grimace	-	-	-	-	
Nesting + Acid	F(7.77, 8.848)=2.076; p=0.1837	0.644	0.304	16	-
Nesting	F(1.117, 5.583)=2.343; p=0.1816	0.684	0.255	19	-
Locomotor	F(1.367, 6.833)=0.5788; p=0.5242	0.341	0.106	57	-
			URB-597		
Stretch + Acid	F(1.609, 8.043)=0.2694; p=0.7249	0.232	0.078	>100	-
Rear + Acid	F(1.088, 5.44)=1.249; p=0.317	0.157	0.06	>100	-
Grimace	-	-	-	-	
Nesting + Acid	F(1.475, 7.376)=4.29; p=0.0658	0.927	0.502	10	-
Nesting	F(1.0, 5.0)=1.0; p=0.3632	0.448	0.13	43	-
Locomotor	F(1.913, 9.563)=3.596; p=0.0699	0.847	0.513	10	-
			PF-3845		
Stretch + Acid	F(2.376, 11.88)=0.7164; p=0.5311	0.378	0.149	33	-

Rear + Acid	F(1.625, 8.127)=0.3943; p=0.6458	0.378	0.128	42	-
Grimace	-	-	-	-	
Nesting + Acid	F(1.626, 8.131)=1.302; p=0.3138	0.511	0.197	24	-
Nesting	F(1.334, 6.668)=13.67; p=0.0064*	0.511	0.197	24	-
Locomotor	F(1.913, 9.563)=3.596; p=0.0699	0.847	0.513	10	-

Supplemental Table IV.II. Summary of power analysis results from female one-way ANOVA data from Figures IV.II-VI.

Supplemental Table IV.II					
	△9-Tetrahydrocannabinol				
Male & Female	F Statistic, p value	Current Effect Size (Cohen's f)	Current Power	Sample Size: Power≥ 0.8	Friedman statistic; p value
Stretch + Acid	F(1.956, 9.780)=4.514; p=0.0415*	0.150	0.063	>100	-
Rear + Acid	F(1.722, 8.608)=0.5581; p=0.5669	0.333	0.112	51	-
Grimace	-	-	-	-	
Nesting + Acid	F(1.577, 7.883)=1.043; p=0.3775	0.457	0.164	30	-
Nesting	F(1.298, 6.492)=31.63; p=0.0007*	2.521	0.999	4	-
Locomotor	F(2.353, 11.77)=4.574; p=0.0296*	0.957	0.697	7	-
	MJN-110				
Stretch + Acid	F(2.378, 11.89)=4.829; p=0.025*	0.982	0.725	7	-
Rear + Acid	F(1.722, 8.608)=0.5581; p=0.5669	0.418	0.156	32	-
Grimace	-	-	-	-	
Nesting + Acid	F(2.581, 12.91)=6.962; p=0.0062*	1.33	0.957	5	-
Nesting	F(1.647, 8.236)=2.867; p=0.1185	0.757	0.385	13	-
Locomotor	F(1.230, 6.15)=0.962; p=0.3855	0.291	0.088	83	-
	JZL-184				
Stretch + Acid	F(2.509, 10.04)=1.801; p=0.2127	0.67	0.314	12	-
Rear + Acid	F(1.390, 5.559)=0.5091; p=0.5635	0.67	0.218	17	-
Grimace	-	-	-	-	

Nesting + Acid	F(1.760, 8.800)=1.370; p=0.2988	0.523	0.214	22	-
Nesting	F(2.097, 10.49)=0.597; p=0.5755	0.346	0.126	42	-
Locomotor	F(1.230, 6.15)=0.962; p=0.3855	0.291	0.088	83	-
			JZL-195		
Stretch + Acid	F(2.203, 11.01)=0.9629; p=0.4198	0.438	0.18	26	-
Rear + Acid	F(1.770, 8.850)=0.5697; p=0.5652	0.337	0.114	49	-
Grimace	-	-	-	-	
Nesting + Acid	F(2.316, 11.58)=1.035; p=0.3962	0.456	0.165	30	-
Nesting	F(1.618, 8.091)=1.041; p=0.3792	0.456	0.165	30	-
Locomotor	F(1.560, 7.801)=2.19; p=0.1784	0.662	0.296	16	-
			SA-57		
Stretch + Acid	F(1.631, 8.153)=9.812; p=0.0084*	1.399	0.879	6	-
Rear + Acid	F(1.768, 8.840)=0.9036; p=0.4273	0.425	0.155	32	-
Grimace	-	-	-	-	
Nesting + Acid	F(1.532, 7.659)=2.968; p=0.1175	0.562	0.222	22	-
Nesting	F(1.0, 5.0)=2.5; p=0.1747	0.707	0.252	19	-
Locomotor	F(1.560, 7.801)=2.19; p=0.1784	0.662	0.296	16	-
			URB-597		
Stretch + Acid	F(1.728, 8.641)=1.530; p=0.2668	0.553	0.231	21	-
Rear + Acid	F(1.301, 6.504)=0.2285; p=0.7097	0.215	0.071	>100	-
Grimace	-	-	-	-	
Nesting + Acid	F(1.257, 5.027)=0.6671; p=0.4858	0.408	0.106	43	-
Nesting	F(1.0, 5.0)=1.0; p=0.3632	0.448	0.13	43	-
Locomotor	F(1.93, 9.651)=0.6194; p=0.5529	0.352	0.124	43	-
			PF-3845		

Stretch + Acid	F(1.693, 8.464)=0.4552; p=0.6181	0.301	0.099	63	-
Rear + Acid	F(1.559, 7.793)=0.2239; p=0.7519	0.212	0.073	>100	-
Grimace	-	-	-	-	
Nesting + Acid	F(1.492, 7.460)=0.9055; p=0.4147	0.425	0.144	36	-
Nesting	F(2.113, 10.57)=5.743; p=0.0195*	1.07	0.761	7	-
Locomotor	F(1.93, 9.651)=0.6194; p=0.5529	0.352	0.124	43	-

Supplemental Table IV.III. Summary of power analysis results from two-way ANOVA data from Figures IV.II.

Supplemental Table IV.III				
	△9-Tetrahydrocannabinol			
Main Effect of Dose	F Statistic, p value	Current Effect Size (Cohen's f)	Current Power	Sample Size: Power≥ 0.8
Stretch + Acid	F(2.276, 22.76) = 11.11; p=0.0003*	1.050	1	4
Rear + Acid	F(1.42, 14.20)=0.3329; p=0.6496	0.182	0.178	72
Nesting + Acid	F(2.468, 24.68)=1.91; p=0.1622	1.294	1	4
Nesting	F(2.362, 23.62)=48.89; p<0.0001*	2.211	1	<3
Locomotor	F(2.353, 23.53)=10.89; p=0.0003*	1.312	1	4
Main Effect of Sex	F Statistic, p value	Current Effect Size (Cohen's f)	Current Power	Sample Size: Power≥ 0.8
Stretch + Acid	F(1,10)=0.0089; p=0.9267	0.146	0.075	>100
Rear + Acid	F(1,10) = 1.310; p=0.2791	0.19	0.092	>100
Nesting + Acid	F(1, 10)=0.032; p=0.8615	0.0744	0.0563	>100
Nesting	F(1, 10)=1.109; p=0.3172	0.167	0.082	>100
Locomotor	F(1,10)=2.674; p=0.1331	0.293	0.15	89
Dose x Sex Interaction	F Statistic, p value	Current Effect Size (Cohen's f)	Current Power	Sample Size: Power≥ 0.8
Stretch + Acid	F(3,30)=0.3275; p=0.8054	0.182	0.257	43
Rear + Acid	F(3,30)=0.1170; p=0.9495	0.11	0.118	>100
Nesting + Acid	F(4, 40)=0.08749; p=0.9858	0.094	0.102	>100
Nesting	F(4 40)=1.878; p=0.1331	0.433	0.964	8
Locomotor	F(3, 30)=0.2928; p=0.8302	0.17	0.228	49

Supplemental Table IV.IV. Summary of power analysis results from two-way ANOVA for MJN110 from Figure IV.III.

Supplemental Table 4				
	MJN-110			
Main Effect of Dose	F Statistic, p value	Current Effect Size (Cohen's f)	Current Power	Sample Size: Power≥ 0.8
Stretch + Acid	F(2.651, 26.51)=6.940; p=0.0019*	0.834	1	5
Rear + Acid	F(2.063, 20.36)=0.9685; p=0.3979	0.311	0.507	22
Nesting + Acid	F(2.32, 23.30)=6.99; p=0.003*	0.837	1	5
Nesting	F(1.913, 19.13)=2.748; p=0.0912	0.525	0.922	8
Locomotor	F(1.440, 14.10)=1.986; p=0.1788	0.446	0.796	13
Main Effect of Sex	F Statistic, p value	Current Effect Size (Cohen's f)	Current Power	Sample Size: Power≥ 0.8
Stretch + Acid	F(1, 10)=4.719; p=0.0550	0.33	0.179	75
Rear + Acid	F(1,10)=1.851; p=0.2035	0.234	0.114	>100
Nesting + Acid	F(1,10)=8.235; p=0.0167*	0.461	0.306	40
Nesting	F(1, 10)=1.359; p=0.2708	0.209	0.101	>100
Locomotor	F(1, 10)=0.6880; p=0.4262	0.301	0.156	89
Dose x Sex Interaction	F Statistic, p value	Current Effect Size (Cohen's f)	Current Power	Sample Size: Power≥ 0.8
Stretch + Acid	F(4, 40)=2.006; p=0.1121	1.415	1	<3
Rear + Acid	F(4,40)=0.5332; p=0.7121	0.232	0.451	24
Nesting + Acid	F(4, 40)=1.842; p=0.1398	0.43	0.961	8
Nesting	F(4, 40)=0.839; p=0.5088	0.289	0.658	16
Locomotor	F(2, 20)=0.08436; p=0.9194	0.092	0.092	>100

Supplemental Table IV.V. Summary of power analysis results from two-way ANOVA for JZL184 from Figure IV.III.

Supplemental Table IV.V				
	JZL-184			
Main Effect of Dose	F Statistic, p value	Current Effect Size (Cohen's f)	Current Power	Sample Size: Power≥ 0.8
Stretch + Acid	F(3.392, 30.53)=2.732; p=0.0549	0.551	0.991	7
Rear + Acid	F(1.942, 17.48)=0.3787; p=0.6843	0.204	0.217	49
Nesting + Acid	F(2.623, 26.23)=5.031; p=0.0089*	0.71	1	6
Nesting	F(2.037, 20.39)=0.5950; p=0.5639	0.234	0.351	32
Locomotor	F(1.440, 14.10)=1.986; p=0.1788	0.446	0.796	13
Main Effect of Sex	F Statistic, p value	Current Effect Size (Cohen's f)	Current Power	Sample Size: Power≥ 0.8
Stretch + Acid	F(1, 9)=5.388; p=0.0454*	2.788	1	5
Rear + Acid	F(1, 9)=9.663; p=0.0125*	0.341	0.173	70
Nesting + Acid	F(1, 10)=0.5152; p=0.4893	0.167	0.082	>100
Nesting	F(1, 10)=5.922; p=0.0352	0.293	0.151	94
Locomotor	F(1, 10)=0.6880; p=0.4262	0.301	0.156	89
Dose x Sex Interaction	F Statistic, p value	Current Effect Size (Cohen's f)	Current Power	Sample Size: Power≥ 0.8
Stretch + Acid	F(4, 36)=0.8497; p=0.5033	0.3025	0.653	15
Rear + Acid	F(4, 36)=0.3130; p=0.8674	0.188	0.275	36
Nesting + Acid	F(4, 40)=0.4105; p=0.800	0.201	0.346	31
Nesting	F(3, 30)=0.1895; p=0.9027	0.138	0.161	74
Locomotor	F(2, 20)=0.08436; p=0.9194	0.092	0.092	>100

Supplemental Table IV.VI. Summary of power analysis results from two-way ANOVA for JZL195 from Figure IV.IV.

Supplemental Table IV.VI				
	JZL-195			
Main Effect of Dose	F Statistic, p value	Current Effect Size (Cohen's f)	Current Power	Sample Size: Power≥ 0.8

Stretch + Acid	F(2.472, 24.72)=5.210; p=0.009*	0.721	1	5
Rear + Acid	F(2.420, 24.20)=0.259; p=0.8133	0.16	0.186	64
Nesting + Acid	F(2.191, 21.91)=3.973; p=0.0306*	0.6298	0.994	7
Nesting	F(1.599, 15.99)=1.109; p=0.3407	0.333	0.522	21
Locomotor	F(1.55, 15.50)=2.732; p=0.1039	0.446	0.819	12
Main Effect of Sex	F Statistic, p value	Current Effect Size (Cohen's f)	Current Power	Sample Size: Power≥ 0.8
Stretch + Acid	F(1,10)=2.681; p=0.1326	0.522	0.373	31
Rear + Acid	F(1,10)=0.02897; p=0.8683	0.041	0.052	>100
Nesting + Acid	F(1,10)=1.408; p=0.2628	0.309	0.163	85
Nesting	F(1,10)=1.085; p=0.3221	0.132	0.07	>100
Locomotor	F(1, 10)=14.62; p=0.0034*	0.841	0.747	14
Dose x Sex Interaction	F Statistic, p value	Current Effect Size (Cohen's f)	Current Power	Sample Size: Power≥ 0.8
Stretch + Acid	F(3,30)=1.447; p=0.2486	0.38	0.845	11
Rear + Acid	F(3, 30)=0.6602; p=0.5830	0.257	0.486	23
Nesting + Acid	F(3,30)=1.555; p=0.2207	0.395	0.874	11
Nesting	F(3,30)=0.5434; p=0.6564	0.234	0.411	27
Locomotor	F(2, 20)=0.9772; p=0.3936	0.313	0.587	19

Supplemental Table IV.VII. Summary of power analysis results from two-way ANOVA for SA57 from Figure IV.IV.

Supplemental Table IV.VII				
	SA-57			
Main Effect of Dose	F Statistic, p value	Current Effect Size (Cohen's f)	Current Power	Sample Size: Power≥ 0.8
Stretch + Acid	F(2.226, 22.26)=4.922; p=0.0145*	0.702	0.999	4
Rear + Acid	F(2.421, 24.21)=0.3686; p=0.7344	0.193	0.256	44
Nesting + Acid	F(1.913, 19.13)=4.249; p=0.0311*	0.562	0.992	7
Nesting	F(1.101, 11.01)=4.643; p=0.0515	0.681	0.95	9
Locomotor	F(1.55, 15.50)=2.732; p=0.1039	0.446	0.819	12
Main Effect of Sex	F Statistic, p value	Current Effect Size (Cohen's f)	Current Power	Sample Size: Power≥ 0.8
Stretch + Acid	F(1, 10)=5.188; p=0.046*	0.694	0.583	19
Rear + Acid	F(1,10)=0.0222; p=0.8845	0.03	0.051	>100

Nesting + Acid	F(1,10)=0.007; p=0.9347	0.014	0.05	>100
Nesting	F(1,10)=0.3414; p=0.572	0.135	0.071	>100
Locomotor	F(1, 10)=14.62; p=0.0034*	0.841	0.747	14
Dose x Sex Interaction	F Statistic, p value	Current Effect Size (Cohen's f)	Current Power	Sample Size: Power≥ 0.8
Stretch + Acid	F(3, 30)=2.832; p=0.0550	0.533	0.991	7
Rear + Acid	F(3, 30)=1.708; p=0.1864	0.413	0.905	10
Nesting + Acid	F(3,30)=0.6439; p=0.5929	0.253	0.471	23
Nesting	F(3,30)=0.1504; p=0.9286	0.123	0.137	91
Locomotor	F(2, 20)=0.9772; p=0.3936	0.313	0.587	19

Supplemental Table IV.VIII. Summary of power analysis results from two-way ANOVA for URB597 from Figure IV.V.

Supplemental Table IV.VIII				
	URB-597			
Main Effect of Dose	F Statistic, p value	Current Effect Size (Cohen's f)	Current Power	Sample Size: Power≥ 0.8
Stretch + Acid	F(2.656, 26.56)=1.202; p=0.3251	0.346	0.724	14
Rear + Acid	F(1.351, 13.51)=1.138; p=0.3258	0.337	0.483	23
Nesting + Acid	F(1.908, 19.08)=3.360; p=0.0581	0.579	0.972	8
Nesting	F(1.721, 17.21)=0.5996; p=0.5362	0.246	0.324	35
Locomotor	F(1.949, 19.49)=3.229; p=0.0626	0.568	0.983	7
Main Effect of Sex	F Statistic, p value	Current Effect Size (Cohen's f)	Current Power	Sample Size: Power≥ 0.8
Stretch + Acid	F(1,10)=1.181; p=0.3027	0.227	0.11	>100
Rear + Acid	F(1, 10)=0.5780; p=0.4646	0.173	0.084	>100
Nesting + Acid	F(1,10)=0.2623; p=0.6196	0.11	0.064	>100
Nesting	F(1,10)=0.01015; p=0.9217	0.02	0.05	>100
Locomotor	F(1, 10)=2.872; p=0.121	0.41	0.251	49
Dose x Sex Interaction	F Statistic, p value	Current Effect Size (Cohen's f)	Current Power	Sample Size: Power≥ 0.8
Stretch + Acid	F(3, 30)=0.5332; p=0.6630	0.232	0.403	27
Rear + Acid	F(3, 30)=1.088; p=0.3690	0.33	0.719	14
Nesting + Acid	F(3,30)=2.094; p=0.1219	0.11	0.118	>100
Nesting	F(3,30)=1.4; p=0.2619	0.375	0.834	12
Locomotor	F(2, 20)=0.3896; p=0.6824	0.196	0.262	44

Supplemental Table IV.IX. Summary of power analysis results from two-way ANOVA for PF3845 from Figure IV.V.

Supplemental Table IV.IX				
	PF3845			
Main Effect of Dose	F Statistic, p value	Current Effect Size (Cohen's f)	Current Power	Sample Size: Power≥ 0.8
Stretch + Acid	F(2.561, 25.61)=0.5551; p=0.6227	0.237	0.381	29
Rear + Acid	F(1.998, 19.98)=0.24; p=0.7887	0.048	0.06	>100
Nesting + Acid	F(1.706, 17.06)=1.910; p=0.1817	0.436	0.755	14
Nesting	F(2.154, 21.54)=17.29; p<0.0001*	1.312	1	4
Locomotor	F(1.949, 19.49)=3.229; p=0.0626	0.568	0.983	7
Main Effect of Sex	F Statistic, p value	Current Effect Size (Cohen's f)	Current Power	Sample Size: Power≥ 0.8
Stretch + Acid	F(1, 10)=0.1126; p=0.7442	0.072	0.056	>100
Rear + Acid	F(1, 10)=1.031; p=0.3339	0.185	0.089	>100
Nesting + Acid	F(1,10)=0.6999; p=0.4223	0.119	0.066	>100
Nesting	F(1,10)=0.2573; p=0.6230	0.097	0.061	>100
Locomotor	F(1, 10)=2.872; p=0.121	0.41	0.251	49
Dose x Sex Interaction	F Statistic, p value	Current Effect Size (Cohen's f)	Current Power	Sample Size: Power≥ 0.8
Stretch + Acid	F(3, 30)=0.3898; p=0.5654	0.264	0.508	21
Rear + Acid	F(3,30)=0.4743; p=0.7025	0.217	0.357	31
Nesting + Acid	F(4, 40)=0.2741; p=0.8930	0.167	0.22	51
Nesting	F(4, 40)=0.9107; p=0.4670	0.301	0.631	17
Locomotor	F(2, 20)=0.3896; p=0.6824	0.196	0.262	44

Chapter V: Effects of repeated MJN110 on pain-related depression of nesting in male and female mice

Introduction

Chapters III and IV demonstrated IP acid's reproducible and robust acute depression of nesting behavior, and Chapter IV showed acute antinociceptive effectiveness of 1.0 mg/kg MJN110 to attenuate acute IP acid-induced depression of nesting. Previous studies have shown functional tolerance following chronic administration of the MAGL-selective inhibitor JZL184 (Schlosburg et al., 2010), and the few studies that have evaluated the antinociceptive effectiveness of repeated MJN110 show mixed results regarding development of tolerance (Burston et al., 2016; Thompson et al., 2020). Accordingly, the goal of this study was to assess the effects of repeated administration of 1.0 mg/kg MJN110 on IP acid-depressed nesting behavior across 7 days. Male and female mice were divided into four groups that received either MJN110 or its vehicle 2 hours prior to administration of IP acid or its vehicle, and nesting consolidation data was collected to evaluate MJN110 and IP acid effects on nesting behavior.

Materials and Methods

Subjects

Male and female ICR mice (Envigo Laboratories, Indianapolis, IN) were 6-8 weeks old upon arrival, individually housed, and acclimated for at least one week before beginning studies. In an AAALAC-approved facility, mice had ad libitum access to food (Teklad LM-485 Mouse/Rat Diet, Harlan Laboratories) and water in cages (31.75 x 23.50cm^2 floor x 15.25cm high) mounted in a RAIR HD Ventilated Rack (Lab Products, Seaford, DE) with corncob bedding (Harlan Laboratories) and a "nestlet" composed of pressed cotton (Ancare, Bellmore, NY). The temperature-controlled housing room was maintained on a 12-hour light/dark cycle (lights on from 7:00AM to 7:00PM), and all testing occurred during the light phase. Females weighed 20-35g and males weighed 25-45g throughout the study. Animal use protocols were approved by the Virginia Commonwealth University Institutional Animal Care and Use Committee and complied with the National Research Council Guide for the Care and Use of Laboratory Animals.

Behavioral Procedures

Nesting Procedure. Studies were conducted in two cohorts of 48 mice tested five months apart (24 female and 24 male mice in each cohort; 96 mice total). Behavioral and pharmacological procedures were identical between the two cohorts as described below, and all mice met an inclusion criterion that required them to build a nest within 24hr of arrival to the laboratory. After 1 week of acclimation, testing occurred over a 7-day period as shown in Figure V.I, and mice were randomly allocated into the following four treatment groups (N=6/sex/treatment/cohort) to receive daily treatment with SC injection of 1.0 mg/kg MJN110 or its vehicle (Veh) followed 2h later by IP injection of 0.32% lactic acid or its vehicle (H_2O). The routes of administration, doses, and pretreatment times for MJN110 and IP acid were based on previous studies (Niphakis et al., 2013; Ignatowska-Jankowska et al., 2015a; Diester et al., 2021b), and IP injections alternated between the subject's left and right sides across the 7-day study. Immediately after the IP injection, old nesting material was removed from the subject's home cage, two 1-in^2 nestlet squares were placed 11 inches apart in the center of the opposing short walls of the cage, and the mouse was returned to its home cage for a 90-min nesting session as described previously (Diester et al., 2021a). At the conclusion of the session, the position of the nestlets was photographed from above and the distance between the center of mass for each nestlet was measured to the nearest quarter inch. Studies were conducted at the same time each day in each mouse (starting at 10:00 AM) to minimize potential environmental or light-cycle confounds. Additionally, mice were weighted prior to injections on each test day. At 24-28h after the last nesting session, mice were euthanized by rapid decapitation and the following tissue regions were collected for studies of cannabinoid agonist-stimulated GTPγS binding: spinal cord (lumbar, rest of cord), cingulate cortex, caudate putamen, nucleus accumbens, amygdala, periaqueductal gray, ventral tegmentum area, cerebellum, and hippocampus. These data are not shown within this dissertation, but they will be analyzed and prepared for publication with this chronic behavioral dataset.

Data Analysis

Nesting Data. The primary dependent variable was % Maximal Nestlet Consolidation on each test day in each mouse, defined as [(11-End)/11] x 100], where 11 and End were the distances in inches between the nestlets at the start and end of the observation period, respectively. This nesting measure was treated as a ratio variable and analyzed by parametric statistics. Because results from the two cohorts were similar (Supp. Figure 1, Supp. Table 4), all data from the two cohorts were combined to yield 24 mice (12 female, 12 male) for each of the four treatment groups. Data analysis proceeded in a series of steps similar to our previously described method for assessment of sex as a biological variable in studies that include both sexes but are not intended *a priori* to be powered for detection of sex differences (Diester et al., 2019), with expansion to include the factor of time (days). The approach complies with the National Institutes of Health mandate to include both sexes in preclinical research and to include analyses that segregate results by sex (Miller et al., 2017; Tannenbaum et al., 2019). All analyses described below were conducted using GraphPad Prism (LaJolla, CA) with a criterion of significance set to $p<0.05$, inclusion of a Geisser-Greenhouse correction for repeated measures to correct for unequal variance, and post hoc analysis for significant ANOVAs using the Holm-Sidak test.

Our primary analysis focused on data across the 7-day study. Pooled data from both sexes and segregated data for each sex were first analyzed by a repeated-measures three-way ANOVA, with MJN110 and IP acid treatments as between-subject variables and days as a within-subject variable. If the three-way interaction was significant, follow-up two-way ANOVAs were conducted to evaluate variance of any two variables across each level of the third variable (MJN110, Acid, Days) (Kirk, 1995). If the three-way interaction and main effect of days were not significant but there was a significant MJN110 x Acid interaction, data were collapsed across days and analyzed by a two-way ANOVA. Lastly, to directly compare data from males and females, results were collapsed across days and analyzed by three-way ANOVA, with MJN110 treatment, IP acid treatment, and sex as the three between-subject variables.

Weight Data. Repeated IP acid may decrease body weight as a surrogate measure for pain-related and analgesic-reversible depression of feeding behavior (Stevenson et al., 2006; Legakis et al., 2020). Accordingly, weights for each subject were collected daily immediately prior to MJN110 or Veh administration. As with nesting data, our primary analysis focused on pooled data across both sexes and data segregated by sex. Specifically, Day-7 body weights for pooled data, females, and males were expressed as a percentage of Day-1 weights and analyzed by two-way ANOVA (MJN110 x Acid). As a secondary analysis, raw Day-1 weights and transformed Day-7 weights were also analyzed by three-way ANOVA with treatment groups (MJN110 x Acid) and sex as the three variables.

Drugs

Lactic acid (Fischer Scientific, NH) was diluted in sterile water and administered intraperitoneally. The MAGL-selective inhibitor MJN110 was kindly provided by Dr. Micah Niphakis (currently at Lundbeck La Jolla Research Center) and diluted in a vehicle (Veh) of 1:1:18 ethanol, emulphor (Alkamuls-620; Sanofi-Aventis, Bridgewater, NJ) and saline, and administered subcutaneously. All injections were administered in volumes of 0.1-0.9mL.

Results

Overview of Data Presentation

The effectiveness of repeated administration of MJN110 to alleviate IP acid-induced nesting depression was assessed across 7 days, with evaluation of pooled data shown in Figure V.I and data segregated by sex in Figure V.II. The effect of repeated MJN110 treatment on bodyweight in the absence and presence of repeated IP acid is shown in Figure V.III. Data evaluating the comparison between cohorts, effects of sex on MJN110 and IP acid treatment in pooled data collapsed across days, follow-up two-way ANOVAs for Figure V.IIC, and baseline weights are shown in Supplemental Figures V.I-IV, respectively. Tables with results for statistical analyses are shown as follows: three-way ANOVA results in Supplemental Table V.I, two-way ANOVA results collapsed

across days in Supplemental Table V.II, two-way ANOVA results per day (Figure V.IIC) in Supplemental Table V.III, and Welch's t-tests in Supplemental Table V.IV.

Effects of repeated MJN110±IP Acid in pooled data from both sexes. Figure V.I shows the effectiveness of repeated 1.0 mg/kg SC MJN110 to alleviate daily IP acid-induced nesting depression in pooled data from both female and male mice. Briefly, the three-way ANOVA indicated a significant MJN110 x Acid interaction with no main effect of Day or Day x MJN110 x Acid interaction (Figure V.IB, Supp. Table V.I). Accordingly, data were collapsed across days and analyzed by two-way ANOVA (Figure V.IC, Supp. Table V.II). Vehicle-control mice (Veh/H_2O) nested at high and stable rates across the 7-day study, and MJN110-alone treatment did not alter nesting behavior following repeated administration (MJN110/H_2O). Repeated treatment with IP acid alone (Veh/Acid) produced a significant and sustained depression of nesting, and repeated dosing of MJN110 produced partial but significant alleviation of IP acid-depressed nesting (MJN110/Acid). Evaluation of sex as a determinant of treatment effects in Figure V.IC showed no main effect of Sex or interaction between Sex and Treatment (Supp. Figure V.II, Supp. Table V.I).

Effects of repeated MJN110±IP Acid on nesting in males and females. Although analysis of pooled data found no significant main effect of Sex or Sex x Treatment interaction, data segregated by sex suggests a differential trajectory of treatment effects over time in males and females (Figure V.II). In males, each treatment produced a relatively consistent effect over time, with no significant main effect of Day or Day x Treatment interaction in the three-way ANOVA (Supp. Table V.I). As with the pooled data, the resulting two-way ANOVA collapsed across days (Fig. V.IIB) indicated both acid-induced depression of nesting and a weak but significant partial antinociception by repeated 1.0 mg/kg MJN110 (Supp. Table V.II).

Conversely, the three-way ANOVA in females showed a significant three-way interaction between Day, MJN110 dose, and IP Acid concentration (Supp. Table V.I). Follow-up two-way ANOVAs of MJN110 x Acid

treatment effects for each day indicated significant acid-induced depression of nesting for all 7 days and significant MJN110 partial antinociception only on Days 1, 3, and 5. Supplemental Table V.III shows these two-way ANOVA results for each treatment day, and Figure V.IID highlights the results for Days 1 and 7. On Day 1, in agreement with our previously published acute study described in Chapter IV (Diester et al., 2021b), MJN110 significantly alleviated IP acid-induced depression of nesting; however, on Day 7 there was only a main effect of acid treatment and no antinociceptive effect of MJN110 (Supp. Table V.III). Additional follow-up two-way ANOVAs evaluating variance across levels of MJN110 and acid are shown in Supplemental Figure V.III, with significant interactions followed by a Dunnett's post-hoc comparison to Day 1 data. These analyses showed no change in Veh/H_2O, Veh/Acid, and MJN110/H_2O treatment groups across the 7-day study, and a significant change in MJN110/Acid treatment effects only on Day 6.

Effects of repeated MJN110±IP Acid on Body Weights. Figure V.III shows treatment effects on body weights at the end of the study. Two-way ANOVA of pooled data showed main effects of MJN110 treatment (to increase body weights) and IP acid treatment (to decrease body weights), but the interaction was not significant (Supp. Table V.II). Thus, although MJN110 alleviated IP acid-induced depression of body weight, this effect could not be attributed to antinociception because MJN110 increased body weight regardless of IP acid treatment. Segregation of data by sex indicated that the main effect of MJN110 treatment was driven by the females, with significant main effects of MJN110 and IP acid treatments for females but only a main effect of IP acid in the males. Supplemental Figure V.IV shows body weight data with sex included as a variable (Supp. Table V.I). On Day 1, males were heavier than females, but there were no significant differences in basal weights across treatment groups. When Day-7 data were expressed as a percentage of Day-1 weights, there was no main effect of sex and no sex x treatment interaction (Supplemental Figure V.IVB).

Discussion

Chapter V evaluated the effects of repeated administration of 1.0 mg/kg MJN110 on episodic IP acid-induced depression of nesting across 7 days of treatment. There were four main findings. First, vehicle control mice (Veh/H2O) nested at high and steady rates across the 7-day study, suggesting that nesting behavior in mice can serve as a robust and stable behavioral endpoint for studies of repeated exposure to experimental manipulations. Second, repeated treatment with MJN110 alone (MJN110/H2O) across 7 days did not alter nesting behavior. Thus, repeated treatment with this dose of MJN110 alone did not produce evidence of general behavioral disruption. Third, repeated IP acid alone treatment (Veh/Acid) produced a significant and sustained depression of nesting across all seven days of testing, with a potential trend for decreased effectiveness in females. Taken together, these findings of sustained, repeatable, and pain-related nesting depression by IP acid enables repeated dosing studies with candidate analgesics like MJN110. Lastly, in evaluation of pooled data from both sexes, MJN110 produced partial but sustained antinociception throughout the 7 days of treatment. Segregation of data by sex revealed differential effects, with MJN110 producing a weak but sustained partial attenuation of IP acid-induced depression of nesting in males and a loss of antinociceptive effect in females. Overall, the weak antinociceptive effect in males and variable effects following repeated dosing in females suggest that MJN110 may not be an ideal candidate analgesic for treatment of visceral episodic pain.

Figures

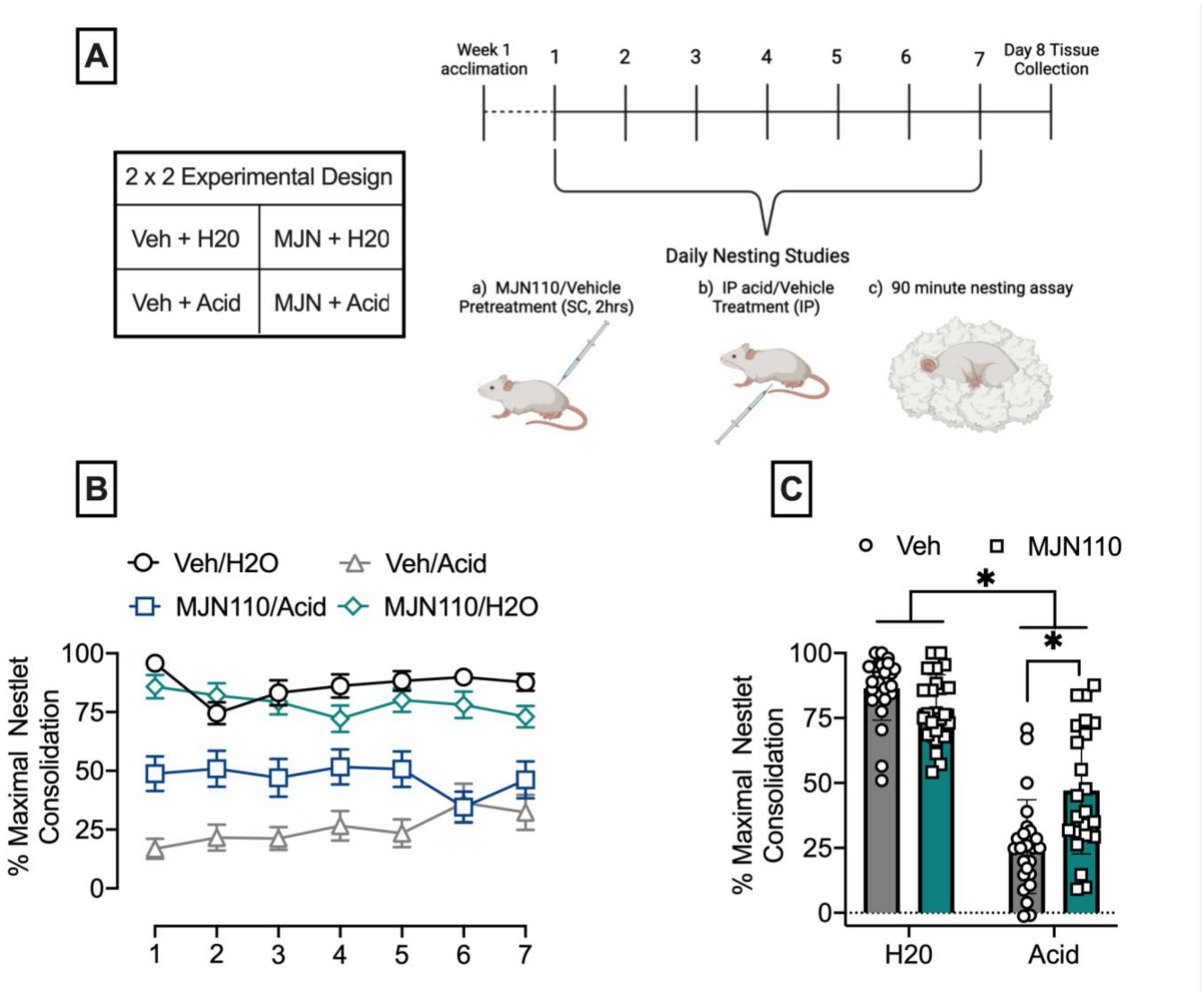

Figure V.I. Study overview and effects of repeated administration of MJN110 on daily IP acid-induced nesting depression in mice. (A) Graphical illustration of experimental design for the study. (B) Treatment effects on nesting behavior across the seven days of treatment. Abscissa: experimental days. Ordinate: nesting behavior expressed as percent maximal nestlet consolidation. Each point shows mean±SEM for 24 mice (12 per sex). (C) Data from Panel B collapsed across days. Abscissa: treatment with IP H_2O or IP Acid. Ordinate: nesting behavior expressed as percent maximal nestlet consolidation. Bars show mean±SEM for 24 mice (12 per sex) in each treatment group, and circles (Veh pretreatment) and squares (MJN110 pretreatment) show individual data. Asterisks (*) indicates a significant difference as determined by two-way ANOVA and Holm-

Sidak post hoc test, $p<0.05$. Three-way ANOVA results for (B) are shown in Supp. Table V.I, and two-way ANOVA results for (C) are shown in Supp. Table V.II.

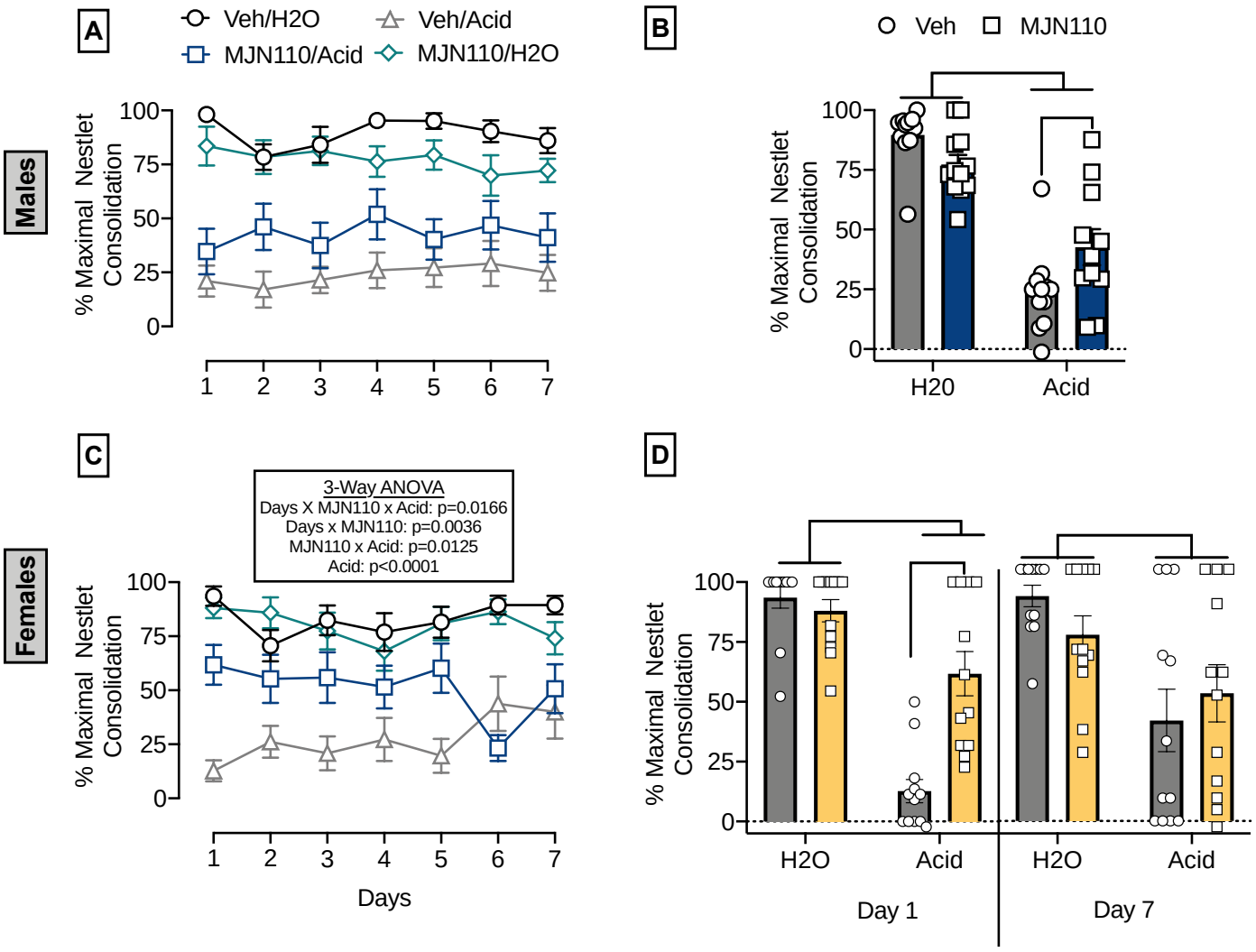

<u>Figure V.II.</u> Differential effects of repeated MJN110±IP acid treatment in female and male mice.

Treatment effects on nesting behavior across seven days of treatment in males (Panel A&B) and females (Panel C&D). Abscissae for panels A&C: experimental days. Ordinates for panels A&C: nesting behavior expressed as percent maximal nestlet consolidation, with each point representing mean±SEM for 12 mice per treatment. Abscissae for panels B&D: treatment with IP H_2O or IP Acid. Ordinates for panels B&D: nesting behavior expressed as percent maximal nestlet consolidation, with bars representing mean±SEM for 12 mice in each treatment group, and circles (Veh pretreatment) and squares (MJN110 pretreatment) showing individual data. For males in Panel A, the three-way interaction was not significant, and there was no significant effects of Day or Day x Treatment interaction. Accordingly, data were collapsed across days, evaluated by two-way ANOVA,

and results are shown in Panel B. For females in Panel C, the three-way interaction was significant, and data on each day were analyzed by two-way ANOVA, with data for Days 1 and 7 highlighted in Panel D. Asterisks (*) indicate significant effects determined by two-way ANOVA and Holm-Sidak post hoc tests ($p<0.05$). Three-way ANOVA results for (A) and (C) are shown in Supp. Table V.I, two-way ANOVA results for (B) are shown in Supp. Table V.II, and two-way ANOVA results for (D) are shown in Supp. Table V.III.

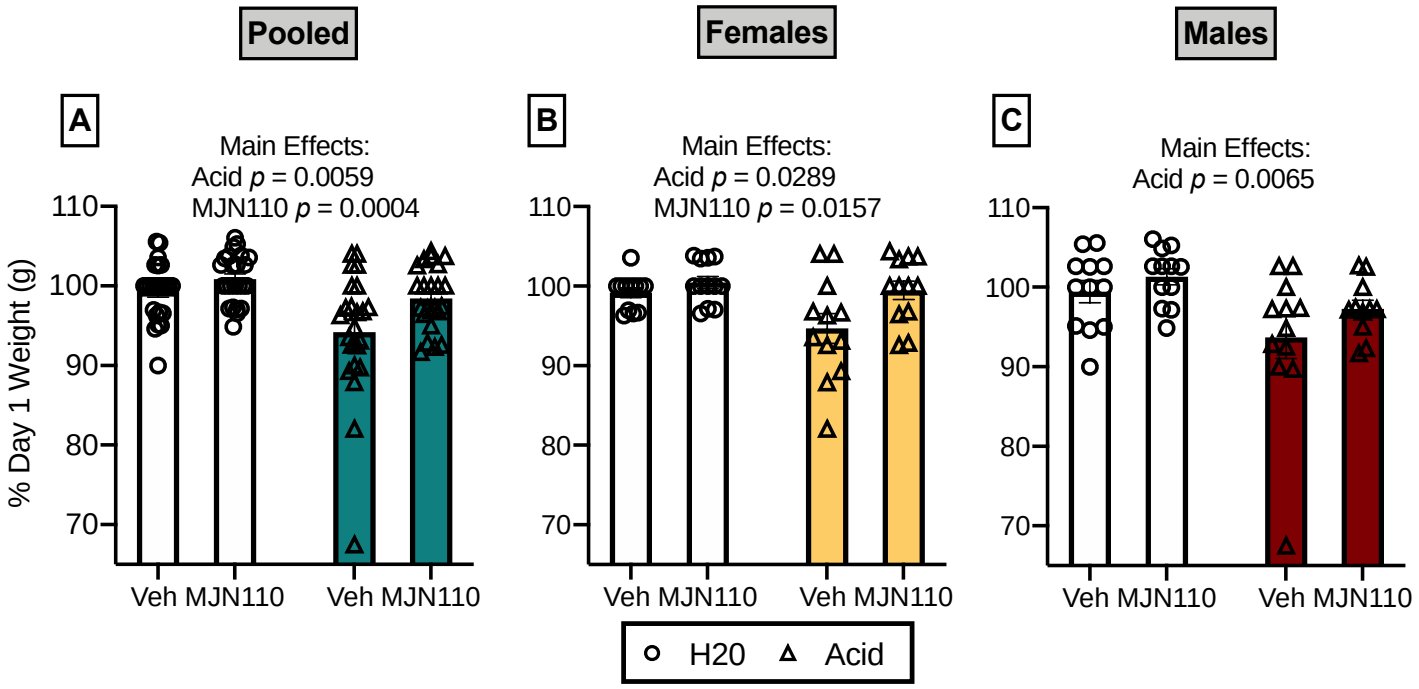

<u>Figure V.III.</u> Opposing effects of MJN110 and IP acid treatment on body weight. Abscissae: MJN110 or Veh treatment, delivered SC in a volume of 10 ml/kg. Ordinates: bodyweight expressed as percent of baseline Day 1 weights. Bars show mean±SEM for 12 mice per sex in each treatment group, and circles (H_2O treatment) and triangles (IP acid treatment) show individual data. Significant main effects determined by two-way ANOVA and Holm-Sidak post hoc test ($p<0.05$) are displayed above each panel. Detailed two-way ANOVA results for all above panels are shown in Supp. Table V.II.

Supplemental Table V.I: Summary of statistical analyses from three-way ANOVA data. Asterisks (*) indicate a significant main effect or interaction ($p<0.05$).

Figure	F statistic	p value
1B	Days: F(5.592, 508.9) = 0.4017	0.8666
	MJN110: F(1, 91) = 3.667	0.0586
	Acid: F(1, 91) = 165.1	<0.0001*
	Days x MJN110: F(6, 546) = 2.762	0.0118*
	Days x Acid: F(6, 546) = 1.507	0.1736
	MJN110 x Acid: F(1, 91) = 16.70	<0.0001*
	Days x MJN110 x Acid: F(6, 546) = 1.207	0.3010
2A	Days: F(5.262, 226.3) = 0.6207	0.6924
	MJN110: F(1, 43) = 0.4142	0.5233
	Acid: F(1, 43) = 100.2	<0.0001*
	Days x MJN110: F(6, 258) = 0.6973	0.6520
	Days x Acid: F(6, 258) = 1.011	0.4188
	MJN110 x Acid: F(1, 43) = 9.627	0.0034*
	Days x MJN110 x Acid: F(6, 258) = 0.3625	0.9022
2C	Days: F(5.218, 229.6) = 0.5829	0.7203
	MJN110: F(1, 44) = 3.908	0.0544
	Acid: F(1, 44) = 65.62	<0.0001*
	Days x MJN110: F(6, 264) = 3.326	0.0036*
	Days x Acid: F(6, 264) = 1.338	0.2404
	MJN110 x Acid: F(1, 44) = 6.790	0.0125*
	Days x MJN110 x Acid: F(6, 264) = 2.643	0.0166*
Supp. 1A	Sex: F(1, 87) = 0.3477	0.5569
	MJN110: F(1, 87) = 3.506	0.0645
	Acid: F(1, 87) = 162.9	<0.0001*
	Sex x MJN110: F(1, 87) = 0.9676	0.3280
	Sex x Acid: F(1, 87) = 1.121	0.2926
	MJN110 x Acid: F(1, 87) = 16.20	0.0001*
	Sex x MJN110 x Acid: F(1, 87) = 0.06765	0.7954
Supp. 2A	MJN110: F(1, 87) = 0.5851	0.4464
	Sex: F(1, 87) = 255.7	<0.0001*
	Acid: F(1, 87) = 0.1580	0.6820
	MJN110 x Sex: F(1, 87) = 0.0009	0.9761
	MJN110 x Acid: F(1, 87) = 1.637	0.2042
	Sex x Acid: F(1, 87) = 0.0019	0.9655
	MJN110 x Sex x Acid: F(1, 87) = 0.2346	0.6294
Supp. 2B	MJN110: F(1, 87) = 7.614	0.0071*
	Sex: F(1, 87) = 0.2260	0.6357
	Acid: F(1, 87) = 13.35	0.0004*
	MJN110 x Sex: F(1, 87) = 0.02271	0.8806
	MJN110 x Acid: F(1, 87) = 1.565	0.2142
	Sex x Acid: F(1, 87) = 1.079	0.3017
	MJN110 x Sex x Acid: F(1, 87) = 0.1923	0.6621

Supplemental Table V.II: Summary of statistical analyses from two-way ANOVA data**.** Asterisks (*) indicate a significant main effect or interaction ($p<0.05$).

Figure	F statistic	p value
1C	Acid: F(1, 91) = 165.1 MJN110: F(1, 91) = 3.667 Acid x MJN110: F(1, 91) = 16.70	<0.0001* 0.0586 <0.0001*
2B	Acid: F(1, 43) = 100.2 MJN110: F(1, 43) = 0.4142 Acid x MJN110: F(1, 43) = 9.627	<0.0001* 0.5233 0.0034*
3A	Acid: F(1, 91) = 13.57 MJN110: F(1, 91) = 7.964 Acid x MJN110: F(1, 91) = 1.670	0.0004* 0.0059* 0.1995
3B	Acid: F(1, 44) = 5.104 MJN110: F(1, 44) = 6.319 Acid x MJN110: F(1, 44) = 2.130	0.0289* 0.0157* 0.1515
3C	Acid: F(1, 43) = 8.190 MJN110: F(1, 43) = 2.530 Acid x MJN110: F(1, 43) = 0.2456	0.0065* 0.1190 0.6227

Supplemental Table V.III: Summary of two-way ANOVA results for Figure V.IIC. Asterisks (*) indicate a significant main effect or interaction ($p<0.05$).

Day	F statistic	p value
1	Acid: F(1, 44) = 76.66 MJN110: F(1, 44) = 12.66 Acid x MJN110: F(1, 44) = 19.85	<0.0001* 0.0009* <0.0001*
2	Acid: F(1, 44) = 19.91 MJN110: F(1, 44) = 6.951 Acid x MJN110: F(1, 44) = 0.6952	<0.0001* 0.0115* 0.4089
3	Acid: F(1, 44) = 21.60 MJN110: F(1, 44) = 2.834 Acid x MJN110: F(1, 44) = 4.990	<0.0001* 0.0994 0.0306*
4	Acid: F(1, 44) = 12.24 MJN110: F(1, 44) = 0.6592 Acid x MJN110: F(1, 44) = 3.077	0.0011* 0.4212 0.0864
5	Acid: F(1, 44) = 22.24 MJN110: F(1, 44) = 5.233 Acid x MJN110: F(1, 44) = 5.535	<0.0001* 0.0270* 0.0232*
6	Acid: F(1, 44) = 47.61 MJN110: F(1,44) = 2.222 Acid x MJN110: F(1, 44) = 1.223	<0.0001* 0.1432 0.2748
7	Acid: F(1, 44) = 14.73 MJN110: F(1, 44) = 0.05755 Acid x MJN110: F(1, 44) = 1.903	0.0004* 0.8115 0.1748

Supplemental Table V.IV: Summary of statistical analyses from Welch's t-tests in Supp. Figure V.I**.** Asterisks (*) indicate a significant effect ($p<0.05$).

Cohort 1 vs 2 Treatment Groups	Welch's corrected t; p value	F-test (variance); p value
Veh/H2O	t = 0.7201; p = 0.7201	F = 4.067; p = 0.0284*
Veh/Acid	t = 0.417; p = 0.6422	F = 1.263; p = 0.7057
MJN110/H2O	t = 0.2496; p = 0.8052	F = 1.048; p = 0.9392
MJN110/Acid	t = 0.3899; p = 0.7022	F = 3.853; p = 0.0366*

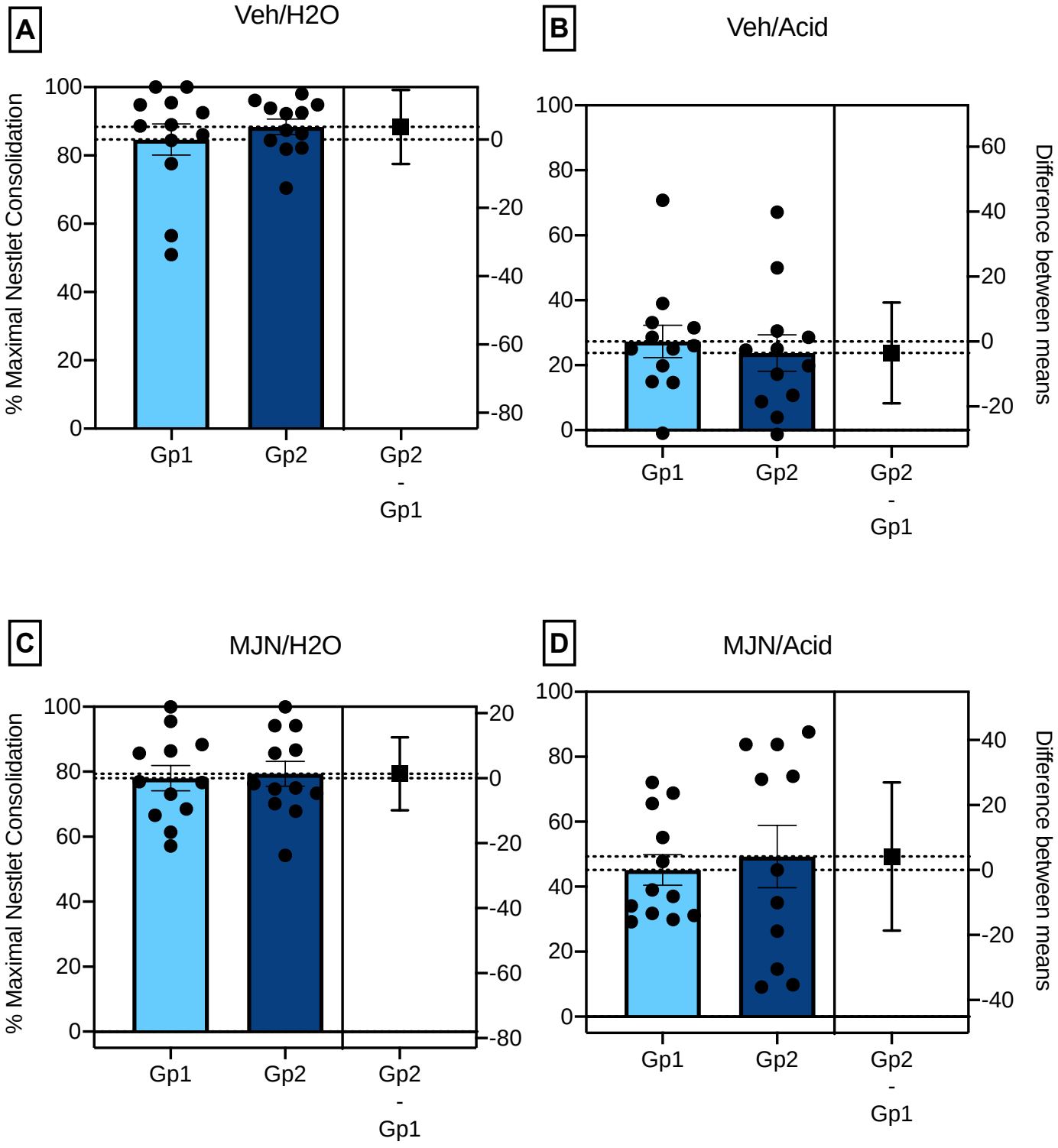

<u>Supplemental Figure V.I.</u> Comparison of treatment effects between Cohorts 1 and 2. Each panel shows one of the four treatment groups of Veh/H_2O (A), Veh/Acid (B), MJN110/H_2O (C), and MJN110/Acid (D). Abscissae: cohort number (left bars) and Difference Score between cohorts (right point). Ordinates: the left axis

denotes nestlet consolidation expressed as percent maximal nestlet consolidation, and the right axis denotes the difference between the means for each cohort calculated as Group2 – Group1. Circles represent an average for each subject across the 7-day study (N=12/Cohort/Group). Dashed lines represent means from each respective group, and squares represent the difference between means for each respective treatment group. Data across cohorts were compared by a two-tailed t-test with Welch's correction for unassumed equal standard deviation. There was not a significant difference in the means between cohorts in any treatment group, so cohorts were combined for all subsequent analyses. Welch's t-test results for all panels are shown in Supp. Table V.IV.

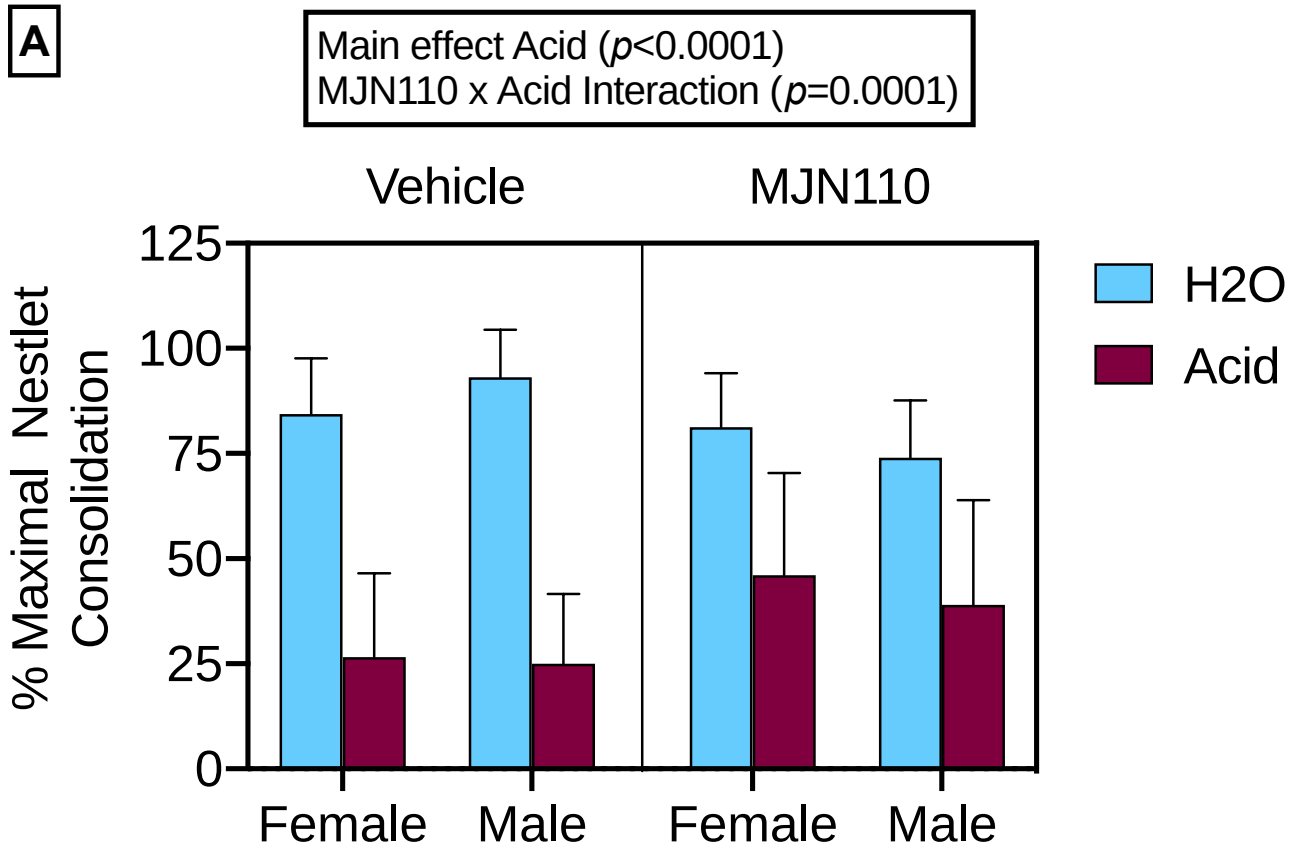

<u>Supplemental Figure V.II.</u> Evaluation of sex as a determinant of MJN110 effects on pooled data collapsed across days. Abscissae: male or female subjects (N=12/sex/treatment) with data collapsed across days. Ordinates: nestlet consolidation expressed as percent maximal nestlet consolidation. Data are visualized across the three variables, with bars representing H_2O (blue) and IP acid (maroon) treatments and boxed groups representing Vehicle (left group) and MJN110 (right group). 0.32% IP acid or H_2O were delivered IP, and 1.0 mg/kg MJN110 or Vehicle were administered SC, with all administered in a volume of 10 ml/kg. Data were analyzed by three-way ANOVA and Holm-Sidak post hoc test, $p<0.05$. Significant main effects and interactions are shown above the graph. Complete three-way ANOVA results are shown in Supp. Table V.I.

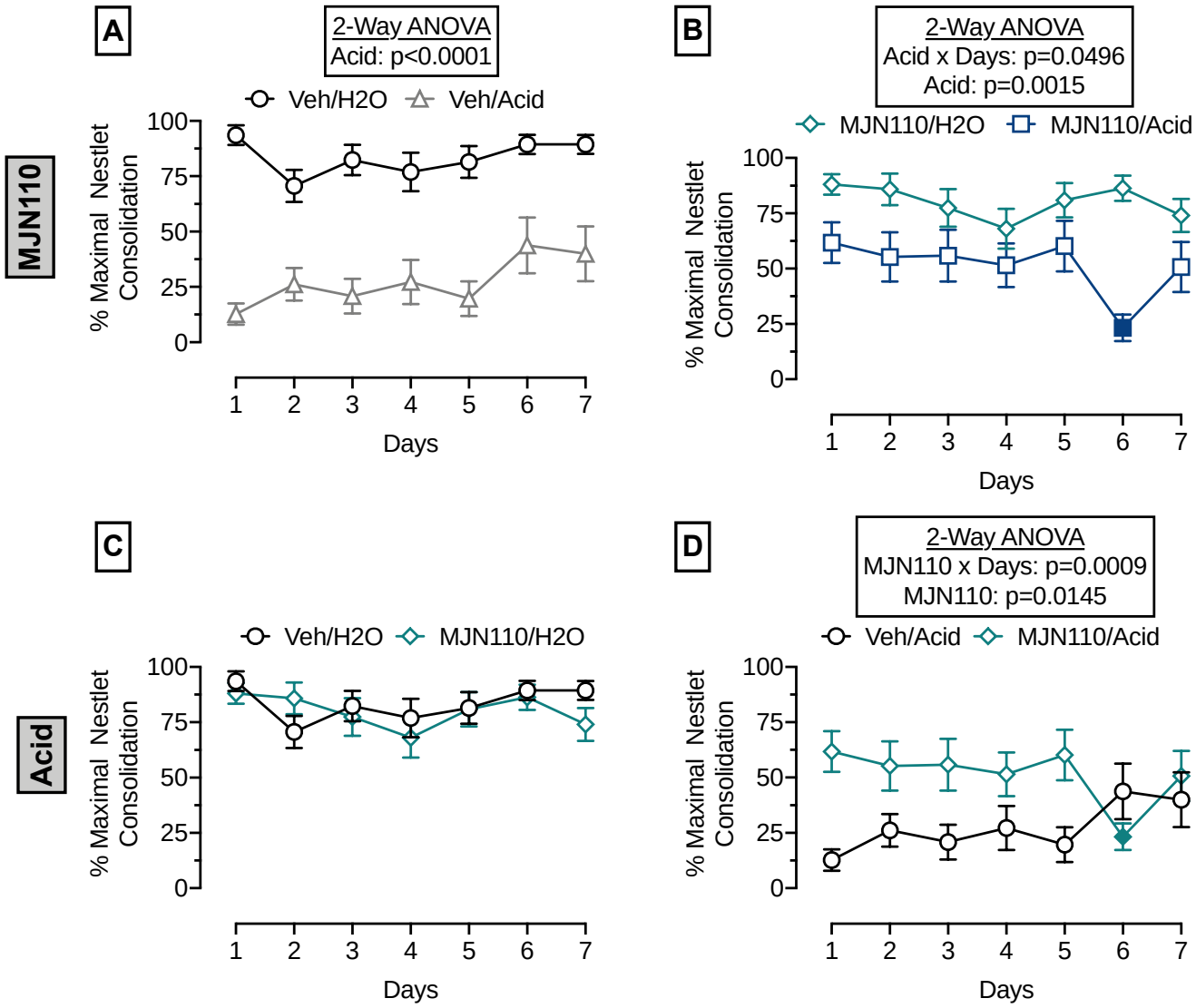

<u>Supplemental Figure V.III.</u> Follow-up two-way ANOVA analyses for female nesting data across MJN110 and Acid levels. Abscissae: experimental days. Ordinates: nesting behavior expressed as percent maximal nestlet consolidation. Each point shows mean±SEM for 12 female mice. Given the significant Days x MJN110 x Acid interaction in female nesting data (Supp. Table V.I), follow-up two-way ANOVAs were conducted to evaluate variance of days and acid across levels of MJN110 (Panels A&B) and variance of days and MJN110 across levels of acid treatment (Panels C&D). Significant interactions and main effects are displayed above each panel, with a significant Dunnett post hoc comparison to Day 1 indicated by a filled symbol ($p<0.05$).

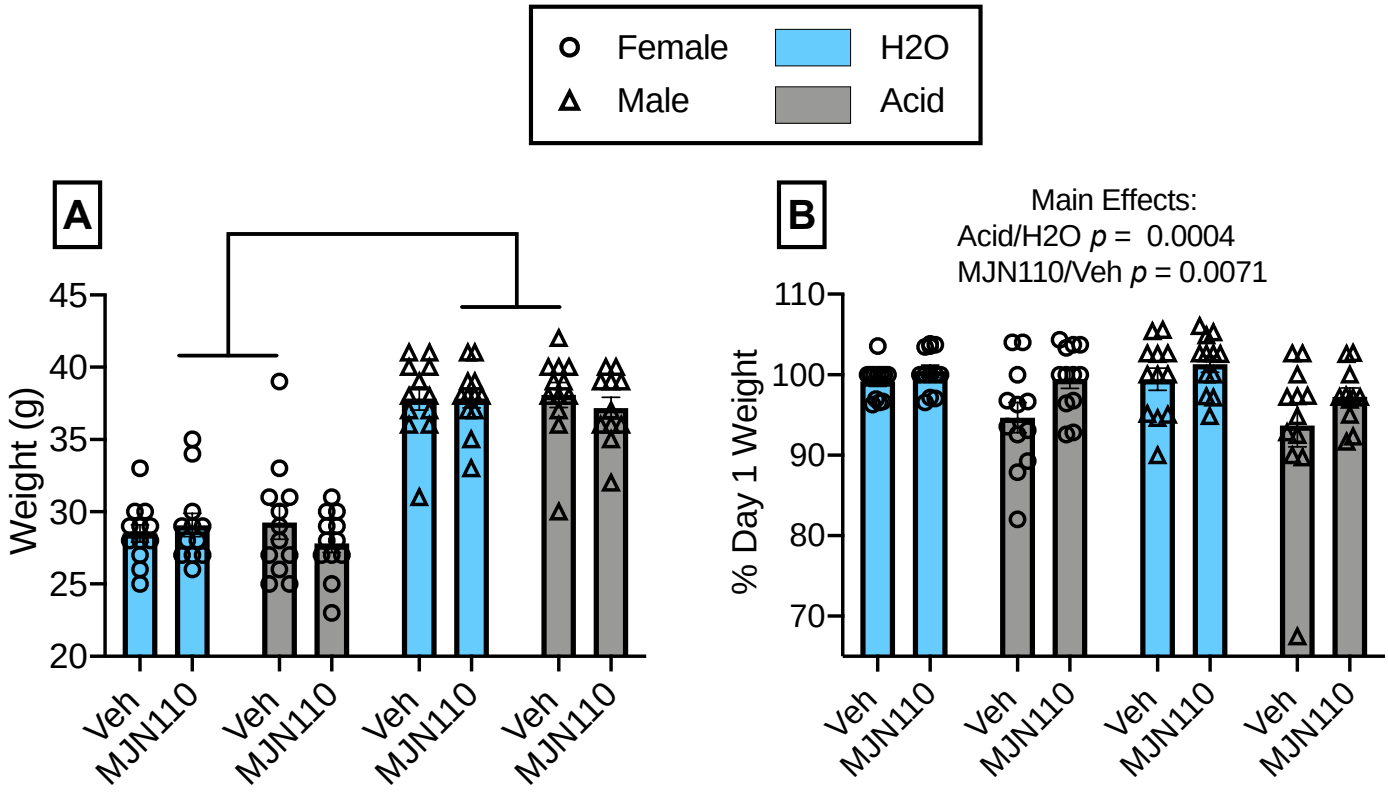

<u>Supplemental Figure V.IV.</u> Baseline weights and evaluation of sex as a determinant of repeated MJN110±IP Acid effects on weight. Abscissae: Veh or 1.0 mg/kg MJN110 treatment delivered SC in a volume of 10 ml/kg. Ordinates: baseline Day 1 weight in grams of male and female mice (A) and Day 7 bodyweight expressed as percent of baseline Day 1 weights (B), N=12/sex/treatment. Symbols and colors for groups are as follows: circles represent female data, triangles represent male data, blue represents H_2O treatment, and gray represents IP acid treatment. An asterisk (*) indicates a significant difference as determined by a three-way ANOVA, $p<0.05$. Main effects for panel (B) are shown at the top of the panel. Complete three-way ANOVA results for both panels are shown in Supp. Table V.I.

Chapter VI: Discussion

Summary

One of the largest discrepancies between preclinical and clinical assessment of pain and analgesia is the type of behavioral endpoint used. Although most preclinical research has historically focused on drug effectiveness to block reflexive withdrawal behaviors stimulated by a noxious stimulus, increasing evidence shows that drug-induced restoration of pain-depressed behaviors provides increased clinical translation with decreased susceptibility to false-positives. Accordingly, the first portion of this dissertation designed a behavioral battery that featured pain-depressed behaviors as well as more conventional pain-stimulated behaviors for testing candidate analgesics in male and female mice. The main findings are as follows. (1) Intraperitoneal injection of dilute lactic acid (IP acid) served as an effective visceral chemical noxious stimulus to produce concentration-dependent stimulation of two behaviors (stretching and facial grimace; pain-stimulated behaviors) and depression of two behaviors (rearing and nesting; pain-depressed behaviors). (2) Pharmacological characterization with two positive control analgesics (ketoprofen, oxycodone) and two active negative controls (diazepam, amphetamine) validated a strategy for distinguishing analgesics from nonanalgesics by profiling drug effects in this battery of complementary pain-stimulated and pain-depressed behaviors along with two additional pain-independent behaviors (nesting and locomotor activity in the absence of the IP acid noxious stimulus). (3) A National Institutes of Health mandate for consideration of Sex as a Biological Variable (SABV) was published at the start of this dissertation research. Accordingly, we developed an experimental design for considering SABV when sex differences are not the principle independent variable, with emphases on exploratory power analyses (effect size, power, predicted N) and segregation of data by sex to allow transparent analysis of SABV and help guide future study designs.

The second portion of this dissertation applied this behavioral battery and SABV data-analysis strategy to evaluate a spectrum of endocannabinoid (eCB) catabolic enzyme inhibitors ranging in selectivity for the eCB catabolic enzymes monoacylglycerol lipase (MAGL) and fatty acid amide hydrolase (FAAH), which have received increasing interest for development of candidate analgesics. The main findings are as follows: (1)

antinociceptive effectiveness decreased as MAGL-selectivity decreased, with the most MAGL-selective inhibitor MJN110 producing the most effective antinociceptive profile, (2) time course and antagonism studies for MJN110 showed a long duration of antinociceptive action (40min – 6hrs), mediation by CB_1R but not CB_2-R, a tendency for greater effects in females, and (3) repeated administration of MJN110 produced partial but sustained attenuation of IP acid-induced depression of nesting, with segregation of data by sex demonstrating sustained but weak antinociception in males and variable effects following repeated dosing in females.

Overall, these data provide a framework for predicting the analgesic potential of test drugs in preclinical pain models in male and female mice, and suggest that MJN110 may have only partial effectiveness as a candidate analgesic for treatment of visceral episodic pain.

Implications for Chapter II

Overview

Chapter II establishes a general, multi-step approach to address The Four Cs articulated by the National Institutes of Health (NIH) when preclinical investigation of sex differences is not the primary aim and sample sizes required to detect sex differences are not known. Inclusion of both males and females is responsive to the "Consider" mandate for the experimental design that takes sex into account. The pooling of data across sex permits focus on the primary variable(s) of interest, while segregation of data by sex addresses the "Collect" mandate for tabulating sex-based data. The secondary analyses address the "Characterize" mandate by using ANOVAs to analyze sex-based differences with existing sample sizes and power analyses to guide both interpretation of the ANOVA results and design of any future studies that might focus on sex differences. Finally, the results of ANOVAs (F statistics) and power analyses (effect size, power, and predicted Ns) provide a useful array of statistical outcome measures that fulfill the "Communicate" mandate for reporting and publishing sex-based data.

Following the NIH mandate for inclusion of sex as a biological variable (SABV) in 2015, multiple groups have evaluated incorporation of SABV across preclinical disciplines (Guizzetti et al., 2016; Galea et al., 2020; Garcia-Sifuentes and Maney, 2021; Li et al., 2021). These studies almost exclusively operate under the assumption that analyses for sex differences should be conducted prior to any other statistical analyses, regardless of initial study design. For studies designed with sex as a primary variable, initial sex difference analyses would be appropriate. However, it should be noted sex is one of many secondary variables present within most preclinical study designs, and these other variables including species, age, strain, and environment. Any variable intended for secondary analysis should not be treated as a primary variable, regardless of highlighted interest.

Reporting of underpowered comparisons between males and females may lead to misleading false negatives and contradictory conclusions within the literature. As sex-dependent conclusions can only be determined through direct comparisons of males and females, studies underpowered for such analyses should practice transparency in reporting of sex differences (i.e. study design and power analyses) and segregate data by sex to identify possible underlying sex differences that would otherwise be masked through underpowered ANOVA comparisons and pooled datasets (Miller et al., 2017; Galea et al., 2020; Duffy and Epperson, 2021). Chapter 5 nicely displays examples where only relying on direct comparison of males vs females via ANOVAs would have shown no sex differences for MJN110 antinociceptive effectiveness to alleviate IP acid-induced depression of nesting, while segregation of data by sex elucidated this effect to be predominately driven by females.

Intentional design of studies that include SABV as a secondary variable for preliminary studies does not imply that there is not a need for increased inclusion of SABV in preclinical research. There is a growing literature detailing how fundamental neurobiological processes differ between sexes that may help rectify clinical discrepancies in male and female treatments (Anderson, 2008; Sorge et al., 2011; Kokras and Dalla, 2014; Bangasser and Wicks, 2017; Golden and Voskuhl, 2017; Fullerton et al., 2018; Shansky, 2018; De Bellis et al., 2020). As fields of research evolve to continually improve our understanding of a plethora of multifaceted

clinical diseases, it will be crucial to ensure clear frameworks for appropriate study designs (with attention to behavioral contingencies of researchers) are developed to generate reproducible and clinically impactful research.

Implications for Chapter III

Overview

Chapter III compared the effects of two clinically effective analgesics (ketoprofen, oxycodone) and two active negative controls (diazepam and amphetamine) on a panel of pain-stimulated, pain-depressed, and pain-independent behaviors in male and female mice. There were three main findings. First, IP acid served as an effective chemical noxious stimulus to produce a concentration-dependent stimulation of stretching and facial grimace and depression of rearing and nesting as putative pain-related behaviors. Test drugs could then be evaluated for their profiles of antinociceptive effectiveness to alleviate these IP acid effects. Second, the positive-control analgesics ketoprofen and oxycodone produced antinociception in assays of both pain-stimulated and pain-depressed outcome measures (with ketoprofen being the most efficacious) at doses below those that altered nesting and/or locomotion in the absence of the IP acid noxious stimulus, whereas the negative controls diazepam and amphetamine did not. These results suggest that analgesic potential of test drugs can be predicted by higher potency to alleviate pain-related stimulation and depression of behavior than to produce pain-independent motor disruption in mice. Lastly, sex differences in drug effects were not a primary focus of the present study and few sex differences were identified; however, the inclusion of equal numbers of male and female mice permitted exploratory power analysis of sex differences that could guide future studies designed to focus on sex as a primary variable of interest. Overall, this study outlines an experimental design and a framework of results with positive and negative controls that can be used to study and interpret effects of candidate analgesic drugs.

Effects of IP lactic acid as a noxious stimulus

The results in Chapter III confirm and extend previous studies in finding that IP injection of dilute acid serves as an effective noxious stimulus to stimulate stretching (Koster et al., 1959; Collier et al., 1968; Stevenson et al., 2006; Booker et al., 2009; Do Carmo et al., 2009; Miller et al., 2012; Bagdas et al., 2016; de la Puente et al., 2017; Alexander et al., 2019) and facial grimace (Langford et al., 2010) and to depress rearing (Cho et al., 2013; Cobos and Portillo-Salido, 2013) and nesting (Negus et al., 2015; Lewter et al., 2017; Alexander et al., 2019). The present study builds on these previous results by showing that potency of IP lactic acid was similar across all four endpoints. Additionally, our approach assessed stretching, facial grimace, and rearing simultaneously during the same video sessions to provide cost- and time-efficient data collection on both pain-stimulated and pain-depressed behaviors in the same subject. Nesting was assessed in different subjects tested in their home cages, which provided an opportunity to assess generality of results across different subjects and testing environments. Finally, the current study improved the primary dependent measure of IP acid-depressed nesting from an ordinal variable (Negus et al., 2015) to a ratio variable to decrease subjectivity and enable utility of parametric statistical analyses.

Effects of ketoprofen and oxycodone

The data presented in Chapter III agree with previous evidence that ketoprofen and other COX inhibitors are effective to produce antinociception against a range of chemical and inflammatory pain stimuli producing an array of pain-related behaviors including stretching (Seguin et al., 1995; Bagdas et al., 2016; Alexander et al., 2019), facial grimace (Leach et al., 2012; Matsumiya et al., 2012; Tuttle et al., 2018a; Cho et al., 2019; de Almeida et al., 2019), depression of rearing (Matson et al., 2007; Nagase et al., 2012) and depression of nesting (Negus et al., 2015; Oliver et al., 2018; Alexander et al., 2019). In the present study, ketoprofen potency and efficacy were similar to alleviate IP acid-induced stimulation of stretching and facial grimace and depression of nesting, and although ketoprofen was less potent to alleviate IP acid-induced depression of rearing, it did significantly restore rearing at 10 mg/kg. The antinociceptive effectiveness of ketoprofen on endpoints of both pain-stimulated and pain-depressed behaviors provides one source of evidence to suggest that ketoprofen effects

reflected sensory blockade of the acid noxious stimulus rather than production of nonspecific motor effects that might impede expression of nociceptive behaviors. This conclusion is further supported by the finding that antinociceptive ketoprofen doses did not alter nesting or locomotion in the absence of the IP acid noxious stimulus. Previous studies have also reported ketoprofen antinociception at doses without evidence of motor disruption (Niemegeers et al., 1975; Julou et al., 1976; Negus et al., 2015; Alexander et al., 2019). Taken together, these findings are consistent with the clinical analgesic efficacy of ketoprofen and other COX inhibitors for treatment of inflammatory pain (Moore and McQuay, 2013), and they also demonstrate sensitivity of this panel of behavioral endpoints to a clinically effective analgesic as a positive control.

The MOR agonist oxycodone is also a clinically effective analgesic to treat inflammatory and other types of pain, but it produced a profile of effects distinct from that of ketoprofen. Like ketoprofen, oxycodone attenuated acid-induced stimulation of stretching and facial grimace and depression of nesting at doses that did not alter locomotion or nesting in the absence of the noxious stimulus. This agrees with other evidence to suggest that MOR agonists can alleviate some inflammation-related pain-stimulated and pain-depressed behaviors at doses that do not alter other pain-independent behaviors (Matson et al., 2007; Cobos et al., 2012; Cobos and Portillo-Salido, 2013; Bagdas et al., 2016; Lewter et al., 2017; Negus, 2019). However, unlike ketoprofen, oxycodone produced only a partial alleviation of acid-induced depression of nesting, and it failed to alleviate acid-induced depression of rearing. Previous studies have also reported limited effectiveness of MOR agonists to alleviate some types of pain-related behavioral depression, and this limited efficacy appears to reflect MOR agonist-induced motor effects that prevent antinociceptive restoration of function in assays of pain-depressed behavior (Matson et al., 2007; Cobos et al., 2012; Elhabazi et al., 2012; Cho et al., 2013; Kendall et al., 2016; de la Puente et al., 2017). In the present study, for example, oxycodone significantly increased locomotion and produced a small though nonsignificant decrease in control nesting at 3.2 mg/kg. These motor effects could have contributed to the descending limb of the inverted-U shaped dose-effect curve for oxycodone effects on IP acid-induced nesting depression and prevented expression of oxycodone antinociception on acid-induced rearing depression (which was also less responsive to ketoprofen, see above).

Taken together, these results suggest that this panel of behaviors is also sensitive to MOR agonist analgesics and provides data that can be used to interpret interactions between analgesic and motoric drug effects.

Effects of diazepam and amphetamine

The $GABA_A$ receptor positive allosteric modulator diazepam produced significant antinociception against both IP acid-stimulated stretching and grimace, a finding that agrees with other evidence for antinociception by diazepam and related benzodiazepines in preclinical assays of pain-stimulated behaviors elicited by chemical noxious stimuli (Rosland et al., 1987; Fidecka and Pirogowicz, 2002; Munro et al., 2008; Chiba et al., 2009). However, as in these previous studies, diazepam antinociception was observed only at a high dose that also produced evidence of motor impairment in the absence of the noxious stimulus, suggesting that apparent antinociception reflected motor impairment rather than analgesia. This conclusion was further supported by the failure of diazepam to alleviate IP acid-induced depression of either rearing or nesting, and indeed, diazepam only exacerbated IP acid-induced depression of rearing. Moreover, this conclusion is also consistent with the lack of diazepam analgesic effectiveness in humans (Raft et al., 1977) and for the absence of a clinical indication for diazepam as a stand-alone treatment for pain (Physician's Desk Reference, 2020).

Overall, these results illustrate the vulnerability of traditional assays of pain-stimulated behavior to false-positive effects with drugs that produce sedation or motor impairment. A traditional strategy to address this vulnerability has been to compare drug potency to produce antinociception with potency to impair motor performance in the absence of the noxious stimulus, but this approach is not always reliable (Seguin et al., 1995). Combined drug evaluation in complementary assays of both pain-stimulated and pain-depressed behavior as shown here can further reduce false positives and enhance selectivity for clinically effective analgesics while also probing drug effects on clinically relevant outcome measures related to behavioral depression and functional impairment (Cobos et al., 2012; Negus et al., 2015; Bagdas et al., 2016; Negus, 2019).

Like the non-analgesic behavioral depressant diazepam, the psychostimulant and dopamine/norepinephrine releaser amphetamine also failed to produce antinociception at doses lower than those that altered locomotor activity as a pain-independent behavior. This data demonstrates the utility of including locomotion to capture pain-independent increases, as basal nesting occurs near assay capacity. This data is consistent with previous evidence that amphetamine and other related psychostimulants (e.g. dopamine transporter inhibitors like cocaine) can produce antinociception in assays of both pain-stimulated behavior (Tocco and Maickel, 1984; Gatch et al., 1999; Connor et al., 2000; Alexander et al., 2019) and pain-depressed behavior (Matson et al., 2007; Negus et al., 2012; Rosenberg et al., 2013). However, amphetamine and related psychostimulants generally produce antinociception only at doses that also stimulate behavior in the absence of a noxious stimulus (suggesting a lack of behavioral selectivity), and they do not always restore pain-related behavioral depression in preclinical studies (Matson et al., 2007; Alexander et al., 2019) (suggesting limited effectiveness). Nonetheless, it is noteworthy that amphetamine produced antinociception on all four nociceptive endpoints in this study. Although amphetamine is not approved for use as an analgesic, it has been found to produce weak analgesic effects in humans and can augment the analgesic effects of opioids (Dalal and Melzack, 1998; Westfall and Westfall, 2011). These analgesic effects may be related to effectiveness of amphetamine and related psychostimulants to alleviate pain-related depression of mesolimbic dopamine signaling (Wood, 2008; Leitl et al., 2014; Martikainen et al., 2018; Watanabe and Narita, 2018). As increased dopamine also can cause increases in general motor behavior, this proves difficult to parse true analgesia from psychostimulant effects.

With regard to its effects on pain-independent behaviors in the present study, the inverted-U shaped dose-effect curve for amphetamine in the assay of locomotor activity is consistent with previous studies (Rethy et al., 1970; Tyler and Tessel, 1979). In particular, the decrease in locomotion at 10 mg/kg likely reflected recruitment of stereotypies that competed with and reduced horizontal locomotion (Tyler and Tessel, 1979; Matson et al., 2007). High baseline nesting near the ceiling of the assay's dynamic range may have prevented detection of any stimulation of nesting by lower amphetamine doses; however, depression of nesting by 10 mg/kg amphetamine may also have reflected stereotypies that competed with and reduced nesting behavior.

Implications for Chapter IV

Chapter IV characterized THC and a spectrum of endocannabinoid catabolic enzyme inhibitors ranging in selectivity from MAGL-selective to FAAH-selective in a battery of pain-stimulated, pain-depressed, and pain-independent behaviors pharmacologically characterized in Chapter III. There were three main findings in this study. First, THC significantly attenuated IP acid-stimulated stretching and facial grimace at doses that did not produce general motor disruption, but THC did not alleviate IP acid-induced depression of either rearing or nesting. Second, for the eCB catabolic enzyme inhibitors, the MAGL-selective inhibitor MJN110 produced antinociception without motor disruption on three of four endpoints, including significant alleviation of IP acid-induced depression of nesting, whereas the FAAH-selective inhibitor PF3845 failed to produce antinociception on any endpoint up to a dose that produced motor disruption. Other eCB catabolic enzyme inhibitors produced effects between these extremes. Lastly, time course and antagonism studies for MJN110 in the assay of IP acid-induced depression of nesting indicated a long duration of antinociceptive action (40 min to 6 hrs) and mediation by CB_1R but not CB_2R. Overall, these results support further consideration of MAGL-selective inhibitors, especially MJN110, as candidate analgesics.

Effects of Δ9-THC

The results in Chapter IV agree with previous work that showed subcutaneous THC to be more potent to decrease IP acid-stimulated stretching than to produce locomotor impairment (Booker et al., 2009). In contrast, THC is less potent in assays with acute thermal and mechanical noxious stimuli, resulting in relatively similar potencies to produce antinociception and locomotor impairment (Sofia et al., 1975; Cravatt et al., 2001; Varvel, 2005; Grim et al., 2016; Britch et al., 2017; Grim et al., 2017). The present study extended this literature by including facial grimace as a second pain-stimulated behavior and assessment of the two pain-depressed endpoints nesting and rearing. THC was less potent and effective to decrease IP acid-stimulated facial grimace than stretching. Moreover, in agreement with our previous work with pain-depressed behaviors in rats (Kwilasz

and Negus, 2012; Leitl and Negus, 2016), THC failed to attenuate IP acid-induced depression of either nesting or rearing. The poor efficacy of THC to alleviate signs of pain-related behavioral depression aligns with clinical studies that show weak or no analgesic efficacy of THC on measures of acute pain in humans (Raft et al., 1977; Greenwald and Stitzer, 2000; Wallace et al., 2007; Lötsch et al., 2018; Mun et al., 2020). As such, these results support the translational validity of preclinical assays of pain-depressed behaviors.

Effects of MAGL>>FAAH-selective inhibitors

Previous studies have demonstrated that selective MAGL inhibition produces antinociception in assays of pain-stimulated behavior through increasing central 2-AG levels and enhancing endogenous eCB tone (Niphakis et al., 2013; Ignatowska-Jankowska et al., 2015a; Donvito et al., 2018). While other studies have shown antinociceptive effectiveness of MAGL-selective inhibitors in models of acute thermal pain and chronic inflammatory or neuropathic pain (Niphakis et al., 2013; Ignatowska-Jankowska et al., 2015a; Burston et al., 2016; Wilkerson et al., 2018; Thompson et al., 2020), our study extended this literature by assessing their effectiveness using an acute visceral inflammatory stimulus. MJN110 potency to decrease IP acid-stimulated stretching was similar to its potency in inflammatory/neuropathic models and higher than its potency for acute thermal nociception. We further extended the literature by assessing IP acid-stimulated facial grimace and IP acid-depressed nesting and rearing. The potency of MJN110 was similar in assays of IP acid-stimulated grimace and stretching, but the effect on grimace was small and not dose dependent. Although MJN110 did not alleviate IP acid-induced depression of rearing, it did alleviate IP acid-depressed nesting with a stable level of antinociceptive effectiveness across a 10-fold dose range. Doses that produced antinociception did not alter pain-independent behaviors in our study; however, MJN110 doses of 1.25 and 2.5 mg/kg increased locomotor speed and distance traveled in another study (Ignatowska-Jankowska et al., 2015a). Accounting for possible differences in sensitivity between these two measures of locomotion, this hyperlocomotive effect is particularly intriguing as it is diametrically opposed to typical $CB_{1/2}R$ agonist-induced hypolocomotion (Figure 6) (Stark and Dews, 1980; Varvel, 2005; Wiebelhaus et al., 2015; Grim et al., 2017).

Further assessment for the antinociceptive time course of 1.0 mg/kg MJN110 in the assay of IP acid-depressed nesting agreed with previous studies that showed behavioral effects and increased 2-AG levels starting after ~1 hour and lasting several hours (Niphakis et al., 2013; Ignatowska-Jankowska et al., 2015a). While all reports agree with our results showing MJN110 antinociception is blocked by rimonabant to implicate CB_1R, the role of CB_2R is less clear (Ignatowska-Jankowska et al., 2015a; Burston et al., 2016; Thompson et al., 2020). This may reflect differential recruitment of CB_2R across the noxious stimuli assessed in these studies, with neuropathic and chronic inflammatory manipulations being more likely to enhance CB_2R expression and signaling (Burston et al., 2013; Donvito et al., 2018). Our studies agree with previous evidence that CB_2R are not necessary for MJN110 antinociception in acute-pain models (Ignatowska-Jankowska et al., 2015a). The role of sex as a determinant of MNJ110 effects is discussed below.

The other MAGL-selective inhibitor JZL184 did not significantly alleviate IP acid-stimulated stretching (Long et al., 2009a; Sakin et al., 2015). Similar to MJN110, it weakly reduced facial grimace and alleviated IP acid-induced depression of nesting but not rearing at doses that did not alter pain-independent behaviors. The poor effectiveness of JZL184 on the present measures of pain-stimulated behavior contrasts with previous evidence for antinociception across multiple acute pain-stimulated endpoints (Long et al., 2009b; Long et al., 2009c; Schlosburg et al., 2010; Kamimura et al., 2018). Additionally, the failure of JZL184 to alter pain-independent behaviors contrasts with previous evidence that JZL184 doses of 20-40 mg/kg increase (Aliczki et al., 2013; Bedse et al., 2018) or decrease (Long et al., 2009b; Kinsey et al., 2011; Ignatowska-Jankowska et al., 2015a; Wiebelhaus et al., 2015) other behaviors. These discrepancies may reflect two issues. First, these previous studies only included male subjects, and the role of sex as a determinant of drug effects is discussed below. Second, JZL184 was delivered subcutaneously as a suspension in this study. Methods for JZL184 preparation in previous reports are unclear, but communication with authors and published results show varying preparation techniques aimed at enhancing solubility, including preparation immediately prior to injection, heating JZL184 solutions, and use of different vehicles (Kinsey et al., 2009; Long et al., 2009b; Long et al., 2009c). These alterations alongside intraperitoneal administration may produce pharmacokinetic differences

that result in higher effective doses and stronger antinociception than observed here. However, effectiveness of JZL184 to alleviate IP acid-induced nesting depression suggests that behaviorally active doses were tested.

Effects of dual MAGL and FAAH inhibitors

Previous evidence supports enhanced antinociceptive effects for dual inhibition of MAGL and FAAH in comparison to selective inhibition for either enzyme alone to alleviate acute thermal noxious stimuli (Long et al., 2009c). Our results did not support this for an acute visceral noxious stimulus because the dual MAGL/FAAH inhibitors JZL195 and SA57 were not more effective than the selective MAGL inhibitors to produce antinociception. Specifically, both JZL195 and SA57 alleviated IP acid-induced stimulation of stretching and depression of nesting at doses that did not alter pain-independent behaviors, but neither drug alleviated IP acid-induced grimace or depression or rearing. The potency of JZL195 to reduce IP acid effects on stretching and nesting in the present study (32 mg/kg SC) was similar to its potency to produce antinociception in an assay of warm-water tail-withdrawal in mice (20 mg/kg IP) (Long et al., 2009c). Long et al. (2009c) also found that 20 mg/kg IP JZL195 decreased locomotor activity and produced catalepsy, and other groups have also shown decreased locomotor activity or rotarod performance at similar or lower doses (Anderson et al., 2014; Adamson Barnes et al., 2016). Similarly, SA57 decreased IP acid-stimulated stretching in the present study at a similar potency (10 mg/kg SC) shown to produce acute thermal antinociception (12.5 mg/kg IP) (Wilkerson et al., 2017), but previous studies also found that intraperitoneal administration of similar SA57 doses produced many undesirable cannabimimetic effects including increased immobility, catalepsy, and decreased rectal temperature (Wiebelhaus et al., 2015; Wilkerson et al., 2017). The more selective effects of JZL195 and SA57 on pain-related vs. pain-independent behaviors in the present study may again reflect pharmacokinetic differences due to use of subcutaneous vs. intraperitoneal administration.

Effects of MAGL<<FAAH-selective inhibitors

Our results do not support FAAH-selective inhibitors as candidate analgesics for acute visceral pain. URB597 produced antinociception on only one endpoint (IP acid-induced nesting depression), and PF3845 failed to produce antinociception on any endpoint up to a dose that depressed locomotion. The effectiveness of URB597 to alleviate IP acid-induced nesting suppression agrees with previous evidence for URB597 antinociception in other assays of pain-depressed behavior (Miller et al., 2012; Kwilasz et al., 2014); however, URB597 did not alleviate depression of rearing, and in contrast to previous studies (Naidu et al., 2009; Miller et al., 2012; Kwilasz et al., 2014), URB597 was not effective to alleviate IP acid-stimulated behaviors. There is a similar discrepancy in the literature on URB597 antinociception in assays of acute thermal pain-stimulated behaviors (Kathuria et al., 2003; Miller et al., 2012). PF3845 was the most FAAH-selective inhibitor in this study, and it produced the least favorable profile of effects. Previous studies have reported small but significant antinociceptive effectiveness of PF3845 on some acute pain-stimulated behaviors (Schlosburg et al., 2009; Grim et al., 2014; Ghosh et al., 2015), but such effects were not detected here. Moreover, the failure of PF3845 to alleviate behavioral depression produced by IP acid in the present study agrees with failure of PF3845 to alleviate depression of marble burying in mice by a chronic constriction injury to the sciatic nerve (Wilkerson et al., 2018). The decrease in IP acid-independent nesting supports previous studies that have shown a similar potency to decrease marble burying and intracranial self-stimulation in mice (Kinsey et al., 2011; Wiebelhaus et al., 2015); however, these same doses were shown to have no effect on immobility time, operant food responding, or distance traveled (Kinsey et al., 2011; Ghosh et al., 2015; Wiebelhaus et al., 2015).

Sex as a determinant of drug effects

The present study was not powered to detect sex differences, but both females and males were included to conduct a secondary analysis using a strategy to provide preliminary insights on the role of sex as a determinant of drug effects (Diester et al., 2019). In general, sex-dependent antinociception was rare, and there were no sex x dose interactions for any drug on any endpoint. However, MJN110 consistently produced higher

antinociceptive effects in females than males in the assay of IP acid-induced nesting depression, whereas JZL184 produced a larger effect in males across three of the six endpoints. This discrepancy may be due in part to tissue-dependent differential activity of MJN110 and JZL184 with serine hydrolases other than MAGL, such as ABHD6, C16:0 and C18:1 MAGs (Long et al., 2009b; Niphakis et al., 2013). Further studies will be required to examine expression and mechanisms of sex differences in effects of eCB catabolic enzyme inhibitors.

Implications for Chapter V

Overview

Chapter V evaluated the effects of repeated administration of 1.0 mg/kg MJN110 on episodic IP acid-induced depression of nesting across 7 days of treatment. There were four main findings. First, vehicle control mice (Veh/H2O) nested at high and steady rates across the 7-day study, suggesting that nesting behavior in mice can serve as a robust and stable behavioral endpoint for studies of repeated exposure to experimental manipulations. Second, repeated treatment with MJN110 alone (MJN110/H2O) across 7 days did not alter nesting behavior. Thus, repeated treatment with this dose of MJN110 alone did not produce evidence of general behavioral disruption. Third, repeated IP acid alone treatment (Veh/Acid) produced a significant and sustained depression of nesting across all seven days of testing, with a potential trend for decreased effectiveness in females. Taken together, these findings of sustained, repeatable, and pain-related nesting depression by IP acid enables repeated dosing studies with candidate analgesics like MJN110. Lastly, in evaluation of pooled data from both sexes, MJN110 produced partial but sustained antinociception throughout the 7 days of treatment. Segregation of data by sex revealed differential effects, with MJN110 producing a weak but sustained partial attenuation of IP acid-induced depression of nesting in males and a loss of antinociceptive effect in females. Overall, the weak antinociceptive effect in males and variable effects following repeated dosing in females suggest that MJN110 may not be an ideal candidate analgesic for treatment of visceral episodic pain.

Effects of repeated IP acid-induced depression of nesting

Results from Chapter V showing repeatable IP acid-induced nesting depression and decreased body weight in male and female mice support previous studies from our laboratory showing that daily administration of IP acid produces reliable depression of operant responding and depression of body weights in male and female rats (Altarifi et al., 2015; Lazenka et al., 2018; Legakis et al., 2020). Additionally, these results extend the utility of IP acid-induced depression of nesting from acute studies suitable for acute evaluation of test-drug effects to this model of repeated episodic visceral pain suitable for evaluating effects of repeated test-drug administration. Chronic pain is a broad umbrella term for multiple pain etiologies and outcome measures. In preclinical research, chronic pain models often involve inflammatory or neuropathic manipulations that produce long-term hypersensitive withdrawal responses from mechanical or thermal stimuli. While advancements have been made in preclinical chronic pain models, such as inclusion of noxious stimuli that model specific disease states (i.e. bone cancer) and measurement of more clinically relevant endpoints (e.g. effects on spontaneous behavior) , the temporal pattern of the underlying pain state is often presumed to be relatively constant for periods of weeks to months (Mercadante et al., 2002; Burma et al., 2017). By contrast, IP acid treatment produces a relatively transient pain state lasting ~1-2 hr (Koster et al., 1959; Bagdas et al., 2016), with repeated daily IP acid administration producing repeatable expression of this transient pain state as a model of visceral episodic chronic pain. Thus, our study provides a model for temporal evaluation of candidate analgesic effectiveness on non-movement related episodic visceral pain (Mercadante et al., 2002), with concentration-dependent control of the IP acid noxious stimulus intensity (Diester et al., 2021a).

Partial and sustained antinociceptive effectiveness of MJN110

This study used the assay of repeated IP acid-induced nesting depression to examine antinociceptive effects of repeated treatment with 1.0 mg/kg MJN110, with the dose selected based on our previous acute-dosing study in Chapter IV. Our finding in the present study that repeated 1.0 mg/kg MJN110 produced

sustained partial attenuation of IP acid-induced depression of nesting in analysis of pooled data from both sexes and in males agrees with previous studies evaluating repeated administration of MJN110 in chronic models of cancer-induced bone pain (CIBP) (Thompson et al., 2020), and osteoarthritic pain (Burston et al., 2016). Interestingly, while both studies report sustained antinociceptive effects following repeated MJN110 administration, they suggest opposing conclusions regarding dosing parameters. Thompson *et al.* show repeated administration of MJN110 (1-10mg/kg) promoted sensitization to antinociceptive attenuation of CIBP-stimulated flinching behavior, while Burston *et al.* showed dose-dependent (1-5 mg/kg) development of tolerance to MJN110's antinociceptive effects on monosodium iodoacetate-stimulated behaviors. As our repeated dosing study assessed a single dose (1.0 mg/kg) within the lower dosing ranges of these studies, additional testing would be needed to determine whether repeated higher doses (3.2 & 10 mg/kg) produce sensitization or tolerance to MJN110's partial attenuation of IP acid-induced depression of nesting in male mice.

This work also agrees with studies investigating other MAGL-selective inhibitors, such as JZL184, which show sustained antinociception during repeated treatment of low JZL184 doses, with development of antinociceptive tolerance following persistent pharmacological inhibition of MAGL to be dose-dependent and likely contingent upon inflammatory mediators recruited within different pain models (Schlosburg et al., 2010; Ghosh et al., 2013; Kinsey et al., 2013). More specifically, repeated 4 mg/kg JZL184 did not produce tolerance in a variety of behavioral and neurochemical measures, while repeated 40 mg/kg JZL184 administration produced functional antagonism of antinociceptive effects, cross-tolerance to CB_1R agonists and FAAH-selective inhibitors, reduced CB_1R function and expression, and increased expression of off-target eCB lipids (Schlosburg et al., 2010; Ghosh et al., 2013; Kinsey et al., 2013). Based on this work, the 32 mg/kg JZL184 dose necessary to attenuate acute IP acid-induced depression of nesting in Chapter IV (Diester et al., 2021b) would likely lead to functional tolerance of the eCB system following repeated administration.

Finally, it should be noted that partial effectiveness of MJN110 in the present study contrasts with the more robust effectiveness of repeated treatment with other clinically effective analgesics, particularly for

treatment of pain-depressed behaviors. Examples for treatments that can fully block IP acid-induced behavioral depression in rodents include the MOR agonist morphine, the NSAID/COX-inhibitors ketorolac and ketoprofen, and the dopamine transport inhibitor buproprion (Stevenson et al., 2006; Altarifi et al., 2015; Legakis et al., 2020; Diester et al., 2021b).

Effects of repeated MJN110 and IP acid in females

Chapter IV shows that acute MJN110 tended to yield greater effectiveness in females compared to males in the assay of IP acid-induced nesting depression (Diester et al., 2021b). Chapter V extends this to evaluate the effectiveness of daily 1.0 mg/kg MJN110 treatment in repeated IP acid-induced depression of nesting in female mice across 7 days. Consistent with our previous acute studies, MJN110 significantly alleviated IP acid-induced depression of nesting on Day 1 of the study (Diester et al., 2021b). This antinociceptive effect was variable across the 7-day study, with only three of the seven days significantly different from Veh/Acid treated females. The basis for the loss of antinociception in this study requires further investigation, but the present results suggests that two processes may have contributed.

First, IP acid administered alone produced a significant and sustained depression of nesting throughout the 7-day treatment period; however, there was a trend for declining IP acid effects over time in females. While the mechanism for this remains to be determined, studies tracking the estrous cycle following neuropathic or repeated administration of chemical noxious stimuli have shown cycle disruption in adult female rats and mice (Hernandez-Leon et al., 2018; Guindon et al., 2019). Other studies have shown models of visceral pain-related behaviors can fluctuate with the female mouse and rat estrous cycle, demonstrating a generally protective and antinociceptive role for estrogen (Ji et al., 2008; Escudero-Lara et al., 2021; Tramullas et al., 2021). Additionally, this study delivers the chemical noxious stimulus to the peritoneal cavity, which is open through the genital canal in females but not in males, providing a potential mechanism for IP acid-induced alterations on estrous cycle and its associated hormones (Solass et al., 2016). Accordingly, additional work evaluating the estrous cycle across repeated IP acid treatment should be conducted.

Second, tolerance may have developed to MJN110-induced antinociception. While it is difficult to dissociate possible loss of antinociception of MJN110 from decreased nociception masking an antinociceptive effect, decreased intensity of the noxious stimulus would suggest complementary trends for increased antinociceptive effectiveness, which was not observed in this study. This behavioral effect was paralleled by evidence for CB_1R desensitization in the lumbar spinal cord of female but not male mice from the MJN110+IP acid treatment group (data not shown). Overall, the loss of significant antinociception by repeated MJN110 in females could reflect a decline in IP acid nociception, tolerance to MJN110 antinociception, or both, with future studies needed to further elucidate these antinociceptive versus nociceptive effects.

Loss of MJN110 antinociception following repeated dosing does not agree with previous studies that show 1 & 3 mg/kg MJN110 produces sustained antinociceptive effectiveness following 7-day repeated administration (Burston et al., 2016; Thompson et al., 2020). There are multiple factors for consideration of this difference in MJN110 antinociception. First, the previous studies were only conducted in males despite growing evidence for sex differences in pain processing (Greenspan et al., 2007; Sorge et al., 2011; Fullerton et al., 2018), cannabinoid pharmacology (Craft et al., 2013; Cooper and Craft, 2018; Farquhar et al., 2019), and endocannabinoid-mediated antinociception (Blanton et al., 2021). Our results showing a tendency for greater effectiveness of acute MJN110 antinociception in females and potential decreased effectiveness over time in females (but not males) agree with other reports within the literature that show general trends for increased sensitivity to antinociceptive effects of cannabinoids in females compared to males (Craft et al., 2013; Blanton et al., 2021) and increased development of tolerance in females following repeated dosing of CB_1R agonists (Wakley et al., 2015; Farquhar et al., 2019).

Second, previous studies showing continued antinociception of MJN110 used more sustained models of chronic pain and demonstrated antinociceptive effectiveness of MJN110 to be CB_2R-dependent (Burston et al., 2016; Thompson et al., 2020). We previously demonstrated a lack of CB_2R necessity for MJN110 antinociception in IP acid-induced depression of nesting (Diester et al., 2021b). The differential dependency on CB_1Rs vs CB_2Rs between various noxious stimuli is not yet fully understood; however, because CB_2Rs are

predominantly expressed on immune cells, it is possible that repeated MJN110 produces more sustained antinociception in models that recruit inflammatory mediators and produce more sustained pain-related behaviors. As MAGL inhibitors such as MJN110 have dual inhibitory capacity for neuronal signaling and proinflammatory mediators through decreased production of arachidonic acid (AA), antinociception dependent upon both CBRs combine CB_1R-inhibited neuronal signaling, CB_2R-activation on infiltrating immune cells, and decreased proinflammatory prostaglandins (e.g. (Thompson et al., 2020)). While it has not been directly studied, these additional mechanisms for antinociceptive effects aside from CB_1R-activation likely play an important role for antinociceptive effectiveness, receptor downregulation, and desensitization following repeated dosing.

Taken together, future studies would need to quantify effects of MJN110 treatment and IP acid treatment on AA and prostaglandins following acute and repeated dosing alongside identifying primary sites of nociceptive and antinociceptive actions (see Chapter VI), with the goal to better understand the role prostaglandins and other inflammatory mediators might play in MJN110's weak CB_1R-mediated attenuation of IP acid-induced depression of nesting in males and variable effects in females. However, given the weak antinociceptive effect of MJN110 in males and variable effects in females on IP acid-induced depression of nesting paired with the non-specific weight increase in females, our work provides little support for further consideration of MJN110 for treatment of episodic visceral pain.

IP acid-independent effects of MJN110 on bodyweights.

Our observation of IP acid-induced depression of body weights in male and female mice agrees with previous findings from our laboratory showing that 7-day repeated IP acid administration depressed body weight in male and female rats (Legakis et al., 2020). Moreover, the IP acid-induced depression of body weight in rats was blocked by the clinically effective analgesic ketoprofen, suggesting that is pain-related (Legakis et al., 2020). Decreases in body weight may serve as a surrogate measure for pain-related decreases in feeding behavior, and consistent with this conclusion, IP acid treatment has been shown to reduce more direct measures of feeding behavior in both mice and rats (Stevenson et al., 2006; Kwilasz and Negus, 2012). As a result, body

weight may serve as an additional endpoint for assessment of MJN110 effectiveness to alleviate pain-related behavioral depression.

Repeated MJN110 treatment did alleviate IP acid-induced weight loss in analysis of pooled data from both sexes and in females; however, this effect manifested as a significant main effect of MJN110 treatment in the two-way ANOVAs and not as a significant interaction between MJN110 and IP acid treatment, indicating that MJN110 increased body weight in females regardless of the presence or absence of the noxious stimulus. Accordingly, MJN110 attenuation of IP acid-induced weight loss cannot be attributed to antinociception in the pooled data or in females.

Our finding of MJN110-induced and IP acid-independent increases in body weight in females agrees with studies showing CB_1R agonists to produce robust appetite stimulation and antiemetic effects (Sticht et al., 2015; Brunton et al., 2018). Moreover, our results showing no effect of MJN110 on IP acid-independent body weight in males agrees with previous work in male rats (Sticht et al. 2019). In Sticht *et al.*'s study, acute treatment with a systemic dose of 10 mg/kg MJN110 did not alter body weight in unstressed rats, but it did significantly decrease feeding in both stressed and unstressed male rats. MJN110-induced depression of feeding was indicated to be peripherally mediated as centrally administered MJN110 (5 ug i.c.v) did not alter feeding or body weight (Sticht et al., 2019). Interestingly, pharmacological inhibition of MAGL seems to produce different effects than genetic deletion from birth, as knockout of MAGL in mice produced sustained body weight decreases from birth (Chanda et al., 2010). Accordingly, future work will be needed to elucidate the effects of MJN110 on weight and feeding behavior in male and female mice. For the purposes of the data in Chapter V, MJN110 alleviation of IP acid-induced decreases in body weight cannot be interpreted as evidence for antinociception.

Our results in female mice and previous work in male rats support further evaluation of MJN110 for treatment of emesis. It may be beneficial if future studies aim to optimize MJN110 effects through identification of pain states clinically shown with nausea or pain-related weight loss as a co-morbidity, such as chemotherapy

patients with peripheral neuropathy, as MJN110 may be able to alleviate pain-related weight loss even if it produces only modest pain relief (Rock and Parker, 2016).

Appendix: Development of Functional Immunohistochemical Staining for Chemical Phenotyping of Activated Neurons

Introduction

Chapters III-V show that IP acid is an effective acute noxious stimulus that can be employed for assessment of episodic pain-depressed nesting across 7 days. Based on work from our lab and others (Leitl et al., 2014; Taylor et al., 2019; Jhou, 2021; Markovic et al., 2021), we hypothesize that pain-depressed behaviors are mediated in part by depression of dopamine signaling in the mesolimbic system. More specifically, mesolimbic dopamine signaling is depressed by IP acid in part via negative regulation of VTA dopamine neurons by local GABAergic neurons in the RMTg. To evaluate mechanisms that might underlie the differential antinociceptive effectiveness of ketoprofen and MJN110 on IP acid-depressed nesting, the neuroanatomical signaling of the noxious stimulus must first be characterized. Accordingly, this study aimed to validate a method for assessment of neuroanatomical patterns of IP acid-induced cFos expression in mouse spinal cord, NAc, VTA, and RMTg alongside chemical phenotyping of activated neurons.

Materials and Methods

Subjects

Adult 6-8 week old male and female ICR mice (Envigo Laboratories, Indianapolis, IN) were acclimated for at least one week following arrival before beginning neuroanatomical studies. In cages (31.75 x 23.50cm^2 floor x 15.25cm high) mounted in a RAIR HD Ventilated Rack (Lab Products, Seaford, DE) with corncob bedding (Harlan Laboratories) and a "nestlet" composed of pressed cotton (Ancare, Bellmore, NY), mice had ad libitum access to food (Teklad LM-485 Mouse/Rat Diet, Harlan Laboratories) and water. Animals were maintained on a 12-hour light/dark cycle (lights on from 7:00AM to 7:00PM) in a temperature controlled AAALAC approved facility, with testing occurring during the light phase. All mice used for immunohistochemical studies were individually housed upon arrival, with females weighing 20-30g and males weighing 25-35g throughout the handling week. Animal use protocols were approved by the Virginia Commonwealth University Institutional

Animal Care and Use Committee and complied with National Research Council Guide for the Care and Use of Laboratory Animals.

Animal Handling and Tissue Collection

Following one week of acclimation, all animals were handled for four days in the experimental room prior to tissue collection, with at least 2 hours acclimation in the experimental room before handling. On day 1, mice were handled by the experimenter until one of the two endpoints: (1) the mouse settled and started grooming, or (2) 10 minutes passed. For all studies, only two mice reached the 10-minute time-out before grooming (total 44). For days 2-4, animals received daily intraperitoneal (IP) sterile water (H2O) injections, followed by handling until mice groomed. On day 5, mice were brought to the experimental room and acclimated for 2 hours. One hour prior to tissue collection, animals were given IP treatments of either 0.32% lactic acid or H2O and returned to their respective home cages, with a 30 minute between-subject window to account for perfusion and tissue collection time. Subjects were deeply anesthetized with 0.07mL of phenytoin-pentobarbital (390 mg/mL pentobarbital sodium, 50mg/mL phenytoin sodium; Euthasol, Virbac Animal Health, Patterson, Greeley, CO), followed by transcardial perfusion of ~5 mL 1x PBS and ~7 mL of 4% paraformaldehyde (PFA). Brains and spinal cords were immediately collected and post-fixed in 4% PFA for 24 hours. Laminectomies were performed to collect spinal cord tissue, with thoracic 10-13 (T10-13) and lumbar 1-5 (L1-5) collected based on peritoneal innervation of the spinal cord(Gebhart, 2000) as separate sections and post-fixed in 4% PFA for 24 hours. The iliac crest was used as the anchoring landmark for identification of spinal cord segments starting at L5, and the first rib was used to check placement of T13. Following 24 hours post-fixation in 4% PFA, brains and spinal cords were washed in cold PBS and placed in 30% sucrose for cryoprotection. Brains were mounted directly to the chuck with Tissue Plus®O.C.T compound (Fisher Health Care, 4585) for coronal sectioning, and spinal cord sections embedded in O.C.T. in cryomolds (Peel-A-Way™, Sigma-Aldrich, St. Louis, MO). Tissue was then cryosectioned (Leica CM 1950) at 40μm and placed into cold PBS with 0.02%

sodium azide (ThermoFisher, AAJ2161022) at 4°C for storage, with serial brain sections collected from the nucleus accumbens to start of the cerebellum and every 4th spinal cord section collected.

Overview of Experimental Design

The goal of this study was to develop a comprehensive method for animal handling, tissue collection, cryosectioning, immunohistochemical staining, and imaging for assessment of IP acid-related neuronal activation, followed by identification and correction of issues preventing reliable assessment of cellular biomarkers. Accordingly, the data from this study is presented in two parts. For the first study (Study 1), methods are detailed for immunohistochemical staining and image analysis, followed by results and a brief discussion evaluating the IHC protocol, with particular emphasis on necessary alterations that are detailed in Table 1. For the second study (Study 2), full amended IHC staining and image analysis methods are described, followed by results and a brief discussion on the effectiveness of the amended IHC protocol for reliable assessment of cellular biomarkers in mouse brain and spinal cord.

Study I

Immunohistochemistry I

Free-floating immunohistochemical staining was performed on spinal cord sections and sections from brain regions of interest (NAc, VTA and RMTg) identified through referencing the Mouse Brain Atlas (Paxinos, 2007). NAc sections were collected from +1.18mm AP to +0.74mm AP, VTA from -2.70 AP to -3.52, and RMTg from -3.55 AP to -4.75 AP. Tissue processed for GAD67 staining first underwent an antigen retrieval, with sections heated to 80°C in 10mM Citrate Buffer (pH 6) for 30 min. After cooling to room temperature for 15 min, sections were washed 3 times in PBS, then placed in a blocking buffer of 3% normal goat serum (NGS) (ThermoFisher, Waltham, MA, 10000C) and 0.25% Triton X-100 (Invitrogen, ThermoFisher, HFH10) in PBS for 1 hour at room temperature. Sections were then incubated in primary antibodies in blocking buffer for 2 days on a rocker at 4°C. Following 3 washes in cold 0.25% Triton solution, sections were light protected with

foil and incubated in secondary antibodies in blocking solution at room temperature for 3 hours on a rocker, followed by a final PBS wash. Sections were mounted on glass slides and cover slipped with VECTASHIELD HardSet Antifade Mounting Medium with DAPI (Vector Laboratories, H-1500). The following antibodies were used for each target: cFos: primary rabbit anti-cFos polyclonal antibody (1:1000, Synaptic Systems, 266 003) and secondary goat anti-rabbit IgG Alexa Fluor 488 (1:500, Invitrogen, ThermoFisher, A-11008, green); GAD67: primary mouse anti-GAD67 monoclonal antibody (1:1000, Abcam, ab26116) and secondary goat anti-mouse IgG Alexa Fluor 594 (1:500, Invitrogen, ThermoFisher, A-11005, red); TH: primary chicken anti-TH polyclonal antibody (1:1000, Abcam, ab76442) and secondary goat anti-chicken IgY Alexa Fluor 594 (1:500, Invitrogen, ThermoFisher, A-11042, red). For VTA and RMTg sections, every other section was split to form two groups co-labeled with either TH + cFos or GAD67 + cFos, and NAc and spinal cord sections were co-labeled with GAD67 + cFos.

Imaging and Analysis I

Images were obtained using an Olympus BX53 microscope with an X-Cite Series 120Q mercury short arc lamp (Excelitas Technologies, Mississauga, Canada) and a Keyence BZ-X800 automated microscope (Keyence, Osaka, Japan) with a halide lamp. Both instruments are equipped with GFP, Texas Red, and DAPI filters. Images for validation of stains in brain sections were acquired first on the Keyence at 4x and 10x magnification (Nikon objectives, Tokyo, Japan), with images stitched for whole-section observations, followed by 60x oil immersion (Olympus objectives, Tokyo, Japan) on the Olympus microscope. Spinal cord sections were imaged on the Keyence at 10x and 40x magnification. For all sections, the optimal plane for cFos observation was selected for image acquisition. Only qualitative analysis was performed to evaluate correct co-labeling and regional specificity of target stains.

Results I

General Protocol

In Study I, the animal handling, perfusions, and tissue collection provided high-quality fixed brain and spinal cord tissue for further sectioning and immunohistochemical processing. Figure A.I displays successful staining and image acquisition for VTA and spinal cord sections. More specifically, Figure A.IA shows representative images for the TH (red) and cFos (green) co-labeled VTA sections. In particular, inclusion of a laminectomy for spinal cord dissection yielded excellent anatomical preservation (Figure A.IB), and utilization of the iliac crest of the pelvis provided a reliable landmark for rapid lumbar vertebral segment identification. The free-floating method provided robust staining with decreased IHC solution volumes per tissue section (1 mL/well, ~16 sections/well).

Characterization and co-localization of TH, cFos, and GAD67 in VTA and Spinal Cord

Figure A.IA shows the 10x stitched image demonstrates a robust and anatomically-selective TH signal for identification of VTA and substantia nigra (SN) regions. The 60x oil immersion images demonstrate clear identification of cFos + TH positive cells. Two different types of co-labeled cells were identified as cFos + TH positive. Due to the nuclear localization of the cFos immunostain and cytosolic localization of the TH immunostain, most co-labeled neurons were identified as TH+ cells with a distinct cFos+ nucleus (yellow arrows). The clear TH signal also enabled identification of a second set of co-labeled cells that showed overlapping TH and cFos fluorescence (orange arrow), likely due to the focal plane capturing the top or bottom of the cell. Due to the thickness of sections, future quantification will focus on the first type for reliable counting of cFos+ and TH+ neurons (yellow arrows). Importantly, white arrows denote distinction of cFos+ only cells. Figure A.IB shows representative images for lumbar spinal cord sections co-labeled with GAD67 (red) and cFos (green) at 10x and 40x. The 10x image demonstrates the higher expression of GAD67 staining in the dorsal horn of the spinal cord, and the 40x images within the dorsal horn demonstrate a clear cFos signal and a sharp boundary for the GAD67 stain between the white matter and laminae I.

Protocol Issues

Table A.I provides an overview of issues encountered throughout the IHC protocol, with examples illustrated in Figure A.II. The primary issue encountered during initial protocol development was bacterial contamination of tissue sections during storage in PBS at 4°C following cryosectioning, resulting in little tissue for further immunohistochemical processing. The secondary issue was evaporation of mounting media, resulting in poor or unattainable image acquisition (Figure A.IIA). The third issue was uneven illumination across sections (Figure A.IIA), making stitched image acquisition or imaging of low signal-to-noise markers like GAD67 unreliable, along with cFos quantification across images. The fourth issue was poor reliability of GAD67 staining for identification of the RMTg, as shown in Figure A.IIB. Representative dashed white circles are placed where previous studies have described the RMTg to be (example image from (Taylor et al., 2019) in Figure A.IIB). The fifth issue during Study I was a low signal-to-noise ratio for cFos staining, creating difficult quantification across sections dependent upon regional autofluorescence. The sixth and final issue was fragility of spinal cord sections, which is especially important considering the peripheral location of the dorsal horn region of interest.

Discussion I

The protocol developed in Study I established a solid basis for immunohistochemical neuronal identification of cFos and TH in brain and spinal cord; however, a variety of issues needed to be addressed before reliable image analysis could be conducted. The necessary protocol amendments listed below in accordance to the issues described above are listed in Table A.VI.

For the issue of bacterial contamination, 0.02% sodium azide was added to all PBS solutions used during IHC processing, with exception of the final PBS wash before cover slipping. Evaporated media was initially addressed by pairing the VECTASHIELD Hardset Antifade mounting media with a clear nail polish seal, followed by transition to Fluoromount-G™ mounting medium with DAPI. The uneven illumination had a two-

fold cause. The first was due to tissue drying too long between mounting on slides and cover-slipping, which was identified due to bright peripheral DAPI and dim central staining (Figure A.IIA). This was addressed by ensuring slides did not dry longer than 10 min before cover slipping. The second cause was a light path issue within the Keyence microscope, presenting as decreased illumination on the edges of images. Aside from instrument maintenance, this was addressed by only capturing qualitative 10x images with high stitching overlap on the Keyence for whole brain section observation, and quantitative images for spinal cord sections and brain regions of interest were only acquired on the Olympus microscope (10x and 20x).

The poor reliability of GAD67 staining for RMTg identification presents a large problem as identification of cFos-activated GABAergic neurons within the RMTg is key to address our hypothesis. Recent studies have demonstrated FoxP1 as a remarkably reliable marker for RMTg GABAergic cells projecting to VTA dopaminergic neurons (Smith et al., 2019; Jhou, 2021). Accordingly, the second portion of this study aimed to characterize the expression of FoxP1 in VTA and RMTg sections for improved identification of GABAergic RMTg neurons.

For the fifth issue of low signal-to-noise ratio of cFos staining, inclusion of sodium azide enabled cFos-stained sections to be incubated overnight at room temperature following Synaptic Systems data sheet recommendations, followed by a 4°C for the remaining incubation. Finally, the sixth issue of peripheral damage of spinal cord sections was addressed by keeping sections within the same 5mL glass vial, with additional wash steps added to ensure minimal carryover.

Table A.I: Protocol Amendments

Protocol Section	Issue	Amendment
Tissue storage	Bacterial contamination	Sodium Azide in all PBS-based solutions

Section mounting	Evaporated mounting media	Fluoromount-G™ with DAPI
Imaging	Uneven illumination	Dry sections on slides <10 min
Imaging	Uneven illumination: light path	Olympus BX53: images for quantification
Target identification	Poor RMTg identification via GAD67 staining	FoxP1 antibody
IHC staining	Peripheral spinal cord damage	Decreased tissue transfers (single glass vial)

Study II

Immunohistochemistry II

Free-floating immunohistochemical staining was performed on spinal cord sections and sections from brain regions of interest (VTA and RMTg) identified through referencing the Mouse Brain Atlas (Paxinos, 2007). VTA was sequentially collected from -2.70 AP to -3.52, and RMTg from -3.55 AP to -4.75 AP. All spinal cord tissue was processed in the same 5 mL glass vial with additional wash for every PBS-based wash step to decrease tissue handling. Tissue processed for GAD67 or FOXP1 staining first underwent an antigen retrieval, with sections heated to 80°C in 10mM Citrate Buffer (pH 6) for 30 min. After cooling to room temperature for 15 min, sections were washed 3 times in PBS, then placed in a blocking buffer of 3% normal goat serum (NGS) (ThermoFisher, Waltham, MA, 10000C) and 0.25% Triton X-100 (Invitrogen, ThermoFisher, HFH10) in PBS for 1 hour at room temperature. Sections were then incubated in primary antibodies in blocking buffer for 2 days on a rocker, with cFos-stained sections at room temperature overnight followed by 4°C and all other sections at 4°C for the entire incubation.

Following 3 washes in cold 0.25% Triton solution, sections were light protected with foil and incubated in secondary antibodies in blocking solution at room temperature for 3 hours on a rocker, followed by a final PBS wash. Sections were mounted on glass slides (<10 min drying time) and cover slipped with Fluoromount-G™

mounting media with DAPI (ThermoFisher, 00-4959-52). The following antibodies were used for each target: cFos: primary rabbit anti-cFos polyclonal antibody (1:1000, Synaptic Systems, 266 003) and either secondary goat anti-rabbit IgG Alexa Fluor 488 or 594 (1:500, Invitrogen, ThermoFisher, A-11008, green or red, respectively); GAD67: primary mouse anti-GAD67 monoclonal antibody (1:1000, Abcam, ab26116) and secondary goat anti-mouse IgG Alexa Fluor 594 (1:500, Invitrogen, ThermoFisher, A-11005, red); TH: primary chicken anti-TH polyclonal antibody (1:1000, Abcam, ab76442) and secondary goat anti-chicken IgY Alexa Fluor 594 (1:500, Invitrogen, ThermoFisher, A-11042, red); FoxP1: primary mouse anti-FoxP1 monoclonal antibody (1:1000, Abcam, ab32010) and secondary goat anti-mouse IgG2a Alexa Fluor 488 (1:500, ThermoFisher, A-21131, green). For VTA and RMTg sections, every other section was split to form two groups co-labeled with either TH + FoxP1 or cFos + FoxP1, and spinal cord sections were co-labeled with GAD67 + cFos.

Imaging and Analysis II

Spinal cord and RMTg FoxP1 images were acquired using an Olympus BX53 microscope with X-Cite Series 120Q mercury short arc lamp using 10x, 20x, or 40x objectives (Olympus). Whole-section VTA and RMTg stitched images were acquired with the Keyence BZ-X800 automated microscope using 10x objectives (Nikon). For all sections, the optimal plane for either cFos observation or FoxP1 observation was selected for image capture. Qualitative analysis was performed to evaluate correct co-labeling and regional specificity for VTA and RMTg sections. ImageJ 1.53c software was used to manually count the number of cFos positive cells in spinal cord sections using the cell counter plugin software, with all count-marked images saved alongside original images.

Results II

General Protocol Amendments

The addition of 0.02% sodium azide eliminated all issues of bacterial contamination within samples. Transition to Fluoromount-G™ with DAPI provided durable tissue visualization for at least 3 weeks without need of a clear nail polish seal. Decreasing the drying time of sections during tissue mounting resulted in even DAPI stain across brain and spinal cord sections, and 10x stitching with ImageJ for generation of composite images decreased shadowing issues in whole-section images (Figure A.IIIA). Additionally, processing spinal cord sections in a single 5mL glass vial reduced both peripheral damage and tissue processing time. Finally, Figure A.IIIA shows dorsal crystal-like green fluorescence. This was seen randomly distributed across VTA, RMTg, and spinal cord sections and was identified as remaining PBS producing salts while drying before cover slipping.

Characterization of FoxP1 as a marker for RMTg

Figure A.III shows representative images for the FoxP1 signal in mouse VTA at approximately -3.74 AP. Figure A.IIIA demonstrates the well-defined TH signal (red) as seen in Study I, enabling visual identification of various regions, including the SN, medial lemniscus (ml), paranigral nucleus (PN), parabrachial pigmented nucleus (PBP), parainterfascicular nucleus (PIF), interfascicular nucleus (IF), the rostral linear nucleus (RLi), and the interpeduncular nucleus (IPC). Surprisingly, the FoxP1 signal (green) lies dorsal to all TH + regions and appears to be within the red nucleus (RMC) and oculomotor nucleus (OM). Figure A.IIIB shows this FoxP1 signal at 20x, highlighting the clear boundary between the TH and FoxP1 signals.

IP acid-induced cFos expression in mouse thoracic and lumbar spinal cord

Figure A.IV shows representative images for dorsal horn cFos quantification in mouse thoracic and lumbar spinal cord sections, with the merged image including the exported ImageJ cell counter marks. Interestingly, spinal cord sections from Study II possess high levels of autofluorescence in the white matter that was not

present in sections from Study I (see Figure A.IB). Figure A.IVB shows quantification results for cFos+ cells in the lumbar (L1-5) and thoracic (T10-13) spinal cords of two IP acid and two H2O treated male mice. cFos+ cell quantification was divided into two categories: dorsal horn (Figure A.IV, counted, pink markers) and rest of grey matter (Figure A.IVA, counted, orange markers). There was a significant increase in cFos+ cells in T10-T13 sections in the dorsal horn and rest of section, but no difference in cFos+ cells from L1-5 spinal cord sections (Figure A.IVB). While data cannot be retroactively separated into smaller combinations of lumbar and thoracic sections for analysis, these preliminary data indicate that future studies evaluating IP acid-induced neuronal activation in mouse spinal cord can collect a smaller tissue section closer to where the lumbar and thoracic spinal cord sections meet (e.g. L3-T13).

Discussion II

This appendix was broken into Study I and Study II, with the overarching goal to develop a comprehensive method for assessment of IP acid-related neuronal activation. There were five main findings. First, the animal handling, perfusions, tissue collection (particularly development of spinal cord laminectomy method), cryosectioning, and free-floating IHC protocol yielded high-quality brain and spinal cord sections for imaging and quantification. Second, TH provided a robust fluorescent signal with good anatomical selectivity and clear axonal versus cell body profiles. Third, cFos produced a reliable nuclear signal that was enhanced following overnight room temperature incubation, with TH and cFos co-labeled neurons easily identifiable. Fourth, GAD67 provides valuable identification of dorsal horn laminae; however, identification of co-labeled cFos and GAD67 + cells remain difficult due to GAD67's expression in the cell body and synaptic terminals. This issue is further highlighted by the inability to readily identify the RMTg due to diffuse GAD67 staining (Figure VI.IIB). Finally, the FoxP1 antibody used in Study II for RMTg identification did not produce staining patterns as described in the literature (Smith et al., 2019), with a very low signal to noise ratio and main detected signal in the RMC and oculomotor nucleus. Overall, Studies I and II establish a strong foundation for cellular

biomarkers in mouse brain and spinal cord, especially TH and cFos. Further validation needs to be conducted to develop robust quantification methods and neuroanatomical characterization of the RMTg.

Implications for Appendix Studies

Neurochemical staining to identify GABAergic neurons

The above GAD67 IHC data shows poor resolution for cellular identification of GABAergic cell bodies due to diffuse axonal and cytoplasmic staining. While some studies have shown good cell body resolution with the anti-GAD67 ab26116 (Kasper et al., 2016; Li et al., 2017; Han et al., 2019; Ishiyama et al., 2019), our results agree with a number of reports in the literature showing diffuse ab26116 staining, which they addressed through pairing with high-magnification and Z-stack image acquisition (Kaufling et al., 2010; Wang et al., 2014; Ativie et al., 2018; Bednarova et al., 2018; Fan et al., 2018; Ge et al., 2019) or pretreating animals with colchicine to increase somatic antigen binding (Wang et al., 2014; Buhler et al., 2018). While reports suggest improved clarification of GABAergic cells through fluorescent *in situ* hybridization (FISH) methods (Esclapez et al., 1994; Takakura et al., 2007; Zhao et al., 2013; Chowdhury et al., 2019), communication with other research groups and trends in the literature propose utility of genetic mouse lines paired with neurochemical staining as a more robust method for GABAergic cell body identification (Wang et al., 2014; Gotts et al., 2016; Chowdhury et al., 2019; Das Gupta et al., 2021). For example, Chowdhury *et al.* injected a Cre-inducible AAV virus carrying GFP into the VTA of GAD67-Cre mice and used FISH to show clear somatic GFP staining that co-labeled with GAD67 but not TH (Chowdhury et al., 2019). These GAD67-Cre mice can then be used for development of chemogenetic studies to test necessity and sufficiency of neural circuits (also demonstrated in Chowdhury *et al.* 2019). However, our specific research question is targeted to the VTA and RMTg, which will likely be benefited most through staining with FoxP1.

While the GAD67 stain in the spinal cord dorsal horn produced slightly improved identification of individual cell bodies, similar issues for individual cell identification exist due to the dense GABAergic interneuron

population present throughout the laminae of the spinal cord dorsal horn (Todd and Koerber, 2013). If quantification of GABAergic cells in the dorsal horn of the spinal cord is desired, data from this appendix would suggest higher resolution acquisition methods (e.g. Z-stack, higher magnification), or transition to another method for GABAergic cell identification, as described above.

FoxP1 staining for identification of RMTg GABAergic neurons

An emerging body of research demonstrates the transcription factor FoxP1 as a powerful tool for reliably identifying GABAergic neurons in the RMTg (Lahti et al., 2016; Smith et al., 2019; Jhou, 2021). More specifically, mRNA and protein characterization demonstrating robust labeling of GABAergic neurons with direct projects to VTA DA neurons along with surprisingly distinct anatomical levels of expression showing RMTg boundaries better than previous GABAergic markers that show high expression levels in adjacent regions to the RMTg. Despite these promising reports, the mouse anti-FoxP1 antibody ab32010 did not produce staining patterns as observed by other groups using the same antibody (Anderson et al., 2020) and a rabbit anti-FoxP1 antibody (Smith et al., 2019; Jhou, 2021). It should be noted that a majority of the literature utilizes the same rabbit anti-FoxP1 antibody ab16645 from Abcam, and a mouse anti-FoxP1 antibody was selected for this study to provide compatible co-labeling with our validated rabbit anti-cFos antibody. Direct comparison of ab32010 to ab16645 was kindly performed by Dr. Thomas Jhou's lab, which confirmed the ab32010 antibody to not produce standard FoxP1 staining, with no observable signal in the RMTg and higher levels of staining in the RMC and oculomotor nucleus (data not shown). A pilot study with the rabbit anti-FoxP1 antibody ab16645 showed staining patterns in agreement with those reported in the literature (N=2 male ICR adult mice, data not shown). As such, validation with the Abcam ab16645 antibody co-labeled with a cFos antibody from a non-rabbit host will need to be conducted before hypothesis testing of IP acid-induced effects can be conducted.

Figures

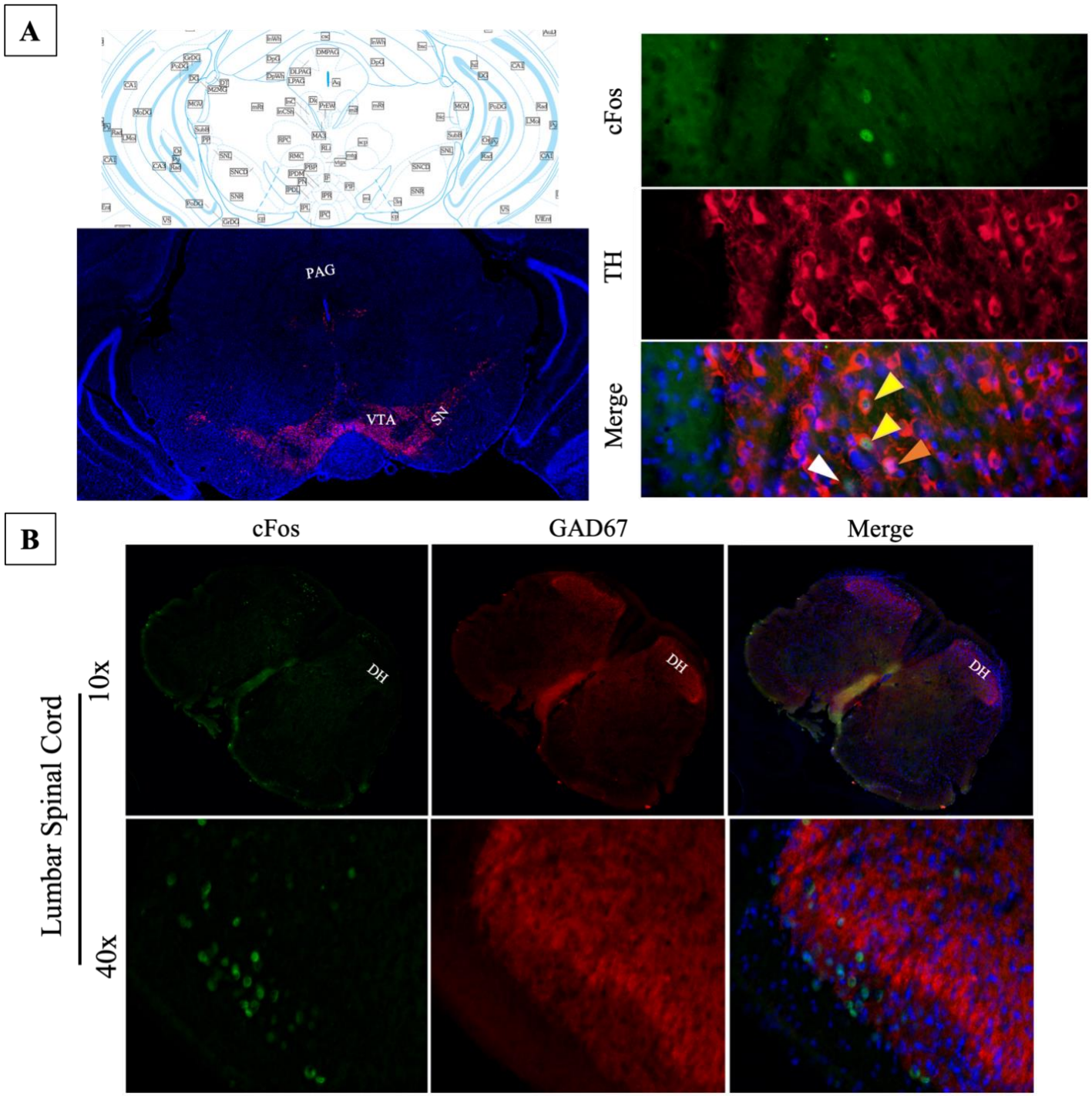

Figure A.I: Characterization and co-localization of TH, cFos, and GAD67 in mouse VTA and spinal cord. (A) The left column shows a representative coronal mouse section imaged at 10x (stitched) stained with TH (red) and counterstained with DAPI (blue), with labels denoting major regions of interest and reference image from Paxinos 3rd edition. The right column shows representative 60x oil immersion images for cFos + cells,

TH+ cells, and co-localization, with arrows denoting the following: yellow = cFos+TH non-overlapping co-localization (most common), white = cFos+, orange = cFos+TH overlapping co-localization (least common). (B) Examples of lumbar spinal cord sections stained with cFos (green), GAD67 (red), and counterstained with DAPI (blue). Region abbreviations: VTA = ventral tegmentum area; SN = substantia nigra; PAG = periaqueductal grey, DH = dorsal horn.

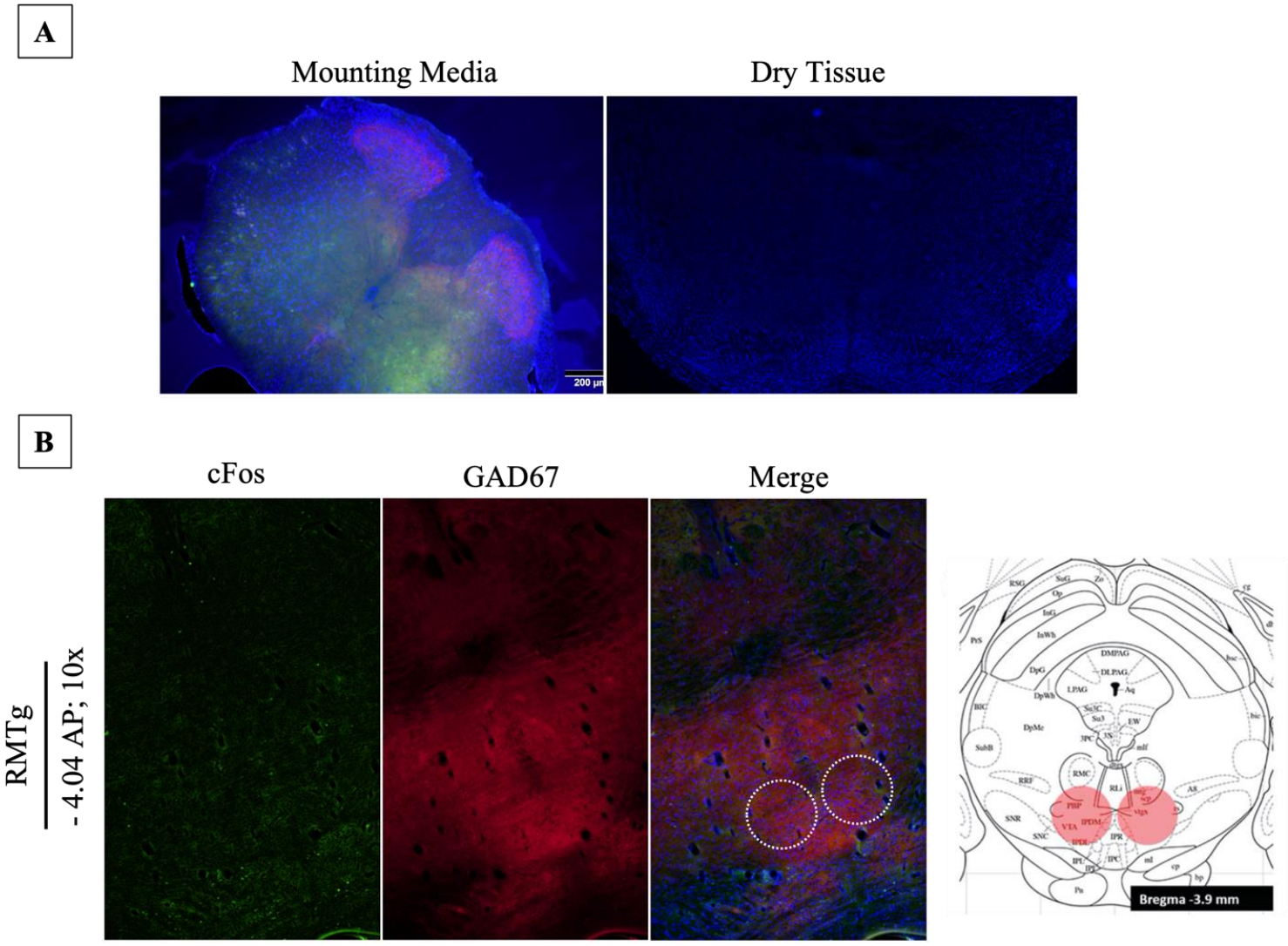

Figure A.II: Image illumination and target quality issues. (A) The left image demonstrates how mounting media evaporation produced high levels of autofluorescence preventing identification of cFos signal. The right image shows uneven DAPI illumination across a coronal brain section due to prolonged drying time before cover slipping. (B) Representative coronal brain sections at approximately -4.04 AP (10x) demonstrating the diffuse GAD67 stain with poor RMTg regional identification. White dashed circles illustrate the suggested location of RMTg per the literature, as shown in the reference example from Taylor *et al.* 2019. For all above images, cFos = green, GAD67 = red, and DAPI = blue.

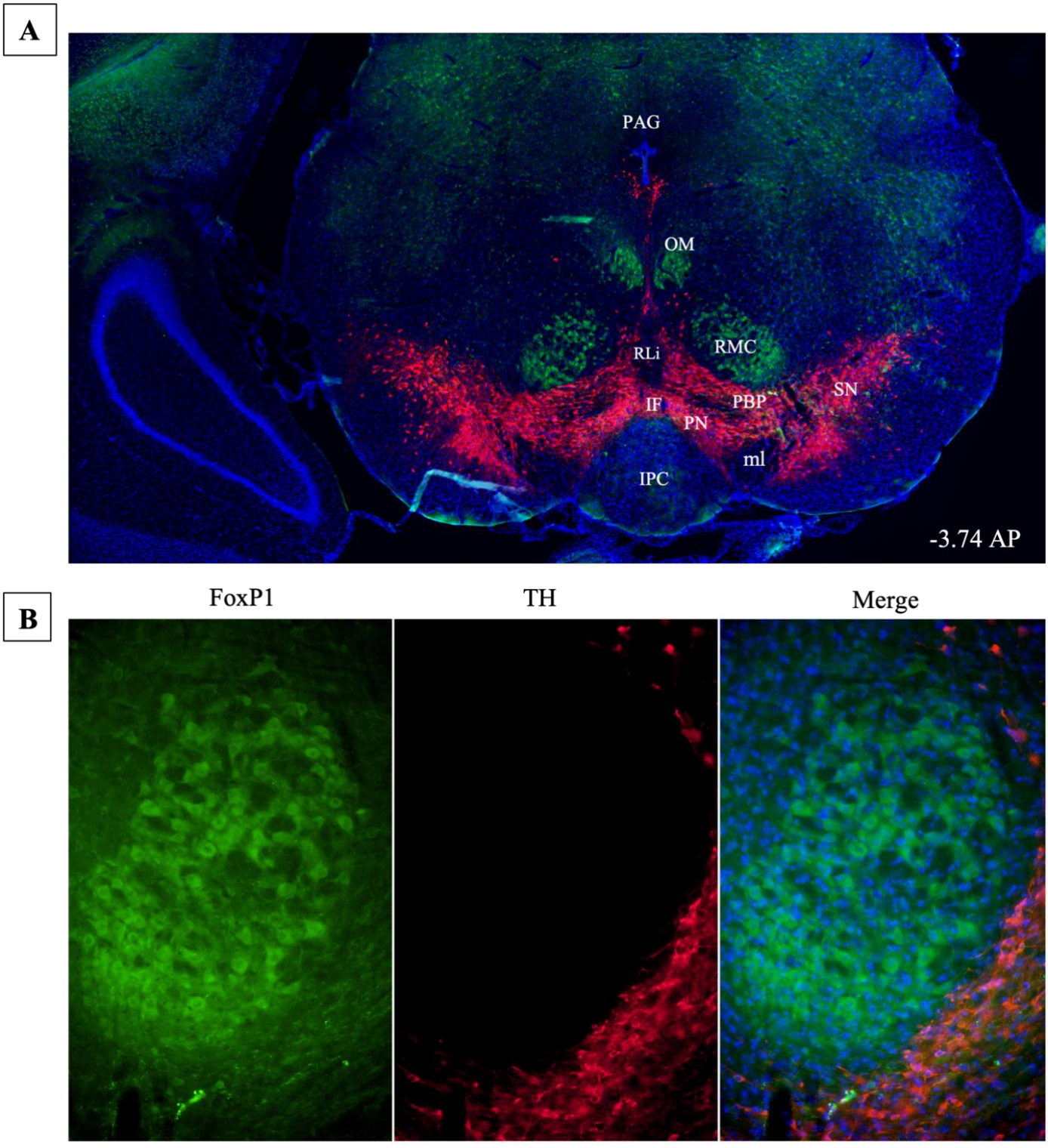

<u>Figure A.III.</u> Characterization of FoxP1 as a marker for RMTg. (A) Representative coronal mouse section at approximately -3.74 AP (10x stitch) stained with TH (red), FoxP1 (green), and DAPI (blue). Identification of

VTA regions, SN, and additional landmarks are denoted in white. (B) Representative 20x images of FoxP1 (green) and TH (red) staining, with the merged image showing clear delineation between the two markers. Abbreviated regions: IF = interfascicular nucleus; IPC = interpeduncular nucleus; ml = medial lemniscus; OM = oculomotor nucleus; periaqueductal gray (PAG); PBP = parabrachial pigmented nucleus, PN = paranigral nucleus, RLi = rostral linear nucleus; the red nucleus (RMC), and SN = substantia nigra.

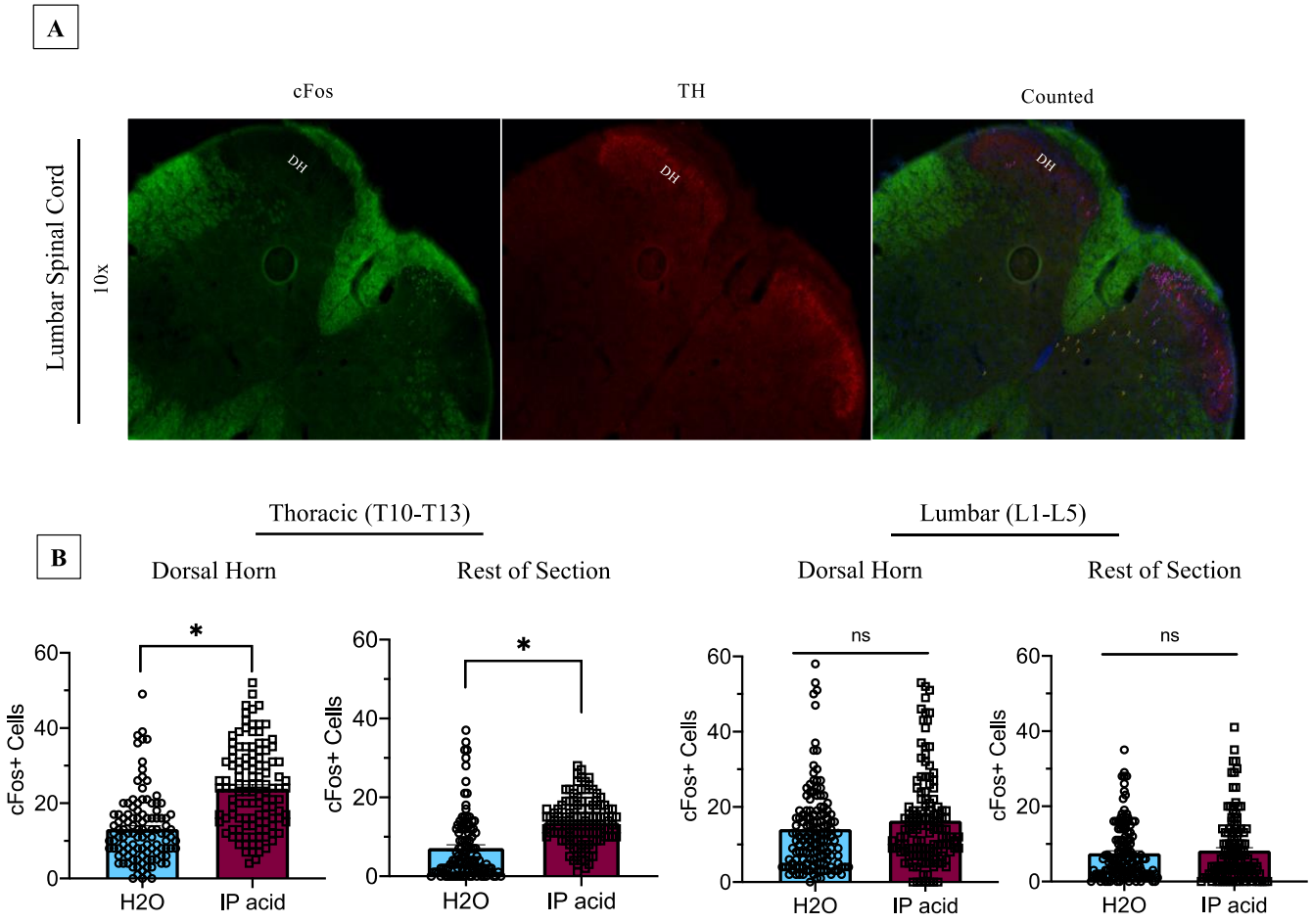

<u>Figure A.IV</u>. IP acid-induced cFos expression in mouse thoracic and lumbar spinal cord. (A) Representative images (10x) from mouse lumbar spinal cord for cFos (green) and GAD67 (red) staining. The right "counted" image shows the merged channels (DAPI = blue) with ImageJ CellCounter Markers inlaid on the image. Pink markers denote cFos+ cells in the dorsal horn and orange markers denote cFos+ cells in the remaining gray matter. (B) Quantified cFos+ cells in lumbar vs thoracic sections in male ICR mice (N = 2/treatment) that received either IP acid or IP veh 1 hr before tissue collection. Abscissae: treatment with IP H_2O or IP acid. Ordinates: number of cFos+ cells. Asterisks (*) indicate significant difference by Welch's two-tailed t-test, $p<0.05$.

References

Adamson Barnes NS, Mitchell VA, Kazantzis NP and Vaughan CW (2016) Actions of the dual FAAH/MAGL inhibitor JZL195 in a murine neuropathic pain model. *British Journal of Pharmacology* **173**:77-87.

Ahn K, Johnson DS, Mileni M, Beidler D, Long JZ, McKinney MK, Weerapana E, Sadagopan N, Liimatta M, Smith SE, Lazerwith S, Stiff C, Kamtekar S, Bhattacharya K, Zhang Y, Swaney S, Van Becelaere K, Stevens RC and Cravatt BF (2009) Discovery and Characterization of a Highly Selective FAAH Inhibitor that Reduces Inflammatory Pain. *Chemistry & Biology* **16**:411-420.

Alexander KS, Rodriguez TR, Sarfo AN, Patton TB and Miller LL (2019) Effects of monoamine uptake inhibitors on pain-related depression of nesting in mice. *Behav Pharmacol* **30**:463-470.

Aliczki M, Zelena D, Mikics E, Varga ZK, Pinter O, Bakos NV, Varga J and Haller J (2013) Monoacylglycerol lipase inhibition-induced changes in plasma corticosterone levels, anxiety and locomotor activity in male CD1 mice. *Horm Behav* **63**:752-758.

Almeida TF, Roizenblatt S and Tufik S (2004) Afferent pain pathways: a neuroanatomical review. *Brain Res* **1000**:40-56.

Altarifi AA, Rice KC and Negus SS (2015) Effects of mu-opioid receptor agonists in assays of acute pain-stimulated and pain-depressed behavior in male rats: role of mu-agonist efficacy and noxious stimulus intensity. *J Pharmacol Exp Ther* **352**:208-217.

Anderson AG, Kulkarni A, Harper M and Konopka G (2020) Single-Cell Analysis of Foxp1-Driven Mechanisms Essential for Striatal Development. *Cell Rep* **30**:3051-3066 e3057.

Anderson GD (2008) Chapter 1 Gender Differences in Pharmacological Response, in *Epilepsy in Women - The Scientific Basis for Clinical Management* pp 1-10.

Anderson WB, Gould MJ, Torres RD, Mitchell VA and Vaughan CW (2014) Actions of the dual FAAH/MAGL inhibitor JZL195 in a murine inflammatory pain model. *Neuropharmacology* **81**:224-230.

Ativie F, Komorowska JA, Beins E, Albayram O, Zimmer T, Zimmer A, Tejera D, Heneka M and Bilkei-Gorzo A (2018) Cannabinoid 1 Receptor Signaling on Hippocampal GABAergic Neurons Influences Microglial Activity. *Front Mol Neurosci* **11**:295.

Babalonis S, Lofwall MR, Sloan PA, Nuzzo PA, Fanucchi LC and Walsh SL (2019) Cannabinoid modulation of opioid analgesia and subjective drug effects in healthy humans. *Psychopharmacology (Berl)* **236**:3341-3352.

Bagdas D, Muldoon PP, AlSharari S, Carroll FI, Negus SS and Damaj MI (2016) Expression and pharmacological modulation of visceral pain-induced conditioned place aversion in mice. *Neuropharmacology* **102**:236-243.

Ballantyne JC and Sullivan MD (2015) Intensity of Chronic Pain--The Wrong Metric? *N Engl J Med* **373**:2098-2099.

Bangasser DA and Wicks B (2017) Sex-specific mechanisms for responding to stress. *J Neurosci Res* **95**:75-82.

Barrot M, Sesack SR, Georges F, Pistis M, Hong S and Jhou TC (2012) Braking dopamine systems: a new GABA master structure for mesolimbic and nigrostriatal functions. *J Neurosci* **32**:14094-14101.

Basbaum AI, Bautista DM, Scherrer G and Julius D (2009) Cellular and molecular mechanisms of pain. *Cell* **139**:267-284.

Beardsley PM, Aceto MD, Cook CD, Bowman ER, Newman JL and Harris LS (2004) Discriminative stimulus, reinforcing, physical dependence, and antinociceptive effects of oxycodone in mice, rats, and rhesus monkeys. *Exp Clin Psychopharmacol* **12**:163-172.

Bednarova V, Grothe B and Myoga MH (2018) Complex and spatially segregated auditory inputs of the mouse superior colliculus. *J Physiol* **596**:5281-5298.

Bedse G, Bluett RJ, Patrick TA, Romness NK, Gaulden AD, Kingsley PJ, Plath N, Marnett LJ and Patel S (2018) Therapeutic endocannabinoid augmentation for mood and anxiety disorders: comparative profiling of FAAH, MAGL and dual inhibitors. *Translational Psychiatry* **8**.

Benarroch EE (2016) Involvement of the nucleus accumbens and dopamine system in chronic pain. *Clinical Implications of Neuroscience Research* **87**:1720-1726.

Blankman JL and Cravatt BF (2013) Chemical probes of endocannabinoid metabolism. *Pharmacol Rev* **65**:849-871.

Blanton HL, Barnes RC, McHann MC, Bilbrey JA, Wilkerson JL and Guindon J (2021) Sex differences and the endocannabinoid system in pain. *Pharmacol Biochem Behav* **202**:173107.

Booker L, Kinsey SG, Abdullah RA, Blankman JL, Long JZ, Ezzili C, Boger DL, Cravatt BF and Lichtman AH (2012) The fatty acid amide hydrolase (FAAH) inhibitor PF-3845 acts in the nervous system to reverse LPS-induced tactile allodynia in mice. **165**:2485-2496.

Booker L, Naidu PS, Razdan RK, Mahadevan A and Lichtman AH (2009) Evaluation of prevalent phytocannabinoids in the acetic acid model of visceral nociception. **105**:42-47.

Britch SC, Wiley JL, Yu Z, Clowers BH and Craft RM (2017) Cannabidiol-Δ 9 -tetrahydrocannabinol interactions on acute pain and locomotor activity. *Drug and Alcohol Dependence* **175**:187-197.

Brunton L, Hilal-Dandan R and Knollmann B (2018) Goodman & Gilman's: The Pharmacological Basis of Therapeutics, in *Goodman & Gilman's: The Pharmacological Basis of Therapeutics*, McGraw-Hill.

Buhler AVK, Tachibana S, Zhang Y and Quock RM (2018) nNOS immunoreactivity co-localizes with GABAergic and cholinergic neurons, and associates with beta-endorphinergic and met-enkephalinergic opioidergic fibers in rostral ventromedial medulla and A5 of the mouse. *Brain Res* **1698**:170-178.

Burma NE, Leduc-Pessah H, Fan CY and Trang T (2017) Animal models of chronic pain: Advances and challenges for clinical translation. *J Neurosci Res* **95**:1242-1256.

Burston JJ, Mapp PI, Sarmad S, Barrett DA, Niphakis MJ, Cravatt BF, Walsh DA and Chapman V (2016) Robust anti-nociceptive effects of monoacylglycerol lipase inhibition in a model of osteoarthritis pain. *British Journal of Pharmacology* **173**:3134-3144.

Burston JJ, Sagar DR, Shao P, Bai M, King E, Brailsford L, Turner JM, Hathway GJ, Bennett AJ, Walsh DA, Kendall DA, Lichtman A and Chapman V (2013) Cannabinoid CB2 Receptors Regulate Central Sensitization and Pain Responses Associated with Osteoarthritis of the Knee Joint. **8**:e80440.

Calcaterra NE and Barrow JC (2014) Classics in Chemical Neuroscience: Diazepam (Valium). *ACS Chemical Neuroscience* **5**:253-260.

Chanda PK, Gao Y, Mark L, Btesh J, Strassle BW, Lu P, Piesla MJ, Zhang MY, Bingham B, Uveges A, Kowal D, Garbe D, Kouranova EV, Ring RH, Bates B, Pangalos MN, Kennedy JD, Whiteside GT and Samad TA (2010) Monoacylglycerol lipase activity is a critical modulator of the tone and integrity of the endocannabinoid system. *Mol Pharmacol* **78**:996-1003.

Chapman CR and Vierck CJ (2017) The Transition of Acute Postoperative Pain to Chronic Pain: An Integrative Overview of Research on Mechanisms. *J Pain* **18**:359 e351-359 e338.

Chiba S, Nishiyama T, Yoshikawa M and Yamada Y (2009) The antinociceptive effects of midazolam on three different types of nociception in mice. *J Pharmacol Sci* **109**:71-77.

Cho C, Michailidis V, Lecker I, Collymore C, Hanwell D, Loka M, Danesh M, Pham C, Urban P, Bonin RP and Martin LJ (2019) Evaluating analgesic efficacy and administration route following craniotomy in mice using the grimace scale. *Sci Rep* **9**:359.

Cho H, Jang Y, Lee B, Chun H, Jung J, Kim S, Hwang S and Oh U (2013) Voluntary movements as a possible non-reflexive pain assay. **9**:25.

Chowdhury S, Matsubara T, Miyazaki T, Ono D, Fukatsu N, Abe M, Sakimura K, Sudo Y and Yamanaka A (2019) GABA neurons in the ventral tegmental area regulate non-rapid eye movement sleep in mice. *Elife* **8**.

Chung L (2015) A Brief Introduction to the Transduction of Neural Activity into Fos Signal. *Dev Reprod* **19**:61-67.

Cisar JS, Weber OD, Clapper JR, Blankman JL, Henry CL, Simon GM, Alexander JP, Jones TK, Ezekowitz RAB, O'Neill GP and Grice CA (2018) Identification of ABX-1431, a Selective Inhibitor of Monoacylglycerol Lipase and Clinical Candidate for Treatment of Neurological Disorders. *J Med Chem* **61**:9062-9084.

Clement CI, Keay KA, Podzebenko K, Gordan BD and Bandler R (2000) Spinal Sources of Noxious Visceral andNoxious Deep Somatic Afferent DriveOnto the Ventrolateral PeriaqueductalGray of the Rat. *The Journal of Comparative Neurology* **425**:323-344.

Cobos E and Portillo-Salido E (2013) "Bedside-to-Bench" Behavioral Outcomes in Animal Models of Pain: Beyond the Evaluation of Reflexes. *Current Neuropharmacology* **11**:560-591.

Cobos EJ, Ghasemlou N, Araldi D, Segal D, Duong K and Woolf CJ (2012) Inflammation-induced decrease in voluntary wheel running in mice: A nonreflexive test for evaluating inflammatory pain and analgesia. *Pain* **153**:876-884.

Collier HOJ, Dinneen LC, Johnson CA and Schneider C (1968) The Abdominal Constriction Response and its Suppression by Analgesic Drugs in the Mouse. *British Journal of Pharmac Chemother* **32**:295-310.

Connor J, Makonnen E and Rostom A (2000) Comparison of analgesic effects of khat (Catha edulis Forsk) extract, D-amphetamine and ibuprofen in mice. *J Pharm Pharmacol* **52**:107-110.

Cooper ZD and Craft RM (2018) Sex-Dependent Effects of Cannabis and Cannabinoids: A Translational Perspective. *Neuropsychopharmacology* **43**:34-51.

Craft RM, Marusich JA and Wiley JL (2013) Sex differences in cannabinoid pharmacology: a reflection of differences in the endocannabinoid system? *Life Sci* **92**:476-481.

Cravatt BF, Demarest K, Patricelli MP, Bracey MH, Giang DK, Martin BR and Lichtman AH (2001) Supersensitivity to anandamide and enhanced endogenous cannabinoid signaling in mice lacking fatty acid amide hydrolase. *Proc Natl Acad Sci U S A* **98**:9371-9376.

Cruz FC, Koya E, Guez-Barber DH, Bossert JM, Lupica CR, Shaham Y and Hope BT (2013) New technologies for examining the role of neuronal ensembles in drug addiction and fear. *Nat Rev Neurosci* **14**:743-754.

Curtis MJ, Bond RA, Spina D, Ahluwalia A, Alexander SP, Giembycz MA, Gilchrist A, Hoyer D, Insel PA, Izzo AA, Lawrence AJ, MacEwan DJ, Moon LD, Wonnacott S, Weston AH and McGrath JC (2015) Experimental design and analysis and their reporting: new guidance for publication in BJP. *Br J Pharmacol* **172**:3461-3471.

Dalal S and Melzack R (1998) Potentiation of Opioid Analgesia by Psychostimulant Drugs. *Journal of Pain and Symptom Management* **16**:245-253.

Dalmann R, Daulhac L, Antri M, Eschalier A and Mallet C (2015) Supra-spinal FAAH is required for the analgesic action of paracetamol in an inflammatory context. **91**:63-70.

Das Gupta RR, Scheurer L, Pelczar P, Wildner H and Zeilhofer HU (2021) Neuron-specific spinal cord translatomes reveal a neuropeptide code for mouse dorsal horn excitatory neurons. *Sci Rep* **11**:5232.

de Almeida AS, Rigo FK, De Pra SD, Milioli AM, Dalenogare DP, Pereira GC, Ritter CDS, Peres DS, Antoniazzi CTD, Stein C, Moresco RN, Oliveira SM and Trevisan G (2019) Characterization of Cancer-Induced Nociception in a Murine Model of Breast Carcinoma. *Cell Mol Neurobiol* **39**:605-617.

De Bellis A, De Angelis G, Fabris E, Cannata A, Merlo M and Sinagra G (2020) Gender-related differences in heart failure: beyond the "one-size-fits-all" paradigm. *Heart Fail Rev* **25**:245-255.

de la Puente B, Zamanillo D, Romero L, Vela JM, Merlos M and Portillo-Salido E (2017) Pharmacological sensitivity of reflexive and nonreflexive outcomes as a correlate of the sensory and affective responses to visceral pain in mice. *Sci Rep* **7**:13428.

Deuis JR, Dvorakova LS and Vetter I (2017) Methods Used to Evaluate Pain Behaviors in Rodents. *Front Mol Neurosci* **10**:284.

Devane WA, Hanus L, Breuer A, Pertwee RG, Stevenson LA, Griffin G, Gibson D, Mandelbaum A, Etinger A and Mechoulam R (1992) Isolation and structure of a brain constituent that binds to the cannabinoid receptor. *Science* **258**:1946-1949.

Diester C, Santos E, Moerke M and Negus S (2021a) Behavioral Battery for Testing Candidate Analgesics in Mice. I. Validation with Positive and Negative Controls. *Journal of Pharmacology and Experimental Therapeutics*.

Diester CM, Banks ML, Neigh GN and Negus SS (2019) Experimental design and analysis for consideration of sex as a biological variable. *Neuropsychopharmacology* **44**:2159-2162.

Diester CM, Lichtman AH and Negus SS (2021b) Behavioral Battery for Testing Candidate Analgesics in Mice. II. Effects of Endocannabinoid Catabolic Enzyme Inhibitors and 9-Tetrahydrocannabinol. *J Pharmacol Exp Ther* **377**:242-253.

Do Carmo GP, Stevenson GW, Carlezon WA and Negus SS (2009) Effects of pain- and analgesia-related manipulations on intracranial self-stimulation in rats: Further studies on pain-depressed behavior. *Pain* **144**:170-177.

Donvito G, Nass SR, Wilkerson JL, Curry ZA, Schurman LD, Kinsey SG and Lichtman AH (2018) The Endogenous Cannabinoid System: A Budding Source of Targets for Treating Inflammatory and Neuropathic Pain. *Neuropsychopharmacology* **43**:52-79.

Dostrovsky J and Craig A (2013) Ascending projection systems, in *Textbook of Pain* (McMahon S, Koltzenburg M, Tracey I and Turk DC eds) pp 182-198, Elsevier.

Dowell D, Haegerich TM and Chou R (2016) CDC Guideline for Prescribing Opioids for Chronic Pain--United States, 2016. *JAMA* **315**:1624-1645.

Duffy KA and Epperson CN (2021) Evaluating the evidence for sex differences: a scoping review of human neuroimaging in psychopharmacology research. *Neuropsychopharmacology*.

Elhabazi K, Trigo J, Mollereau C, Moulédous L, Zajac JM, Bihel F, Schmitt M, Bourguignon J, Meziane H, Petit-Demoulière B, Bockel F, Maldonado R and Simonin F (2012) Involvement of neuropeptide FF receptors in neuroadaptive responses to acute and chronic opiate treatments. *British Journal of Pharmacology* **165**:424-435.

Esclapez M, Tillakaratne NJK, Kaufman DL, Tobin AJ and Houser CR (1994) Comparative Localization of Two Forms of Glutamic Acid

Decarboxylase and Their mRNAs in Rat Brain Supports the Concept

of Functional Differences between the Forms. *The Journal of Neuroscience* **14**:1834-1855.

Escudero-Lara A, Cabanero D and Maldonado R (2021) Kappa opioid receptor modulation of endometriosis pain in mice. *Neuropharmacology* **195**:108677.

Fan XC, Fu S, Liu FY, Cui S, Yi M and Wan Y (2018) Hypersensitivity of Prelimbic Cortex Neurons Contributes to Aggravated Nociceptive Responses in Rats With Experience of Chronic Inflammatory Pain. *Front Mol Neurosci* **11**:85.

Farquhar CE, Breivogel CS, Gamage TF, Gay EA, Thomas BF, Craft RM and Wiley JL (2019) Sex, THC, and hormones: Effects on density and sensitivity of CB1 cannabinoid receptors in rats. *Drug Alcohol Depend* **194**:20-27.

Faul F, Erdfelder E, Lang A-G and Buchner A (2007) G*Power 3: A flexible statistical power analysis program for the social, behavioral, and biomedical sciences. *Behavior Research Methods* **39**:175-191.

Ferreira GS, Veening-Griffioen DH, Boon WPC, Moors EHM, Gispen-De Wied CC, Schellekens H and Van Meer PJK (2019) A standardised framework to identify optimal animal models for efficacy assessment in drug development. *PLOS ONE* **14**:e0218014.

Fidecka S and Pirogowicz E (2002) Lack of Interaction Between the Behavioral Effects of Ketoprofen and Benzodiazepines in Mice. *Polish Journal of Pharmacology* **54**:111-117.

Finnerup NB, Attal N, Haroutounian S, McNicol E, Baron R, Dworkin RH, Gilron I, Haanpää M, Hansson P, Jensen TS, Kamerman PR, Lund K, Moore A, Raja SN, Rice ASC, Rowbotham M, Sena E, Siddall P, Smith BH and Wallace M (2015) Pharmacotherapy for neuropathic pain in adults: a systematic review and meta-analysis. *The Lancet Neurology* **14**:162-173.

Fowler C (2012) Monoacylglycerol lipase - a target for drug development? *British Journal of Pharmacology* **166**:1568-1585.

Fullerton EF, Doyle HH and Murphy AZ (2018) Impact of sex on pain and opioid analgesia: a review. *Curr Opin Behav Sci* **23**:183-190.
Galea LAM, Choleris E, Albert AYK, McCarthy MM and Sohrabji F (2020) The promises and pitfalls of sex difference research. *Front Neuroendocrinol* **56**:100817.
Garcia-Larrea L and Peyron R (2013) Pain matrices and neuropathic pain matrices: a review. *Pain* **154 Suppl 1**:S29-S43.
Garcia-Sifuentes Y and Maney DL (2021) Reporting and misreporting of sex differences in the biological sciences. *Elife* **10**.
Gatch MB, Negus SS and Mello NK (1999) Antinociceptive Effects of Cocaine in Rhesus Monkeys. *Pharmacoogy Biochemistry and Behavior* **62**:291-297.
Ge MM, Chen SP, Zhou YQ, Li Z, Tian XB, Gao F, Manyande A, Tian YK and Yang H (2019) The therapeutic potential of GABA in neuron-glia interactions of cancer-induced bone pain. *Eur J Pharmacol* **858**:172475.
Gebhart G (2000) Visceral pain—peripheral sensitization. *Pain* **47**:54-55.
Ghosh S, Kinsey SG, Liu Q-S, Hruba L, McMahon LR, Grim TW, Merritt CR, Wise LE, Abdullah RA, Selley DE, Sim-Selley LJ, Cravatt BF and Lichtman AH (2015) Full Fatty Acid Amide Hydrolase Inhibition Combined with Partial Monoacylglycerol Lipase Inhibition: Augmented and Sustained Antinociceptive Effects with Reduced Cannabimimetic Side Effects in Mice. *Journal of Pharmacology and Experimental Therapeutics* **354**:111-120.
Ghosh S, Wise LE, Chen Y, Gujjar R, Mahadevan A, Cravatt BF and Lichtman AH (2013) The monoacylglycerol lipase inhibitor JZL184 suppresses inflammatory pain in the mouse carrageenan model. *Life Sci* **92**:498-505.
Goldberg DSM, S.J. (2011) Pain as a global public health priority. *BMC Public Health* **11**:770.
Golden LC and Voskuhl R (2017) The importance of studying sex differences in disease: The example of multiple sclerosis. *J Neurosci Res* **95**:633-643.
Gonzalez-Cano R, Montilla-Garcia A, Ruiz-Cantero MC, Bravo-Caparros I, Tejada MA, Nieto FR and Cobos EJ (2020) The search for translational pain outcomes to refine analgesic development: Where did we come from and where are we going? *Neurosci Biobehav Rev* **113**:238-261.
Gotts J, Atkinson L, Yanagawa Y, Deuchars J and Deuchars SA (2016) Co-expression of GAD67 and choline acetyltransferase in neurons in the mouse spinal cord: A focus on lamina X. *Brain Res* **1646**:570-579.
Greenspan JD, Craft RM, LeResche L, Arendt-Nielsen L, Berkley KJ, Fillingim RB, Gold MS, Holdcroft A, Lautenbacher S, Mayer EA, Mogil JS, Murphy AZ, Traub RJ, Consensus Working Group of the Sex G and Pain SIGotI (2007) Studying sex and gender differences in pain and analgesia: a consensus report. *Pain* **132 Suppl 1**:S26-S45.
Greenwald MK and Stitzer ML (2000) Antinociceptive, subjective and behavioral effects of smoked marijuana in humans. *Drug and Alcohol Dependence* **59**:261-275.
Grim TW, Ghosh S, Hsu KL, Cravatt BF, Kinsey SG and Lichtman AH (2014) Combined inhibition of FAAH and COX produces enhanced anti-allodynic effects in mouse neuropathic and inflammatory pain models. *Pharmacol Biochem Behav* **124**:405-411.
Grim TW, Morales AJ, Gonek MM, Wiley JL, Thomas BF, Endres GW, Sim-Selley LJ, Selley DE, Negus SS and Lichtman AH (2016) Stratification of Cannabinoid 1 Receptor (CB1R) Agonist Efficacy: Manipulation of CB1R Density through Use of Transgenic Mice Reveals Congruence between In Vivo and In Vitro Assays. *J Pharmacol Exp Ther* **359**:329-339.
Grim TW, Morales AJ, Thomas BF, Wiley JL, Endres GW, Negus SS and Lichtman AH (2017) Apparent CB 1 Receptor Rimonabant Affinity Estimates: Combination with THC and Synthetic Cannabinoids in the Mouse In Vivo Triad Model. *Journal of Pharmacology and Experimental Therapeutics* **362**:210-218.
Grossman ML, Basbaum AI and Fields HL (1982) Afferent and Efferent Connections of the Rat Tail Flick Reflex (A Model Used to Analyze Pain Control Mechanisms). *The Journal of Comparative Neurology* **206**:9-16.

Guindon J and Beaulieu P (2009) The role of the endogenous cannabinoid system in peripheral analgesia. *Curr Mol Pharmacol* **2**:134-139.
Guindon J, Blanton H, Brauman S, Donckels K, Narasimhan M and Benamar K (2019) Sex Differences in a Rodent Model of HIV-1-Associated Neuropathic Pain. *Int J Mol Sci* **20**.
Guindon J and Hohmann AG (2009) The Endocannabinoid System and Pain. *CNS Neurol Disord Drug Targets* **8**:403-421.
Guizzetti M, Davies DL, Egli M, Finn DA, Molina P, Regunathan S, Robinson DL and Sohrabji F (2016) Sex and the Lab: An Alcohol-Focused Commentary on the NIH Initiative to Balance Sex in Cell and Animal Studies. *Alcohol Clin Exp Res* **40**:1182-1191.
Habib AM, Okorokov AL, Hill MN, Bras JT, Lee M-C, Li S, Gossage SJ, Van Drimmelen M, Morena M, Houlden H, Ramirez JD, Bennett DLH, Srivastava D and Cox JJ (2019) Microdeletion in a FAAH pseudogene identified in a patient with high anandamide concentrations and pain insensitivity. *British Journal of Anaesthesia* **123**:e249-e253.
Han P, Welsh CT, Smith MT, Schmidt RE and Carroll SL (2019) Complex Patterns of GABAergic Neuronal Deficiency and Type 2 Potassium-Chloride Cotransporter Immaturity in Human Focal Cortical Dysplasia. *J Neuropathol Exp Neurol* **78**:365-372.
Health NIo (2015) Consideration of Sex as a Biological Variable in NIH-funded Research. *NOT-OD-15-102*.
Heinricher MM and Fields HL (2013) Central Nervous System Mechanisms of Pain Modulation, in *Wall and Melzack's Textbook of Pain* (McMahon S, Koltzenburg M, Tracey I and Turk DC eds) pp 129-142, Elsevier.
Herkenham M, Lynn AB, Johnson MR, Melvin LS, de Costa BR and Riche KC (1991) Characterization and localization of cannabinoid receptors in rat brain: a quantitative *in vitro* autoradiographic study. *The Journal of Neuroscience* **11**:563-583.
Hernandez-Leon A, De la Luz-Cuellar YE, Granados-Soto V, Gonzalez-Trujano ME and Fernandez-Guasti A (2018) Sex differences and estradiol involvement in hyperalgesia and allodynia in an experimental model of fibromyalgia. *Horm Behav* **97**:39-46.
Hohmann AG (2002) Spinal and peripheral mechanisms of cannabinoid
antinociception: behavioral, neurophysiological and
neuroanatomical perspectives. *Chemistry and Physics of Lipids* **121**:173-190.
Holzer P (2009) Acid-Sensitive Ion Channels and Receptors, in pp 283-332, Springer Berlin Heidelberg.
Hruba L, Seillier A, Zaki A, Cravatt BF, Lichtman AH, Giuffrida A and McMahon LR (2015) Simultaneous Inhibition of Fatty Acid Amide Hydrolase and Monoacylglycerol Lipase Shares Discriminative Stimulus Effects with Δ9-Tetrahydrocannabinol in Mice. *Journal of Pharmacology and Experimental Therapeutics* **353**:261-268.
Huggins JP, Smart TS, Langman S, Taylor L and Young T (2012) An efficient randomised, placebo-controlled clinical trial with the irreversible fatty acid amide hydrolase-1 inhibitor PF-04457845, which modulates endocannabinoids but fails to induce effective analgesia in patients with pain due to osteoarthritis of the knee. *Pain* **153**:1837-1846.
Hutson PH, Tarazi FI, Madhoo M, Slawecki C and Patkar AA (2014) Preclinical pharmacology of amphetamine: Implications for the treatment of neuropsychiatric disorders. **143**:253-264.
Ignatowska-Jankowska B, Wilkerson JL, Mustafa M, Abdullah R, Niphakis M, Wiley JL, Cravatt BF and Lichtman AH (2015a) Selective Monoacylglycerol Lipase Inhibitors: Antinociceptive versus Cannabimimetic Effects in Mice. *Journal of Pharmacology and Experimental Therapeutics* **353**:424-432.
Ignatowska-Jankowska BM, Baillie GL, Kinsey S, Crowe M, Ghosh S, Owens RA, Damaj IM, Poklis J, Wiley JL, Zanda M, Zanato C, Greig IR, Lichtman AH and Ross RA (2015b) A Cannabinoid CB1 Receptor-Positive Allosteric Modulator Reduces Neuropathic Pain in the Mouse with No Psychoactive Effects. *Neuropsychopharmacology* **40**:2948-2959.

Ishiyama M, Tamura S, Ito H, Takei H, Hoshi M, Asano M, Itoh M and Shirakawa T (2019) Early Postnatal Treatment with Valproate Induces Gad1 Promoter Remodeling in the Brain and Reduces Apnea Episodes in Mecp2-Null Mice. *Int J Mol Sci* **20**.

Jalabert M, Bourdy R, Courtin J, Veinante P, Manzoni OJ, Barrot M and Georges F (2011) Neuronal circuits underlying acute morphine action on dopamine neurons. *Proc Natl Acad Sci U S A* **108**:16446-16450.

Jhou TC (2021) The rostromedial tegmental (RMTg) "brake" on dopamine and behavior: A decade of progress but also much unfinished work. *Neuropharmacology* **198**:108763.

Ji Y, Tang B and Traub RJ (2008) The visceromotor response to colorectal distention fluctuates with the estrous cycle in rats. *Neuroscience* **154**:1562-1567.

Jirkof P (2014) Burrowing and nest building behavior as indicators of well-being in mice. *Journal of Neuroscience Methods* **234**:139-146.

Julou L, Guyonnet J, Durcot R, Fournel J and Pasquet J (1976) Ketoprofen (19.583 R.P.) (2-(3-benzoylphenyl)-propionic acid). Main pharmacological properties--outline of toxicological and pharmacokinetic data. *Scan J Rheumatol Suppl*:33-44.

Jurik A, Auffenberg E, Klein S, Deussing JM, Schmid RM, Wotjak CT and Thoeringer CK (2015) Roles of prefrontal cortex and paraventricular thalamus in affective and mechanical components of visceral nociception. *Pain* **156**:2479-2491.

Kaczocha M, Azim S, Nicholson J, Rebecchi MJ, Lu Y, Feng T, Romeiser JL, Reinsel R, Rizwan S, Shodhan S, Volkow ND and Benveniste H (2018) Intrathecal morphine administration reduces postoperative pain and peripheral endocannabinoid levels in total knee arthroplasty patients: a randomized clinical trial. *BMC Anesthesiol* **18**:27.

Kalso E (2005) Oxycodone. *Journal of Pain and Symptom Management* **29**:47-56.

Kamimura R, Hossain MZ, Unno S, Ando H, Masuda Y, Takahashi K, Otake M, Saito I and Kitagawa J (2018) Inhibition of 2-arachydonoylgycerol degradation attenuates orofacial neuropathic pain in trigeminal nerve-injured mice. *Journal of Oral Science* **60**:37-44.

Kandasamy R and Morgan MM (2020) 'Reinventing the wheel' to advance the development of pain therapeutics. *Behav Pharmacol*.

Kantor MD (1986) Ketoprofen: A Review of its Pharmacologic and Clinical Properties. *Pharmacotherapy* **6**:93-102.

Kasper JM, McCue DL, Milton AJ, Szwed A, Sampson CM, Huang M, Carlton S, Meltzer HY, Cunningham KA and Hommel JD (2016) Gamma-Aminobutyric Acidergic Projections From the Dorsal Raphe to the Nucleus Accumbens Are Regulated by Neuromedin U. *Biol Psychiatry* **80**:878-887.

Kathuria S, Gaetani S, Fegley D, Valiño F, Duranti A, Tontini A, Mor M, Tarzia G, Rana GL, Calignano A, Giustino A, Tattoli M, Palmery M, Cuomo V and Piomelli D (2003) Modulation of anxiety through blockade of anandamide hydrolysis. *Nature Medicine* **9**:76-81.

Kaufling J, Veinante P, Pawlowski SA, Freund-Mercier MJ and Barrot M (2009) Afferents to the GABAergic tail of the ventral tegmental area in the rat. *J Comp Neurol* **513**:597-621.

Kaufling J, Waltisperger E, Bourdy R, Valera A, Veinante P, Freund-Mercier MJ and Barrot M (2010) Pharmacological recruitment of the GABAergic tail of the ventral tegmental area by acute drug exposure. *Br J Pharmacol* **161**:1677-1691.

Kendall L, Wegenase D, Dorsey K, Kang S, Lee NY and Hess AM (2016) Efficacy of Sustained-Release Buprenorphine in an Experimental Laparotomy Model in Female Mice. *Journal of the American Association for Laboratory Animal Science* **55**:77-73.

Kinsey SG, Long JZ, O'Neal ST, Abdullah RA, Poklis JL, Boger DL, Cravatt BF and Lichtman AH (2009) Blockade of Endocannabinoid-Degrading Enzymes Attenuates Neuropathic Pain. *Journal of Pharmacology and Experimental Therapeutics* **330**:902-910.

Kinsey SG, O'Neal ST, Long JZ, Cravatt BF and Lichtman AH (2011) Inhibition of endocannabinoid catabolic enzymes elicits anxiolytic-like effects in the marble burying assay. *Pharmacol Biochem Behav* **98**:21-27.

Kinsey SG, Wise LE, Ramesh D, Abdullah R, Selley DE, Cravatt BF and Lichtman AH (2013) Repeated low-dose administration of the monoacylglycerol lipase inhibitor JZL184 retains cannabinoid receptor type 1-mediated antinociceptive and gastroprotective effects. *J Pharmacol Exp Ther* **345**:492-501.

Kirk RE (1995) *Experimental Design: Proceures for the Behavioral Sciences*. Brooks/Cole Publishing, Monterey, California.

Kissin I (2010) The development of new analgesics over the past 50 years: a lack of real breakthrough drugs. *Anesth Analg* **110**:780-789.

Kokras N and Dalla C (2014) Sex differences in animal models of psychiatric disorders. *Br J Pharmacol* **171**:4595-4619.

Koster R, Anderson M and De Beer EJ (1959) Acetic Acid for Analgesic Screening. *Federation Procedings*:412-417.

Kraft B, Frickey NA, Kaufmann RM, Reif M, Frey R, Gustorff B and Kress HG (2008) Lack of Analgesia by Oral Standardized Cannabis Extract on Acute Inflammatory Pain and Hyperalgesia in Volunteers. *Anesthesiology* **109**:101-110.

Kwilasz AJ, Abdullah RA, Poklis JL, Lichtman AH and Negus SS (2014) Effects of the fatty acid amide hydrolase inhibitor URB597 on pain-stimulated and pain-depressed behavior in rats. **25**:119-129.

Kwilasz AJ and Negus SS (2012) Dissociable Effects of the Cannabinoid Receptor Agonists 9-Tetrahydrocannabinol and CP55940 on Pain-Stimulated Versus Pain-Depressed Behavior in Rats. **343**:389-400.

Lahti L, Haugas M, Tikker L, Airavaara M, Voutilainen MH, Anttila J, Kumar S, Inkinen C, Salminen M and Partanen J (2016) Differentiation and molecular heterogeneity of inhibitory and excitatory neurons associated with midbrain dopaminergic nuclei. *Development* **143**:516-529.

Langford DJ, Bailey AL, Chanda ML, Clarke SE, Drummond TE, Echols S, Glick S, Ingrao J, Klassen-Ross T, Lacroix-Fralish ML, Matsumiya L, Sorge RE, Sotocinal SG, Tabaka JM, Wong D, Van Den Maagdenberg AMJM, Ferrari MD, Craig KD and Mogil JS (2010) Coding of facial expressions of pain in the laboratory mouse. *Nature Methods* **7**:447-449.

Lazenka ML, Moerke MJ, Townsend EA, Freeman KB, Carroll FI and Negus SS (2018) Dissociable effects of the kappa opioid receptor agonist nalfurafine on pain/itch-stimulated and pain/itch-depressed behaviors in male rats. *Psychopharmacology (Berl)* **235**:203-213.

Le Bars D, Gozaru M and Cadden SW (2001) Animal Models of Nociception. *Pharmacol Rev* **53**:597-652.

Leach MC, Klaus K, Miller AL, Scotto di Perrotolo M, Sotocinal SG and Flecknell PA (2012) The assessment of post-vasectomy pain in mice using behaviour and the Mouse Grimace Scale. *PLoS One* **7**:e35656.

Legakis LP, Karim-Nejad L and Negus SS (2020) Effects of repeated treatment with monoamine-transporter-inhibitor antidepressants on pain-related depression of intracranial self-stimulation in rats. *Psychopharmacology (Berl)* **237**:2201-2212.

Lehmann EL (2006) *Nonparametrics: Statistical Methods Based on Ranks, Revised*. Springer.

Leitl MD and Negus SS (2016) Pharmacological modulation of neuropathic pain-related depression of behavior. *Behavioural Pharmacology* **27**:364-376.

Leitl MD, Onvani S, Bowers MS, Cheng K, Rice KC, Carlezon WA, Banks ML and Negus SS (2014) Pain-Related Depression of the Mesolimbic Dopamine System in Rats: Expression, Blockade by Analgesics, and Role of Endogenous κ-opioids. *Neuropsychopharmacology* **39**:614-624.

Lewter LA, Fisher JL, Siemian JN, Methuku KR, Poe MM, Cook JM and Li JX (2017) Antinociceptive Effects of a Novel alpha2/alpha3-Subtype Selective GABAA Receptor Positive Allosteric Modulator. *ACS Chem Neurosci* **8**:1305-1312.

Li M, Qu Y, Zhong J, Che Z, Wang H, Xiao J, Wang F and Xiao J (2021) Sex bias in alcohol research: A 20-year comparative study. *Front Neuroendocrinol* **63**:100939.

Li Y, Zhao Z, Cai J, Gu B, Lv Y and Zhao L (2017) The Frequency-Dependent Aerobic Exercise Effects of Hypothalamic GABAergic Expression and Cardiovascular Functions in Aged Rats. *Front Aging Neurosci* **9**:212.

Long JZ, Li W, Booker L, Burston JJ, Kinsey SG, Schlosburg JE, Pavón FJ, Serrano AM, Selley DE, Parsons LH, Lichtman AH and Cravatt BF (2009a) Selective blockade of 2-arachidonoylglycerol hydrolysis produces cannabinoid behavioral effects. *Nature Chemical Biology* **5**:37-44.
Long JZ, Nomura DK and Cravatt BF (2009b) Characterization of Monoacylglycerol Lipase Inhibition Reveals Differences in Central and Peripheral Endocannabinoid Metabolism. **16**:744-753.
Long JZ, Nomura DK, Vann RE, Walentiny DM, Booker L, Jin X, Burston JJ, Sim-Selley LJ, Lichtman AH, Wiley JL and Cravatt BF (2009c) Dual blockade of FAAH and MAGL identifies behavioral processes regulated by endocannabinoid crosstalk in vivo. *Proceedings of the National Academy of Sciences* **106**:20270-20275.
Lötsch J, Weyer-Menkhoff I and Tegeder I (2018) Current evidence of cannabinoid-based analgesia obtained in preclinical and human experimental settings. *European Journal of Pain* **22**:471-484.
Lu H-C and Mackie K (2016) An Introduction to the Endogenous Cannabinoid System. *Biological Psychiatry* **79**:516-525.
Mansour A, Fox CA, Akil H and Watson SJ (1995) Opioid-receptor mRNA expression in rat CNS: anatomical and functional implications. *Trends Neurosci* **18**:22-29.
Mansour A, Khachaturian H, Lewis ME, Akil H and Watson SJ (1987) Autoradiographic Differentiation of Mu, Delta, and Kappa Opioid Receptors in the Rat Forebrain and Midbrain. *The Journal of Neuroscience* **7**:2445-2464.
Marino MJ (2018) How often should we expect to be wrong? Statistical power, P values, and the expected prevalence of false discoveries. *Biochem Pharmacol* **151**:226-233.
Markovic T, Pedersen CE, Massaly N, Vachez YM, Ruyle B, Murphy CA, Abiraman K, Shin JH, Garcia JJ, Yoon HJ, Alvarez VA, Bruchas MR, Creed MC and Morón JA (2021) Pain induces adaptations in ventral tegmental area dopamine neurons to drive anhedonia-like behavior. *Nature Neuroscience*.
Martikainen IK, Hagelberg N, Jaaskelainen SK, Hietala J and Pertovaara A (2018) Dopaminergic and serotonergic mechanisms in the modulation of pain: In vivo studies in human brain. *Eur J Pharmacol* **834**:337-345.
Matson DJ, Broom DC, Carson SR, Baldassari J, Kehne J and Cortright DN (2007) Inflammation-Induced Reduction of Spontaneous Activity by Adjuvant: A Novel Model to Study the Effect of Analgesics in Rats. *Journal of Pharmacology and Experimental Therapeutics* **320**:194-201.
Matsui A and Williams JT (2011) Opioid-sensitive GABA inputs from rostromedial tegmental nucleus synapse onto midbrain dopamine neurons. *J Neurosci* **31**:17729-17735.
Matsumiya LC, Sorge RE, Sotocinal SG, JTabaka JM, Wieskopf JS, Zaloum A, King OD and Mogil JS (2012) Using the Mouse Grimace Scale to Reevaluate the Efficacy of Postoperative Analgesics in Laboratory Mice. *Journal of American Association for Laboratory Animals Science* **51**:42-49.
McCarthy MM, Arnold AP, Ball GF, Blaustein JD and De Vries GJ (2012) Sex differences in the brain: the not so inconvenient truth. *J Neurosci* **32**:2241-2247.
McMahon S, SKoltzenburg M, Tracey I and Turk D (2013) Wall and Melzack's Textbook of Pain, in, Elsevier, Philadelphia.
McReynolds JR, Christianson JP, Blacktop JM and Mantsch JR (2018) What does the Fos say? Using Fos-based approaches to understand the contribution of stress to substance use disorders. *Neurobiol Stress* **9**:271-285.
Mechoulam R, Ben-Shabat S, Hanus L, Ligumsky M, Kaminski NE, Schatz AR, Gopher A, Almog S, Martin BR, Compton DR, Pertwee RG, Griffin G, Bayewitch M, Barg J and Vogel Z (1995) Identification of an endogenous 2-monoglyceride, present in canine gut, that binds to cannabnoid receptors. *Biochemical Pharmacology* **50**:83-90.
Medicine Io (2011) *Relieving Pain in America: A Blueprint for Transforming Preveition, Care, Education, and Research*. The National Academics Press, Washington D.C.
Meng IM, BH; Martin, WJ; Fields, HL (1998) An analgesic circuit inactivated by cannabinoids. *Nature* **395**.
Mercadante S, Radbruch L, Caraceni A, Cherny N, Kaasa S, Nauck F, Ripamonti C, De Conno F and Steering Committee of the European Association for Palliative Care Research N (2002) Episodic (breakthrough)

pain: consensus conference of an expert working group of the European Association for Palliative Care. *Cancer* **94**:832-839.
Miller LL, Picker MJ, Umberger MD, Schmidt KT and Dykstra LA (2012) Effects of Alterations in Cannabinoid Signaling, Alone and in Combination with Morphine, on Pain-Elicited and Pain-Suppressed Behavior in Mice. *Journal of Pharmacology and Experimental Therapeutics* **342**:177-187.
Miller LR, Marks C, Becker JB, Hurn PD, Chen WJ, Woodruff T, McCarthy MM, Sohrabji F, Schiebinger L, Wetherington CL, Makris S, Arnold AP, Einstein G, Miller VM, Sandberg K, Maier S, Cornelison TL and Clayton JA (2017) Considering sex as a biological variable in preclinical research. *FASEB J* **31**:29-34.
Mogil JS (2009) Animal models of pain: progress and challenges. *Nature Reviews Neuroscience* **10**:283-294.
Molinoff PB (2011) Neurotransmission and the Central Nervous System
, in *Goodman & Gilman's The Pharmacological Basis of Therapeutics* (Brunton L ed) pp 363-396, McGraw Hill Medical.
Moore A and McQuay H (2013) Cyclooxygenase Inhibitors: Clinical Use, in *Wall & Melzack's Textbook of Pain* (McMahon S, Koltzenburg M, Tracey I and Turk D eds) pp 455-464, Elsevier, Philadelphia.
Motulsky H (2020) Graphpad Statistics Guide, in.
Muller-Vahl KR, Fremer C, Beals C, Ivkovic J, Loft H and Schindler C (2021) Monoacylglycerol Lipase Inhibition in Tourette Syndrome: A 12-Week, Randomized, Controlled Study. *Mov Disord* **36**:2413-2418.
Mun CJ, Letzen JE, Peters EN, Campbell CM, Vandrey R, Gajewski-Nemes J, DiRenzo D, Caufield-Noll C and Finan PH (2020) Cannabinoid effects on responses to quantitative sensory testing among individuals with and without clinical pain: a systematic review. *Pain* **161**:244-260.
Munro G, Jansen-Olesen I and Olesen J (2017) Animal models of pain and migraine in drug discovery. *Drug Discov Today* **22**:1103-1111.
Munro G, Lopez-Garcia JA, Rivera-Arconada I, Erichsen HK, Nielsen EO, Larsen JS, Ahring PK and Mirza NR (2008) Comparison of the novel subtype-selective GABAA receptor-positive allosteric modulator NS11394 [3'-[5-(1-hydroxy-1-methyl-ethyl)-benzoimidazol-1-yl]-biphenyl-2-carbonitrile] with diazepam, zolpidem, bretazenil, and gaboxadol in rat models of inflammatory and neuropathic pain. *J Pharmacol Exp Ther* **327**:969-981.
Nagase H, Kumakura S and Shimada K (2012) Establishment of a novel objective and quantitative method to assess pain-related behavior in monosodium iodoacetate-induced osteoarthritis in rat knee. *Journal of Pharmacological and Toxicological Methods* **65**:29-36.
Naidu PS, Booker L, Cravatt BF and Lichtman AH (2009) Synergy between Enzyme Inhibitors of Fatty Acid Amide Hydrolase and Cyclooxygenase in Visceral Nociception. **329**:48-56.
Naidu PS, Kinsey SG, Guo TL, Cravatt BF and Lichtman AH (2010) Regulation of Inflammatory Pain by Inhibition of Fatty Acid Amide Hydrolase. **334**:182-190.
Nakagawa S and Cuthill IC (2007) Effect size, confidence interval and statistical significance: a practical guide for biologists. *Biol Rev Camb Philos Soc* **82**:591-605.
Negus SS (2018) Addressing the Opioid Crisis: The Importance of Choosing Translational Endpoints in Analgesic Drug Discovery. *Trends Pharmacol Sci* **39**:327-330.
Negus SS (2019) Core Outcome Measures in Preclinical Assessment of Candidate Analgesics. *Pharmacological Reviews* **71**:225-266.
Negus SS, Neddenriep B, Altarifi AA, Carroll FI, Leitl MD and Miller LL (2015) Effects of Ketoprofen, Morphine, and Kappa Opioids On Pain-Related Depression of Nesting in Mice. *PAIN*:1.
Negus SS, O'Connell R, Morrissey E, Cheng K and Rice KC (2012) Effects of Peripherally Restricted κ Opioid Receptor Agonists on Pain-Related Stimulation and Depression of Behavior in Rats. *Journal of Pharmacology and Experimental Therapeutics* **340**:501-509.
Network P (2020) Physician's Desk Reference, in, Montvale, NJ.
Nevins ME, Nash SA and Beardsley PM (1993) Quantitative grip strength assessment as a means of evaluating muscle relaxation in mice. **110**:92-96.

Niemegeers C, Lenaerts F, Awouters F and Janssen P (1975) Gastrointestinal effects and acute toxicity of suprofen. *Arzneimittelforschung* **10**:1537-1542.
Niphakis MJ, Cognetta AB, Chang JW, Buczynski MW, Parsons LH, Byrne F, Burston JJ, Chapman V and Cravatt BF (2013) Evaluation of NHS Carbamates as a Potent and Selective Class of Endocannabinoid Hydrolase Inhibitors. *ACS Chemical Neuroscience* **4**:1322-1332.
Niphakis MJ, Johnson DS, Ballard TE, Stiff C and Cravatt BF (2012) O-Hydroxyacetamide Carbamates as a Highly Potent and Selective Class of Endocannabinoid Hydrolase Inhibitors. *ACS Chemical Neuroscience* **3**:418-426.
Nomura DK, Morrison BE, Blankman JL, Long JZ, Kinsey SG, Marcondes MCG, Ward AM, Hahn YK, Lichtman AH, Conti B and Cravatt BF (2011) Endocannabinoid Hydrolysis Generates Brain Prostaglandins That Promote Neuroinflammation. *Science* **334**:809-813.
Nyilas R, Gregg LC, Mackie K, Watanabe M, Zimmer A, Hohmann AG and Katona I (2009) Molecular architecture of endocannabinoid signaling at nociceptive synapses mediating analgesia. *Eur J Neurosci* **29**:1964-1978.
Obeng S, Hiranita T, Leon F, McMahon LR and McCurdy CR (2021) Novel Approaches, Drug Candidates, and Targets in Pain Drug Discovery. *J Med Chem* **64**:6523-6548.
Ohno-Shosaku T and Kano M (2014) Endocannabinoid-mediated retrograde modulation of synaptic transmission. *Current Opinion in Neurobiology* **29**:1-8.
Oliver V, Thurston S and Lofgren J (2018) Using Cageside Measures to Evaluate Analgesic Efficacy in Mice (*Mus musculus*) after Surgery. *Journal of the American Association for Laboratory Animal Science* **57**:186-201.
Owens RA, Ignatowska-Jankowska B, Mustafa M, Beardsley PM, Wiley JL, Jali A, Selley DE, Niphakis MJ, Cravatt BF and Lichtman AH (2016) Discriminative Stimulus Properties of the Endocannabinoid Catabolic Enzyme Inhibitor SA-57 in Mice. **358**:306-314.
Paxinos GF, Keith BJ (2007) *The Mouse Brain: In Stereotaxic Coordinates*. Elsevier Inc.
Pogatzki-Zahn EL, P. (2021) Prevention of Chronic Post-Surgical Pain. *IASP Fact Sheet*.
Price DD (2003) Central Neural Mechansims that Interrelate Sensory and Affective Dimensions of Pain. *Mol Interv* **2**:392-403.
Raft D, Gregg J, Ghia J and Harris L (1977) Effects of intravenous tetrahydrocannabinol on experimental and surgical pain; Psychological correlates of the analgesic response. *Clinical Pharmacology & Therapeutics* **21**:26-33.
Reggio PH (2010) Endocannabinoid binding to the cannabinoid receptors: what is known and remains unknown. *Curr Med Chem* **17**:1468-1486.
Rethy C, Smith C and Villarreal J (1970) Effects of narcotic analgesics upon the locomotor activity and brain catecholamine content of the mouse. *The Journal of Pharmacology and Experimental Therapeutics* **176**:472-479.
Rice A, Arendt-Nielsen L, Belton J, Blyth FM, Degenhardt L, Di Forti M, Eccleston C, Finn DA, Finnerup NB, Fisher E, Gilron I, Haroutounian S, Hohmann AG, Kalso E, Krane E, Moore A, Rowbotham M, Soliman N, Wallace M and Zinboonyahgooon N (2021) IASP Position Statement on the Use of Cannabinoids to Treat Pain. *International Association for the Study of Pain*.
Richardson JD, Kilo S and Hargreaves KM (1998) Cannabinoids reduce hyperalgesia and inflammation via interaction withperipheral CB1 receptors. *Pain* **75**:111-119.
Rock EM and Parker LA (2016) Cannabinoids As Potential Treatment for Chemotherapy-Induced Nausea and Vomiting. *Front Pharmacol* **7**:221.
Rosenberg MB, Carroll FI and Negus SS (2013) Effects of Monoamine Reuptake Inhibitors in Assays of Acute Pain-Stimulated and Pain-Depressed Behavior in Rats. *The Journal of Pain* **14**:246-259.
Rosland JH, Hunskaar S and Hole K (1987) The Effect of Diazepam on Nociception in Mice. *Pharmacology & Toxicology* **61**:111-115.
Sagar DR, Gaw AG, Okine BN, Woodhams SG, Wong A, Kendall DA and Chapman V (2009) Dynamic regulation of the endocannabinoid system: implications for analgesia. *Mol Pain* **5**:59.

Sakin YS, Dogrul A, Ilkaya F, Seyrek M, Ulas UH, Gulsen M and Bagci S (2015) The effect of FAAH, MAGL, and Dual FAAH/MAGL inhibition on inflammatory and colorectal distension-induced visceral pain models in Rodents. *Neurogastroenterology & Motility* **27**:936-944.

Sanders-Bush E and Hazelwood L (2011) 5-Hydroxytryptamine (Serotonin) and Dopamine, in *Goodman & Gilman's The Pharmacological Basis of Therapeutics* (Brunton L ed) pp 335-362, McGraw Hill Medical.

Schlosburg JE, Blankman JL, Long JZ, Nomura DK, Pan B, Kinsey SG, Nguyen PT, Ramesh D, Booker L, Burston JJ, Thomas EA, Selley DE, Sim-Selley LJ, Liu Q-S, Lichtman AH and Cravatt BF (2010) Chronic monoacylglycerol lipase blockade causes functional antagonism of the endocannabinoid system. *Nature Neuroscience* **13**:1113-1119.

Schlosburg JE, Kinsey SG and Lichtman AH (2009) Targeting Fatty Acid Amide Hydrolase (FAAH) to Treat Pain and Inflammation. *The AAPS Journal* **11**:39-44.

Schwienteck KL, Li G, Poe MM, Cook JM, Banks ML and Stevens Negus S (2017) Abuse-related effects of subtype-selective GABAA receptor positive allosteric modulators in an assay of intracranial self-stimulation in rats. *Psychopharmacology* **234**:2091-2101.

Seguin L, Le Marouille-Girardon S and Millan MJ (1995) Antinociceptive profiles of non-peptidergic neurokinin1 and neurokinin2 receptor antagonists: a comparison to other classes of antinociceptive agent. **61**:325-343.

Shansky RM (2018) Sex differences in behavioral strategies: avoiding interpretational pitfalls. *Curr Opin Neurobiol* **49**:95-98.

Siemian JN, Arenivar MA, Sarsfield S, Borja CB, Erbaugh LJ, Eagle AL, Robison AJ, Leinninger G and Aponte Y (2021) An excitatory lateral hypothalamic circuit orchestrating pain behaviors in mice. *Elife* **10**.

Sinniger V, Porcher C, Mouchet P, Juhem A and Bonaz B (2004) c-fos and CRF receptor gene transcription in the brain of acetic acid-induced somato-visceral pain in rats. *Pain* **110**:738-750.

Skolnick P and Volkow ND (2016) Re-energizing the Development of Pain Therapeutics in Light of the Opioid Epidemic. *Neuron* **92**:294-297.

Smith RJ, Vento PJ, Chao YS, Good CH and Jhou TC (2019) Gene expression and neurochemical characterization of the rostromedial tegmental nucleus (RMTg) in rats and mice. *Brain Struct Funct* **224**:219-238.

Sofia RD, Vassar HB and Knobloch LC (1975) Comparative analgesic activity of various naturally occurring cannabinoids in mice and rats. *Psychopharmacologia* **40**:285-295.

Solass W, Struller F, Horvath P, Konigsrainer A, Sipos B and Weinreich FJ (2016) Morphology of the peritoneal cavity and pathophysiological consequences. *Pleura Peritoneum* **1**:193-201.

Sorge RE, LaCroix-Fralish ML, Tuttle AH, Sotocinal SG, Austin JS, Ritchie J, Chanda ML, Graham AC, Topham L, Beggs S, Salter MW and Mogil JS (2011) Spinal cord Toll-like receptor 4 mediates inflammatory and neuropathic hypersensitivity in male but not female mice. *J Neurosci* **31**:15450-15454.

Spahn V, Del Vecchio G, Labuz D, Rodriguez-Gaztelumendi A, Massaly N, Temp J, Durmaz V, Sabri P, Reidelbach M, Machelska H, Weber M and Stein C (2017) A nontoxic pain killer designed by modeling of pathological receptor conformations. *Science* **355**:966-969.

St. Sauver JL, Warner DO, Yawn BP, Jacobson DJ, McGree ME, Pankratz JJ, Melton LJ, Roger VL, Ebbert JO and Rocca WA (2013) Why Patients Visit Their Doctors: Assessing the Most Prevalent Conditions in a Defined American Population. *Mayo Clinic Proceedings* **88**:56-67.

Stark P and Dews PB (1980) Cannabinoids. I. Behavioral Effects. *Journal of Pharmacology and Experimental Therapeutics* **214**:124-130.

Stein C (2016) Opioid Receptors. *Annu Rev Med* **67**:433-451.

Stevenson GW, Bilsky EJ and Negus SS (2006) Targeting Pain-Suppressed Behaviors in Preclinical Assays of Pain and Analgesia: Effects of Morphine on Acetic Acid-Suppressed Feeding in C57BL/6J Mice. *The Journal of Pain* **7**:408-416.

Stevenson GW, Cormier J, Mercer H, Adams C, Dunbar C, Negus SS and Bilsky EJ (2009) Targeting pain-depressed behaviors in preclinical assays of pain and analgesia: Drug effects on acetic acid-depressed locomotor activity in ICR mice. *Life Sciences* **85**:309-315.
Sticht MA, Lau DJ, Keenan CM, Cavin JB, Morena M, Vemuri VK, Makriyannis A, Cravatt BF, Sharkey KA and Hill MN (2019) Endocannabinoid regulation of homeostatic feeding and stress-induced alterations in food intake in male rats. *Br J Pharmacol* **176**:1524-1540.
Sticht MA, Rock EM, Limebeer CL and Parker LA (2015) Endocannabinoid Mechanisms Influencing Nausea. *Int Rev Neurobiol* **125**:127-162.
Takakura AC, Moreira TS, West GH, Gwilt JM, Colombari E, Stornetta RL and Guyenet PG (2007) GABAergic pump cells of solitary tract nucleus innervate retrotrapezoid nucleus chemoreceptors. *J Neurophysiol* **98**:374-381.
Tannenbaum C, Ellis RP, Eyssel F, Zou J and Schiebinger L (2019) Sex and gender analysis improves science and engineering. *Nature* **575**:137-146.
Tappe-Theodor A, King T and Morgan MM (2019) Pros and Cons of Clinically Relevant Methods to Assess Pain in Rodents. *Neurosci Biobehav Rev* **100**:335-343.
Taylor NE, Long H, Pei J, Kukutla P, Phero A, Hadaegh F, Abdelnabi A, Solt K and Brenner GJ (2019) The rostromedial tegmental nucleus: a key modulator of pain and opioid analgesia. *Pain* **160**:2524-2534.
Therapeutics A (2017) Abide Therapeutics mines serine hydrolases and finds CNS gold. *Nature Research Custom Media*:821.
Thompson AL, Grenald SA, Ciccone HA, Bassirirad N, Niphakis MJ, Cravatt BF, Largent-Milnes TM and Vanderah TW (2020) The Endocannabinoid System Alleviates Pain in a Murine Model of Cancer-Induced Bone Pain. *Journal of Pharmacology and Experimental Therapeutics* **373**:230-238.
Tocco D and Maickel R (1984) Analgesic Activities of Amphetamine Isomers. *Arch Int Pharmacodyn Ther* **268**:25-31.
Todd AJ and Koerber HR (2013) Neuroanatomical Substrates of Spinal Nociception, in *Wall and Melzack's Textbook of Pain* (SB M, Koltzenburg M, I T and Turk DC eds) pp 77-93, Elsevier.
Tramullas M, Collins JM, Fitzgerald P, Dinan TG, SM OM and Cryan JF (2021) Estrous cycle and ovariectomy-induced changes in visceral pain are microbiota-dependent. *iScience* **24**:102850.
Tsou K, Brown S, Sanudo-Pena MC, Mackie K and Walker JL (1998) Immunohistochemical distribution of cannabinoid CB1 receptors in the rat central nervous system. *Neuroscience* **83**:393-411.
Tuttle AH, Molinaro MJ, Jethwa JF, Sotocinal SG, Prieto JC, Styner MA, Mogil JS and Zylka MJ (2018a) A deep neural network to assess spontaneous pain from mouse facial expressions. *Mol Pain* **14**:1744806918763658.
Tuttle AH, Philip VM, Chesler EJ and Mogil JS (2018b) Comparing phenotypic variation between inbred and outbred mice. *Nat Methods* **15**:994-996.
Tyler TD and Tessel RE (1979) Amphetamine's locomotor-stimulant and norepinephrine-releasing effects: Evidence for selective antagonism by nisoxetine. **64**:291-296.
van Belle G (2008) *Statistical rules of thumb*. John Wiley & Sons, Hoboken, NJ.
Varvel SA (2005) 9-Tetrahydrocannbinol Accounts for the Antinociceptive, Hypothermic, and Cataleptic Effects of Marijuana in Mice. **314**:329-337.
Volkow ND and Collins FS (2017) The Role of Science in Addressing the Opioid Crisis. *The New England Journal of Medicine* **377**:391-394.
von Schaper E (2016) Bial incident raises FAAH suspicions. *Nat Biotechnol* **34**:223.
Wakley AA, Wiley JL and Craft RM (2015) Gonadal hormones do not alter the development of antinociceptive tolerance to delta-9-tetrahydrocannabinol in adult rats. *Pharmacol Biochem Behav* **133**:111-121.
Wallace M, Schulteis G, Atkinson JH, Wolfson T, Lazzaretto D, Bentley H, Gouaux B and Abramson I (2007) Dose-dependent Effects of Smoked Cannabis on Capsaicin-induced Pain and Hyperalgesia in Healthy Volunteers. **107**:785-796.
Wang X, Gao F, Zhu J, Guo E, Song X, Wang S and Zhan RZ (2014) Immunofluorescently labeling glutamic acid decarboxylase 65 coupled with confocal imaging for identifying GABAergic somata in the rat

dentate gyrus-A comparison with labeling glutamic acid decarboxylase 67. *J Chem Neuroanat* **61-62**:51-63.
Watanabe M and Narita M (2018) Brain Reward Circuit and Pain, in *Advances in Pain Research: Mechanisms and Modulation of Chronic Pain* (Shyu B and Tominaga M eds), Springer Nature, Singapore.
Weber K, Hacker R, Hardisty JF, Harris SB and Hayes AW (2020) Oral repeated-dose toxicity studies of BIA 10-2474 in cynomolgus monkeys. *Regul Toxicol Pharmacol* **111**:104547.
Westfall T and Westfall D (2011) Adrenergic Agonists and Antagonists, in *Goodman & Gilman's The Pharmacological Basis of Therapeutics* (Brunton L, Chabner B and Knollmann B eds), McGraw-Hill.
Wiebelhaus JM, Grim TW, Owens RA, Lazenka MF, Sim-Selley LJ, Abdullah RA, Niphakis MJ, Vann RE, Cravatt BF, Wiley JL, Negus SS and Lichtman AH (2015) Δ9-Tetrahydrocannabinol and Endocannabinoid Degradative Enzyme Inhibitors Attenuate Intracranial Self-Stimulation in Mice. *Journal of Pharmacology and Experimental Therapeutics* **352**:195-207.
Wilkerson JL, Curry ZA, Kinlow PD, Mason BL, Hsu K-L, Van Der Stelt M, Cravatt BF and Lichtman AH (2018) Evaluation of different drug classes on transient sciatic nerve injury–depressed marble burying in mice. *PAIN* **159**:1155-1165.
Wilkerson JL, Ghosh S, Mustafa M, Abdullah RA, Niphakis MJ, Cabrera R, Maldonado RL, Cravatt BF and Lichtman AH (2017) The endocannabinoid hydrolysis inhibitor SA-57: Intrinsic antinociceptive effects, augmented morphine-induced antinociception, and attenuated heroin seeking behavior in mice. *Neuropharmacology* **114**:156-167.
Wood PB (2008) Role of central dopamine in pain and analgesia. *Expert Reviews Neurotherapeutics* **8**:781-797.
Woodhams SG, Chapman V, Finn DP, Hohmann AG and Neugebauer V (2017) The cannabinoid system and pain. *Neuropharmacology* **124**:105-120.
Yezierski RP and Hansson P (2018) Inflammatory and Neuropathic Pain From Bench to Bedside: What Went Wrong? *J Pain* **19**:571-588.
Zhang GF, Guo J and Yang JJ (2020) The labteral habenula: role in chronic pain and depression. *Translational Perioperative Pain Medicine* **7**:271-278.
Zhao C, Eisinger B and Gammie SC (2013) Characterization of GABAergic neurons in the mouse lateral septum: a double fluorescence in situ hybridization and immunohistochemical study using tyramide signal amplification. *PLoS One* **8**:e73750.